CASE FILE
COPY

MANUAL FOR STRUCTURAL STABILITY ANALYSIS OF SANDWICH PLATES AND SHELLS

by R. T. Sullins, G. W. Smith, and E. E. Spier

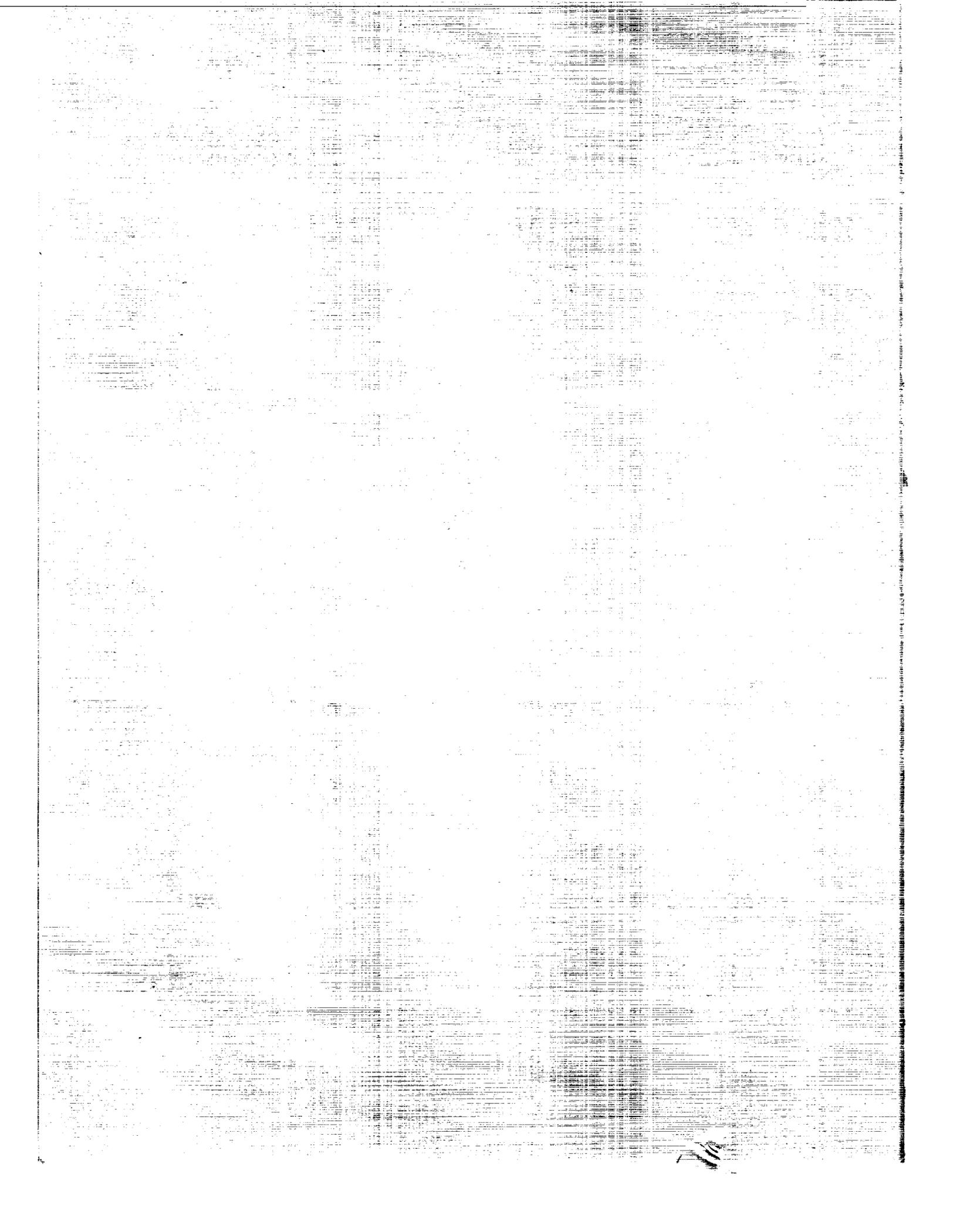# MANUAL FOR STRUCTURAL STABILITY ANALYSIS

OF SANDWICH PLATES AND SHELLS

By R. T. Sullins, G. W. Smith, and E. E. Spier

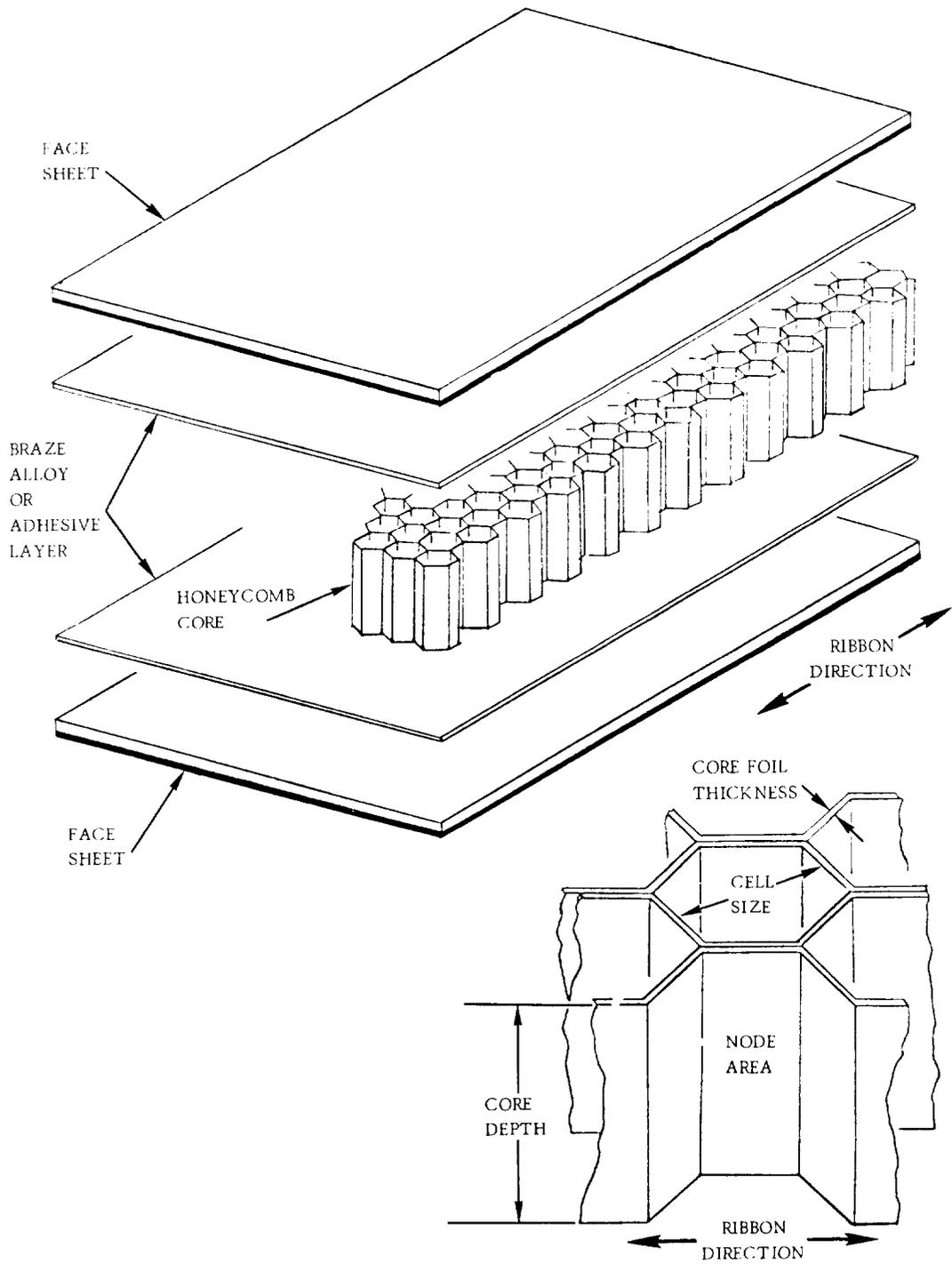Distribution of this report is provided in the interest of information exchange. Responsibility for the contents resides in the author or organization that prepared it.

NATIONAL AERONAUTICS AND SPACE ADMINISTRATION

FACE
SHEET

BRAZE
ALLOY
OR
ADHESIVE
LAYER

HONEYCOMB
CORE

FACE
SHEET

RIBBON
DIRECTION

CORE FOIL
THICKNESS

CELL
SIZE

NODE
AREA

CORE
DEPTH

RIBBON
DIRECTION

HONEYCOMB SANDWICH CONSTRUCTION

ABSTRACT

The basic objective of this study was to develop and compile a manual which would include practical and up-to-date methods for analyzing the structural stability of sandwich plates and shells for typical loading conditions which might be encountered in aerospace applications. The methods proposed for use would include known analytical approaches as modified for correlation with applicable test data.

The data prsented here covers recommended design equations and curves for a wide range of structural configurations and loading conditions, including combined loads. In a number of cases, actual test data points are included on the design curves to substantiate the recommendations made. For those items where little or no test data exists the basic analytical approach is presented along with the notation that this represented the "best available" data and should be used with some caution and judgment until substantiated by test.

The following subjects are among those covered in the manual:

    Local Instability

    General Instability of Flat Panels

    General Instability of Circular Cylinders

    General Instability of Truncated Circular Cones

    General Instability of Dome-Shaped Shells

    Instability of Sandwich Shell Segments

    Effects of Cutouts on the General Instability of Sandwich Shells

    Inelastic Behavior of Sandwich Plates and Shells

TABLE OF CONTENTS

TABLE OF CONTENTS, Cont'd.

LIST OF FIGURES

LIST OF FIGURES, Cont'd.

LIST OF FIGURES, Cont'd.

LIST OF TABLES

a	Panel length, inches. Major semi-axis of an ellipse, inches.
a_R	Axial length of a cylindrical panel, inches.
a_p	Length of the flat panel shown in Figure 7.1-1, inches.
b	Panel width, inches. Minor semi-axis of an ellipse, inches.
b_R	Circumferential width of a cylindrical panel, inches.
b_f	Pitch of corrugated core, inches.
b_p	Width of the flat panel shown in Figure 7.1-1, inches.
C_L	Length parameter defined by Equation (4.7-25), dimensionless.
C_o	Parameter defined by Equations (4.2-21) and (6.2-19), dimensionless.
C_p	Buckling coefficient for sandwich cylinders subjected to external lateral pressure, dimensionless.
D	Bending stiffness of sandwich wall or panel $= \dfrac{\eta(E_1 t_1)(E_2 t_2)h^2}{\lambda(E_1 t_1 + E_2 t_2)}$, inch-lbs.
D_q	Shear stiffness of sandwich wall or panel $= h^2(G_{xz})/t_c$, lb/inch.
d	Total thickness of sandwich wall or panel $(d = t_1 + t_2 + t_c)$, inches.
E	Young's modulus, psi.
E_c	Young's modulus of the core in the direction normal to the facings, psi.
E_f	Young's modulus of facing, psi.
E_s	Secant modulus of facing, psi.
E_t	Tangent modulus of facing, psi.

E_1, E_2	Young's moduli for facings 1 and 2 respectively, psi.
e_i	Strain intensity defined by Equation (9.2-2), in./in.
F_v	Transverse shear force, lbs.
$(F_v)_{cr}$	Critical transverse shear force, lbs.
F_c	Flatwise sandwich strength (the lower of flatwise core compressive, flatwise core tensile, and flatwise core-to-facing bond strengths), psi.
G_c	Transverse shear modulus of core, psi.
G_{ca}	Core shear modulus associated with the plane perpendicular to the facings and parallel to side a of panel, psi.
G_{cb}	Core shear modulus associated with the plane perpendicular to the facings and parallel to side b of panel, psi.
G_f	Elastic shear modulus of facing, psi.
G_{ij}	Core shear modulus associated with the plane perpendicular to the facings and parallel to the direction of loading, psi.
G_s	Secant shear modulus of facing, psi.
G_{xz}	Core shear modulus associated with the plane perpendicular to the facings and parallel to the axis of revolution of a cylinder, psi.
G_{yz}	Core shear modulus associated with the plane perpendicular to the axis of revolution of a cylinder, psi.
h	Distance between middle surfaces of the two facings of a sandwich construction, inches.
K	Buckling coefficient for an isotropic (non-sandwich) flat plate, dimensionless. Buckling coefficient for flat rectangular sandwich panel under edgewise compression (K_c), edgewise shear (K_s), or edgewise bending (K_b). $K = K_F + K_M$.
K_F	Theoretical flat panel buckling coefficient which is dependent on facing stiffness and panel aspect ratio, dimensionless.

K_M Theoretical flat panel buckling coefficient which is dependent on sandwich bending and shear rigidities, panel aspect ratio, and applied loading, dimensionless.

K_c Buckling coefficient for sandwich cylinders under axial compression and sandwich domes under external pressure, dimenionless.

K_c' Buckling coefficient for short sandwich cylinders under axial compression, dimensionless.

K_p Parameter defined by Equation (4.4-2), dimensionless.

K_s Buckling coefficient for sandwich cylinder subjected to torsion, dimensionless.

K_δ Parameter defined by Equation (2.2-4), dimensionless.

k Buckling coefficient, dimensionless.

k_x Buckling coefficient associated with compressive stress acting in the x direction, dimensionless.

k_x' Loading coefficient for applied compressive stress which is acting in the x direction, dimensionless.

k_y Buckling coefficient associated with compressive stress acting in the y direction, dimensionless.

k_y' Loading coefficient for applied compressive stress which is acting in the y direction, dimensionless.

L Over-all length, inches.

L_e Effective length, inches.

M Applied bending moment, in-lbs.

M_{cr} Critical bending moment, in-lbs.

M.S.   Margin of safety, dimensionless.

N_{cr} Critical compressive running load, lbs/inch.

n Number of circumferential full-waves in the buckle pattern, dimensionless.

P	Axial load, lbs.
P′	Equivalent axial load defined by Equation (5.6-32), lbs.
P_{cr}	Critical axial load, lbs.
$(\bar{P}_{cr})_{Empirical}$	Empirical lower-bound value for critical axial load when acting alone, lbs.
p	External pressure, psi.
p_{cr}	Critical value for external pressure, psi.
$(p_{cr})_{Test}$	Experimental value for critical external pressure, psi.
$(\bar{p}_x)_{CL}$	Classical theoretical critical pressure for a cylinder subjected to external pressure acting only on the end closures, psi.
p_y	External pressure acting only on the lateral surface of a cylinder, psi.
$(\bar{p}_y)_{CL}$	Classical theoretical critical pressure for a cylinder subjected to external pressure acting only on the lateral surface, psi.
Q	The relative minimum, with respect to ζ, of expression (2.2-2), dimensionless.
q	Quantity defined by Equation (2.2-3), dimensionless.
R	Degree of core shear modulus orthotropicity = G_{ca}/G_{cb}, dimensionless. Radius to middle surface, inches.
R_b	Stress ratio defined by Equation (4.7-9), dimensionless.
$(R_b)_{CL}$	Stress ratio defined by Equation (4.7-5), dimensionless.
R_c	Load, stress, or pressure ratios as defined in appropriate sections of this handbook, dimensionless.
$(R_c)_{CL}$	Stress ratios as defined in appropriate sections of this handbook, dimensionless.
R_e	Effective radius, inches.

R_i — Stress or load ratio for the particular type of loading associated with the subscript i, dimensionless.

R_j — Stress or load ratio for the particular type of loading associated with the subscript j, dimensionless.

R_{large} — Radius to middle surface at the large end of a truncated conical shell, measured perpendicular to the axis of revolution, inches.

R_{Max} — Maxium radius of curvature for middle surface of a dome-shaped shell, inches.

R_p — Pressure ratios as defined in appropriate sections of this handbook, dimensionless.

$(R_p)_{CL}$ — Pressure ratio defined by Equation (4.7-15), dimensionless.

R_s — Load or stress ratios as defined in appropriate sections of this handbook, dimensionless.

$(R_s)_{CL}$ — Stress ratio defined by Equation (4.7-29), dimensionless.

R_{small} — Radius to middle surface at the small end of a truncated conical shell, measured perpendicular to the axis of revolution, inches.

R_x — Stress or load ratio corresponding to the x direction, dimensionless.

R_y — Stress or load ratio corresponding to the y direction, dimensionless.

R_2 — Middle-surface radius of curvature in the plane perpendicular to the meridian, inches.

r_a — Parameter defined by Equation (4.2-37), dimensionless.

s — Cell size of honeycomb core, inches.

T — External torque, in-lbs.

T_{cr} — Critical external torque, in-lbs.

$(\bar{T}_{cr})_{Empirical}$ — Empirical lower-bound value for critical torque when acting alone, in-lbs.

t — Thickness, inches.

t_R	Total thickness of the cylindrical panel shown in Figure 7.1-1, inches.
t_c	Thickness of core (measured in the direction normal to the facings), inches.
t_f	Thickness of a single facing, inches.
t_p	Total thickness of the flat panel shown in Figure 7.1-1, inches.
t_o	Thickness of material from which corrugated core is formed, inches.
t_1, t_2	Thicknesses of the respective facings of a sandwich construction (there is no preference as to which facing is denoted by the subscript 1 or 2), inches.
U	Sandwich transverse shear stiffness, defined as $U = \dfrac{h^2}{t_c} G_c \approx h\,G_c$, lbs. per inch.
V	Bending and shear rigidity parameter which is defined as $V = \dfrac{\pi^2 D}{b^2 U}$, dimensionless.
V_c	Parameter defined in Sections 4.2 and 6.2, dimensionless.
V_p	Parameter defined by Equation (4.4-4), dimensionless.
V_s	Parameter defined by Equation (4.5-4), dimensionless.
V_{xz}	Parameter defined by Equation (4.7-13), dimensionless.
V_{yz}	Parameter defined by Equation (4.7-14), dimensionless.
W	Bending and shear rigidity parameter for flat sandwich panels with corrugated core which is defined as $W = \dfrac{\pi^2 t_c (E_1 t_1)(E_2 t_2)\,\eta}{\lambda b^2 G_{cb}(E_1 t_1 + E_2 t_2)}$, dimensionless.
w_c	Running compression load, lbs/inch.
Z	Length parameter defined by Equation (4.2-33), dimensionless.
Z_s	Length parameter defined by Equation (4.5-3), dimensionless.

α Angle of rotation at appropriate joint in corrugated-core sandwich construction (see Figure 2.1-5), degrees. Vertex half-angle of conical shell, degrees.

β Angle of rotation at appropriate joint in corrugated-core sandwich construction (see Figure 2.1-5), degrees.

γ Knock-down factor, dimensionless. Ratio $= \sigma_y / \sigma_x$, dimensionless.

γ_b Knock-down factor associated with general instability under pure bending, dimensionless.

γ_c Knock-down factor associated with general instability under axial compression, dimensionless.

γ_d Knock-down factor associated with the general instability of a dome-shaped shell under external pressure, dimensionless.

$(\gamma_i)_{Test}$ Knock-down factor determined from a test specimen subjected to the loading condition corresponding to the subscript i, dimensionless.

γ_p Knock-down factor associated with general instability of a cylinder under uniform external lateral pressure, dimensionless.

γ_s Knock-down factor associated with general instability under pure torsion, dimensionless.

δ Amplitude of initial waviness in facing, inches.

ϵ_x Normal strain in the x direction, in/in.

ϵ_y Normal strain in the y direction, in/in.

ϵ_{xy} Shear strain in the xy plane, in/in.

ζ Parameter involving the core elastic moduli, core thickness, and buckle wavelength, dimensionless.

η Plasticity reduction factor, dimensionless.

η_{Test} Plasticity reduction factor corresponding to an experimental critical stress value, dimensionless.

λ $(1 - \mu_a \mu_b) = (1 - \mu_i^2)$ for isotropic facings, dimensionless. Ratio $= \tau / \sigma_x$, dimensionless.

θ	Ratio of transverse shear moduli of core [see Equation (4.2-1)], dimensionless.
ν	Actual Poisson's ratio of facing, dimensionless.
ν_e	Elastic Poisson's ratio of facing, dimensionless.
ρ	Radius of gyration for shell wall of sandwich and non-sandwich constructions ($\rho \approx h/2$ for sandwich constructions whose two facings are of equal thickness), inches.
σ	Stress, psi.
σ_b	Peak compressive stress due solely to an applied bending moment, psi.
$(\bar{\sigma}_b)_{CL}$	Classical theoretical value for the critical peak compressive stress under a bending moment acting alone, psi.
σ_{CL}	Classical value of critical stress, psi.
σ_c	Uniform compressive stress due solely to an applied axial load, psi.
σ'_c	Effective compressive stress defined by Equation (4.7-38), psi.
$(\sigma_c)_b$	Peak axial compressive stress due solely to an applied bending moment, psi.
$(\sigma_c)_c$	Uniform axial compressive stress due solely to an applied axial load, psi.
$(\bar{\sigma}_c)_{CL}$	Classical theoretical value for the critical uniform compressive stress under an axial load acting alone, psi.
σ_{cr}	Critical stress, psi.
$\sigma_{cr_{test}}$	Experimental critical stress obtained from a particular test specimen, psi.
$\sigma'_{cr_{test}}$	Experimental critical stress which would have been attained had the test specimen remained elastic, psi.

σ_{cr_x}	Critical value for the compressive stress acting in the x direction, psi.
$\sigma_{cr_1}, \sigma_{cr_2}$	Compressive stresses in facings 1 and 2, respectively, in the presence of the critical loading for general instability (there is no preference as to which facing is denoted by the subscript 1 or 2), psi.
σ_{crimp}	Uniaxial compressive stress at which shear crimping occurs in sandwich constructions, psi.
σ_i	Stress intensity defined by Equation (9.2-1), psi.
σ_H	Hoop membrane stress, psi.
σ_M	Meridional membrane stress, psi.
σ_{Max}	Maximum possible critical stress corresponding to a particular material, psi.
σ_{MIN}	Minimum value of stress for the post-buckling equilibrium path, psi.
$\sigma_{predicted}$	Predicted value for critical stress, psi.
σ_p	Critical buckling stress for a flat plate, psi.
σ_R	Critical buckling stress for a complete cylinder, psi.
σ_{wr}	Facing wrinkling stress, psi.
σ_x	Stress acting in the x direction, psi. Uniform axial compressive stress due to an applied axial load, psi.
σ'_x	Effective compressive stress defined by Equation (4.7-37), psi.
$(\sigma_x)_b$	Peak axial compressive stress due solely to an applied bending moment, psi.
$(\bar{\sigma}_x)_{CL}$	Classical theoretical value for critical uniform axial compressive stress when acting alone, psi.
$(\sigma'_x)_c$	Uniform axial compressive stress due solely to an applied axial load, psi.
σ_y	Stress acting in the y direction, psi.

τ	Shear stress, psi.
τ'	Effective shear stress defined by Equation (4.7-39), psi.
$(\bar{\tau})_{CL}$	Classical theoretical value for critical uniform shear stress when acting alone, psi.
τ_{cr}	Critical shear stress, psi.
τ'_{cr}	Critical shear stress for an equivalent cylinder subjected to an applied torque, psi.
τ_{crimp}	Pure shear stress, acting coplanar with the facings, at which shear crimping occurs in sandwich constructions, psi.
τ_T	Uniform shear stress due solely to an applied torque, psi.
τ_V	Peak shear stress due solely to an applied transverse shear force, psi.
Φ	Angular dimension of corrugated core (see Figure 2.1-4), degrees. Quantity defined by Equation (4.2-10), dimensionless.
Ψ	Angle of rotation at appropriate joint in corrugated-core sandwich construction (see Figure 2.1-5), degrees. Parameter defined by Equation (4.4-3), dimensionless.

CONVERSION OF U.S. CUSTOMARY UNITS TO THE INTERNATIONAL SYSTEM OF UNITS[1]

(Reference: MIL-HDBK-23)

Quantity	U.S. Customary Unit	Conversion Factor[2]	SI Unit
Density	$lbm/in.^3$ lbm/ft^3	27.68×10^3 16.02	kilograms/meter^3 (kg/m^3) kilograms/meter^3 (kg/m^3)
Length	ft in.	0.3048 0.0254	meters (m) meters (m)
Stress	psi	6.895×10^3	newtons/meter^2 (N/m^2)
Pressure	$lb/in.^2$ lb/ft^2	6.895×10^3 47.88	newtons/meter^2 (N/m^2) newtons/meter^2 (N/m^2)
Moduli { Elasticity Rigidity	psi	6.895×10^3	newtons/meter^2 (N/m^2)
Temperature	(°F + 460)	5/9	degrees Kelvin (°K)
Thermal conductivity	Btu in./hr ft^2 °F	0.1240	kg cal/hr m °C

Prefixes to indicate multiples of units are as follows:

Prefix	Multiple
giga (G)	10^9
mega (M)	10^6
kilo (k)	10^3
milli (m)	10^{-3}
micro (μ)	10^{-6}

---

[1] The International System of Units [Système International (SI)] was adopted by the Eleventh General Conference on Weights and Measures, Paris, October 1960, in Resolution No. 12.

[2] Multiply value given in U.S. Customary Unit by conversion factor to obtain equivalent value in SI unit.

1

INTRODUCTION

1.1 GENERAL

This handbook presents practical methods for the structural stability analysis of sandwich plates and shells. The configurations and loading conditions covered here are those which are likely to be encountered in aerospace applications. Basic equations, design curves, and comparisons of theory against test data are included.

For the purposes of this handbook, a structural sandwich is defined as a layered construction formed by bonding two thin facings to a comparatively thick core as depicted in Figure 1.1-1. The facings provide practically all of the over-all bending and in-plane extensional rigidity to the sandwich. The core serves to position the faces at locations removed from the neutral axis, provides virtually all of the transverse shear rigidity of the sandwich, and stabilizes the facings against local buckling. Thus the structural sandwich concept is quite similar to that of a conventional I beam. The sandwich core plays a role which is analogous to that of the I beam web while the sandwich facings perform a function very much like that of the I beam flanges. The primary difference between these two types of construction lies in the

---

Numbers in brackets [ ] in the text denote references listed at end of each major section (1; 2; etc.).

fact that the transverse shear deflections are usually significant to the sandwich behavior; whereas, for I beams, these deflections are only important for the special case of relatively short, deep beams.
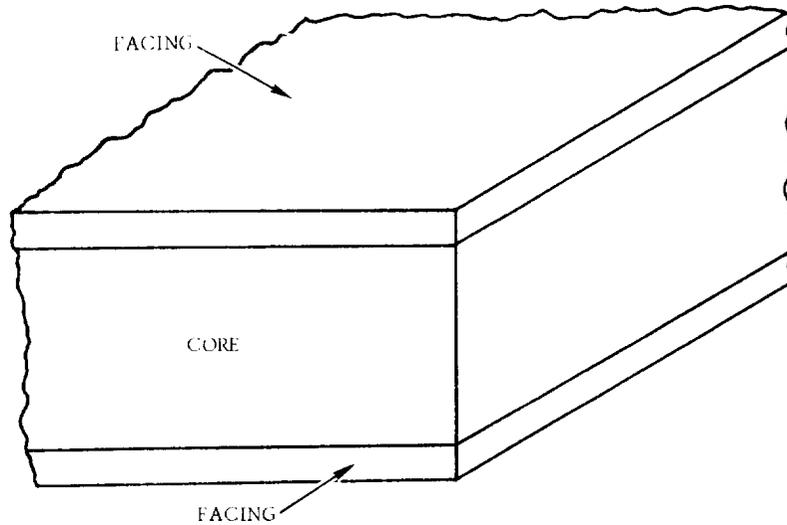
Figure 1.1-1. Typical Sandwich Construction

The sandwich is an attractive structural design concept since, by the proper choice of materials and geometry, constructions having high ratios of stiffness-to-weight can be achieved. Since rigidity is required to prevent structural instability, the sandwich is particularly well suited to applications where the loading conditions are conducive to buckling.

The use of sandwich construction in aerospace vehicles is certainly not a recent innovation. The British de Havilland Mosquito bomber of World War II employed

structural sandwich throughout the airframe. In this case, the sandwich was in the form of birch face sheets bonded to a balsa wood core. Many other airplanes, including the B-58, B-70, F-111, C-5A, etc., have taken advantage of the high strength-to-weight ratio enjoyed by sandwich construction. Space vehicle applications have included the Apollo spacecraft, the Spacecraft LM Adapter (SLA) fairings on the Centaur and other launch vehicles, as well as propellant tank bulkheads.

In view of the ever increasing application of structural sandwich, it has become desirable to assemble a handbook which presents latest design and analysis criteria for the stability of such construction. The practicing designer and stress analyst need this information in a form suitable for easy, rapid use. This document is meant to fulfill that need. However, it should be kept in mind that, in many areas, all practical problems have not yet been fully resolved and one can only employ what might be referred to as a "best-available" approach. In these cases it is advisable to supplement numerical computations with suitable testing. Such areas of uncertainty are identified in this handbook in the sections dealing with the appropriate configurations and loading conditions.

In the sections to follow a discussion is given of the basic principles behind the design equations along with conclusions derived from an analysis of available test data. This is followed by the design equations along with any limitations on their use. Also, to facilitate their use, a table of these equations and restrictions immediately precedes the list of references in Sections 2, 3, 4, and 5 since these sections cover a wide range of loading conditions and considerations.

1.2 FAILURE MODES

Structural instability of a sandwich construction can manifest itself in a number of different modes. The various possibilities are as described below and as shown in Figures 1.2-1 through 1.2-3.

Intracellular Buckling (Face Dimpling) - This is a localized mode of instability which occurs only when the core is not continuous. As depicted in Figure 1.2-1, in the regions directly above core cells (such as those of a honeycomb core), the facings buckle in plate-like fashion with the cell walls acting as edge supports. The progressive growth of these buckles can eventually precipitate the buckling mode identified below as face wrinkling.

Face Wrinkling - This is a localized mode of instability which manifests itself in the form of short wavelengths in the facings, is not confined to individual cells of cellular-type cores, and involves the transverse (normal to facings) straining of the core material. As shown in Figure 1.2-1, one must consider the possible occurrence of wrinkles which may be either symmetrical or antisymmetrical with respect to the middle surface of the original undeformed sandwich. As shown in Figure 1.2-2, final failure from wrinkling will usually result either from crushing of the core, tensile rupture of the core, or tensile rupture of the core-to-facing bond. However, if proper care is exercised in the selection of the adhesive system, one can reasonably assume that the tensile bond strength will exceed both the tensile and compressive strengths of the core proper.

1-4

A - Intracellular Buckling (Face Dimpling)
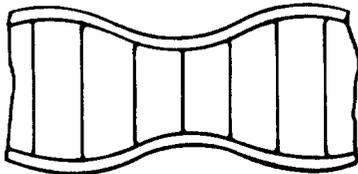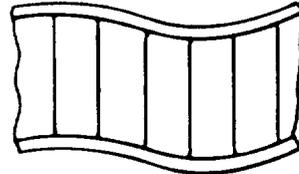
SYMMETRIC   ANTISYMMETRIC

B - Face Wrinkling
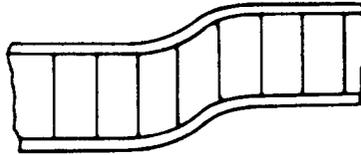
C - Shear Crimping

Figure 1.2-1. Localized Instability Modes

A - Core Crushing

B - Tensile Rupture   C - Tensile Rupture
of Bond   of Core Proper

Figure 1.2-2. Ultimate Failures Precipitated by Face Wrinkling

A – General Instability of Configurations Without Intermediate Stiffening

ORIGINAL LOCATION OF SANDWICH INNER SURFACE

AXIS OF REVOLUTION

B – General Instability of Ring-Stiffened Sandwich Cylinder

ORIGINAL LOCATION OF SANDWICH INNER SURFACE

AXIS OF REVOLUTION
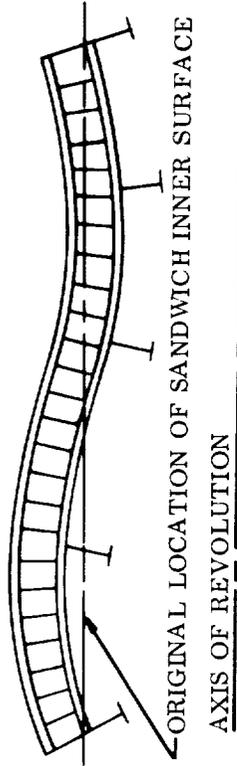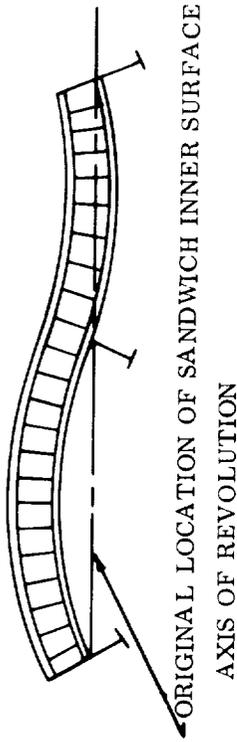
C – Panel Instability of Ring-Stiffened Sandwich Cylinder

Figure 1.2-3. Non-Localized Instability Modes

1-6

Shear Crimping - Shear crimping is often referred to as a local mode of failure but is actually a special form of general instability for which the buckle wavelength is very short due to a low transverse shear modulus for the core. This phenomenon occurs quite suddenly and usually causes the core to fail in shear; however, it may also cause a shear failure in the core-to-facing bond. Crimping will sometimes occur in cases where relatively long-wave general instability first develops. In such instances the crimp appears because of severe local transverse shear stresses at the ends of buckle patterns. As the crimp develops, the general buckle may disappear and a post-test examination would then lead to an erroneous conclusion as to the mechanism which initiated failure.

General Instability - For configurations having no supplementary stiffening (such as rings) except at the boundaries, the general instability mode is depicted in Figure 1.2-3A. The phenomenon involves over-all bending of the composite wall coupled with transverse (normal to facings) shear deformations. Usually, transverse extensional strains do not play a significant role in this behavior. Whereas intracellular buckling and wrinkling are localized phenomena, general instability is of a more gross nature. Except for the special case cited under the identification "Shear Crimping", the wavelengths associated with general instability are normally considerably larger than those encountered in intracellular buckling and face wrinkling.

For configurations having supplementary stiffening at locations other than the boundaries, the term general instability takes on new significance and reference is also made to an additional mode identified as panel instability. For this case, general

1-7

instability is as defined above but with the added provision that the buckle pattern involves simultaneous radial displacement of both the sandwich wall and the intermediate stiffeners. As shown in Figure 1.2-3B, the appropriate half-wavelength of the buckle pattern must therefore exceed the spacing between intermediate stiffeners. The example used in Figure 1.2-3B is that of a sandwich cylinder stiffened by a series of rings which have insufficient stiffness to enforce nodal points at their respective locations.

Panel Instability - This mode of instability applies only to configurations which have supplementary stiffening at locations other than the boundaries. Figure 1.2-3C depicts this mode by again using the example of a sandwich cylinder stiffened by a series of rings. However, in this case the rings have sufficient stiffness to enforce nodal points at their respective locations. The rings experience no radial deformation. Therefore, the half-wavelength of the buckle pattern cannot exceed the spacing between rings. As in the case of general instability, this mode involves over-all bending of the composite wall coupled with transverse shear deformations. Here again, transverse extensional strains do not play a significant role in the behavior.

2

LOCAL INSTABILITY

2.1 INTRACELLULAR BUCKLING (Face Dimpling)

2.1.1 Sandwich with Honeycomb Core

2.1.1.1 Basic Principles

From a practical viewpoint, intracellular buckling can be regarded as flat-plate behavior. Even where curvature is present, as in the cases of cylinders and spheres, the honeycomb core cell size will normally be sufficiently small to justify such an assumption. As noted from Reference 2-1, the critical stress for flat plates can be expressed in the form

$$\sigma_{cr} = \frac{k\pi^2 \eta E_f}{12(1-\nu_e^2)} \left(\frac{t_f}{s}\right)^2 \qquad (2.1\text{-}1)$$

where

σ_{cr} = Critical compressive stress, psi.

k = Coefficient which depends on the plate geometry, boundary conditions, and type of loading, dimensionless.

η = Plasticity reduction factor, dimensionless.

E_f = Young's modulus (for facing material in the case of intracellular buckling), psi.

ν_e = Elastic Poisson's ratio (for facing material in the case of intracellular buckling), dimensionless.

2-1

t_f = Thickness of plate (Facing thickness in the case of intra-
        cellular buckling), inches.

s   = A selected characteristic dimension of the plate, inches.

It is convenient here to combine several of the constants in Equation (2.1-1) to obtain

$$\sigma_{cr} = K \frac{\eta E_f}{(1-\nu_e^2)} \left(\frac{t_f}{s}\right)^2 \qquad (2.1-2)$$

or

$$\left[\frac{\sigma_{cr}(1-\nu_e^2)}{\eta E_f}\right] = K\left(\frac{t_f}{s}\right)^2 \qquad (2.1-3)$$

To apply these equations to the case of intracellular buckling, it is only necessary to

define the dimension s and establish a corresponding value for K. In Reference

2-2, Norris took s to be equal to the honeycomb core cell size. By convention,

this is taken equal to the diameter of the largest circle that can be inscribed within

the cell. Based on the analysis of test data, Norris then chose K = 2.0 for the

case of uniaxial compression. This provides a reasonably good fit to the test results

as shown in Figure 2.1-1 which was taken directly from Reference 2-2. It should be

noted that the choice of K = 2.0 does not provide a lower bound to the data. Six of

the test results fall significantly below the values predicted by the recommended

formula. This situation can be tolerated since the dimpling of several cells in a

honeycomb sandwich construction will not lead to catastrophic failure so long as a

sufficiently large number of cells remain unbuckled. As indicated by the scatter in

Figure 2.1-1, one could reasonably expect the majority of unbuckled cells to possess

considerably greater buckling strengths than would be indicated by the proposed

design curve. Under these conditions, some redistribution of stress would occur
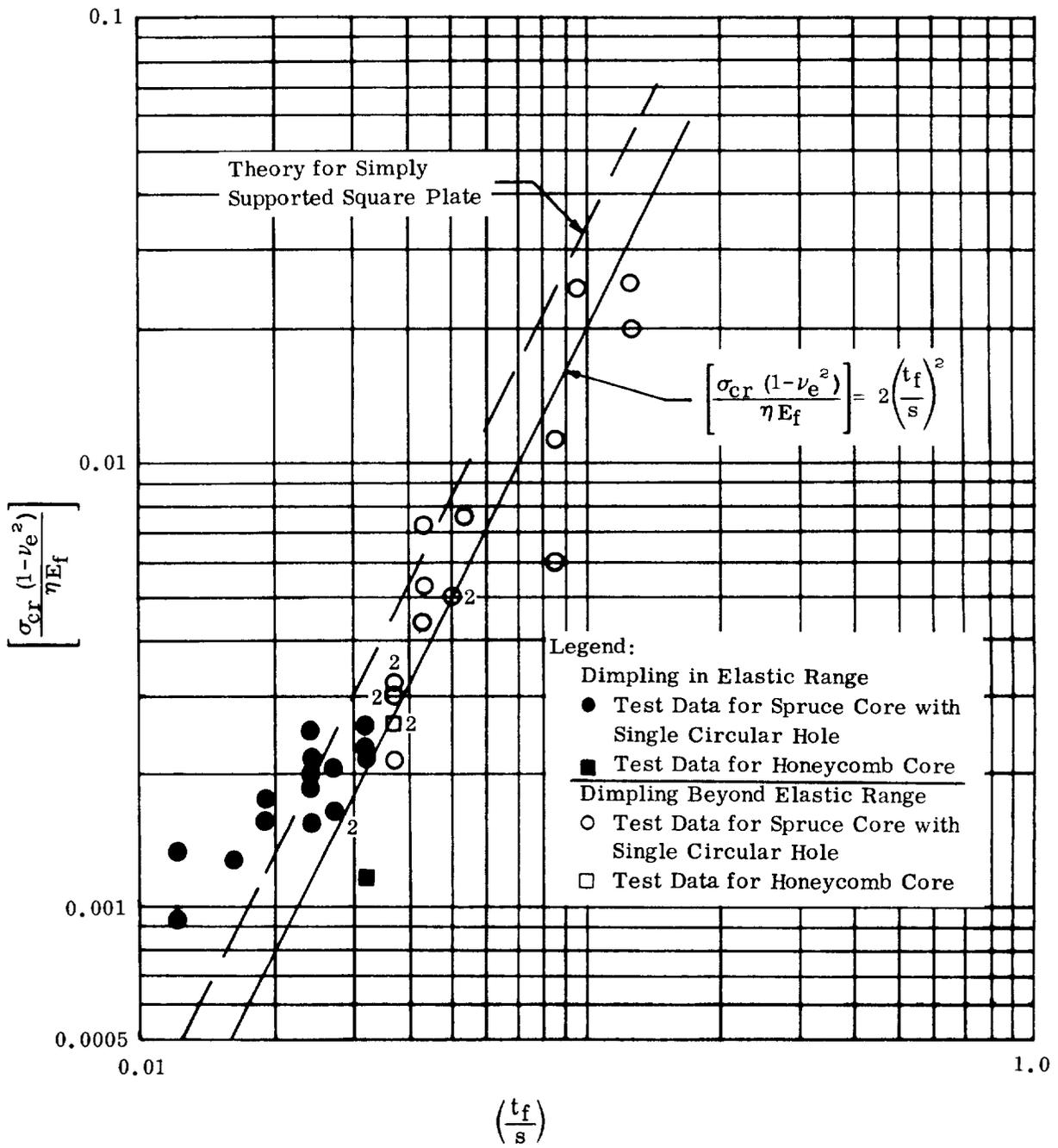
Figure 2.1-1. Critical Stresses for Intracellular Buckling Under Uniaxial Compression

but the structure could continue to support the applied load. In addition, it is pointed out that the dimpled regions retain significant post-buckling load-carrying capability since they behave essentially as flat plates. This does not mean, however, that one can permit the dimples to grow without bound. The point can be reached where these deformations precipitate wrinkling and this cannot be tolerated.

It is also of importance to note here that most of the test data shown in Figure 2.1-1 were obtained from sandwich plates having a solid spruce core through which a single circular hole was drilled to represent a core cell. It is questionable that such specimens truly simulate the cell edge support likely to be encountered in practical honeycomb configurations. Only three data points were obtained for specimens actually having honeycomb cores and, as shown in Figure 2.1-1, these points lie in the lower region of the total band of scatter.

In view of the foregoing discussion, it is evident that the use of Equation 2.1-3 together with the selection of K = 2.0 is certainly not a rigorous approach to the analysis of intracellular buckling. However, until further work is accomplished in this area, it is recommended that this criterion be employed as a "best-available", approximate design tool.

2.1.1.2 Design Equations and Curves

The facing stress at which intracellular buckling will occur under uniaxial compression is given by the following semi-empirical formula:

$$\sigma_{cr} = 2.0 \frac{\eta E_f}{(1-\nu_e^2)} \left(\frac{t_f}{s}\right)^2 \qquad (2.1-4)$$

The dimension s is the diameter of the largest circle that can be inscribed within the cell shape. For example, in the cases of hexagonal and square cells, s is measured as shown below.

Figure 2.1-2. Definition of Dimension s

Solving Equation (2.1-4) for s gives the result

$$s = t_f \sqrt{2} \left[\frac{\sigma_{cr}(1-\nu_e^2)}{\eta E_f}\right]^{-\frac{1}{2}} \qquad (2.1-5)$$

This equation may be used to determine the maximum permissible cell size corresponding to particular facing materials and thicknesses. Figure 2.1-3 presents a family of plots of Equation (2.1-5) for selected values of t_f ranging from $t_f = 0.001$ to $t_f = 0.100$.

For elastic cases, use $\eta = 1$. Whenever the behavior is inelastic, the methods of Section 9 must be employed.
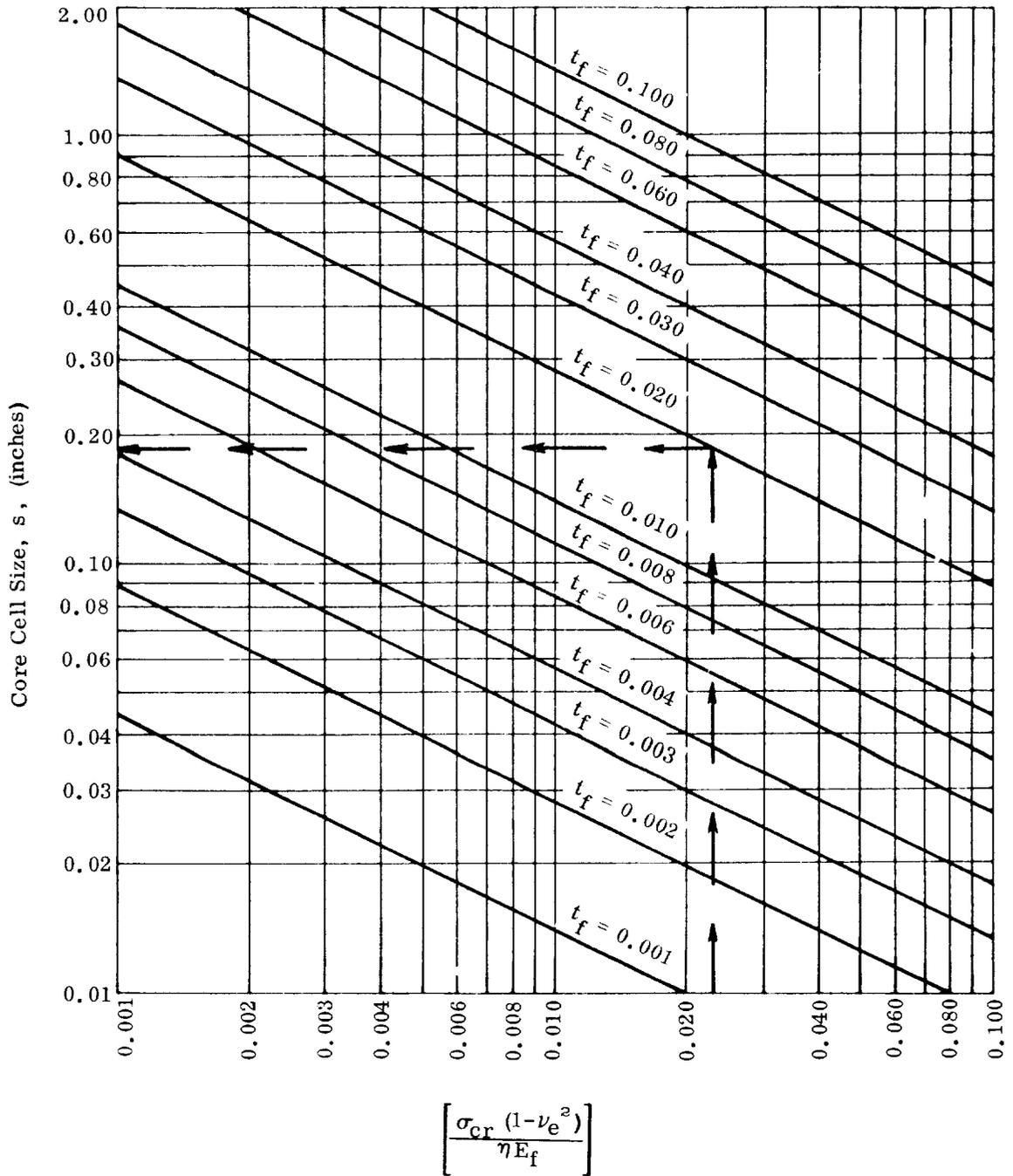
Figure 2.1-3. Chart for Determination of Core Cell Size Such That
Intracellular Buckling Will Not Occur

When the facings are subjected to biaxial compression, it is recommended that one

use the interaction formula

$$R_x + R_y = 1 \qquad (2.1-6)$$

where

$$R_i = \frac{\left[\begin{array}{c}\text{Applied Compressive Loading} \\ \text{in Subscript Direction}\end{array}\right]}{\left[\begin{array}{c}\text{Critical Compressive Loading (when} \\ \text{acting alone) in Subscript Direction}\end{array}\right]} \qquad (2.1-7)$$

This straight-line interaction relationship is based on the information provided in

Reference 2-1 for square flat plates. For cases involving shearing stresses which

are coplanar with the facings, it is recommended that the principal stresses first be

computed and that these values then be used in the above interaction equation. When-

ever one of the principal stresses is tensile and the behavior is elastic, the analysis

should be based on the assumption that the compressive principal stress is acting

alone.

2.1.2 Sandwich With Corrugated Core

2.1.2.1 Basic Principles

This section deals with corrugated-core sandwich constructions whose cross sections

may be idealized as shown in Figure 2.1-4. For cylinders, the only case treated

here is that where the axis of the corrugations is parallel to the axis of revolution.

For flat plates, however, the corrugations can be oriented in either the longitudinal

or transverse directions.

Single-Truss   Double-Truss
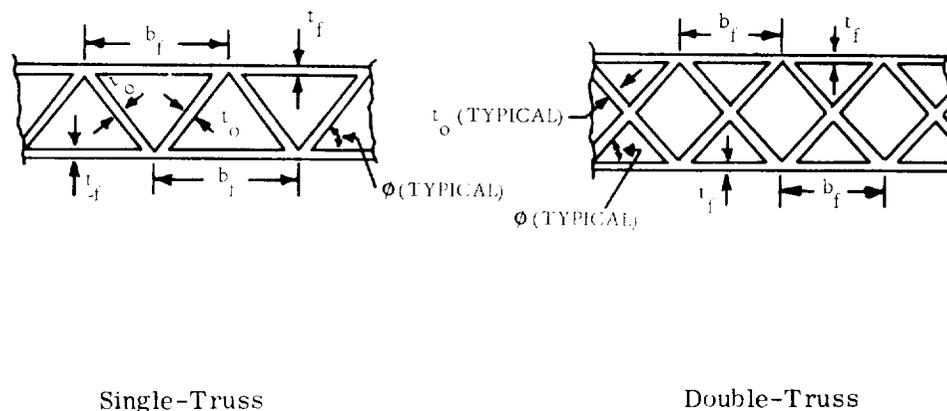
Figure 2.1-4. Corrugation Configurations

Each of the following loading conditions is considered:

a. Uniaxial compression acting parallel to the axis of the corrugations.

b. Uniaxial compression acting parallel to the facings but normal to the axis of the corrugations.

c. Biaxial compression resulting from combinations of a and b above.

The design curves presented here are taken directly from Reference 2-3 and are

based entirely on theoretical considerations. No comparisons are made against test

data to confirm the validity of these solutions. Until such substantiation is obtained, the recommended design curves can only be considered as a "best-available" criterion. It is pointed out, however, that there does not appear to be any reason to suspect that test data would disagree with the curves.

Although Reference 2-3 is devoted solely to flat plates, the results are considered to be applicable to the cylindrical configurations shown in Figure 2.1-4 since the dimensions b_f will usually be small with respect to the radius. Under such conditions, curvature influences will be negligible.

The theoretical development includes consideration of each of the buckling modes shown in Figure 2.1-5. Both of the following possibilities are covered:

    a.   The face sheets are the unstable elements and are restrained by the core.

    b.   The core is the unstable element and is restrained by the face sheets.

Buckling is assumed to be accompanied by rotation of the joints but with no deflection of the joints. The angles between the various elements at any one joint are taken to remain unchanged during buckling. It is also assumed that the over-all sandwich dimensions are sufficiently large such that end effects are negligible.
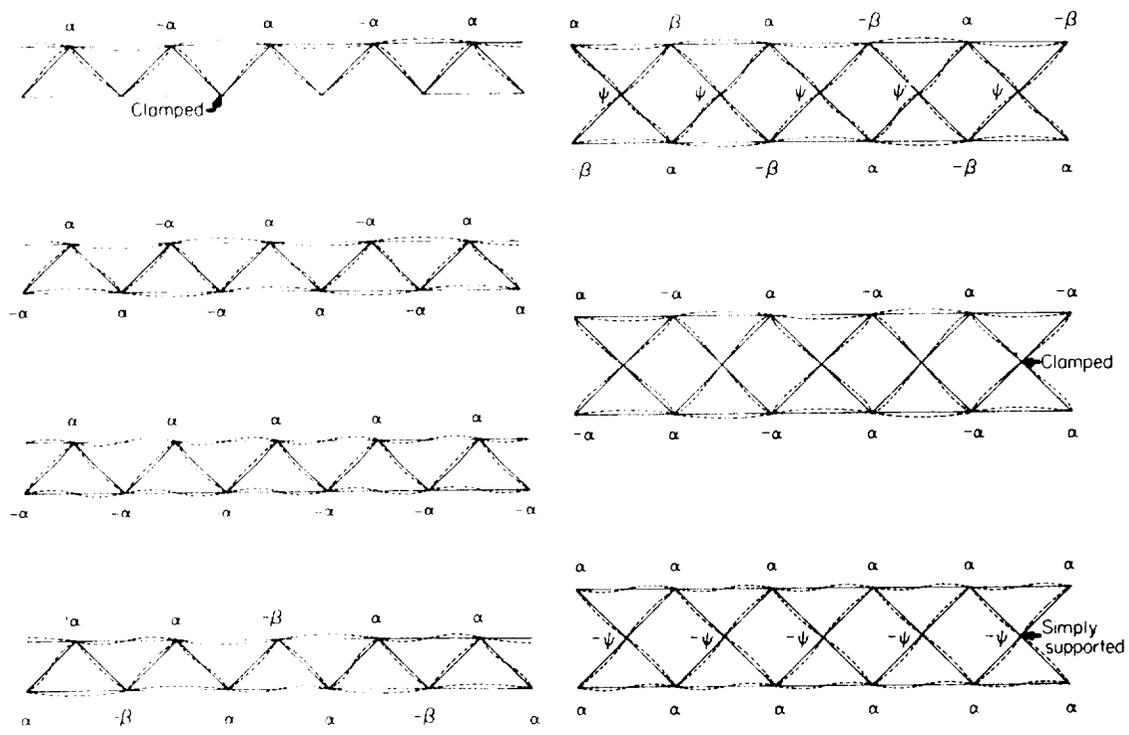
Single-Truss-Core   Double-Truss-Core

(α, β, and ψ denote angles of rotations at the appropriate joints)

Figure 2.1-5. Buckling Modes

2.1.2.2 Design Equations and Curves

The theoretical stress at which intracellular buckling of the facings or buckling of the

corrugated core will occur is given by the following formula:

$$\sigma_{cr} = \frac{k_i \pi^2 \eta E}{12(1-\nu_e^2)} \left(\frac{t_f}{b_f}\right)^2 \tag{2.1-8}$$

where

σ_{cr} = Critical compressive stress, psi.

k_i = Coefficient which depends upon the geometry and loading conditions, dimensionless.

η = Plasticity reduction factor, dimensionless.

E = Young's modulus of facings and core, psi.

ν_e = Elastic Poisson's ratio of facings and core, psi.

t_f = Facing thickness, inches.

b_f = Pitch of corrugated core (see Figure 2.1-4), inches.

The only case considered here is that where the two facings are of the same thickness

and the entire sandwich construction (facings and core) is made of a single material.

Figures 2.1-6 through 2.1-12 give values for k_i for each of the following loading

combinations:

a. k_x when $k_y' = 0$

b. k_x when $k_y' = 0.5$

c. k_x when $k_y' = 1.0$

d. k_y when $k_x' = 0$

The coefficients k_x' and k_y' are defined as follows:

$$k_x' = \frac{12(1-\nu_e^2)}{\pi^2 \eta E} \left(\frac{b_f}{t_f}\right)^2 \quad \text{(Applied Compressive } \sigma_x) \qquad (2.1-9)$$

$$k_y' = \frac{12(1-\nu_e^2)}{\pi^2 \eta E} \left(\frac{b_f}{t_f}\right)^2 \quad \text{(Applied Compressive } \sigma_y) \qquad (2.1-10)$$

The subscript x (for k and k') is used to identify cases where the loading is directed along the axis of the corrugations (x direction). The subscript y (for k and k') is used to identify cases where the loading is acting in the y direction which is parallel to the facings but normal to the axis of the corrugations. For combinations a through c, separate plots are furnished for single-truss-core and double-truss-core configurations. For combination d, a single family of curves covers both arrangements since all of the corresponding applied load is transferred through the facings. The dashed lines in Figures 2.1-6 through 2.1-11 divide the charts into two regions. Above the dashed lines, the face sheets are the unstable elements and are restrained by the core. Below the dashed lines, the core is unstable and is restrained by the face sheets.

To clarify the design charts given in Figures 2.1-6 through 2.1-12, the following additional definitions are provided:

t_o = Thickness of material from which the corrugations are formed (see Figure 2.1-4), inches.

ϕ = Angle shown in Figure 2.1-4, degrees.

In addition, the sample problem given below should be helpful to the user of this handbook.

2-12

Given: Sample Problem Data for Single-Truss Core Type Sandwich Panel

$E = 30 \times 10^6$ psi $\qquad t_o = .016''$ $\qquad b_f = .700''$

$\nu_e = .30$ $\qquad t_f = .020''$ $\qquad \phi = 65°$

Proportional Limit $\sigma = 90,000$ psi $\qquad \sigma_y = 16,300$ psi (Compression)

Required: Find σ_{cr_x} ; Assuming $\eta = 1$, one obtains

$$k_y' = \frac{12\sigma_y(1 - \nu_e^2)}{\pi^2 \eta E}\left(\frac{b_f}{t_f}\right)^2 = \frac{12 \times 16,300 \times .910}{9.87 \times 1 \times 30 \times 10^6}\left(\frac{.700}{.020}\right)^2 = 0.736$$

$$\frac{t_o}{t_f} = \frac{.016}{.020} = .800$$

Using linear interpolation between values given on Figures 2.1-7 and 2.1-8 one obtains $k_x = 2.68$.

Hence, the critical stress in the x direction (parallel to the corrugation axis) is

$$\sigma_{cr_x} = \frac{k_x \pi^2 \eta E}{12(1 - \nu_e^2)}\left(\frac{t_f}{b_f}\right)^2$$

and, assuming $\eta = 1$, one obtains

$$\sigma_{cr_x} = \frac{2.68 \times 9.87 \times 1 \times 30 \times 10^6}{12 \times .910}\left(\frac{.020}{.700}\right)^2 = 59,300 \text{ psi (Compression)}$$

The stress intensity σ_i (See Section 9) can now be computed as follows:

$$\sigma_i = \sqrt{\sigma_x^2 + \sigma_y^2 - \sigma_x\sigma_y + 3\tau^2}$$

$$= 10^3 \sqrt{(59.3)^2 + (16.3)^2 - (59.3 \times 16.3) + 0} = 53,100 \text{ psi}$$

Since this value is below the proportional limit, the assumption $\eta = 1$ is valid.

In cases where the σ_i value exceeds the proportional limit, the methods of Section 9 must be employed.

2-13
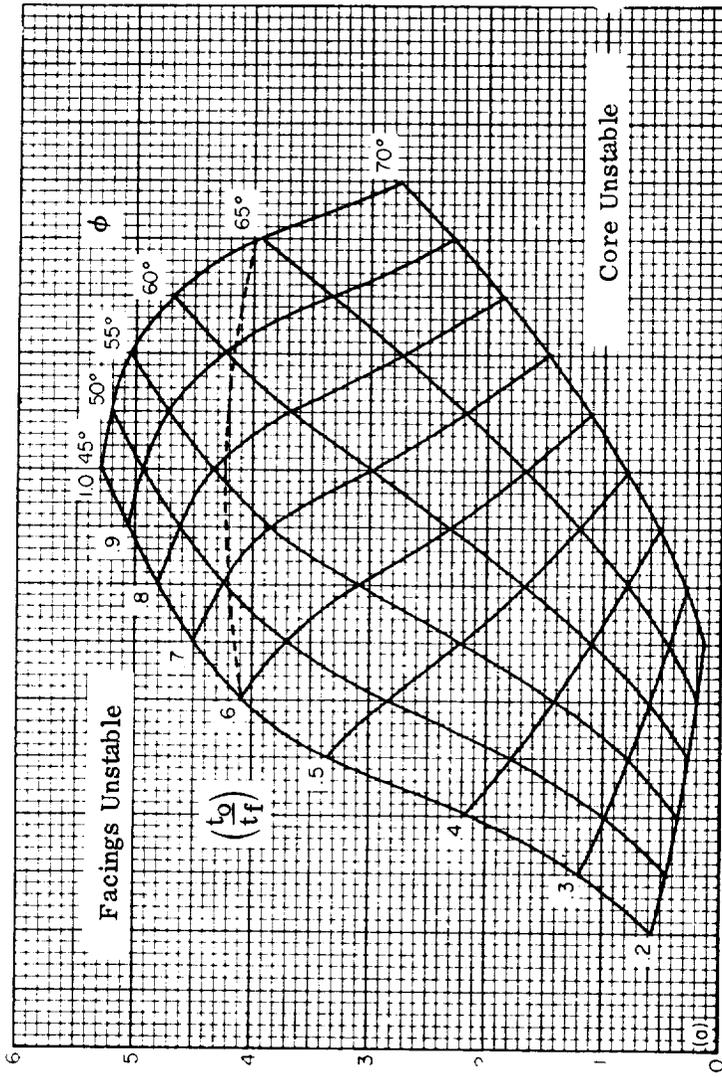
Figure 2.1-6. Local Buckling Coefficient for Single-Truss-Core Sandwich

$k_y' = 0$
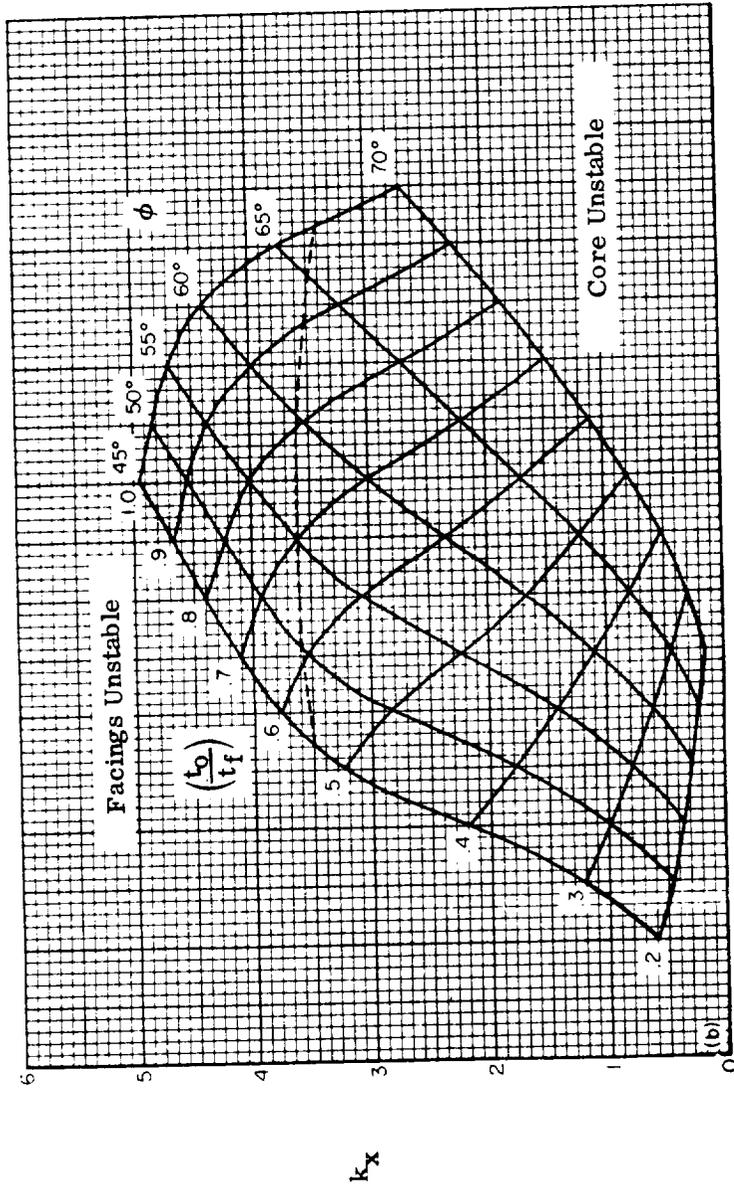
Figure 2.1-7. Local Buckling Coefficient for Single-Truss-Core Sandwich
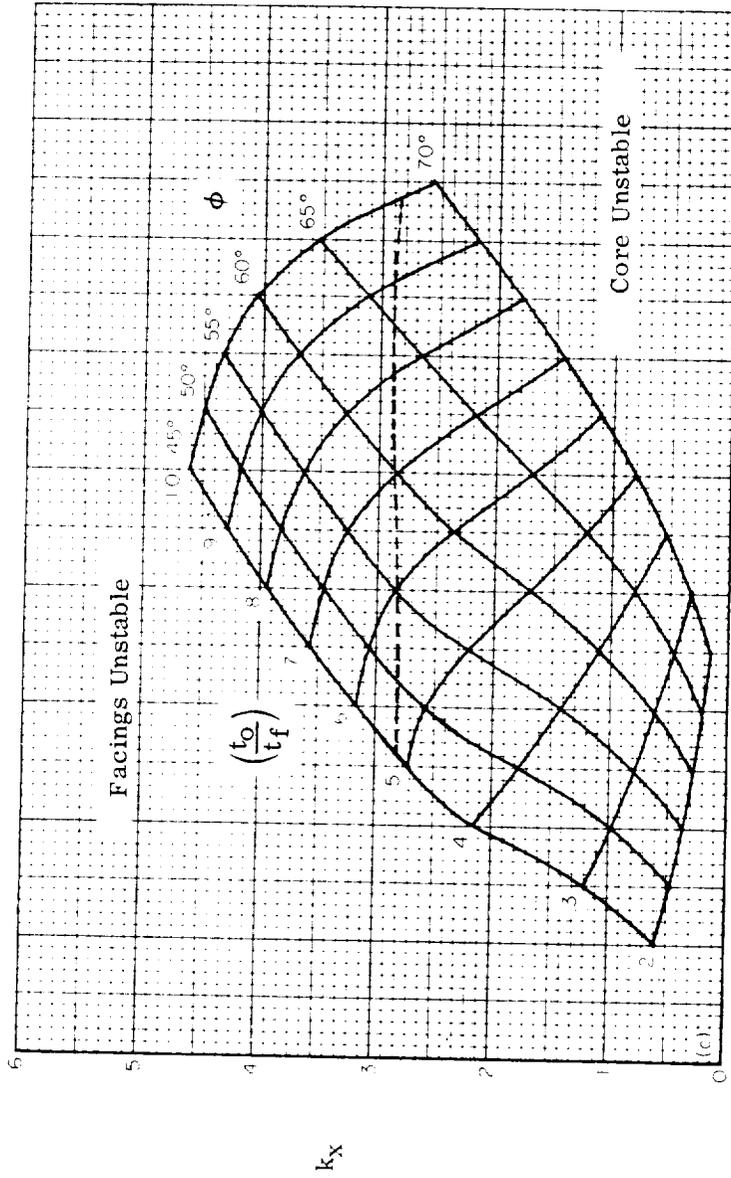
$k_y' = 0.5$

Figure 2.1-8. Local Buckling Coefficient for Single-Truss-Core Sandwich
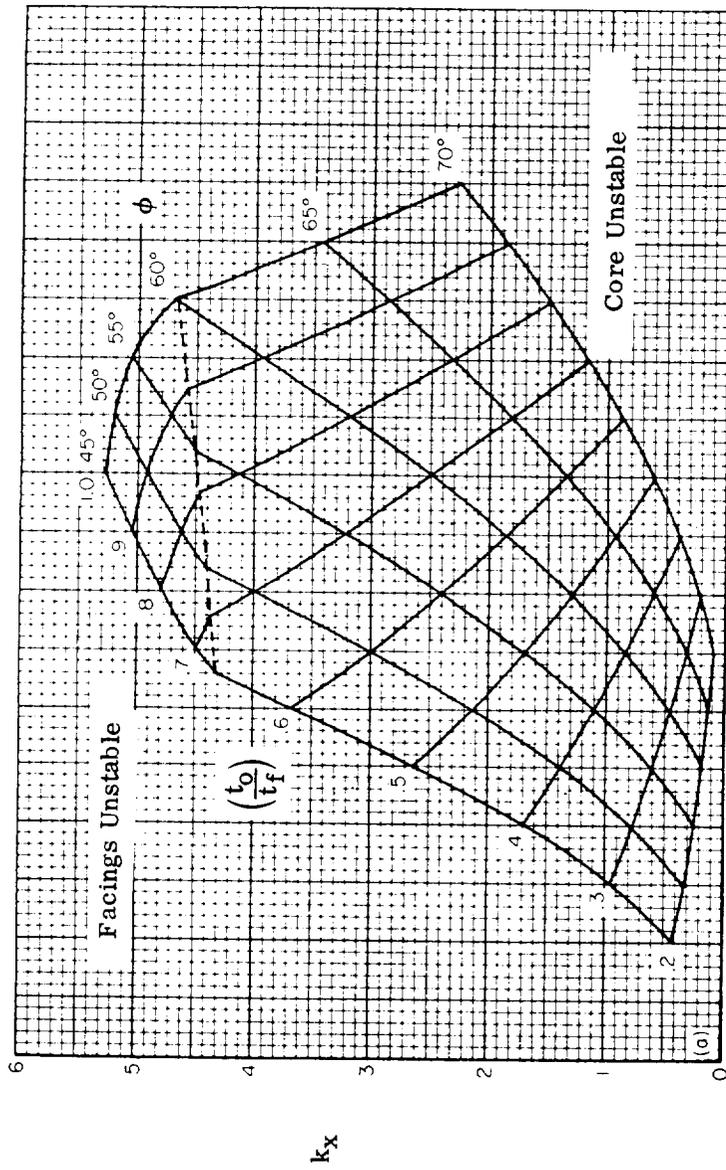
$k_y' = 1.0$

Figure 2.1-9. Local Buckling Coefficient for Double-Truss-Core Sandwich

$k_y' = 0$
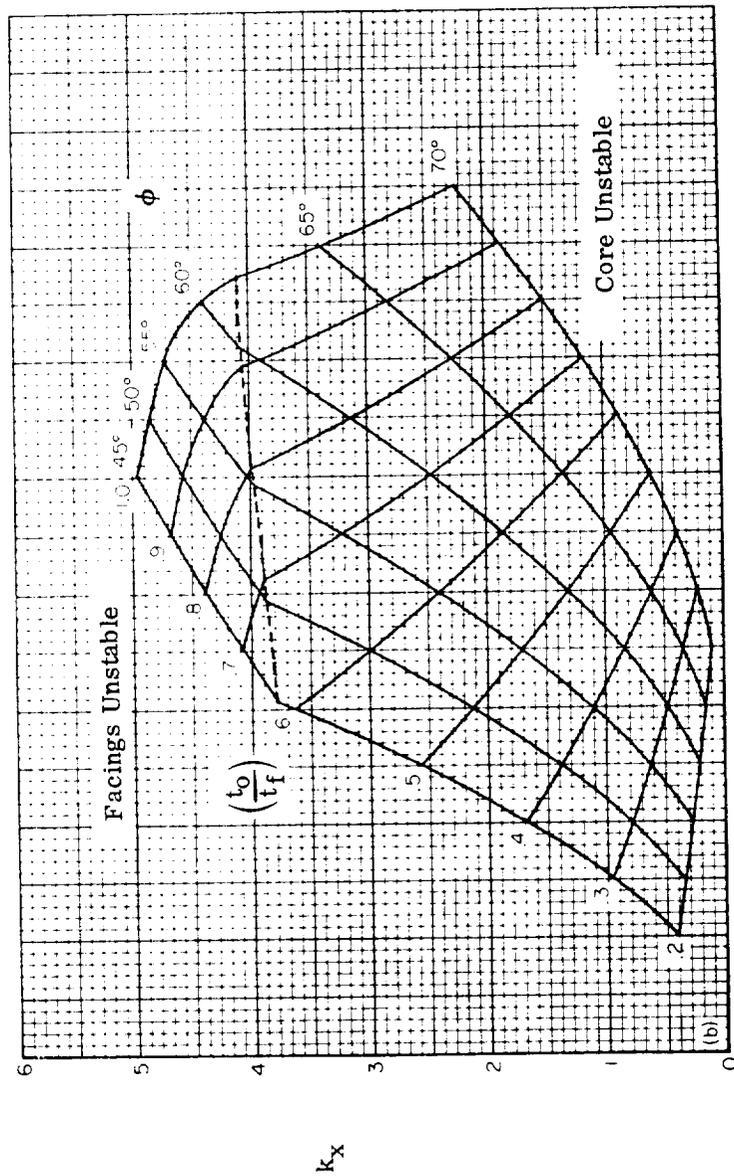
Figure 2.1-10. Local Buckling Coefficient for Double-Truss-Core Sandwich

$k_y' = 0.5$
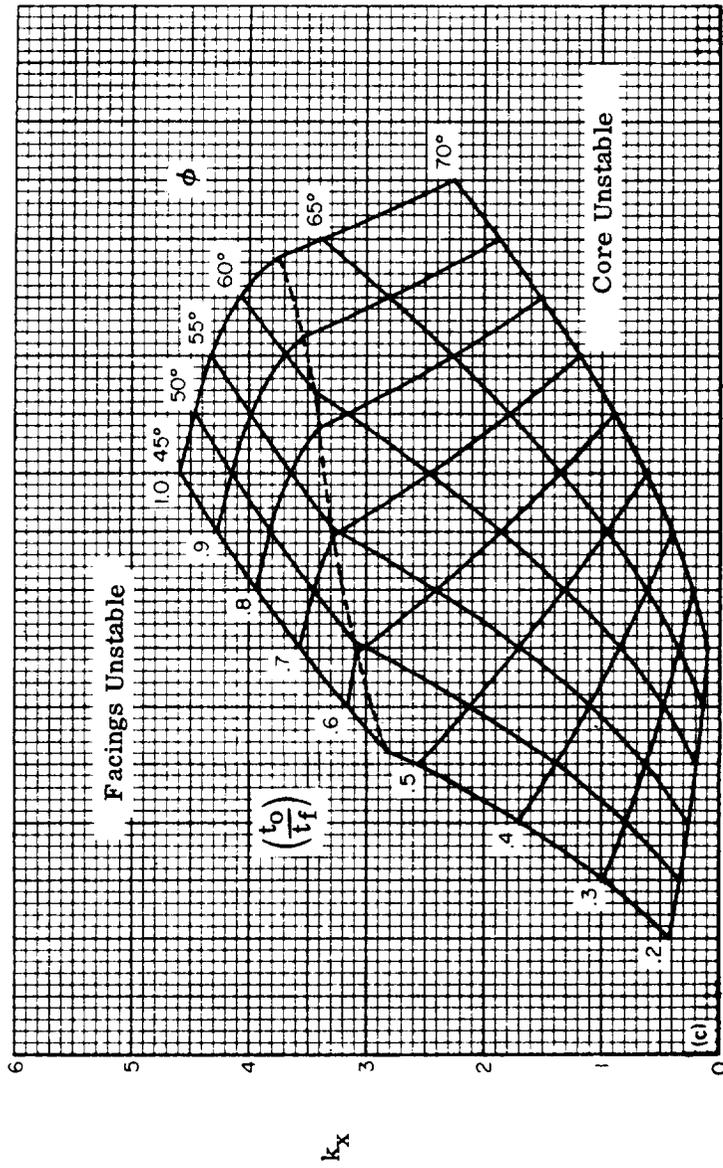
Figure 2.1-11. Local Buckling Coefficient for Double-Truss-Core Sandwich
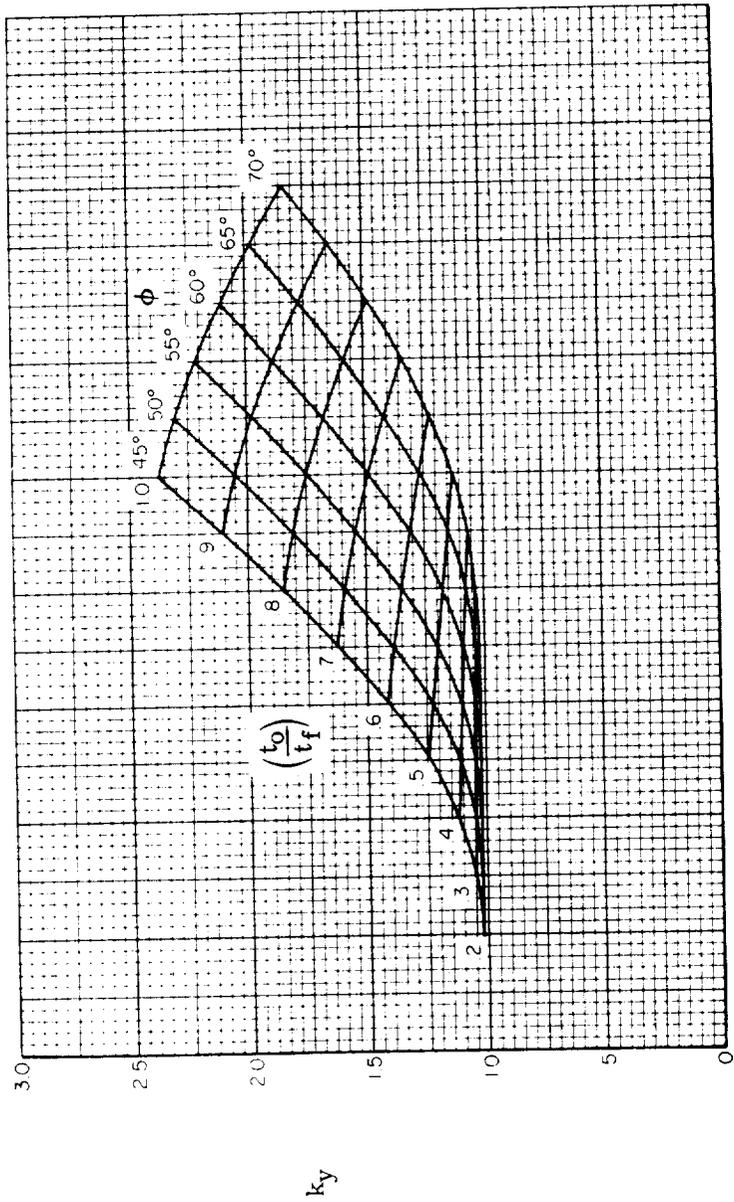
Figure 2.1-12. Local Buckling Coefficient for Truss-Core Sandwich

$k'_x = 0$

2.2 FACE WRINKLING

2.2.1 Sandwich With Solid or Foam Core (Antisymmetric Wrinkling)

2.2.1.1 Basic Principles

The problem of face wrinkling has been treated by many investigators dating back as far as 1940. The most important publications on this subject are listed as References 2-4 through 2-14. For the purposes of this handbook, it was decided that the results in References 2-7 and 2-9 would be the most useful. The latter applies only to sandwich configurations which have solid or foam cores. The development there includes consideration of both the symmetric and antisymmetric modes along with the influences from initial waviness of the facings. It is pointed out that, when the core is sufficiently thick, the wrinkle patterns of the two facings will be independent of each other and the same critical load is obtained for the symmetric and antisymmetric modes. However, for sandwiches having thinner cores, the core strains introduced by one facing influence the wave pattern in the other facing. Under these conditions, it was found that sandwiches having solid or foam cores can be expected to wrinkle antisymmetrically. The following governing equation was derived to predict this form of wrinkling for isotropic facings subjected to uniaxial compression:

$$\sigma_{wr} = Q \left[\frac{\eta E_f E_c G_c}{(1-\nu_e^2)} \right]^{\frac{1}{3}} \qquad (2.2-1)$$

where,

σ_{wr} = Facing wrinkling stress, psi.

η = Plasticity reduction factor, dimensionless.

E_f = Young's modulus of facing, psi.

E_c = Young's modulus of the core in the direction normal to the facings, psi.

G_c = Core shear modulus associated with the plane perpendicular to the facings and parallel to the direction of the applied load, psi.

ν_e = Elastic Poisson's ratio of facings, dimensionless.

The quantity Q is the relative minimum, with respect to ζ, of the expression

$$\frac{\dfrac{\zeta^2}{30\,q^2} + \dfrac{16\,q}{\zeta}\left(\dfrac{\cosh\,\zeta - 1}{11\,\sinh\,\zeta + 5}\right)}{1 + 6.4\,K_\delta\zeta\left(\dfrac{\cosh\,\zeta - 1}{11\,\sinh\,\zeta + 5}\right)} \qquad (2.2\text{-}2)$$

where

$$q = \frac{t_c}{t_f}\,G_c\left[\frac{(1-\nu_e^2)}{\eta E_f\,E_c\,G_c}\right]^{\frac{1}{3}} \qquad (2.2\text{-}3)$$

$$K_\delta = \frac{\delta E_c}{t_c\,F_c} \qquad (2.2\text{-}4)$$

and

ζ = Parameter involving the core elastic moduli, core thickness, and buckle wavelength, dimensionless.

t_c = Thickness of core, inches.

t_f = Thickness of facing, inches.

δ = Amplitude of initial waviness in facing, inches.

F_c = Flatwise sandwich strength (the lower of flatwise core compressive, flatwise core tensile, and flatwise core-to-facing bond strengths), psi.

The initial waviness plays an important role in the wrinkling phenomenon since it causes transverse facing deflections to develop even when the applied loading is very small. As the load increases, these deflections grow at steadily increasing rates and lead to transverse tensile or compressive failure of the core or tensile rupture of the

core-to-facing bond. These failures occur, of course, at load values below the predictions from classical theory in which it is assumed that the facings are initially perfect ($K_\delta = 0$).

The results from Reference 2-9 can be summarized in the form of Equation (2.2-1) accompanied by plots of Q vs q with K_δ as a parameter. A family of such curves is given in Reference 2-9 and they are of the general shape shown in Figure 2.2-1. The limiting values established by the straight line 0A correspond to the shear crimping mode of failure (see Section 2.3). All other points on the curves are for antisymmetric wrinkling. In actual practice, curves of this type do not prove to be very helpful since the K_δ values appropriate to particular structures are rarely known. Therefore, in order to provide a practical means for the prediction of face wrinkling in sandwich constructions having solid or foam cores, it has become common practice to select a single conservative lower-bound Q based on available test data. This approach is followed here. Elastic test data selected from Reference 2-9 are plotted in Figure 2.2-2 from which the value Q = 0.50 has been selected as a safe design value. Additional data are given in Reference 2-6 which are not shown here but lead to the same value for a lower-bound Q. This is in conformance with the observation made by Plantema in Reference 2-15 that the value Q = 0.50 has often been recommended for practical design purposes. However, since much of the existing test data were obtained from specimens that were not very representative of configurations likely to be encountered in realistic structures, the selection of Q = 0.50 can only be regarded as a "best-available" approach. In view of the uncertainties
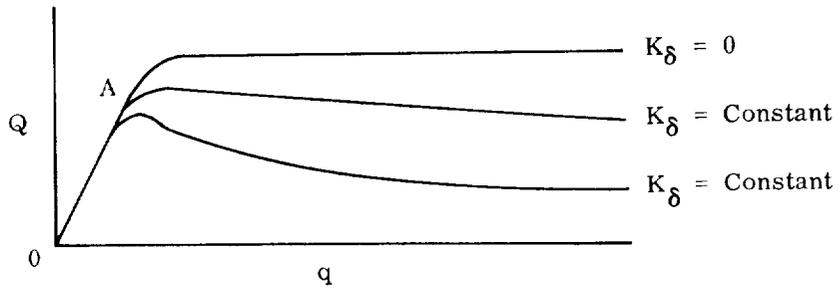
Figure 2.2-1. Typical Variation of Q vs. q

involved, it is recommended that for the verification of final designs, wrinkling tests be performed on specimens which are truly representative of the actual configuration. The method presented here for the prediction of wrinkling should only be regarded as an approximate guideline.
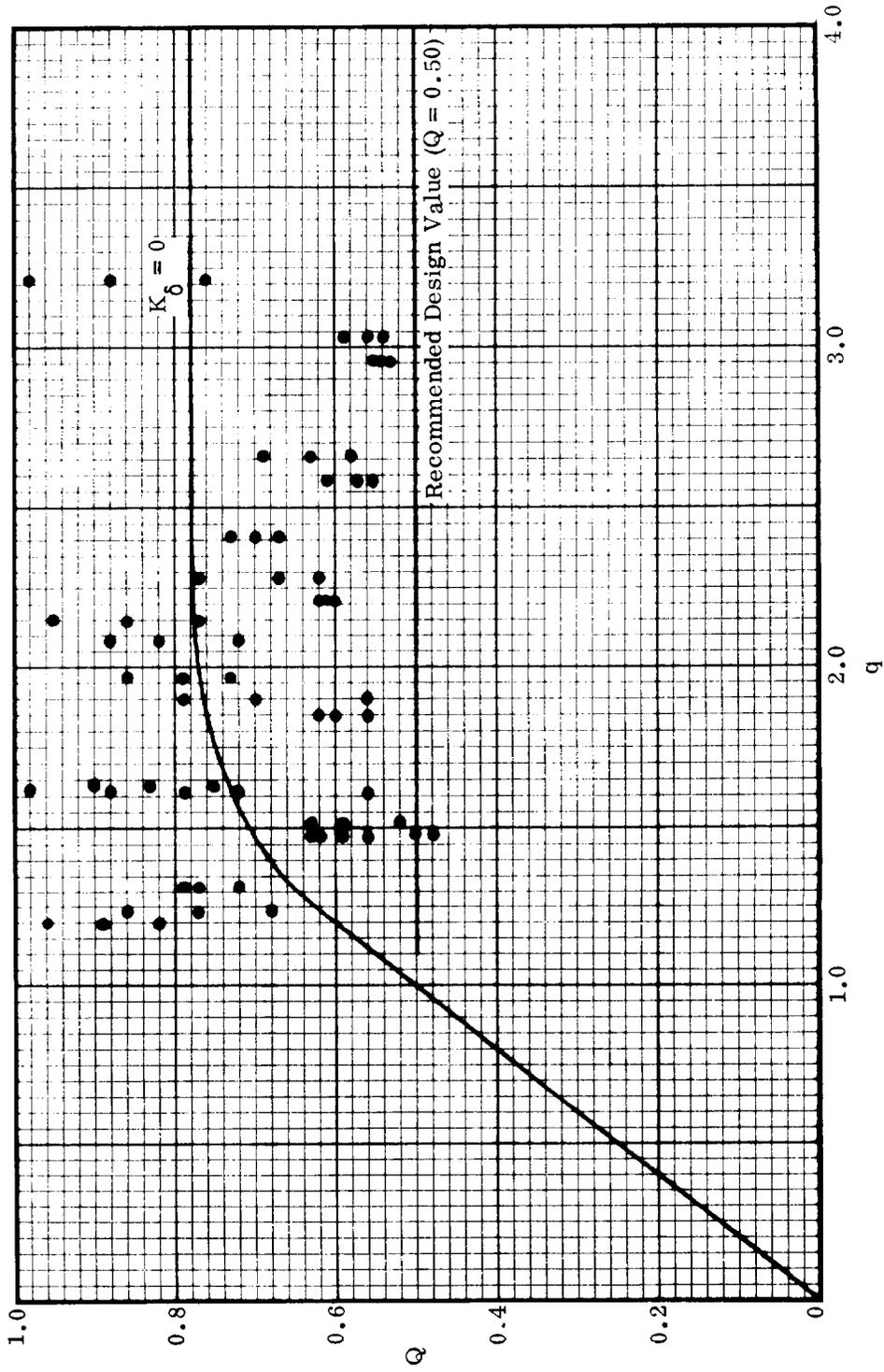
Figure 2.2-2. Comparison of Theory vs Test Results for Face Wrinkling in Sandwich Constructions Having Solid or Foam Cores

2.2.1.2 Design Equations and Curves

The following equation may be used to compute the approximate uniaxial compressive stress at which face wrinkling will occur in sandwich constructions having solid or foam cores:

$$\sigma_{wr} = Q \left[\frac{\eta E_f \, E_c \, G_c}{(1-\nu_e^2)} \right]^{\frac{1}{3}}$$ (2.2-5)

In cases where the amplitude of initial waviness is known, one can use the curves of Figure 2.2-3 to establish Q. Whenever such information is unavailable, it is recommended that the value $Q = 0.50$ be used to obtain a lower-bound prediction.

For elastic cases, use $\eta = 1$. Whenever the behavior is inelastic, the methods of Section 9 must be employed.

When the facings are subjected to biaxial compression, it is recommended that one use the interaction formula

$$R_x^3 + R_y = 1$$ (2.2-6)

where

$$R_i = \frac{\left[\text{Applied Compressive Loading in Subscript Direction}\right]}{\left[\begin{array}{c}\text{Critical Compressive Loading (when acting alone) in}\\ \text{Subscript Direction}\end{array}\right]}$$ (2.2-7)

and the y direction corresponds to the direction of maximum compression. This interaction relationship is based on the information provided in Reference 2-1 for rectangular flat plates having very large aspect ratios. For cases involving shearing stresses which are coplanar with the facings, it is recommended that the principal stresses first be computed and that these values then be used in the above interaction equation. Whenever one of the principal stresses is tensile and the behavior is elastic, the analysis should be based on the assumption that the compressive principal stress is acting alone.

2-26

Figure 2.2-3. Parameters for Determination of Face Wrinkling in Sandwich Constructions Having Solid or Foam Cores

2-27

2.2.2 Sandwich With Honeycomb Core (Symmetric Wrinkling)

2.2.2.1 Basic Principles

As noted in Section 2.2.1.1, the results of Reference 2-9 apply only to sandwich configurations which have solid or foam cores. However, the basic theory of that report is capable of extension to constructions having honeycomb cores and this is accomplished in Reference 2-7. The extension is achieved by incorporating conditions which recognize that the honeycomb core elastic moduli in the plane parallel to the facings are very small in comparison with the core elastic moduli in the direction normal to the facings. Full consideration was given to both the symmetric and antisymmetric wrinkling modes along with the influences from initial waviness of the facings. However, in this case it was found that, except for the region controlled by shear crimping (low q), symmetric wrinkling develops at stress levels which are lower than those at which the antisymmetric mode will occur. Based on this observation, the development of Reference 2-7 resulted in the following equation for the prediction of wrinkling for isotropic facings in sandwich constructions having honeycomb cores and subjected to uniaxial compression:

$$\sigma_{wr} = \frac{0.82 \left(\dfrac{E_c \, t_f}{\eta E_f \, t_c} \right)^{\frac{1}{2}} (\eta E_f)}{1 + 0.64 \, K_\delta} \qquad (2.2\text{-}8)$$

where

$$K_\delta = \frac{\delta \, E_c}{t_c \, F_c} \qquad (2.2\text{-}9)$$

and

σ_{wr} =   Facing wrinkling stress, psi.

E_c =   Young's modulus of the core in the direction normal to the facings, psi.

t_f =   Thickness of facing, inches.

η =   Plasticity reduction factor, dimensionless.

E_f =   Young's modulus of facing, psi.

t_c =   Thickness of core, inches.

δ =   Amplitude of initial waviness in facing, inches.

F_c =   Flatwise sandwich strength (the lower of flatwise core compressive, flatwise core tensile, and flatwise core-to-facing bond strengths), psi.

Equation (2.2-8) can be used to plot a family of design curves of the form shown in Figure 2.2-4. It should be noted that the curve for $K_\delta = 0$ is an upper-bound classical value which is based on the assumption that the facings are initially perfect. This particular curve agrees very closely with the following symmetrical wrinkling equation recently obtained by Bartelds and Mayers [2-14]:

$$\sigma_{wr} = 0.86 \left[\frac{E_c \, t_f}{\eta E_f \, t_c} \right]^{\frac{1}{2}} (\eta E_f) \qquad (2.2\text{-}10)$$

Comparison of Equations (2.2-8) and (2.2-10) shows that, when $K_\delta = 0$, the former gives critical stresses which are approximately 5 percent less than those obtained by Bartelds and Mayers [2-14].

Numbers in brackets [ ] in the text denote references listed at end of each major section (1; 2; etc.)
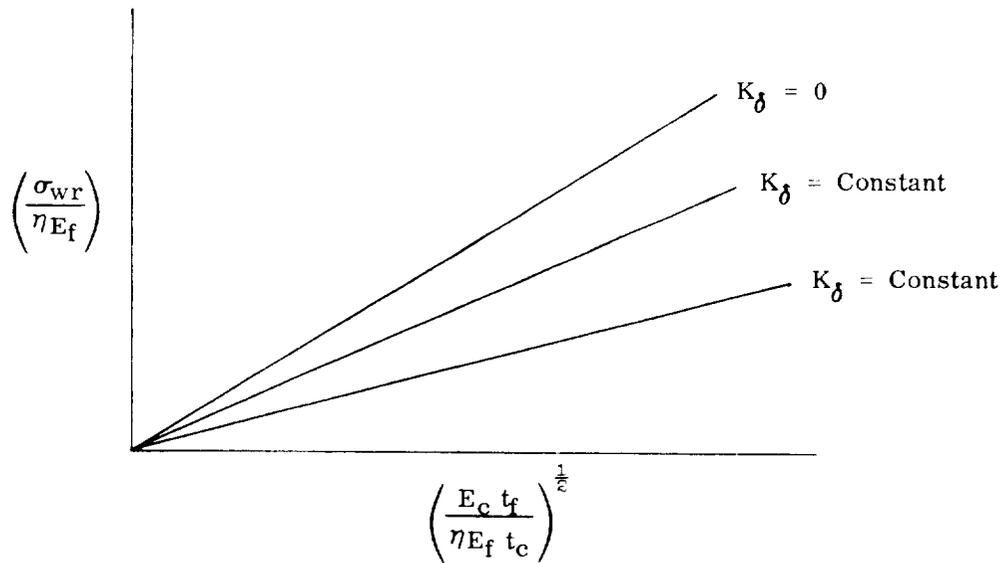
Figure 2.2-4. Typical Design Curves for Face Wrinkling in Sandwich Constructions Having Honeycomb Cores

In actual practice, curves of the type shown in Figure 2.2-4 do not prove to be very helpful since the K_δ values appropriate to particular structures are rarely known. Therefore, in order to provide a practical means for the prediction of face wrinkling in sandwich constructions having honeycomb cores, a lower-bound approach is taken in this handbook. For this purpose, test data selected from References 2-7 and 2-10 are plotted in Figure 2.2-5. All of the specimens from Reference 2-7 failed within the elastic range. Several of these failures occurred by means of shear crimping and these data were discarded. For the remaining tests reported in Reference 2-7, three data points are plotted in Figure 2.2-5 for each group of nominally identical specimens. One point is plotted for the maximum test value for the group, one point for the minimum, and one point for the average. The data from Reference 2-10 were selected in a similar manner with several added restrictions. A number of these specimens wrinkled under highly inelastic conditions. Since rather crude plasticity reduction
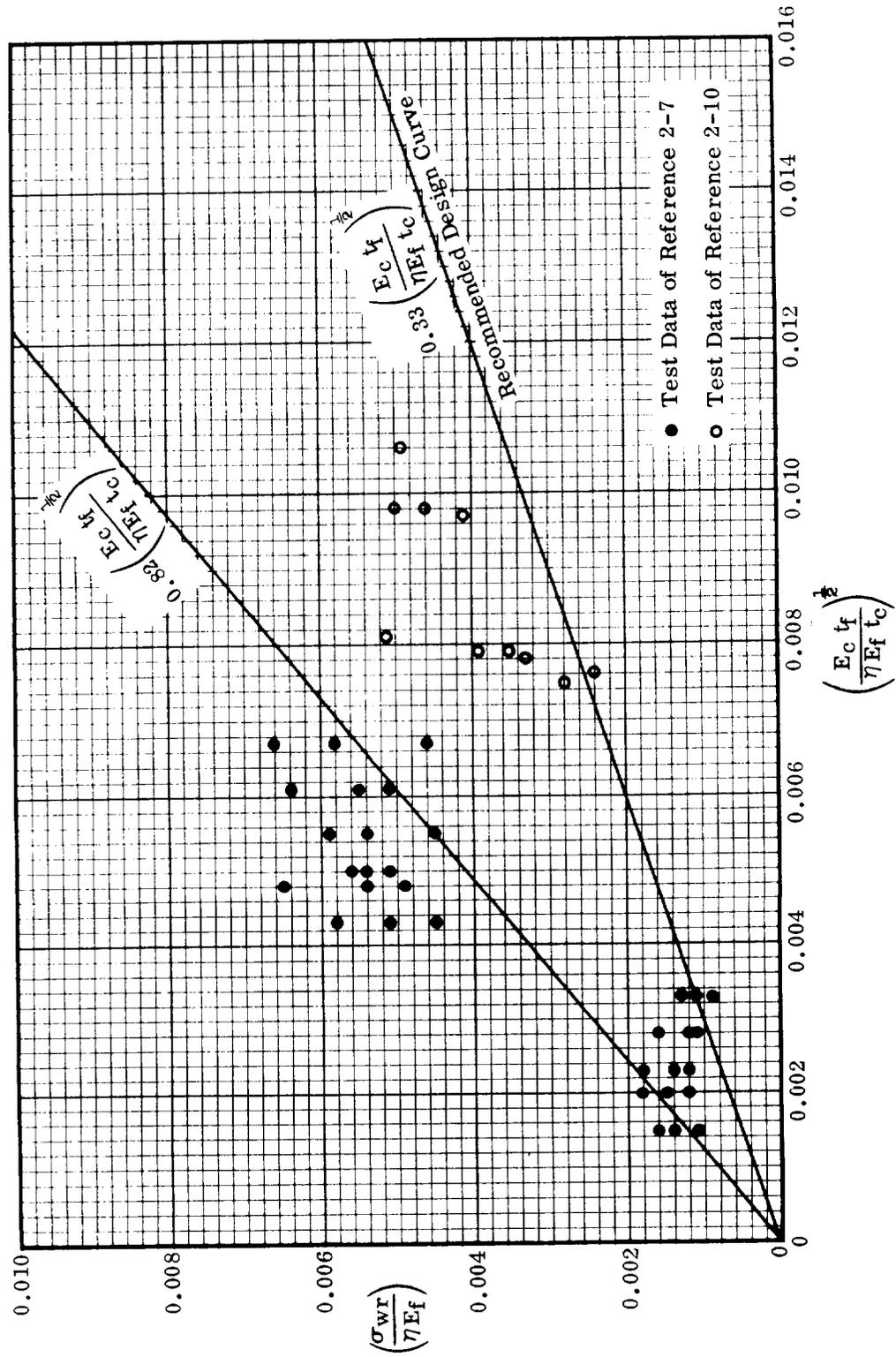
Figure 2.2-5. Comparison of Theory vs Test Results for Face Wrinkling in Sandwich Constructions Having Honeycomb Cores

factors ($\eta = E_t/E_f$) were used in the data reduction, it was decided to plot data only for those specimens which wrinkled at stress levels where (E_t/E_f) ≥ 0.85. In addition, many of the test specimens of Reference 2-10 had very poor core-to-facing bonds as measured by flatwise tensile strengths. It was therefore decided to plot data only for those specimens whose flatwise tensile strengths were at least equal to the flatwise compressive strengths. Adhesive technology has now advanced to the point where, with proper care, one can usually select an adhesive system which satisfies such a requirement.

Based on the plot of Figure 2.2-5, the relationship

$$\sigma_{wr} = 0.33 \left(\frac{E_c \, t_f}{\eta E_f \, t_c} \right)^{\frac{1}{2}} (\eta E_f) \qquad (2.2-11)$$

has been selected here to provide safe design values. This implies that a knock-down factor of approximately 0.4 is applicable to this wrinkling phenomenon. Obviously, this is not a rigorous approach to the problem and it would be advisable to base the design equation on a much wider selection of test data of specimens which were truly representative of contemporary practical designs. Therefore, Equation (2.2-11) can only be regarded as a "best-available" approach and it is recommended that, for verification of final designs, wrinkling tests be performed on specimens that actually duplicate the selected sandwich configuration. The method presented here should only be regarded as an approximate guideline.

2.2.2.2 Design Equations and Curves

The following equation may be used to compute the approximate uniaxial compressive stress at which face wrinkling will occur in sandwich constructions having honeycomb cores:

$$\sigma_{wr} = \frac{0.82 \left(\dfrac{E_c\, t_f}{\eta E_f\, t_c}\right)^{\frac{1}{2}} (\eta E_f)}{1 + 0.64\, K_\delta} \qquad (2.2\text{-}12)$$

where

$$K_\delta = \frac{\delta\, E_c}{t_c\, F_c} \qquad (2.2\text{-}13)$$

In cases where the amplitude of initial waviness is known, one can either use these equations or the curves given in Figures 2.2-6 and 2.2-7 to establish the wrinkling stress. Both of these figures are taken directly from MIL-HDBK-23 [2-16]. Whenever the initial waviness is unknown, it is recommended that the following equation be used to obtain a lower-bound prediction:

$$\sigma_{wr} = 0.33 \left(\frac{E_c\, t_f}{\eta E_f\, t_c}\right)^{\frac{1}{2}} (\eta E_f) \qquad (2.2\text{-}14)$$

For elastic cases, use $\eta = 1$. Whenever the behavior is inelastic, the methods of Section 9 must be employed.

When the facings are subjected to biaxial compression, it is recommended that one use the interaction formula

$$R_x^3 + R_y = 1 \qquad (2.2\text{-}15)$$

where

$$R_i = \frac{\left[\text{Applied Compressive Loading in Subscript Direction}\right]}{\left[\begin{array}{c}\text{Critical Compressive Loading (when acting alone) in}\\ \text{Subscript Direction}\end{array}\right]} \qquad (2.2\text{-}16)$$

2-33
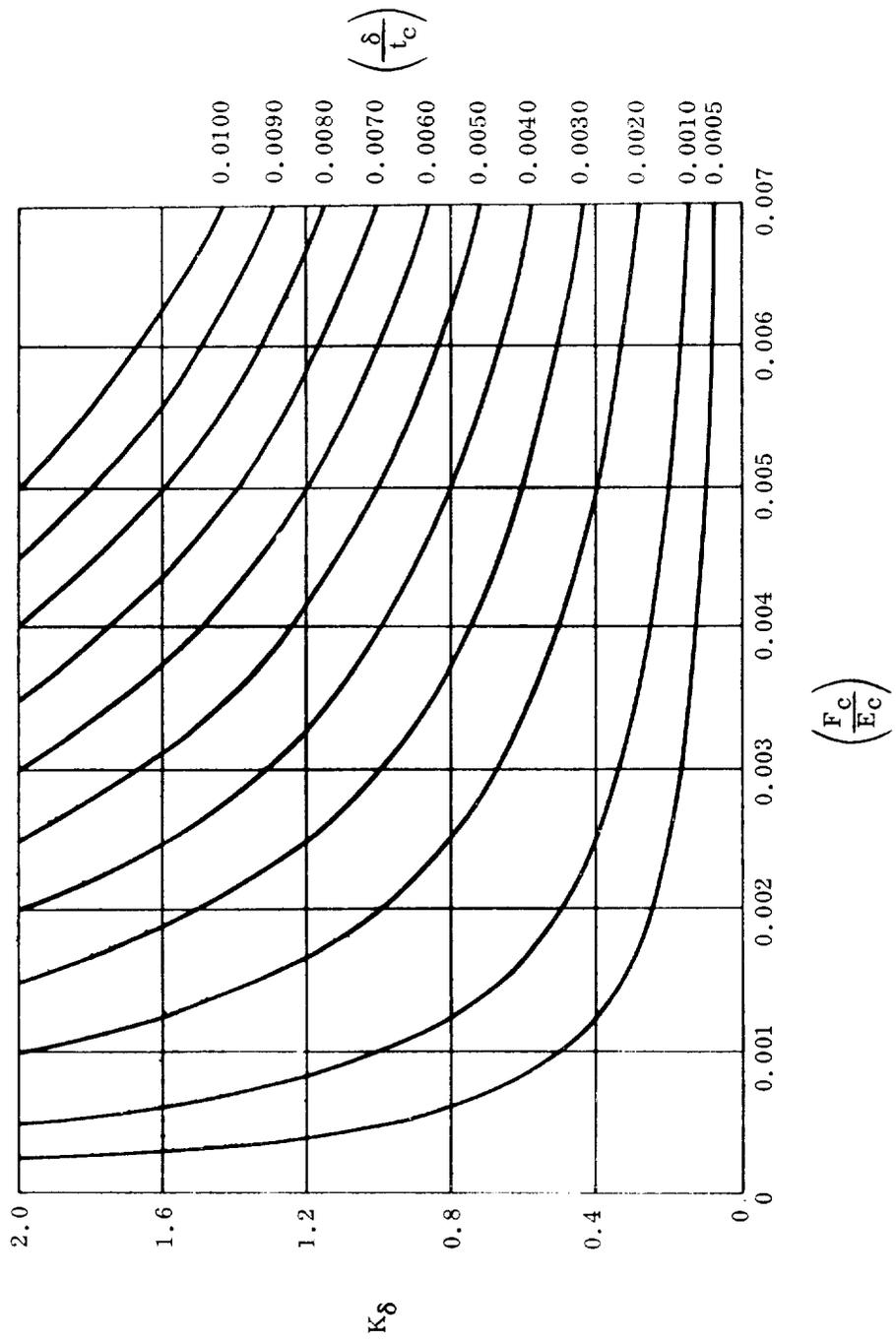
Figure 2.2-6.   Relationship of K_δ to Honeycomb Core Properties (F_c/E_c) and Facing Waviness Parameter (δ/t_c)
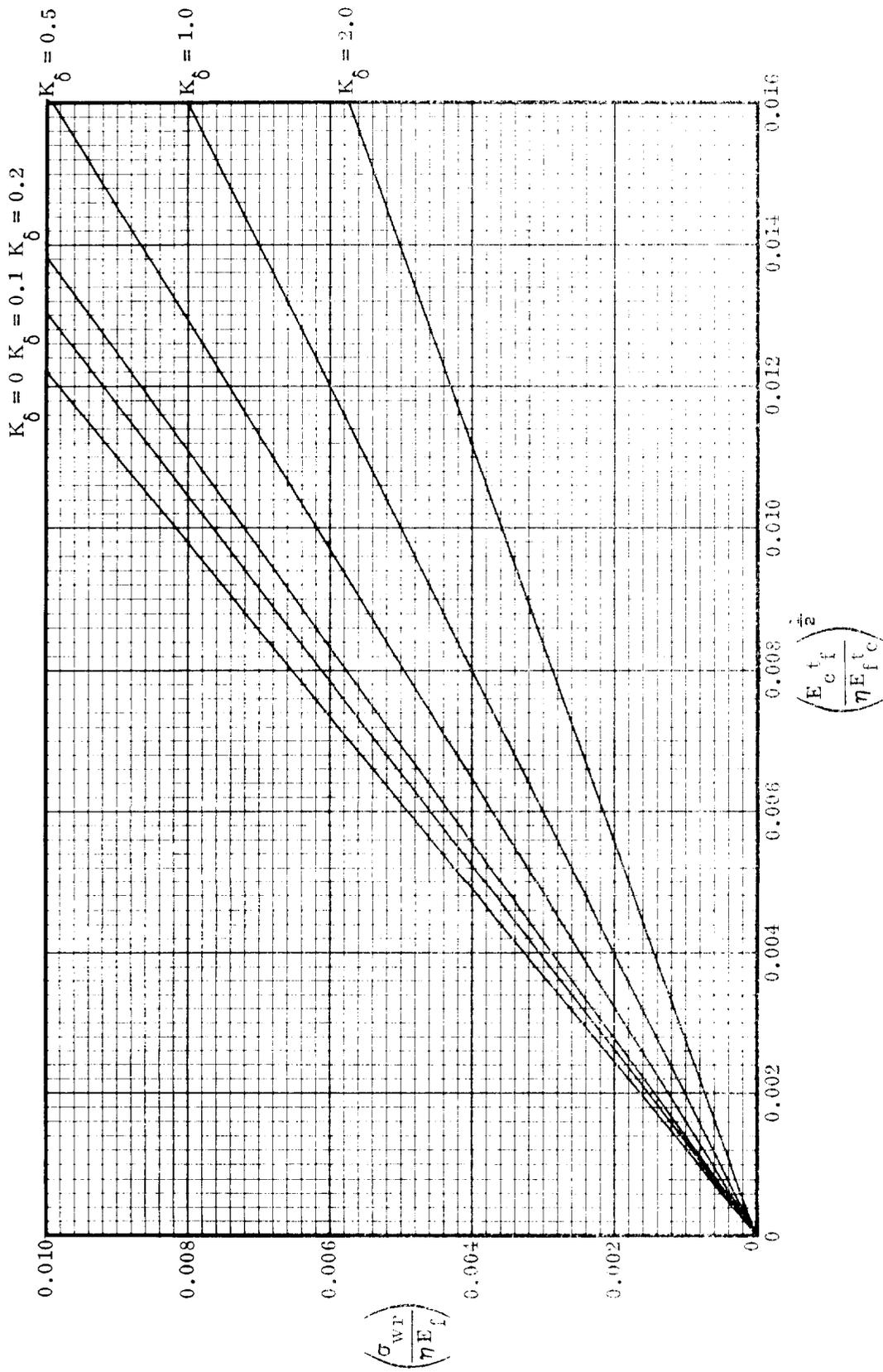
Figure 2.2-7. Graphs of Equation (2.2-12) for the Wrinkling Stress of Facings in Sandwich Constructions Having Honeycomb Cores

2-35

and the y direction corresponds to the direction of maximum compression. This interaction relationship is based on the information provided in Reference 2-1 for rectangular flat plates having very large aspect ratios. For cases involving shearing stresses which are coplanar with the facings, it is recommended that the principal stresses first be computed and that these values then be used in the above interaction equation. Whenever one of the principal stresses is tensile and the behavior is elastic, the analysis should be based on the assumption that the compressive principal stress is acting alone.

2.3 SHEAR CRIMPING

2.3.1 Basic Principles

To understand the phenomenon of shear crimping, one must keep in mind that this mode of failure is simply a limiting case of general instability. The equations for predicting shear crimping emerge from general instability theory when the analytical treatment extends into the region of low shear moduli for the core. For example, the theoretical derivation of Reference 2-17, as reformulated in Section 4.2.1.1 of this handbook, yields the result that, when the two facings are of the same material, shear crimping will occur in axially compressed sandwich cylinders whenever

$$V_c \geq 2 \qquad (2.3-1)$$

where

$$V_c = \frac{\sigma_0}{\sigma_{crimp}} \qquad (2.3-2)$$

$$\sigma_0 = \eta E_f \frac{h}{R} \frac{2\sqrt{t_1 t_2}}{\sqrt{1-\nu_e^2}(t_1 + t_2)} \qquad (2.3-3)$$

$$\sigma_{crimp} = \frac{h^2}{(t_1 + t_2) t_c} G_{xz} \qquad (2.3-4)$$

η = Plasticity reduction factor, dimensionless.

E_f = Young's modulus of facings, psi.

h = Distance between middle surfaces of facings, inches.

R = Radius to middle surface of cylindrical sandwich, inches.

t_1 and t_2 = Thicknesses of the facings (There is no preference as to which facing is denoted by the subscript 1 or 2.), inches.

ν_e = Elastic Poisson's ratio of facings, dimensionless.

2-37

t_c = Thickness of core, inches.

G_{xz} = Core shear modulus associated with the plane perpendicular to the facings and oriented in the axial direction, psi.

The critical stress can be determined from the equation

$$\sigma_{cr} = K_c \, \sigma_0 \qquad\qquad (2.3\text{-}5)$$

and, when the Inequality (2.3-1) holds true, K_c can be computed as follows:

$$K_c = \frac{1}{V_c} \qquad\qquad (2.3\text{-}6)$$

Hence,

$$\sigma_{cr} = \frac{\sigma_{crimp}}{\sigma_0} \, \sigma_0 = \sigma_{crimp} \qquad\qquad (2.3\text{-}7)$$

Therefore, when the two facings are made of the same material, the following equation can be written for the critical stress for shear crimping in a circular sandwich cylinder under axial compression:

$$\sigma_{cr} = \sigma_{crimp} = \frac{h^2}{(t_1 + t_2) \, t_c} \, G_{xz} \qquad\qquad (2.3\text{-}8)$$

An equivalent result can be obtained from Reference 2-18 for sandwich cylinders subjected to uniform external lateral pressure. That is, where the two facings are made of the same material, one can write

$$\sigma_{cr} = \sigma_{crimp} = \frac{h^2}{(t_1 + t_2) \, t_c} \, G_{yz} \qquad\qquad (2.3\text{-}9)$$

where

G_{yz} = Core shear modulus associated with the plane perpendicular to the axis of revolution, psi.

In addition, the development of Reference 2-19 leads one to the following formula for circular sandwich cylinders under pure torsion and having both facings made of the same material:

$$\tau_{cr} = \tau_{crimp} = \frac{h^2}{(t_1 + t_2) t_c} \sqrt{G_{xz} G_{yz}} \qquad (2.3-10)$$

It should be noted that, although Equations (2.3-8) through (2.3-10) were derived for sandwich cylinders, all of these final expressions are independent of curvature. Thus, these equations have a general applicability which is not limited to the cylindrical configuration.

2.3.2 Design Equations

The following equations may be used to compute the facing stresses at which shear crimping will occur in sandwich constructions having both facings made of the same material:

a. For uniaxial compression acting coplanar with the facings (see Figure 2.3-1), use

$$\sigma_{crimp} = \frac{h^2}{(t_1 + t_2) \, t_c} \, G_{ij} \qquad (2.3-11)$$

where

G_{ij} = Core shear modulus associated with the plane perpendicular to the facings and parallel to the direction of loading, psi.
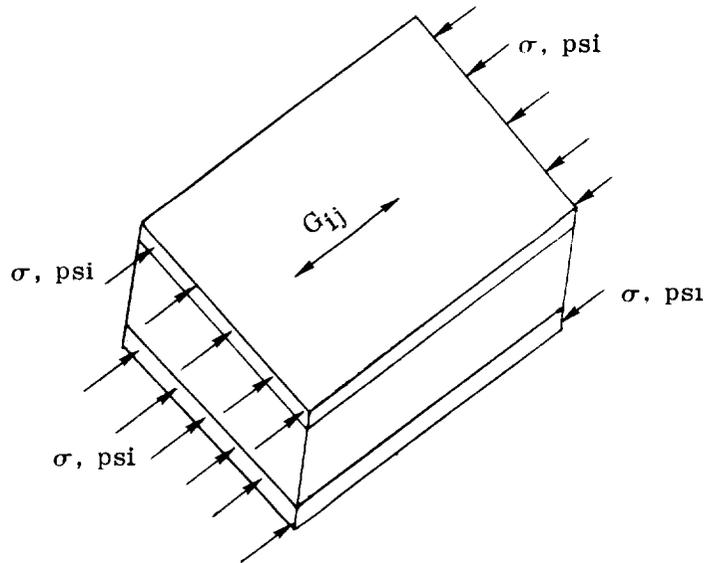
Figure 2.3-1. Uniaxial Compression

b.   For pure shear acting coplanar with the facings (see Figure 2.3-2), use

$$\tau_{crimp} = \frac{h^2}{(t_1 + t_2) t_c} \sqrt{G_{xz} G_{yz}}$$ (2.3-12)
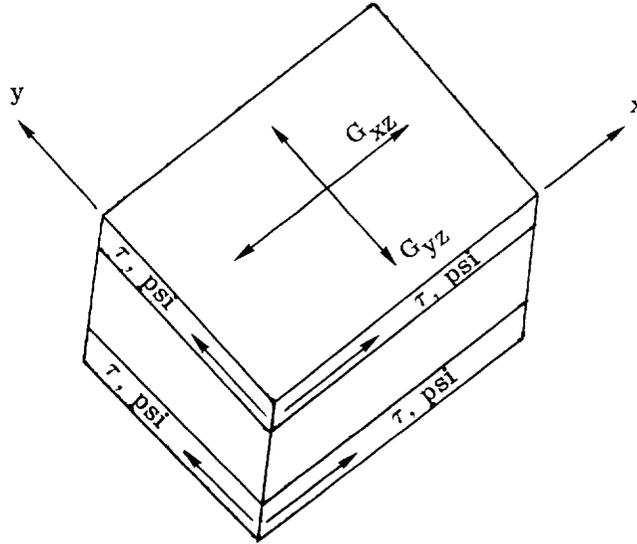
Figure 2.3-2.   Pure Shear

The foregoing equations are valid regardless of the overall dimensions of the structure. In addition, no knock-down factors are required since shear crimping is insensitive to initial imperfections. The predictions from these equations will be somewhat conservative since their derivations neglect bending of the facings about their own middle surfaces. Although such bending is of negligible importance to most sandwich buckling phenomena, in the case of shear crimping this influence can be considerable.

Further mention of the shear crimping mode of failure is made in the various sections on general instability included in this handbook.

Table 2-1. Summary of Design Equations for Local Instability Modes of Failure

NOTATION: σ = Design stress (psi), τ = Design shearing stress (psi), η = Plasticity correction factor (dimensionless), E = Young's modulus (psi), E_c = Young's modulus of the core in the direction normal to the facings (psi), ν_e = Elastic Poisson's ratio (dimensionless), t = Thickness (inches), G = Shear modulus (psi), G_{ij} = Core shear modulus associated with the plane perpendicular to the facings and parallel to the direction of loading (psi), F = Flatwise sandwich strength (the lower value of flatwise core compression, flatwise core tension, or flatwise core-to-facing bond strengths) (psi), δ = Amplitude of initial waviness in facing (inches). Other dimensions and corresponding symbols are indicated on the figures.

SUBSCRIPTS: c, f, cr, and wr designate core, facing, critical, and wrinkling respectively. The subscript xz denotes the plane perpendicular to the facings and parallel to the axis of revolution while yz denotes the plane perpendicular to the axis of revolution.

Failure Mode	Design Formulas	
1. INTRACELLULAR BUCKLING (FACE DIMPLING) (Ref. Page 2-1) Honeycomb Core (Ref. Page 2-1) Corrugated Core (Ref. Page 2-8) See Figure 2.1-5 for all other modes for both single and double-truss-core constructions.	(a) For uniaxial loading $$\sigma_{cr} = 2.0 \; \frac{\eta E_f}{(1-\nu_e^2)} \left(\frac{t_f}{s}\right)^2$$ When designing for cell size $$s = t_f \sqrt{2.0 \; \sqrt{\frac{(1-\nu_e^2)\,\sigma_{cr}}{\eta E_f}}}$$ (b) For biaxial loading conditions refer to the interaction formula page 2-7. (c) For either loading use $\eta = 1.0$ for elastic analysis. Refer to Section 9 for inelastic cases.	Cell Size Also use Figure 2.1-3 for cell sizing.
	(a) Design buckling stress $$\sigma_{cr} = \frac{k_i \, \pi^2 \eta E}{12(1-\nu_e^2)} \left(\frac{t_f}{b_f}\right)^2$$ Definition of the coefficient, k_i, is given on page 2-11. Values are given in Figures 2.1-6 through 2.1-12. (b) Use $\eta = 1.0$ for elastic analysis. Refer to Section 9 for inelastic cases. (c) Equation applies to panels having faceplates and cores of the same material only.	
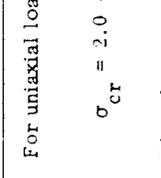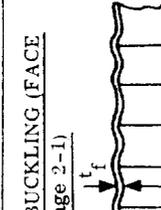
2. FACE WRINKLING (Ref. Page 2-21)
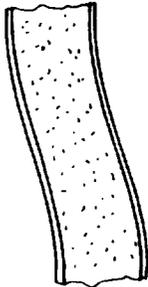
Antisymmetric Wrinkling (Typical of Solid or Foam Core) Ref. Page 2-21

(a) For uniaxial loading

$$\sigma_{wr} = Q \left[\frac{\eta E_f E_c G_c}{(1-\nu_e^2)}\right]^{\frac{1}{3}}$$

The coefficient, Q, is a function of initial waviness. Values for Q may be found from Figure 2.2-3 if the initial waviness is known. For preliminary design or if the initial waviness is unknown use Q = 0.5.

(b) For biaxial loading conditions refer to the interaction formula on page 2-26.

(c) Use η = 1.0 for elastic analysis. Refer to Section 9 for inelastic cases.

Symmetric Wrinkling (Typical of Honeycomb Core) Ref. Page 2-28

(a) For uniaxial loading

For known initial waviness

$$\sigma_{wr} = \frac{0.82 \left(\frac{E_c t_f}{\eta E_f t_c}\right)^{\frac{1}{2}} (\eta E_f)}{1 + 0.64 K_\delta} \qquad \text{where} \quad K_\delta = \frac{\delta E_c}{t_c F_c}$$

Also may use curves of Figures 2.2-6 and 2.2-7.

For unknown initial waviness and preliminary design use

$$\sigma_{wr} = 0.33 \left(\frac{E_c t_f}{\eta E_f t_c}\right)^{\frac{1}{2}} (\eta E_f)$$

(b) For biaxial loading conditions refer to the interaction formula on page 2-33.

(c) Use η = 1.0 for elastic analysis. Refer to Section 9 for inelastic cases.

3. SHEAR CRIMPING (Ref. Page 2-37)

(a) For uniaxial compression acting coplanar with the facings

$$\sigma_{cr} = \frac{h^2}{(t_1 + t_2) t_c} G_{ij}$$

(b) For pure shear acting coplanar with the facings

$$\tau_{cr} = \frac{h^2}{(t_1 + t_2) t_c} \sqrt{G_{xz} G_{yz}}$$

NOTE: Shear crimping is a special case of the general instability problem which is covered in greater detail in other sections.

REFERENCES

2-1   Gerard, George and Becker, Herbert, "Handbook of Structural Stability, Part I - Buckling of Flat Plates," NACA Technical Note 3781, July 1957.

2-2   Norris, C. B., "Short-Column Compressive Strength of Sandwich Constructions as Affected by Size of Cells of Honeycomb Core Materials," U. S. Forest Service Research Note, FPL-026, January 1964.

2-3   Anderson, M. S., "Local Instability of the Elements of a Truss-Core Sandwich Plate," NASA Technical Report R-30, 1959.

2-4   Gough, C. S., Elam, C. F., and deBruyne, N. A., "The Stabilization of a Thin Sheet By a Continuous Supporting Medium," Journal of the Royal Aeronautical Society, January 1940.

2-5   Williams, D., Leggett, D.M.A., and Hopkins, H. G., "Flat Sandwich Panels Under Compressive End Loads," Royal Aircraft Establishment Report No. A.D. 3174, June 1941.

2-6   Hoff, N. J. and Mautner, S. E., "The Buckling of Sandwich Type Panels," Journal of the Aeronautical Sciences, Vol. 12, No. 3, July 1945.

2-7   Norris, C. B., Boller, K. H., and Voss, A. W., "Wrinkling of the Facings of Sandwich Construction Subjected to Edgewise Compression," FPL Report No. 1810-A, June 1953.

2-8   Yusuff, S., "Theory of Wrinkling in Sandwich Construction," Journal of the Royal Aeronautical Society, Vol. 59, January 1955.

2-9   Norris, C. B., Ericksen, W. S., March, H. W., Smith, C. B., and Boller, K. H., "Wrinkling of the Facings of Sandwich Constructions Subjected to Edgewise Compression," FPL Report No. 1810, March 1956.

2-10   Jenkinson, P. M. and Kuenzi, E. W., "Wrinkling of the Facings of Aluminum and Stainless Steel Sandwich Subjected to Edgewise Compression," FPL Report No. 2171, December 1959.

2-11   Yusuff, S., "Face Wrinkling and Core Strength in Sandwich Construction," Journal of the Royal Aeronautical Society, Vol. 64, March 1960.

2-12   Harris, B. J. and Crisman, W. C., "Face-Wrinkling Mode of Buckling of Sandwich Panels," Proceedings of the American Society of Civil Engineers, Journal of the Engineering Mechanics Division, June 1965.

2-13   Benson, A. S. and Mayers, J., "General Instability and Face Wrinkling of Sandwich Plates - Unified Theory and Applications," AIAA Paper No. 66-138 Presented in New York, New York, January 1966.

2-14   Bartelds, G. and Mayers, J., "Unified Theory for the Bending and Buckling of Sandwich Shells - Application to Axially Compressed Circular Cylindrical Shells," Department of Aeronautics and Astronautics, Stanford University Report No. SUDAAR No. 287, November 1966.

2-15   Plantema, F. J., Sandwich Construction, John Wiley & Sons, Inc., New York, Copyright 1966.

2-16   U. S. Department of Defense, Structural Sandwich Composites, MIL-HDBK-23, 30 December 1968.

2-17   Zahn, J. J. and Kuenzi, E. W., "Classical Buckling of Cylinders of Sandwich Construction in Axial Compression - Orthotropic Cores," U. S. Forest Service Research Note FPL-018, November 1963.

2-18   Kuenzi, E. W., Bohannan, B., and Stevens, G. H., "Buckling Coefficients for Sandwich Cylinders of Finite Length Under Uniform External Lateral Pressure," U. S. Forest Service Research Note FPL-0104, September 1965.

2-19   March, H. W. and Kuenzi, E. W., "Buckling of Sandwich Cylinders in Torsion," FPL Report No. 1840, January 1958.

3

GENERAL INSTABILITY OF FLAT PANELS

3.1   RECTANGULAR PLATES

3.1.1   General

As previously noted, one of the potential modes of failure for sandwich panels is that

of general instability. This occurs when the panel becomes elastically unstable under

the application of certain types of in-plane loads. Further, it should be noted, the

loads which are critical for instability may or may not be of such magnitude as to

cause a failure of the basic materials.

The flat, rectangular sandwich panel represents that configuration for which the vast

majority of fabrication and test data has been accumulated over the past decade. This

is probably due to the fact that this configuration was best adapted to the structural

needs for a number of applications and that it represented the minimum in fabrication

problems and costs as far as this type of construction is concerned. By the same

token, analytical solutions have been developed for a wide range of loading applications

for flat panels, and an appreciable amount of testing for correlation with these solu-

tions has been accomplished.

As a consequence of this past work, it is now possible to employ the analytical solu-

tions for flat panels, as given in MIL-HDBK-23, [3-1], with a high degree of con-

fidence. This view is supported by recommendations given in References 3-2 through

3-7, inclusive, for basic panel design. Therefore, with this background in mind, the

buckling coefficients, K, which will be given in this section for the various plate loading conditions will be those taken from the applicable sections of Reference 3-1, with no "knock down" factor to be applied to them.

The development of plate buckling coefficients for sandwich construction requires the consideration of a number of factors, some are: 1) the degree of orthotropicity of the face plates, 2) the use of the same or of dissimilar materials for the face plates and, 3) the degree of orthotropicity of the core material. The general equations given in the following sections account for these possibilities; however, the curves showing K as a function of (a/b), V, the type of loading and edge support conditions will assume the use of isotropic faceplate materials since this is largely typical of aerospace vehicle design practices.

In all cases, the final design of the sandwich panel must comply with the following four basic design principles, Reference 3-1;

a. The sandwich facings shall be at least thick enough to withstand the chosen design stresses under the application of the ultimate design loads.

b. The core shall be thick enough and have sufficient shear rigidity and strength so that over-all sandwich buckling, excessive deflection, and shear failure will not occur under the design loads.

c. The core shall have high enough moduli of elasticity, and the sandwich shall have great enough flatwise tensile and compressive strength such that wrinkling of either facing will not occur under the design loads.

d. If the core is a cellular honeycomb or constructed of corrugated material and dimpling of the facings is not permissible, the cell size or corrugation spacing shall be small enough so that dimpling of either facing into the core spaces will not occur under the design loads.

3-2

Other requirements include the use of moduli of elasticity and stress values representative of those values which prevail under the conditions of use. Also, where the stresses are beyond the proportional limit, the appropriate reduced modulus of elasticity should be used.

The following sections on specific types of panel loads define the appropriate equations for each particular situation and discuss useful limits and other considerations, as applicable. A summary table, (Table 3-1), listing the panel instability equations given in the various parts of this section, along with a definition of terms, equation limitations if any, and references for the appropriate buckling curves immediately precedes the list of references to facilitate use of the manual for specific problem solution.

Figure 3.1-1 shows elastic properties and dimensions for the typical sandwich panel under consideration in this section.
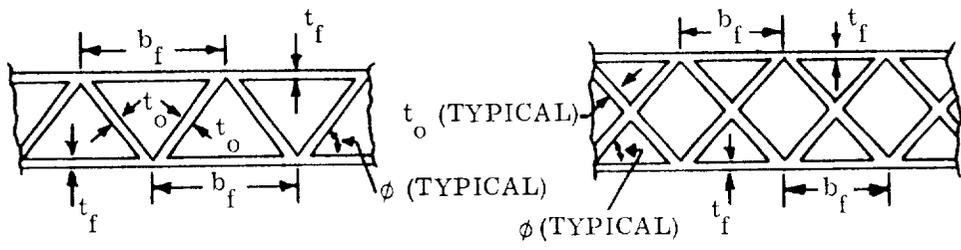
CORRUGATED CORE CONFIGURATIONS
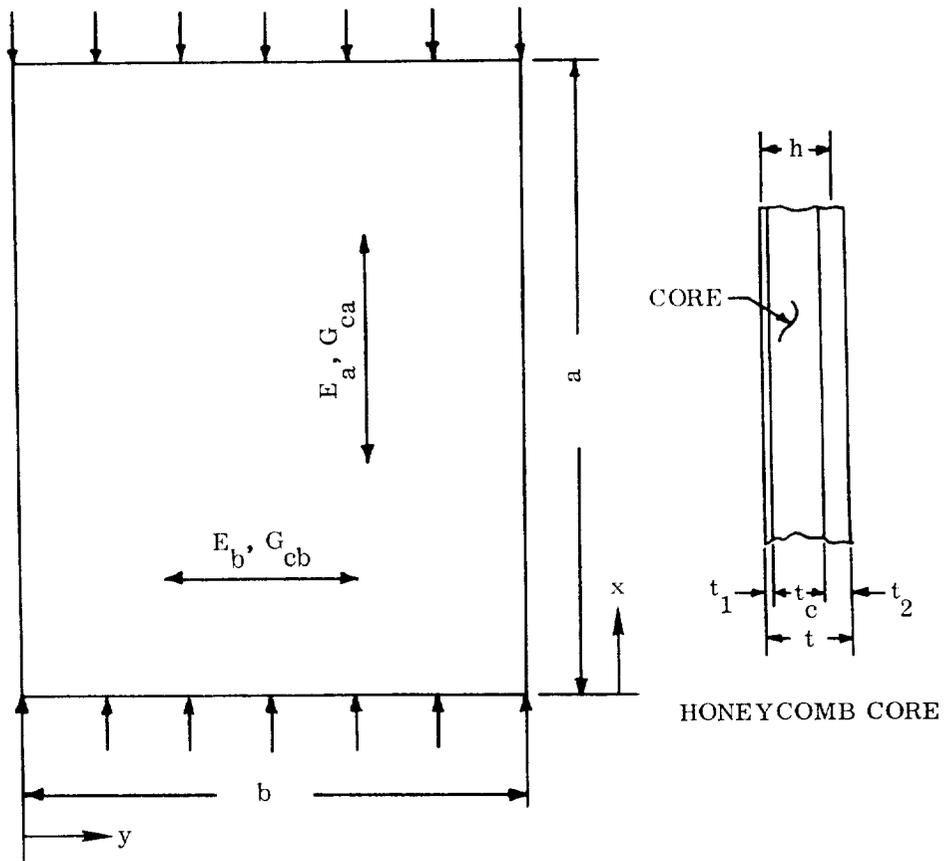
Figure 3.1-1. Elastic Properties and Dimensional Notations
for a Typical Sandwich Panel

3-4

3.1.2　Uniaxial Edgewise Compression

3.1.2.1　Basic Principles

The buckling coefficient equations and curves given here for uniaxial edgewise compression are those originally developed by Ericksen and March, [3-8], and are included in the MIL-HDBK-23 documents, issued since then. The basic principles and assumptions employed in the development of these general instability equations are noted in the references and are not repeated here except where required to limit their use because of the original restrictions imposed.

The basic equations for calculation of the allowable sandwich panel edgewise compression loads are given in the following section. Curves for panel buckling coefficients for panels having isotropic faceplates and both orthotropic and isotropic cores for various panel edge support conditions follow the equations.

3.1.2.2　Design Equations and Curves

As previously noted, the equations presented in this section are those developed by Ericksen and March, and presented in MIL-HDBK-23, as well as in other documents. Supporting data such as pertinent assumptions and definition of terms are also included along with the equations.

Sandwich Panels With Honeycomb Cores

One of the basic assumptions used in the design and analysis of sandwich panels is that the face plates carry the inplane loads applied and that the core provides that shear support to the face plates required for them to act as a unit in preventing early

3-5

individual buckling. From this, the edgewise compression capability of the panel is given by the following equations, which are taken from Section 5.3, Reference 3-1:

$$N_{cr} = (\pi^2/b^2)(K)(D) \tag{3.1-1}$$

where D is the sandwich bending stiffness. Solving this equation for the facing stresses gives the following:

$$F_{c_1,2} = \pi^2 K \frac{(E_1' t_1)(E_2' t_2)}{(E_1' t_1 + E_2' t_2)^2} \frac{(h^2)}{(b^2)} \frac{(E_{1,2}')}{\lambda} \tag{3.1-2}$$

For equal facings:

$$F_c = \frac{\pi^2 K}{4} \frac{(h)^2}{(b)^2} \frac{E_f'}{\lambda} \tag{3.1-3}$$

where

    K = buckling coefficient = $K_F + K_M$ (see definitions in following work).

    E' = $(E_a' E_b')^{\frac{1}{2}}$ = effective modulus of elasticity for orthotropic facings.

    λ = $(1 - \mu_a \mu_b)$

    μ_a, μ_b = Poisson's ratio as measured parallel to the subscript direction.

    f,1,2 = subscripts denoting facings.

    h,b = see Figure 3.1-1.

Since the buckling coefficient curves to be presented here are being limited to the case of isotropic face plates, which is representative of the large majority of structural sandwich applications, the affected equations given previously are revised below for this situation.

For isotropic facings:

$$E'_{ai} = E'_{bi} = E'_i = \eta_i E_i; \text{ and } \mu_{ai} = \mu_{bi} = \mu_i$$

where η_i = plasticity correction factor (see Section 9.0).

As noted above the buckling coefficient for the panel under this loading condition is given by the equation

$$K = K_F + K_M$$

where

$$K_F = \frac{(E'_1 t_1^3 + E'_2 t_2^3)(E'_1 t_1 + E'_2 t_2)}{12 E'_1 t_1 (E'_2 t_2) h^2} K_{M_o} \tag{3.1-4}$$

$$K_{M_o} = K_M \text{ for the case where } V = 0 \text{ [see Figure (3.1-16)]} \tag{3.1-5}$$

Values of K_F are generally quite small relative to K_M, thus a safe first approximation is to assume it is equal to zero until a final panel check is made. On this basis, K = K_M may be used to develop initial face plate and core thicknesses for the panel.

K_M is a theoretical coefficient which is dependent on the sandwich panel bending and shear rigidities and panel aspect ratio. Other factors which influence the magnitude of this coefficient include the panel edge support conditions and the orthotropicity of the core. A discussion of these considerations along with development of the equations for calculation of this coefficient are given in References 3-1 and 3-8. This manual does not propose to repeat these equations here; however, the curves shown in Figures 3.1-2 through 3.1-15 give values of K_M as a function of edge support condition, panel aspect ratio, and the bending-shear rigidity parameter, V which is defined as follows

$$V = \frac{\pi^2 D}{b^2 U} \tag{3.1-6}$$

3-7

which further can be written as:

$$V = \frac{\pi^2 t_c \, E_1' t_1 \, E_2' t_2}{\lambda b^2 G_c \, (E_1' t_1 + E_2' t_2)} \qquad (3.1\text{-}7)$$

$$V = \frac{\pi^2 t_c \, E_f' t_f}{2\lambda b^2 G_c} \quad \text{(for equal facings)} \qquad (3.1\text{-}7a)$$

where U is sandwich shear stiffness; G_c is the core shear modulus associated with the axes parallel to direction of loading (also parallel to panel side of length a) and perpendicular to the plane of the panel.

An indication of the influence and importance of the core shear modulus may be obtained from inspection of the above equations for V and the curves giving values of K_M given later. Holding all terms constant except G_c, an increase in its value reduces the value of V to be used with the buckling coefficient curves, this reduced value then calls for an increased value of K_M.

Sandwich Panels With Corrugated Core

The equations and formulas previously given are for sandwich panels with honeycomb cores; however, they may be adapted to cover the case of panels with corrugated cores by means of the following modifications:

a. For the case where the corrugation flutes are oriented normal to the direction of the load application, the shear modulus in the direction parallel to the flutes, G_{cb}, is very high with respect to the shear modulus parallel to the direction of loading, G_{ca}; thus, the previous curves may be used by letting $G_{cb} = \infty$ and $R = G_{ca}/G_{cb} = 0$.

b. For the case where the corrugation flutes are parallel to the direction of loading, the corrugations may be assumed to carry load in a direct proportion to their area and elastic modulus. The parameter V for this case is replaced by the parameter W, which is defined as

3-8

$$W = \frac{\pi^2 t_c (E_1' t_1)(E_2' t_2)}{\lambda b^2 G_{cb}(E_1' t_1 + E_2' t_2)} \qquad (3.1\text{-}8)$$

Or, for equal facings,

$$W = \pi^2 t_c E_f' t_f / 2\lambda b^2 G_{cb} \qquad (3.1\text{-}8a)$$

Values of K_M as a function of (b/a), $R = (G_{ca}/G_{cb})$, and V, or W, are given for various edge support conditions in Figures 3.1-2 through 3.1-15, with Figures 3.1-14 and 3.1-15 representing the case of panels having corrugated cores.

Figure 3.1-16 gives values of K_{M_0} as a function of panel aspect ratio and edge support conditions for use in determining values of K_F in order that final values for K may be obtained for specific designs.

The curves and equations just given may be used in developing a panel design in addition to checking the adequacy of an existing design; however, this is a slow iterative process. As a consequence, this manual recommends the use of the design-procedures approach described in Reference 3-1 since it was specifically developed to expedite the new design process.
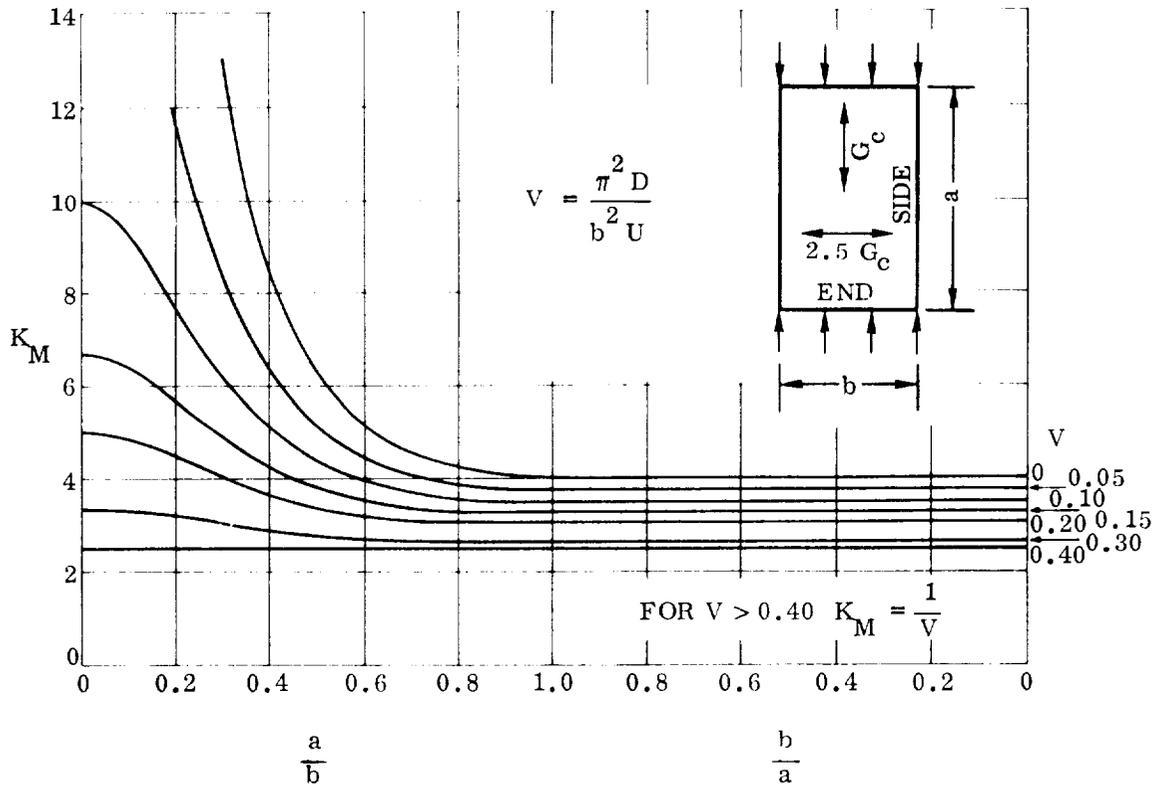
Figure 3.1-2. K_M for a Sandwich Panel with Ends and Sides Simply Supported, Isotropic Facings, and Orthotropic Core, (R = 0.40)

$$V = \frac{\pi^2 D}{b^2 U}$$

FOR $V > 1.00$ $K_M = \frac{1}{V}$
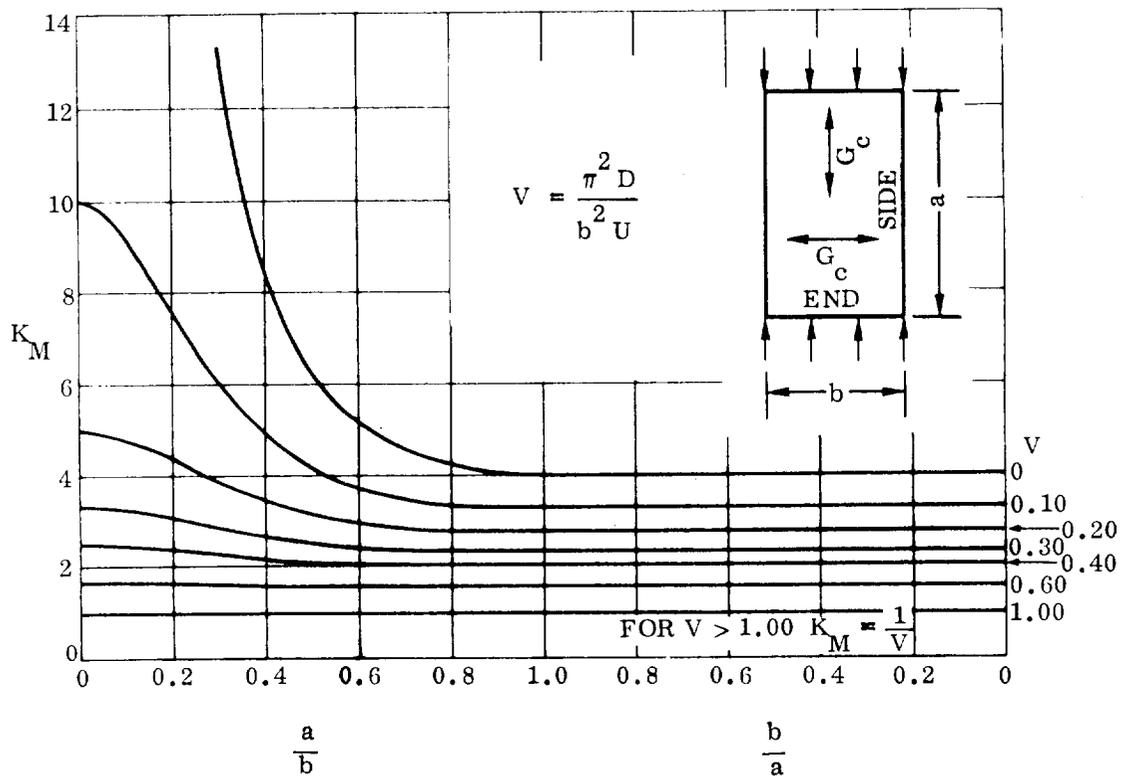
Figure 3.1-3. K_M for Sandwich Panel with Ends and Sides Simply Supported, Isotropic Facings, and Isotropic Core, (R = 1.00)
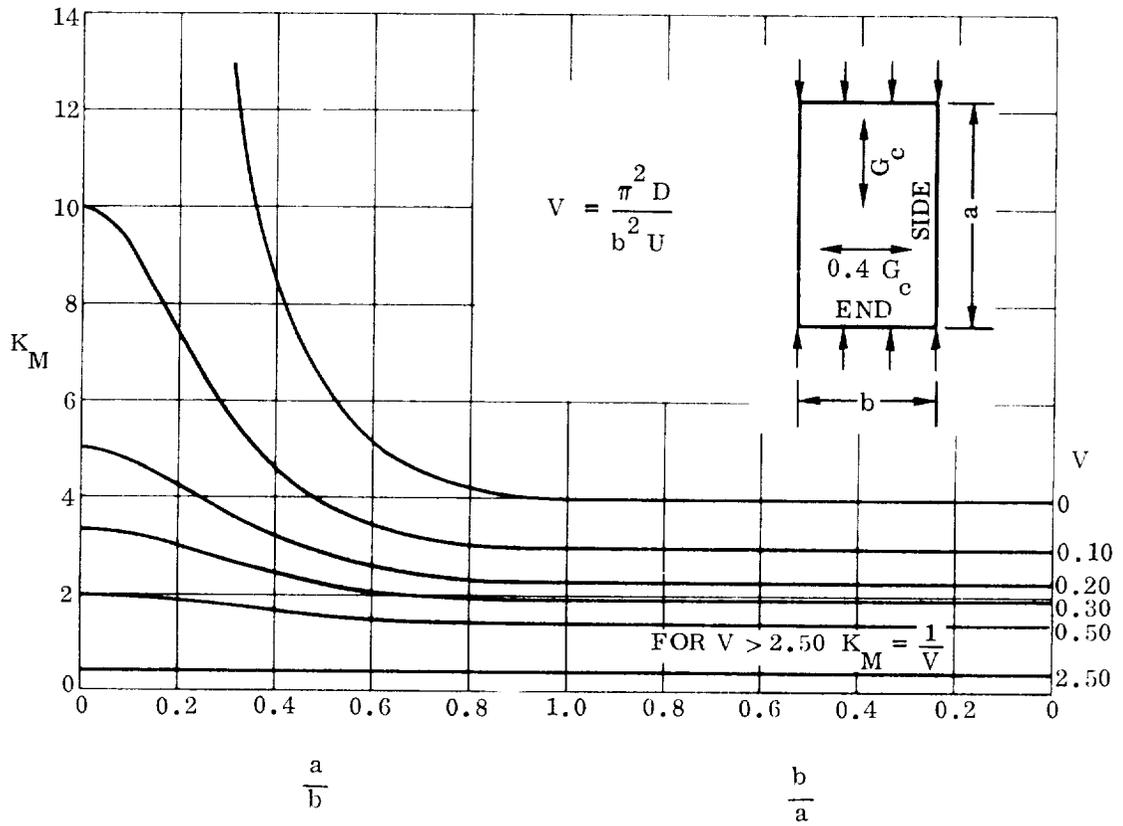
Figure 3.1-4. K_M for Sandwich Panel with Ends and Sides Simply Supported, Isotropic Facings, and Orthotropic Core, (R = 2.50)
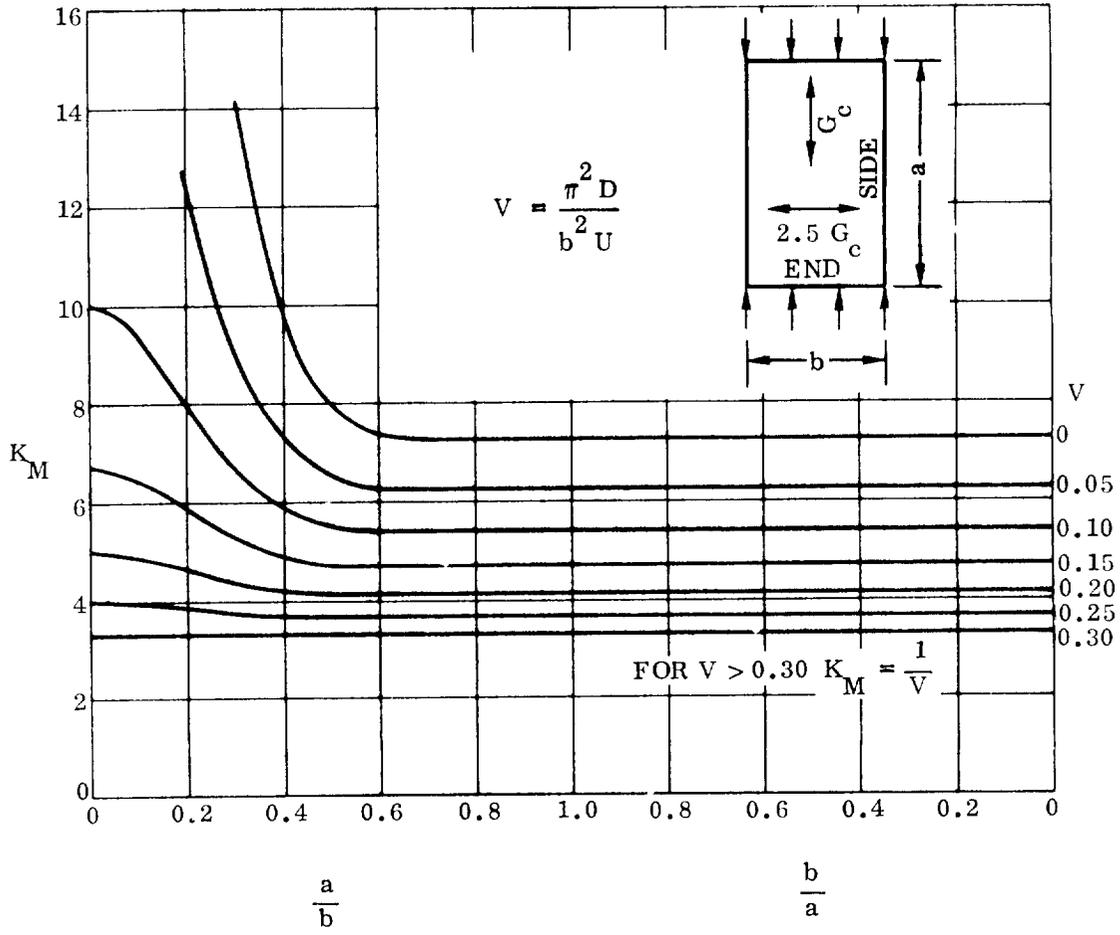
Figure 3.1-5. K_M for Sandwich Panel with Ends Simply Supported and Sides Clamped, Isotropic Facings, and Orthotropic Core, (R = 0.40)

3-13
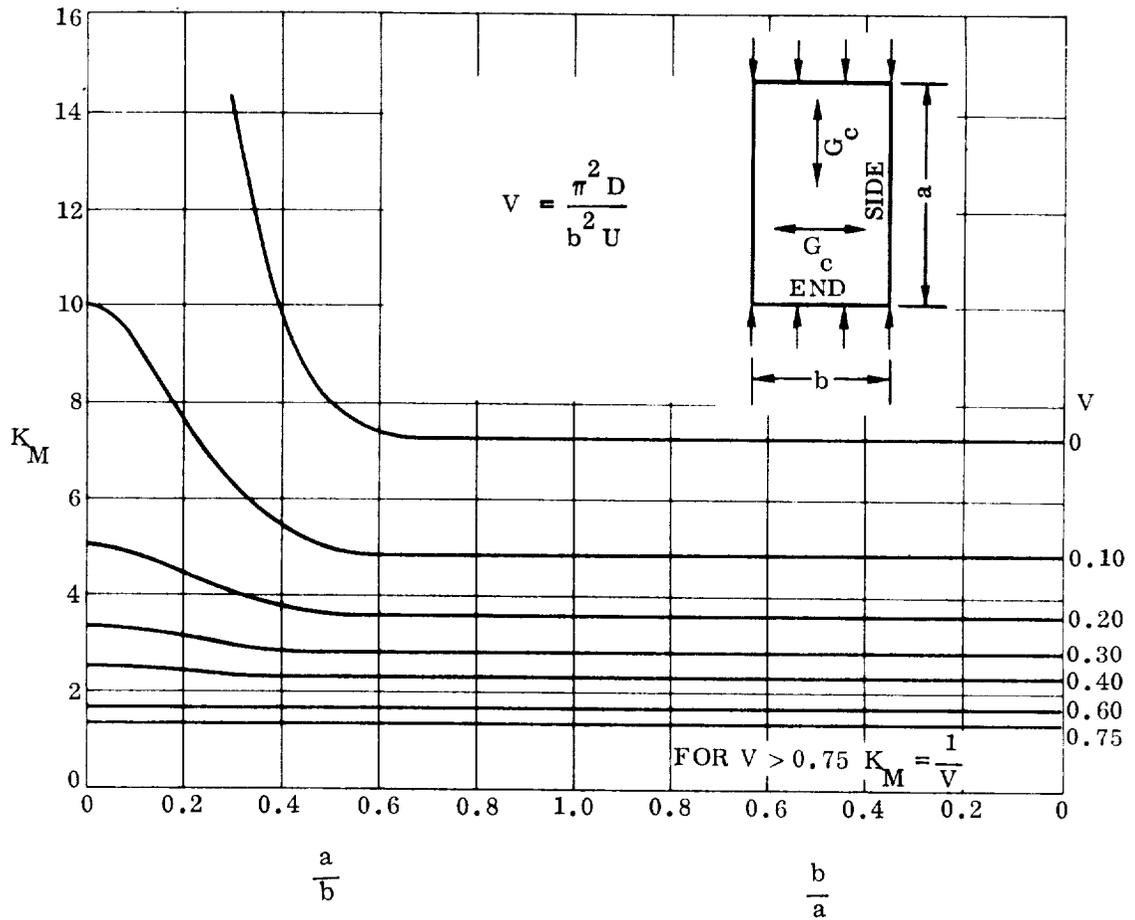
Figure 3.1-6. K_M for Sandwich Panel with Ends Simply Supported and Sides Clamped, Isotropic Facings, and Isotropic Core, (R = 1.00)

3-14
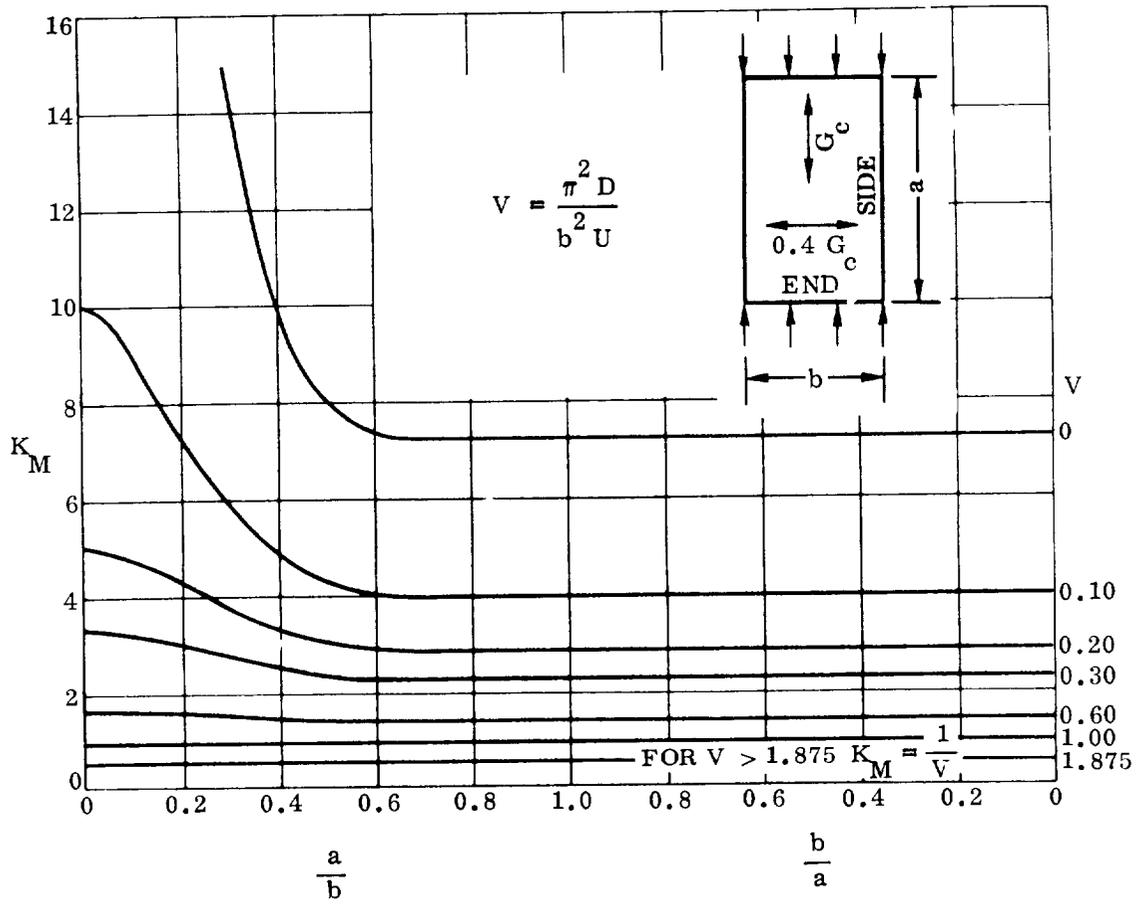
Figure 3.1-7. K_M for Sandwich Panel with Ends Simply Supported and Sides Clamped, Isotropic Facings, and Orthotropic Core, (R = 2.50)

3-15
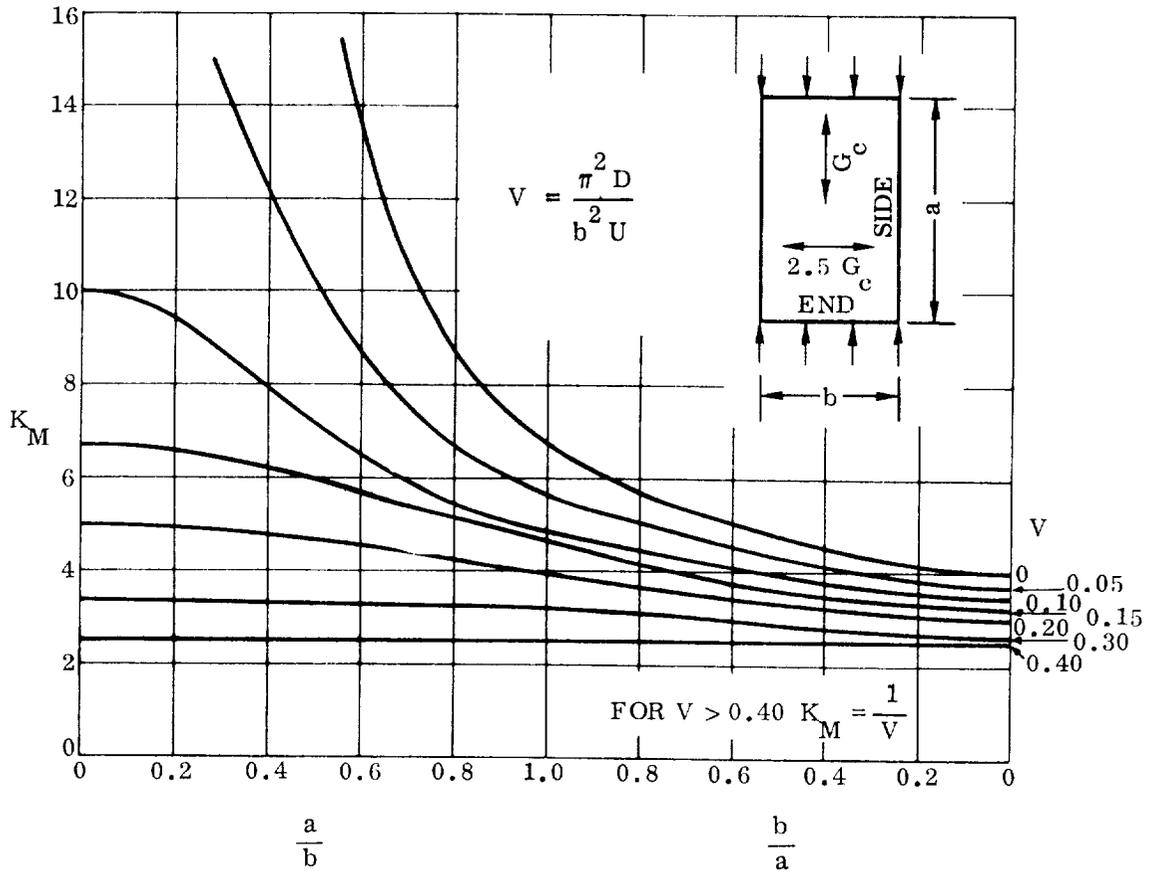
Figure 3.1-8. K_M for Sandwich Panel with Ends Clamped and Sides Simply Supported, Isotropic Facings, and Orthotropic Core, (R = 0.40)

$$V = \frac{\pi^2 D}{b^2 U}$$

K_M

V

0

0.10

0.20

0.30

0.40

0.60

1.00

FOR V > 1.00 $K_M = \dfrac{1}{V}$

16

14

12

10

8

6

4

2

0

0   0.2   0.4   0.6   0.8   1.0   0.8   0.6   0.4   0.2   0

$\dfrac{a}{b}$

$\dfrac{b}{a}$

G_c

SIDE

G_c

END

a

b
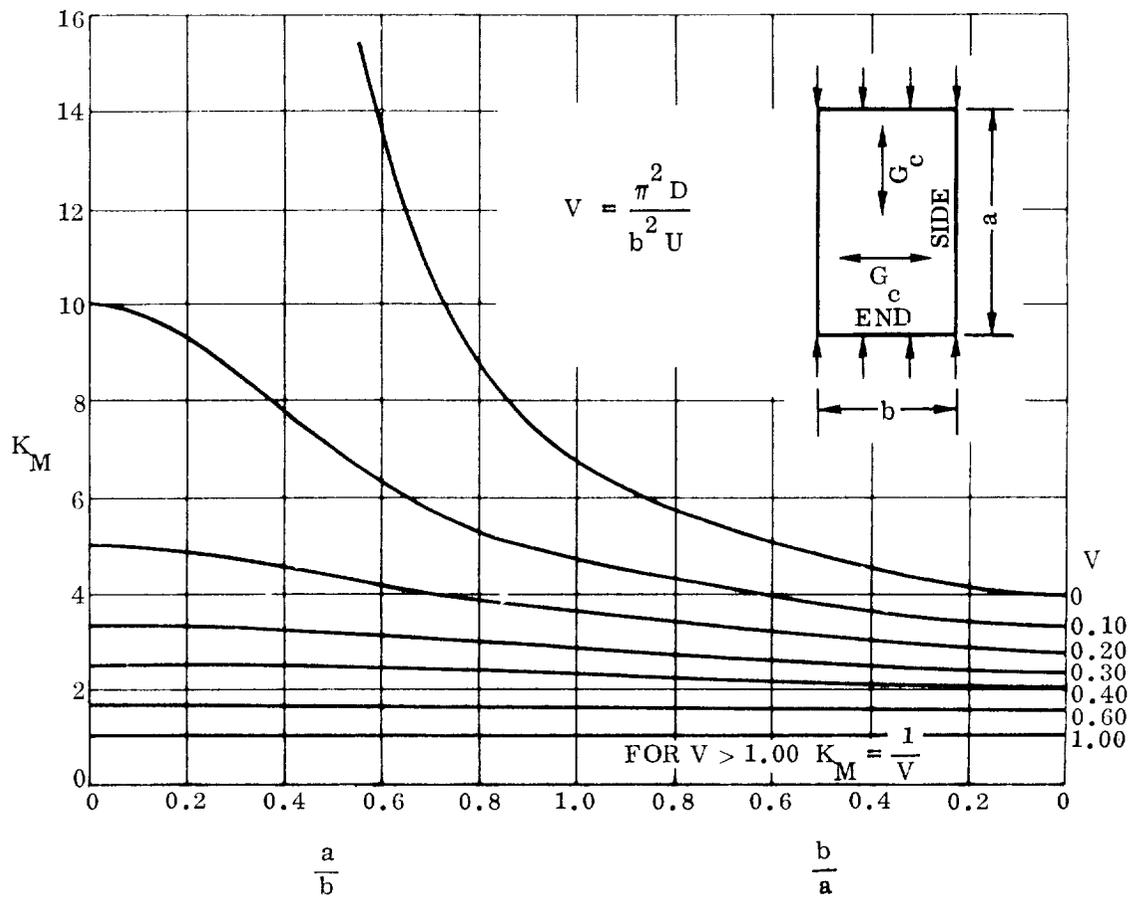
Figure 3.1-9. K_M for Sandwich Panel with Ends Clamped and Sides Simply
Supported, Isotropic Facings, and Isotropic Core, (R = 1.00)

3-17
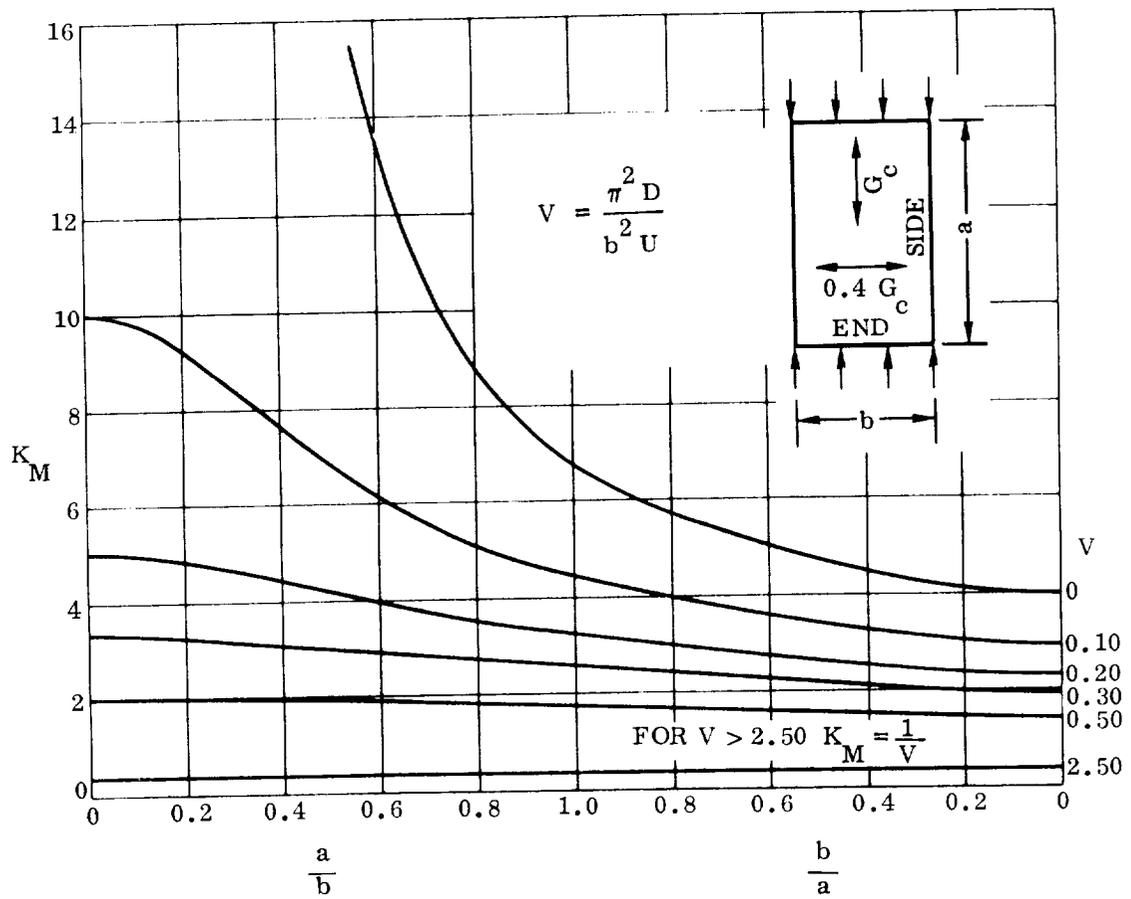
Figure 3.1-10. K_M for Sandwich Panel with Ends Clamped and Sides Simply Supported, Isotropic Facings, and Orthotropic Core, $(R = 2.50)$

3-18
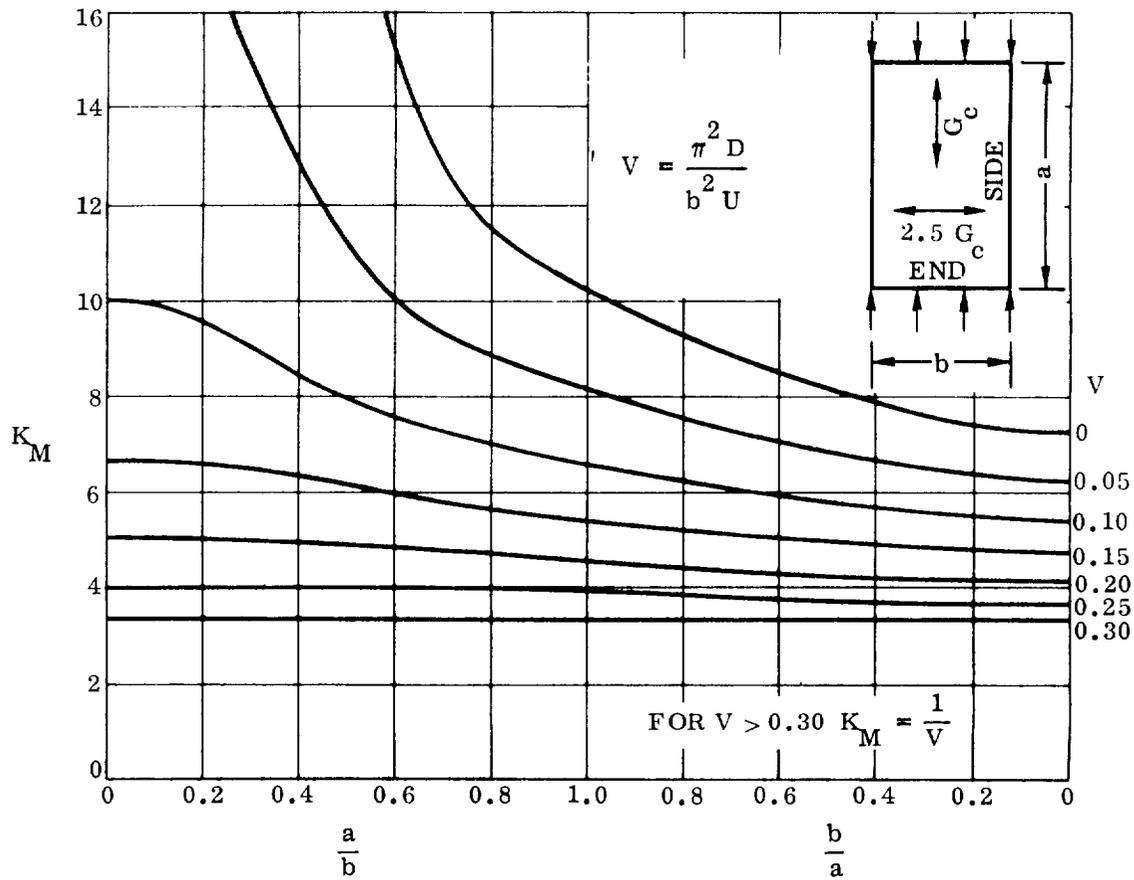
Figure 3.1-11. K_M for Sandwich Panel with Ends and Sides Clamped, Isotropic Facings, and Orthotropic Core, (R = 0.40)

3-19
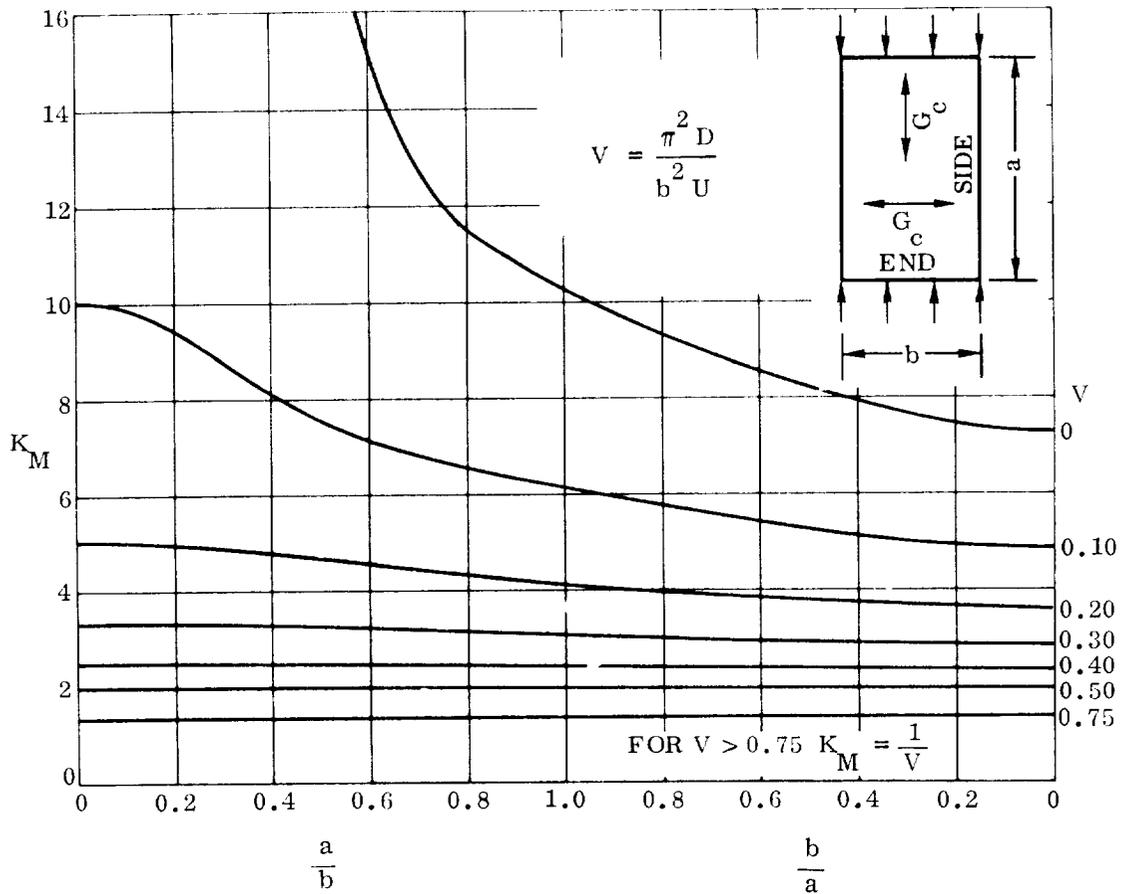
Figure 3.1-12. K_M for Sandwich Panel with Ends and Sides Clamped, Isotropic Facings, and Isotropic Core, (R = 1.00)

$$V = \frac{\pi^2 D}{b^2 U}$$

FOR V > 1.875 $K_M = \frac{1}{V}$
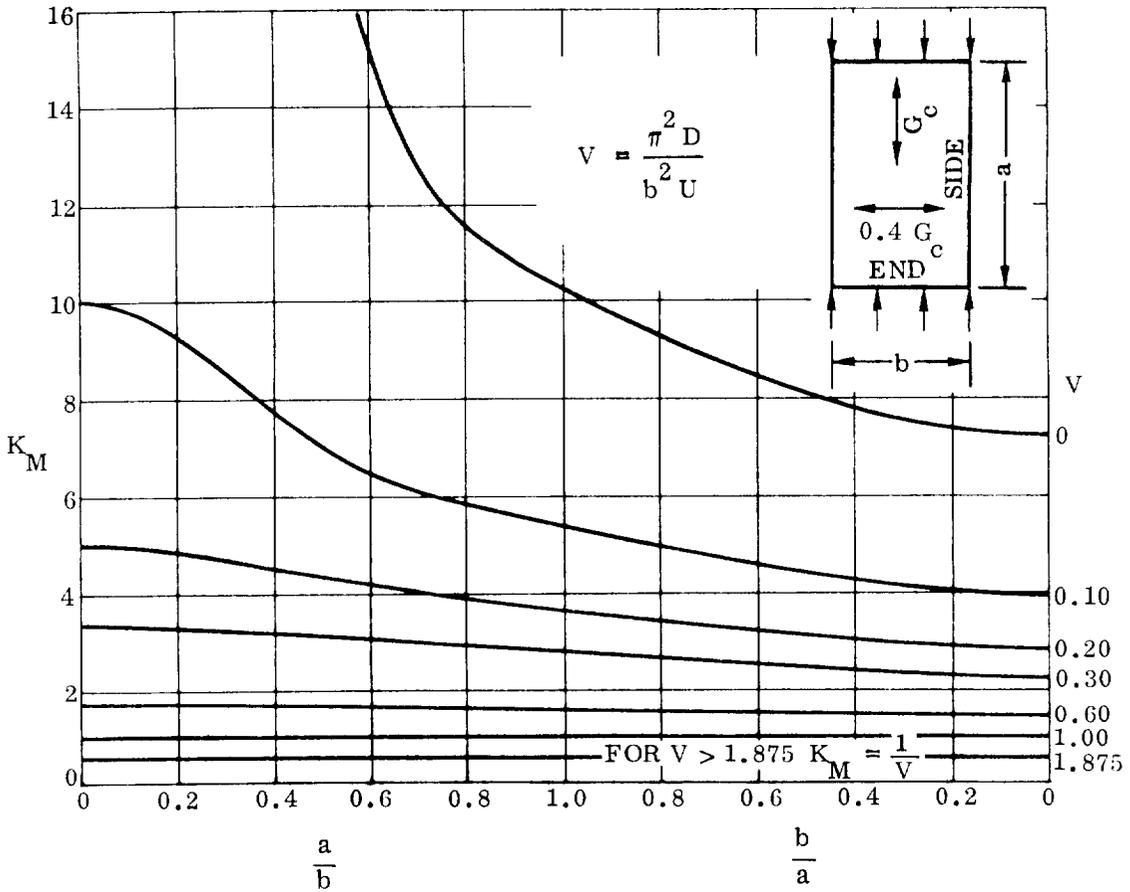
Figure 3.1-13. K_M for Sandwich Panel with Ends and Sides Clamped, Isotropic Facings, and Orthotropic Core, (R = 2.50)
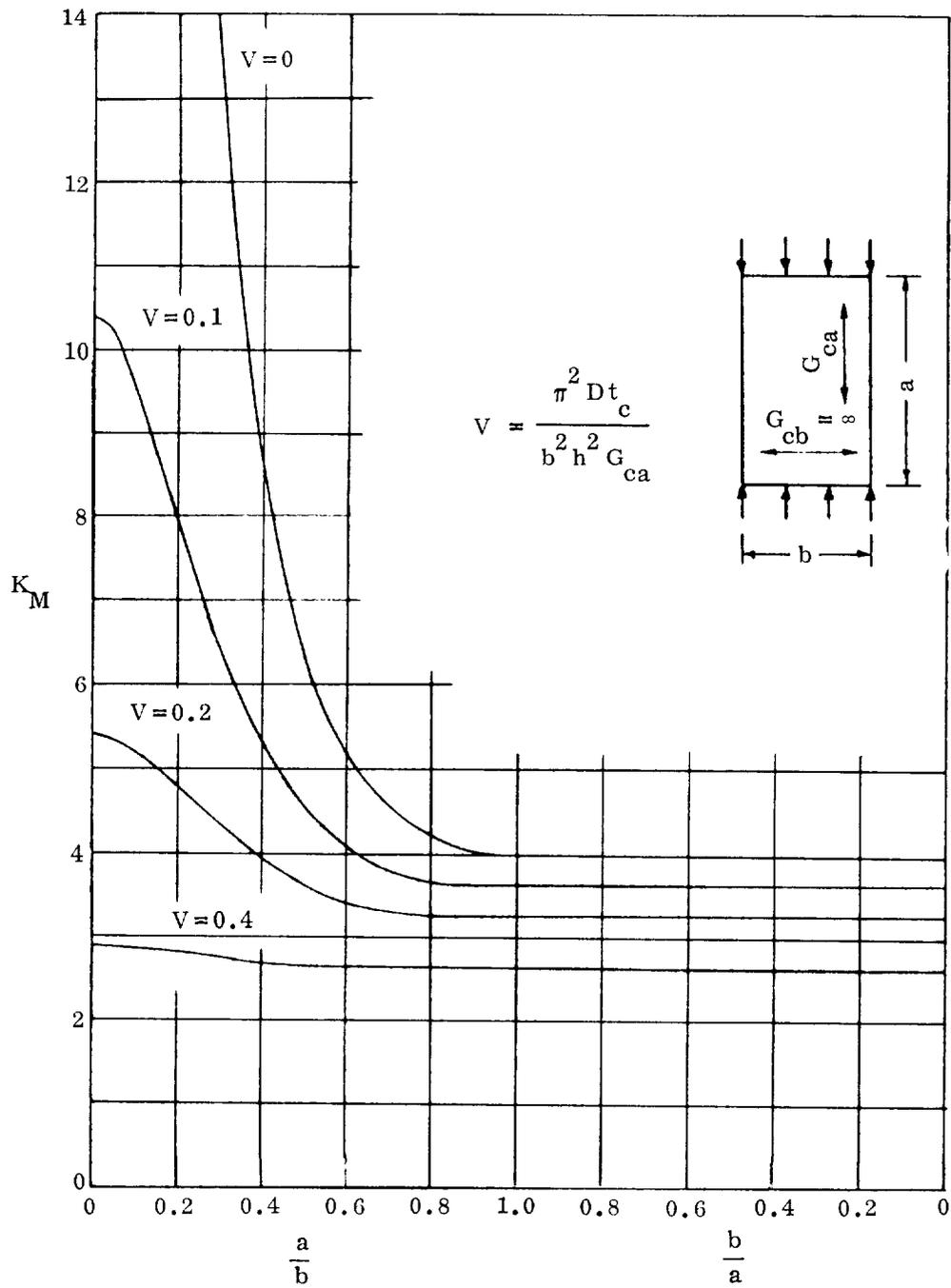
Figure 3.1-14. K_M for Simply Supported Sandwich Panel Having a Corrugated Core. Core Corrugation Flutes are Perpendicular to the Load Direction

3-22

$$W = \frac{\pi^2 D t_c}{b^2 h^2 G_{cb}}$$
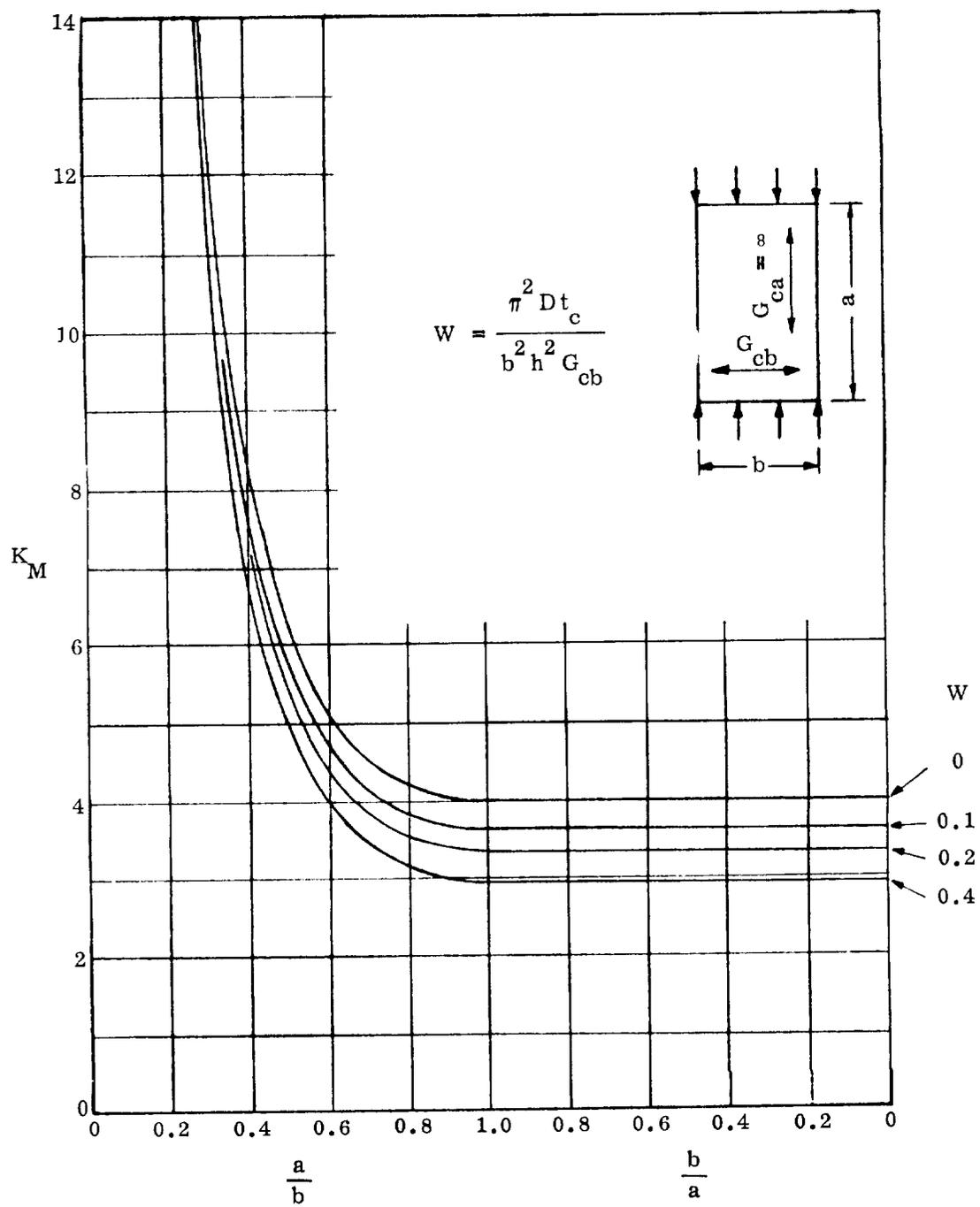
Figure 3.1-15. K_M for Simply Supported Sandwich Panel Having a Corrugated Core. Core Corrugation Flutes are Parallel to the Load Direction
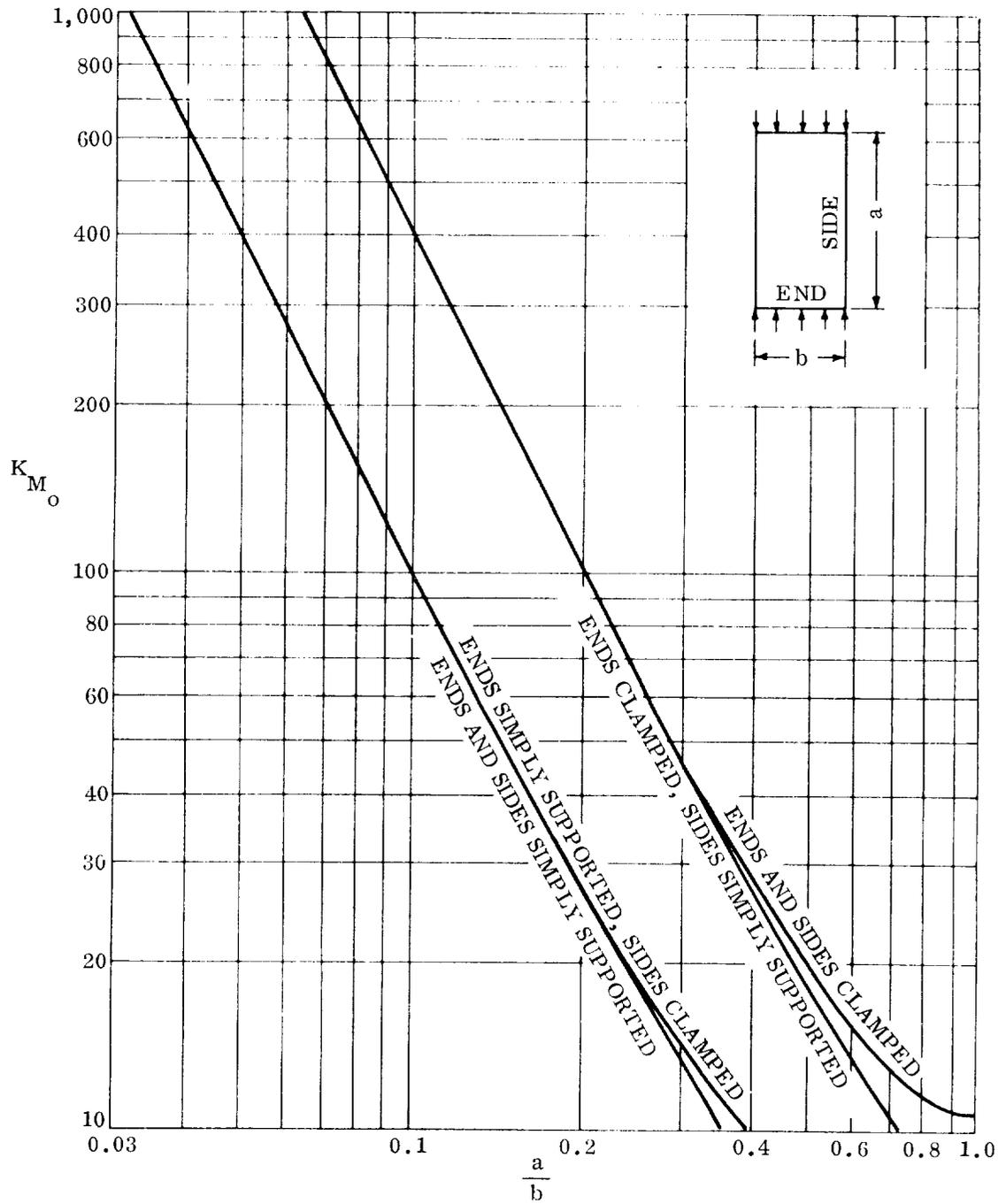
Figure 3.1-16. K_{M_o} for Sandwich Panel with Isotropic Facings in Edgewise Compression

3-24

3.1.3 Edgewise Shear

3.1.3.1 Basic Principles

As noted earlier in Section 3.1.1, sufficient analysis, design, and testing of flat sand-
wich panels has been accomplished to demonstrate the adequacy of the analytical

approaches presently in use. Thus, the panel buckling coefficient equations and

curves given in the following paragraphs for edgewise shear are those taken from the

MIL-HDBK-23 documents presently in use. These equations were originally developed

by Kuenzi and Ericksen [3-13] and employ the same general assumptions as those

described in Section 3.1.1. Specific limitations or restrictions on the use of these

equations will be noted where these require consideration.

The basic equations for use in calculation of the allowable sandwich panel edgewise

shear loads are given in the following section along with applicable background data

and assumptions. Design curves and buckling coefficients for panels having isotropic

faceplates and both orthotropic and isotropic cores for both simply supported and

clamped edge conditions follow the equations.

3.1.3.2 Design Equations and Curves

The design equations presented here are taken from Reference 3-1 and 3-13. Support-

ing data and design constraints are also noted and discussed as required.

The edgewise shear load carrying capability of a sandwich panel is given by the follow-

ing equation:

$$N_{scr} = (\pi^2/b^2)(K_s)(D) \qquad\qquad (3.1-9)$$

where

$$N_{scr} = \text{critical edgewise shear load, lb per inch}$$

$$D = \text{sandwich bending stiffness}$$

Solving this for the facing stresses gives the following equation:

$$F_{s1,2} = \pi^2 K_s \frac{(E_1' t_1)(E_2' t_2)(h^2) E_{1,2}'}{(E_1' t_1 + E_2' t_2)^2 (b^2) \lambda} \tag{3.1-10}$$

Or, for equal facings

$$F_s = \frac{\pi^2 K_s (h^2) E_f'}{4 (b^2) \lambda} \tag{3.1-10a}$$

where

E' is the effective modulus of elasticity of facing at stress $F_s = \eta E$

η = plasticity correction factor (Section 9.0)

$\lambda = 1 - \mu^2$

$\mu = \mu_1 = \mu_2$ = Poisson's ratio of facings

h = distance between facing centroids (Figure 3.1-1)

b = panel width ($\leq a$) (Figure 3.1-1)

$K_s = K_F + K_M$ (Note: These terms differ from those of Section 3.1.2)

where

$$K_F = \frac{(E_1' t_1^3 + E_2' t_2^3)(E_1' t_1 + E_2' t_2) K_{M_0}}{12 (E_1' t_1)(E_2' t_2) h^2} \tag{3.1-11}$$

Or, for equal facings

$$K_F = \frac{(t_f^2) K_{M_0}}{3h^2} \tag{3.1-11a}$$

K_{M_0} = value of K_M for $V = W = 0$

The equation defining the value of K_M is quite complex and involved, being dependent on panel aspect ratio, (a/b), the number of half-waves, (n), for the minimum energy buckle pattern, and the panel bending and shear rigidity parameter, (V, or W). This manual proposes to follow general practice in the literature and provide curves only for the definition of this buckling coefficient. Those interested in the basic equation and its development will find this in Reference 3-13.

Values of K_M are given in Figures 3.1-17 through 3.1-24 as a function of the panel aspect ratio and the parameter V, or W, for various panel edge support conditions. These figures cover panels with isotropic faceplates and both isotropic and orthotropic core, including panels using corrugated flutes for cores. Values of the buckling coefficient, K_{M_O}, may also be obtained from the same set of figures.

The equations defining the parameters V and W are the same as those given in the previous section for edgewise compression; however, they are repeated below to facilitate their use. The equation numbers previously assigned to them are retained below

$$V = \frac{(E_1' t_1) (E_2' t_2) (\pi^2) t_c}{\lambda (E_1' t_1 + E_2' t_2) (b^2) G_{ca}} \qquad (3.1-7)$$

$$V = \pi^2 t_c E_f' t_f / 2\lambda b^2 G_{ca} \quad \text{(equal facings)} \qquad (3.1-7a)$$

For a sandwich panel with a corrugated core in which the corrugation flutes are parallel to the edge of length a, the parameter V is replaced by the parameter W which is defined as follows:

$$W = \frac{\pi^2 t_c (E_1' t_1)(E_2' t_2)}{\lambda b^2 G_{cb} (E_1' t_1 + E_2' t_2)} \qquad (3.1\text{-}8)$$

Or, for equal facings

$$W = \pi^2 t_c E_f' t_f / 2 \lambda b^2 G_{cb} \qquad (3.1\text{-}8a)$$

In checking a particular design for the critical buckling stress, F_{scr}, Figures 3.1-17 through 3.1-21 should be used for those panels having all edges simply supported. Curves of K_M for sandwich panels having all edges clamped are given in Figures 3.1-22 through 3.1-24. These curves may be interpolated in order to obtain the buckling coefficients for other values of core orthotropicity, $(R = G_{ca}/G_{cb})$, and intermediate values of V or W.

It should be noted that if the resulting value of F_{scr} is above the proportional limit value, the value of E′ shall be an effective value based on that stress level, and this effective value shall be used in computing the value of V, Equation (3.1-7) or (3.1-7a) or W, Equation (3.1-8) or (3.1-8a), as the case may be. This same effective value for E′ shall also be used in Equation (3.1-10), or (3.1-10a) when calculating the critical panel buckling stress. Thus, several interations will be required to establish the actual value of F_{scr} in those cases where it exceeds the proportional limit.

The equations and curves just given may be used in the development of panel designs as well as in checking an existing design; however, as was the case for uniaxial compression, this is a lengthy iterative process. Thus, this manual recommends the use of the design-procedures approach described in Reference 3-1 for those cases where the initiation of new designs is required.

3-28
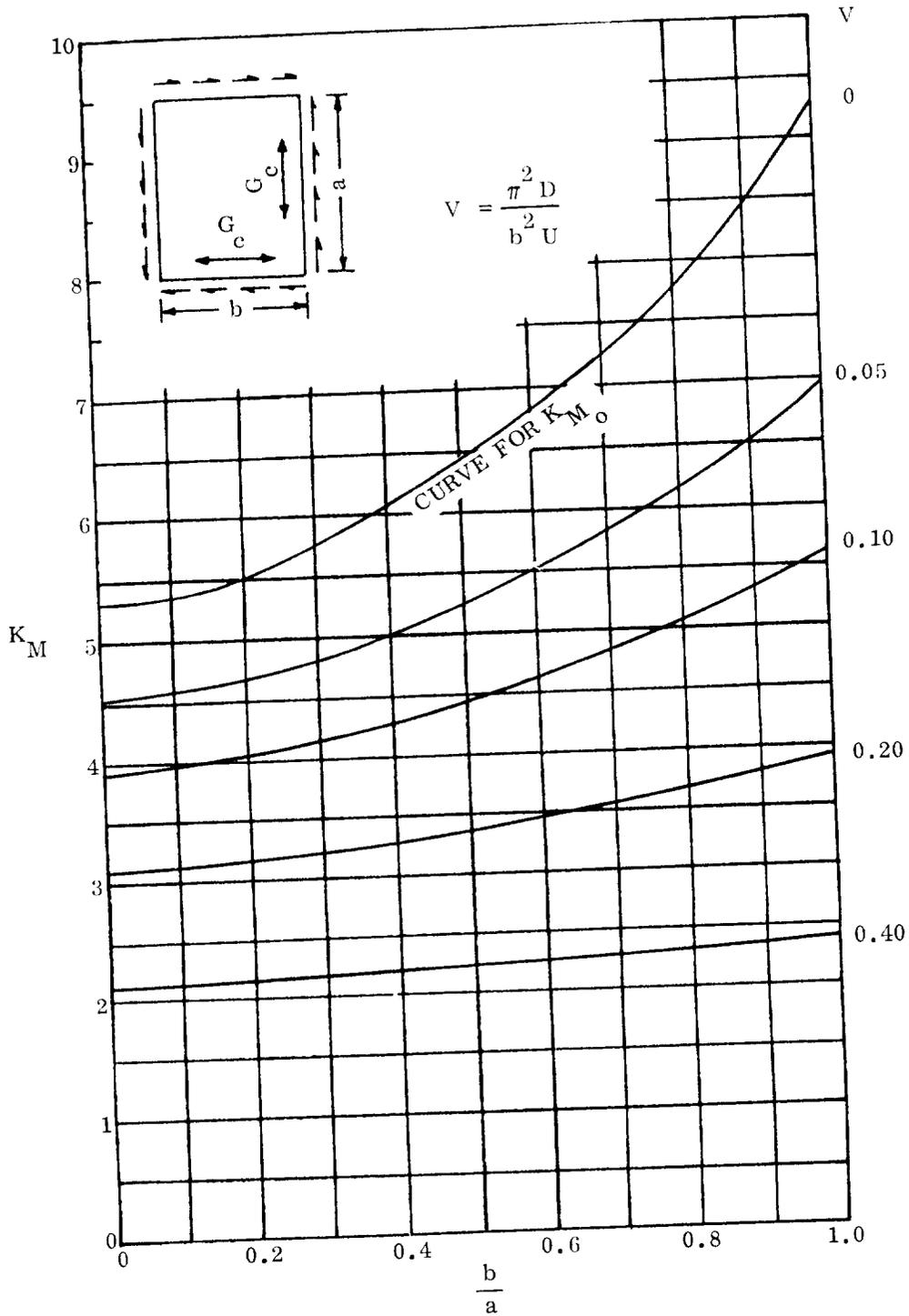
Figure 3.1-17. K_M for a Sandwich Panel with All Edges Simply Supported, and an Isotropic Core, (R = 1.00)
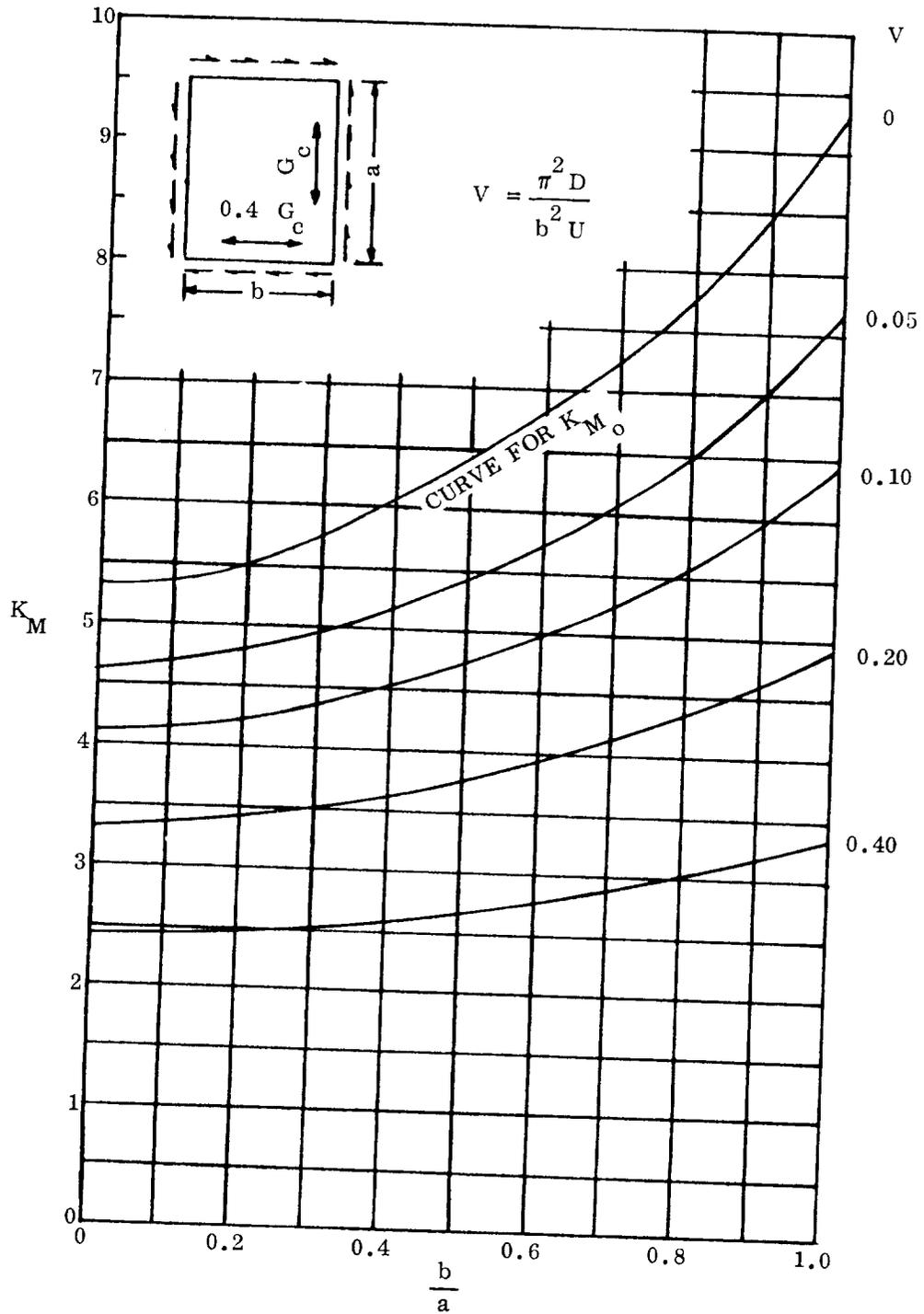
Figure 3.1-18. K_M for a Sandwich Panel with All Edges Simply Supported, and an Orthotropic Core, (R = 2.50)
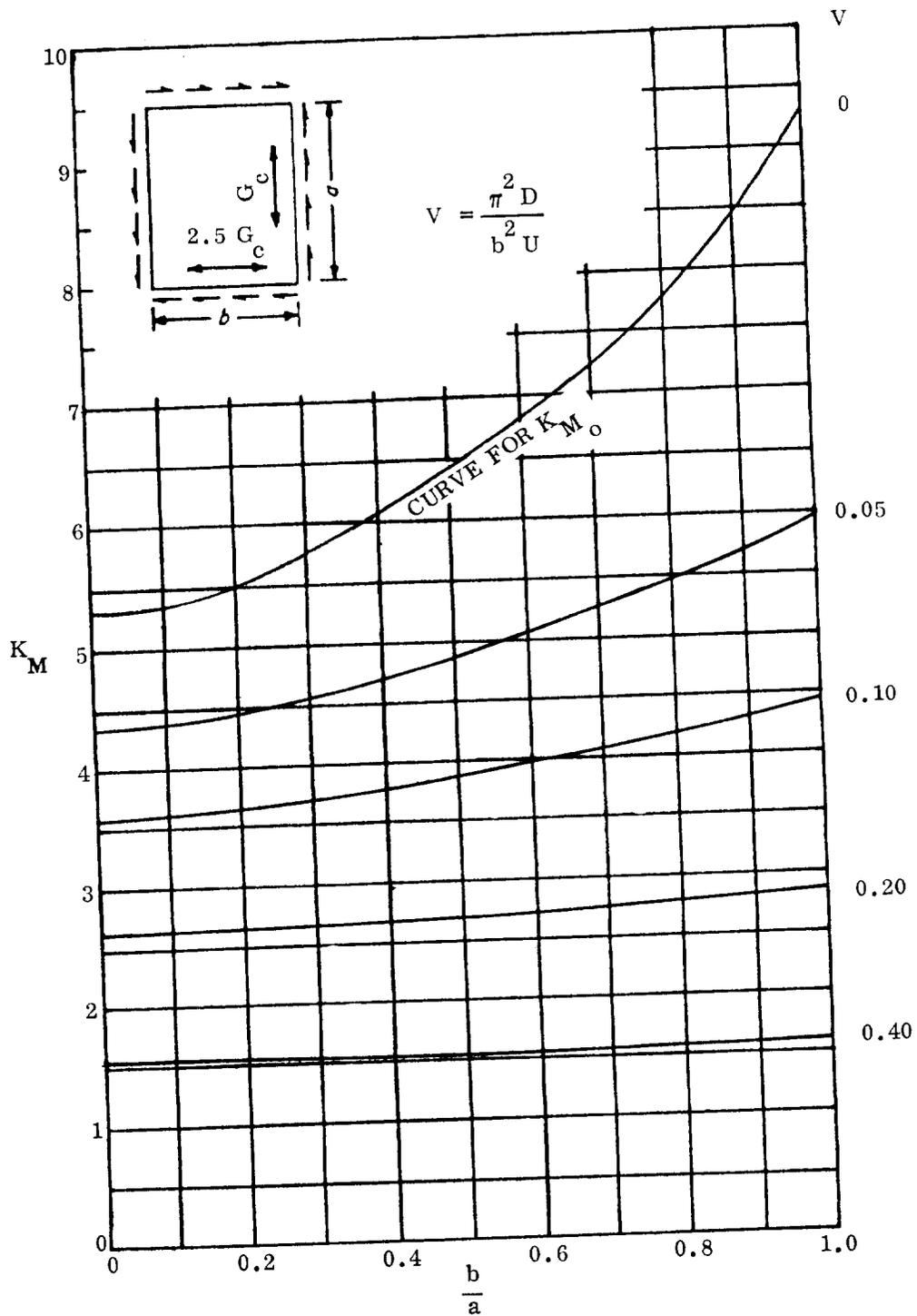
Figure 3.1-19. K_M for a Sandwich Panel with All Edges Simply Supported, and with an Orthotropic Core, (R = 0.40)

3-31
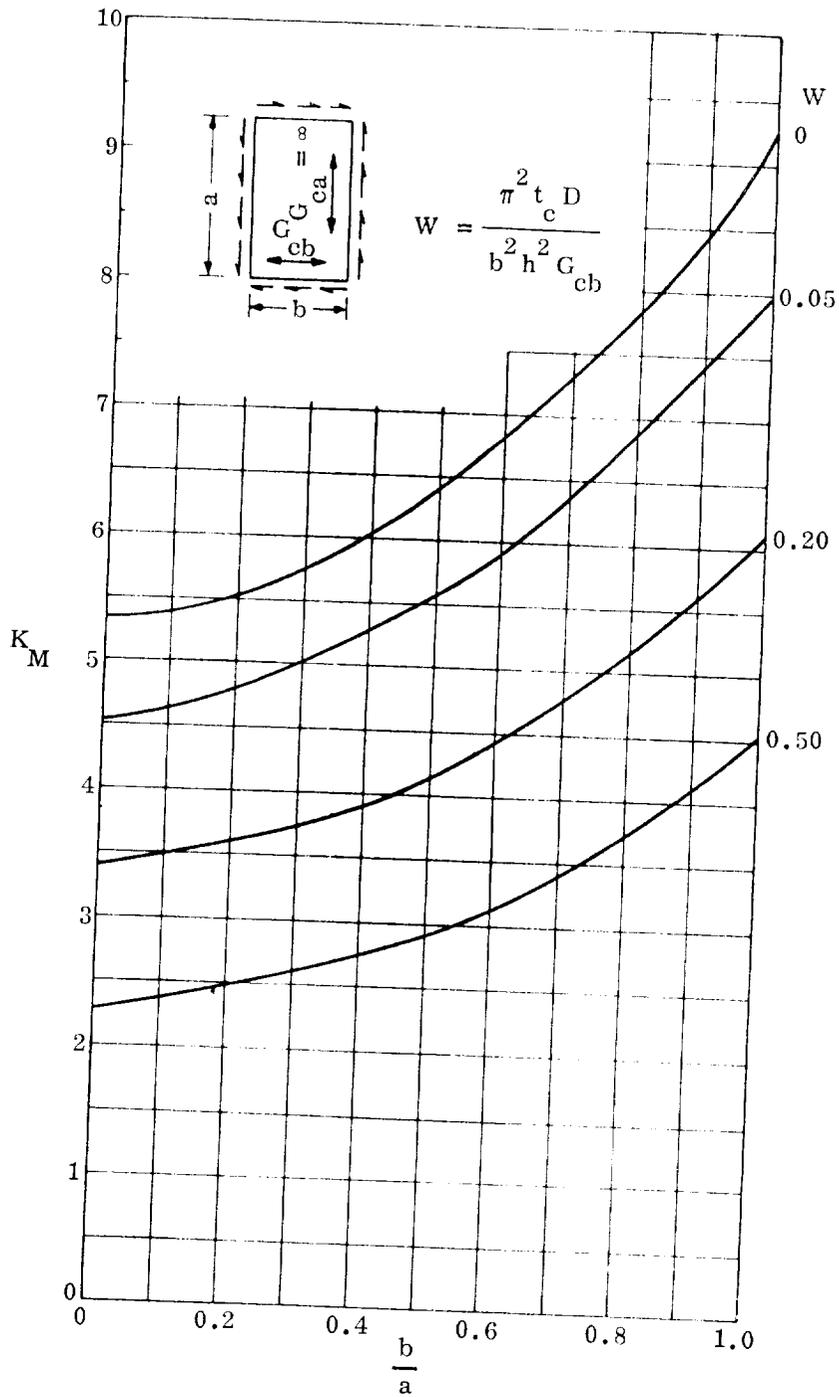
Figure 3.1-20. K_M for a Sandwich Panel with All Edges Simply Supported, Isotropic Facings and Corrugated Core. Core Corrugation Flutes are Parallel to Side a
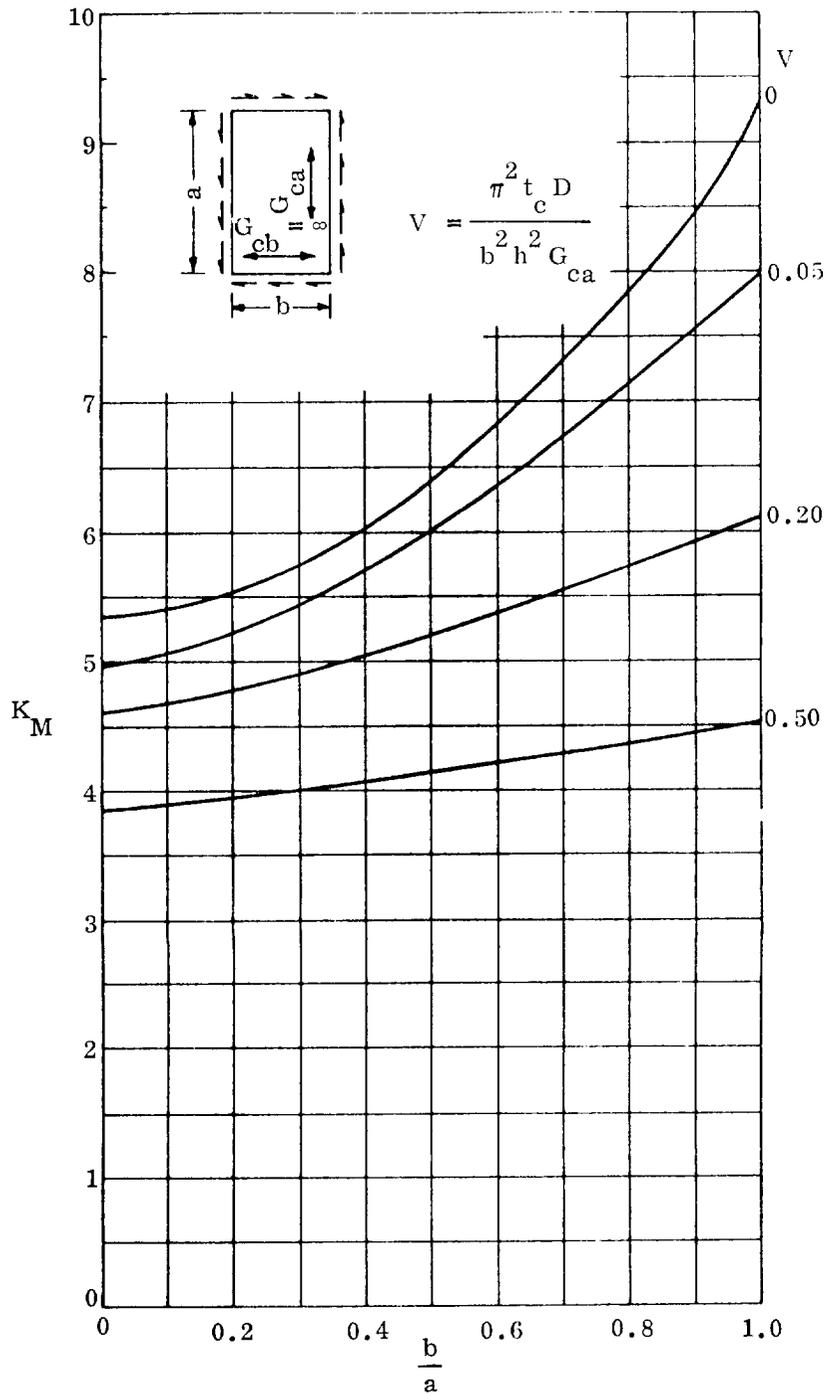
Figure 3.1-21. K_M for a Sandwich Panel with All Edges Simply Supported, Isotropic Facings and Corrugated Core. Core Corrugation Flutes are Parallel to Side b

3-33

$$V = \frac{\pi^2 D}{b^2 U}$$
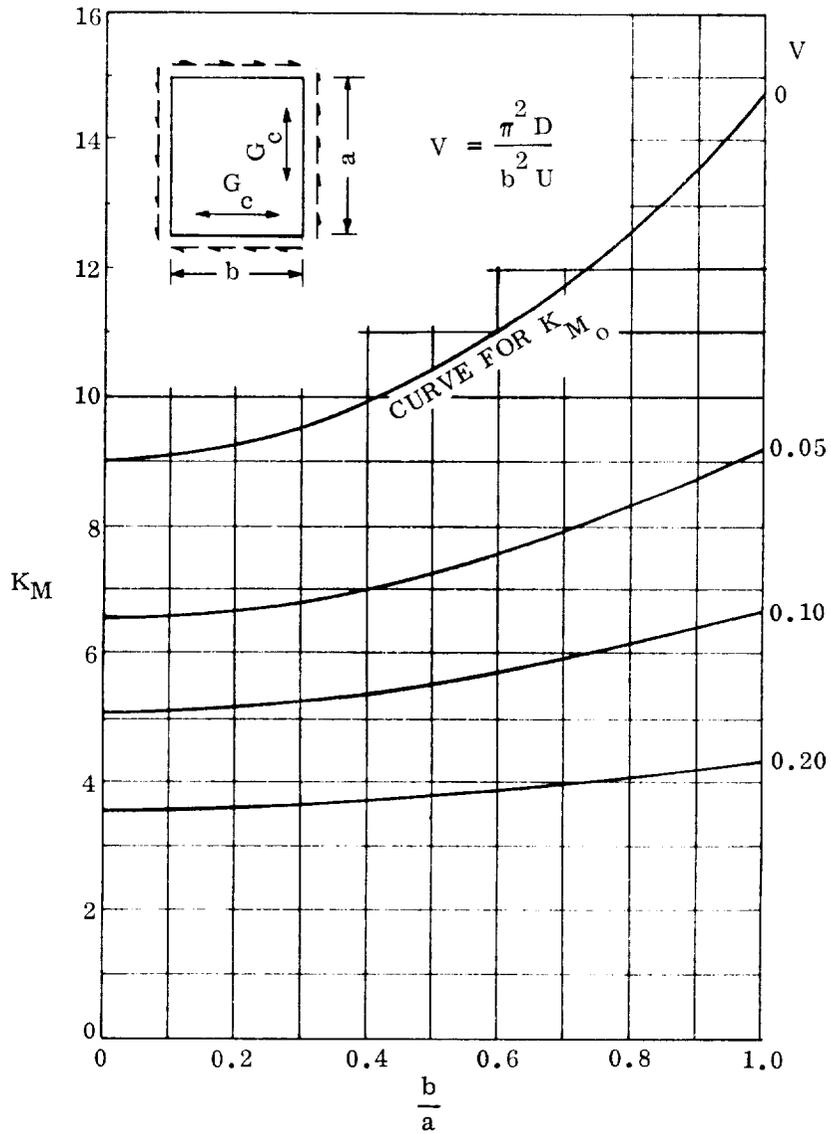
Figure 3.1-22. K_M for a Sandwich Panel with All Edges Clamped, Isotropic Facings and Isotropic Core, (R = 1.00)
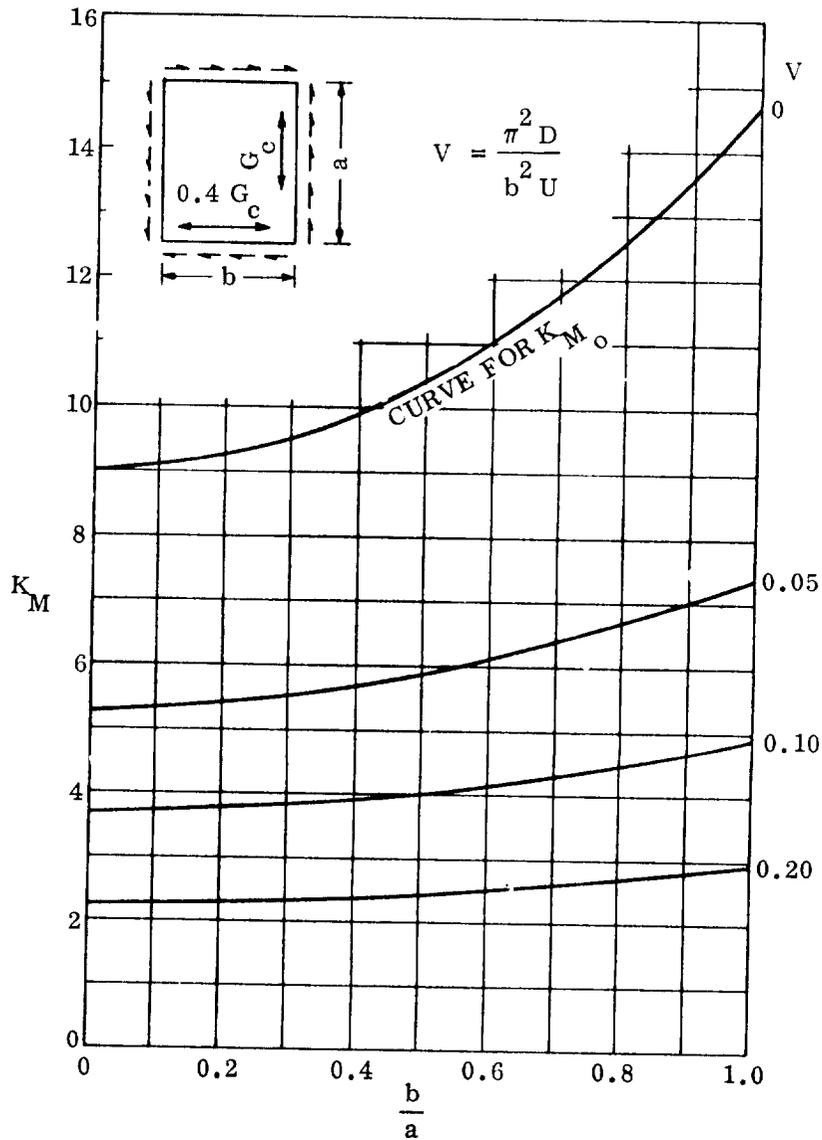
Figure 3.1-23. K_M for a Sandwich Panel with All Edges Clamped, Isotropic Facings and Orthotropic Core, (R = 2.50)

The figure shows a graph with K_M on the vertical axis (0 to 16) and $\frac{b}{a}$ on the horizontal axis (0 to 1.0). An inset shows a square panel with dimensions a and b, core shear moduli G_c and $0.4 G_c$, with the equation:

$$V = \frac{\pi^2 D}{b^2 U}$$

Curves are labeled with V values: 0 (CURVE FOR K_{M_o}), 0.05, 0.10, 0.20.
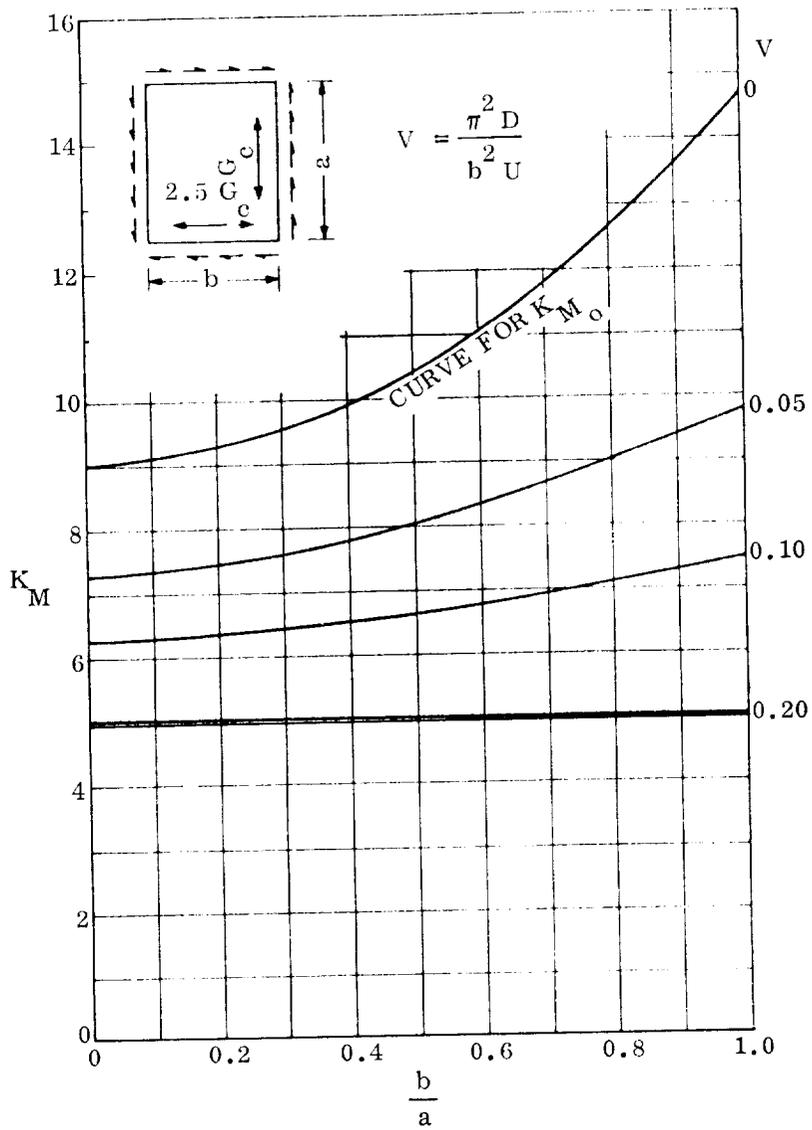
Figure 3.1-24. K_M for a Sandwich Panel with All Edges Clamped, Isotropic Facings and Orthotropic Core, (R = 0.40)

3.1.4   Edgewise Bending Moment

3.1.4.1   Basic Principles

The application of an edgewise bending moment to a flat, rectangular sandwich panel produces a loading condition such as that shown in Figure 3.1-25. This represents a somewhat different situation from the ones previously covered, since the tension loading on one half of the panel represents a stabilizing effect.   The edge compression load on the other half of the panel varies linearly from zero at the neutral axis to a maximum value, N, at the panel edge. It is this compression loading which can produce panel buckling in the same fashion as the uniaxial compression case; however, the presence of the panel edge support along the line of maximum loading forces consideration of a more complex failure mode.

These failure mode considerations for this type of loading have been covered in the development of analytical techniques for the evaluation of flat plates (Reference 3-17). Also, as has been previously noted, sufficient analytical development and testing has been accomplished on flat, rectangular sandwich panels to enable the use of the buckling coefficients given in Reference 3-1 for this loading condition with complete confidence. The general equations for the behavior of flat, rectangular honeycomb sandwich panels under this loading condition were developed by Kimel [3-15] while whose applicable to panels with a corrugated core were developed by Harris and Auelman, [3-14] and [3-16]. The assumptions employed in the development of the basic equation for the panel stability coefficient for this loading condition are generally the same as those described

in Section 3.1.1, with one particular exception. This exception requires that the

critical design faceplate stress, F_{cr}, shall not exceed the elastic buckling stress for

the faceplates. This requirement stresses the fact that the analysis is based on a

linear loading variation across the edge of the panel. Once the elastic buckling stress

is exceeded this variation is no longer linear, and extrapolation to a buckling stress

beyond the elastic range of facing stresses cannot be done by using an effective elastic

modulus such as the tangent modulus, in the buckling formulas. Since the proper

extrapolation to stresses beyond the elastic range must consider the variation of

effective elastic modulus across the panel width associated with the stress variation,

the equations and buckling coefficients given here are thus strictly applicable only to

buckling at facing stresses within the elastic range.

The basic equations to be used in the calculation of the allowable sandwich panel edge

loading are given in the following section. Design curves and buckling coefficients

for panels having isotropic faceplates and both isotropic and orthotropic cores based

on simply supported edge conditions follow these equations.

3.1.4.2   Design Equations and Curves

The design equations presented here are those taken from Reference 3-1. Background

assumptions and any applicable design constraints are also covered.

Using a linear stress variation as previously discussed, the value of N at the panel

edge is given by the equation:

$$N = 6M/b^2 \qquad\qquad (3.1\text{-}12)$$

where

N = load per unit width of edge

M = edgewise bending moment

b = panel width (Figure 3.1-25)

The edgewise bending load capability of a sandwich panel is given by the following

equation, taken from Reference 3-1:

$$N_{cr} = (\pi^2/b^2)(K_b)(D) \tag{3.1-13}$$

where

N_{cr} = critical edgewise loading, lb per inch

D = sandwich bending stiffness

The critical faceplate stresses are obtained by solution of the previous equation and

are as follows:

$$F_{c1,2} = \pi^2 K_b \frac{(E_1 t_1)(E_2 t_2)}{(E_1 t_1 + E_2 t_2)^2} \frac{(h^2)}{(b^2)} \frac{(E_{1,2})}{\lambda} \tag{3.1-14}$$

Or, for equal facings,

$$F_c = \frac{\pi^2 K_b}{4} \frac{(h^2)}{(b^2)} \frac{E}{\lambda} \tag{3.1-14a}$$

where

E = modulus of elasticity of facing

$\lambda = (1 - \mu^2)$

μ = Poisson's ratio of facings: $\mu_a = \mu_b$ assumed above

h = distance between facing centroids

b = length of loaded edge of panel

$K_b = K_F + K_M$ (Note: The values for these buckling terms differ
from those given in Sections 3.1.2 and 3.1.3)

3-39

$$K_F = \frac{(E_1 t_1^3 + E_2 t_2^3)(E_1 t_1 + E_2 t_2)}{12(E_1 t_1)(E_2 t_2)(h^2)} K_{M_o} \qquad (3.1-15)$$

Or, for equal facings

$$K_F = \frac{(t_f^2) K_{M_o}}{2 h^2} \qquad (3.1-15a)$$

where

$$K_{M_o} = \text{value of } K_M \text{ for } V = W = 0$$

Values of K_M for panel buckling are given in Figures 3.1-25 through 3.1-28 as a function of the parameter V or W, and the panel aspect ratio. These cover panels having isotropic faceplates using both isotropic and orthotropic cores, including those using corrugated flute-type cores.

The equations defining the parameters V and W are the same as those given in the previous section for edgewise compression; however, they are repeated below to facilitate their use. The equation numbers previously assigned to them are retained below; however, values of E' are replaced by those of E for this case.

$$V = \frac{(E_1 t_1)(E_2 t_2)(\pi^2) t_c}{\lambda (E_1 t_1 + E_2 t_2)(b^2) G_{ca}} \qquad (3.1-7)$$

$$V = \pi^2 t_c E_f t_f / 2\lambda \, b^2 G_{ca} \qquad \text{(equal facings)} \qquad (3.1-7a)$$

For a sandwich panel with a corrugated core in which the corrugation flutes are parallel to the edge of length a, the parameter V is replaced by the parameter W, which is defined as follows:

$$W = \frac{\pi^2 t_c (E_1 t_1)(E_2 t_2)}{\lambda\, b^2 G_{cb}\, (E_1 t_1 + E_2 t_2)} \qquad (3.1\text{-}8)$$

Or, for equal facings,

$$W = \pi^2 t_c E_f t_f / 2\lambda\, b^2\, G_{cb} \qquad (3.1\text{-}8a)$$

A particular design may be checked by using the graphs given in Figures 3.1-25 through 3.1-28 to determine the appropriate value of the buckling coefficient to use in Equation (3.1-15), or (3.1-15a) to compute the critical buckling stress, F_{cr}. This approach, which involves trial and error solutions by iteration, may also be employed to develop new panel designs; however, this manual recommends that the design-procedures approach described in Reference 3-1 be considered since it was set up to facilitate such design calculations.
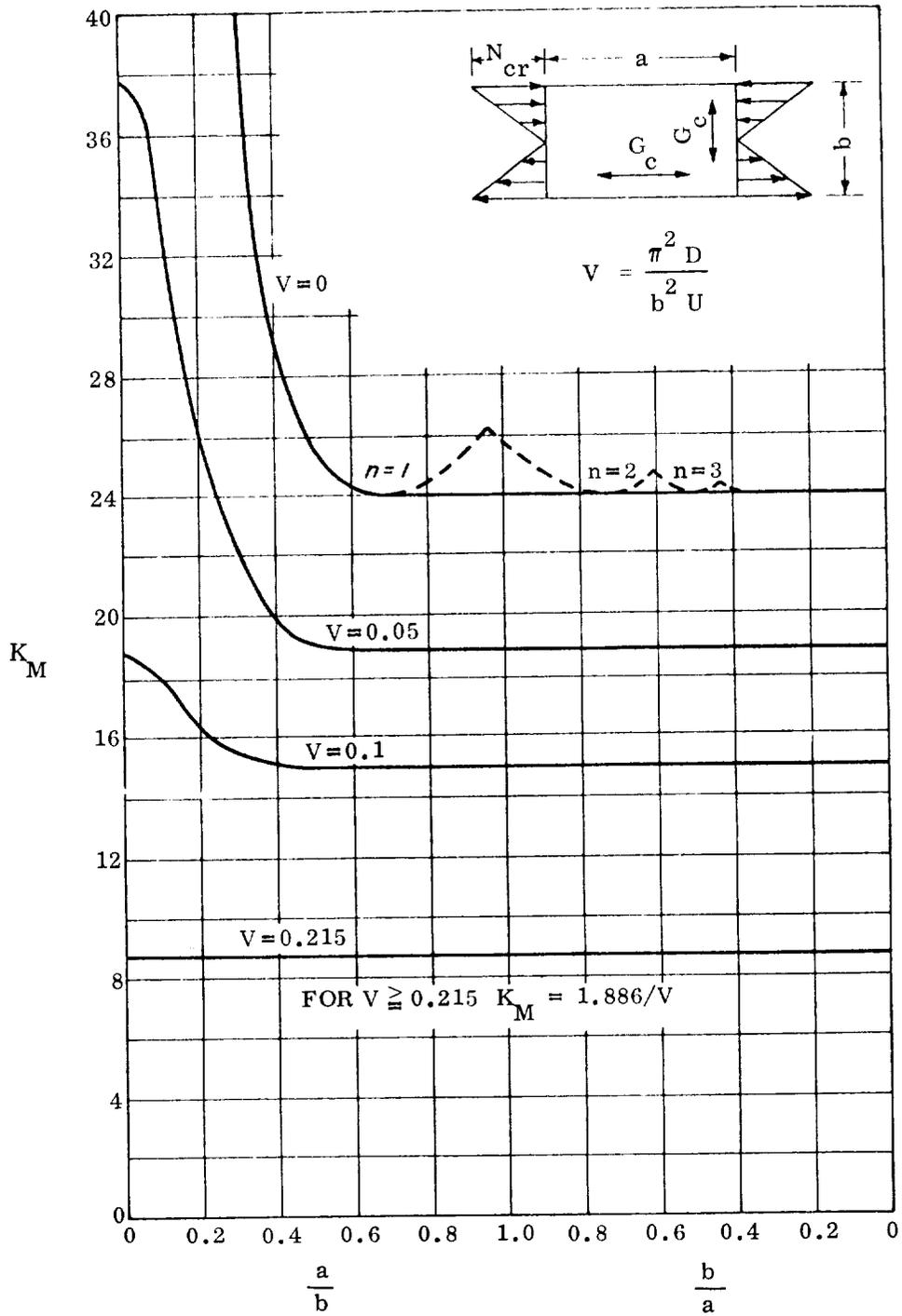
Figure 3.1-25. K_M for a Simply Supported Sandwich Panel with an Isotropic Core, $(R = 1.00)$

The graph contains the following labels and equations:

K_M (vertical axis)

$V = 0$

$V = 0.05$

$V = 0.1$

$V = 0.2$

$V = 0.4$

$n = 1$ $n = 2$ $n = 3$

$$V = \frac{\pi^2 D}{b^2 U}$$

N_{cr} a G_c $0.4\ G_c$ b

FOR $V \geqq 0.4$ $K_M = 1.886/V$

Horizontal axis: 0 0.2 0.4 0.6 0.8 1.0 0.8 0.6 0.4 0.2 0

$\dfrac{a}{b}$ $\dfrac{b}{a}$
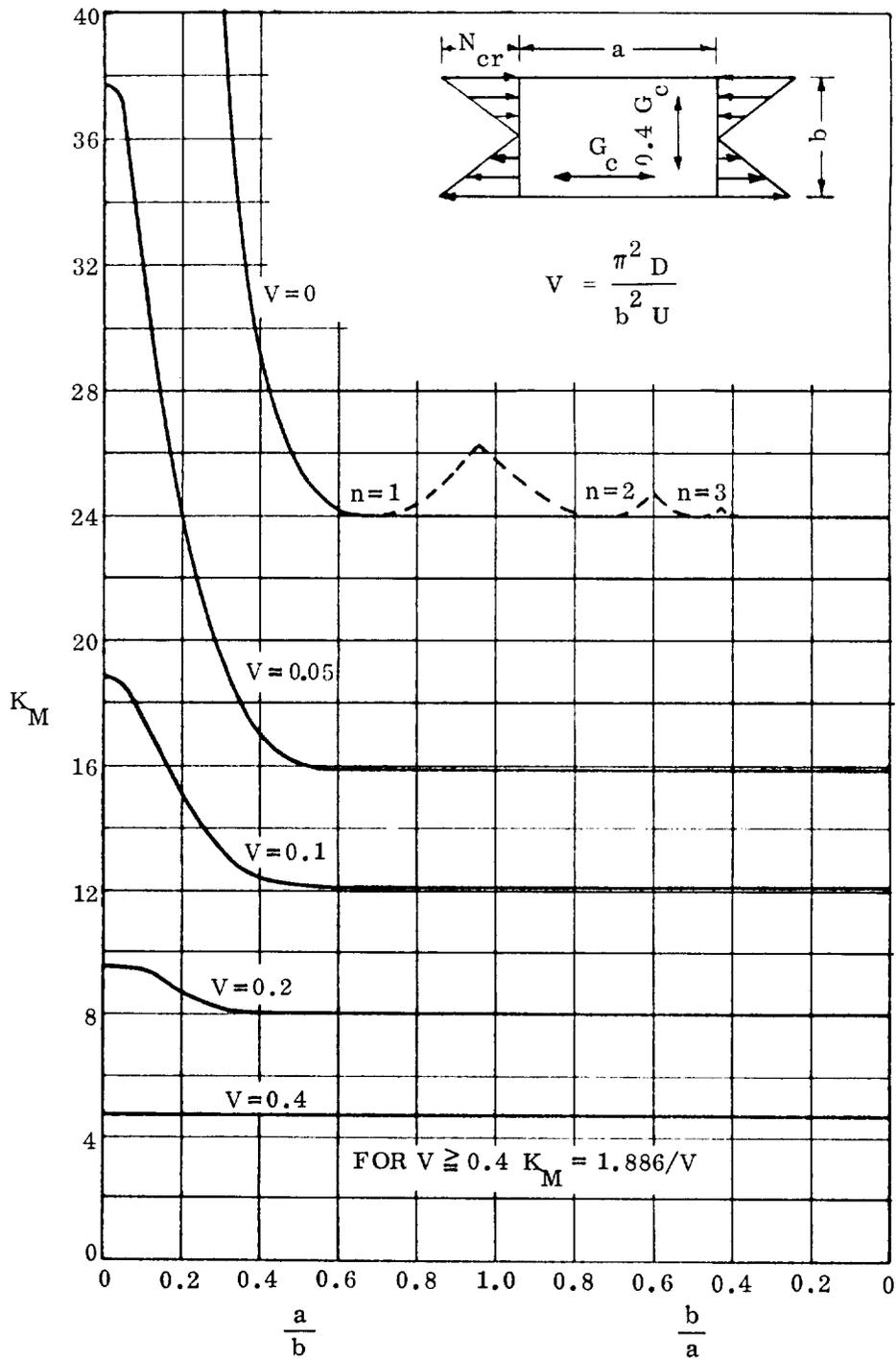
Figure 3.1-26. K_M for a Simply Supported Sandwich Panel with an Orthotropic Core, (R = 2.50)

3-43
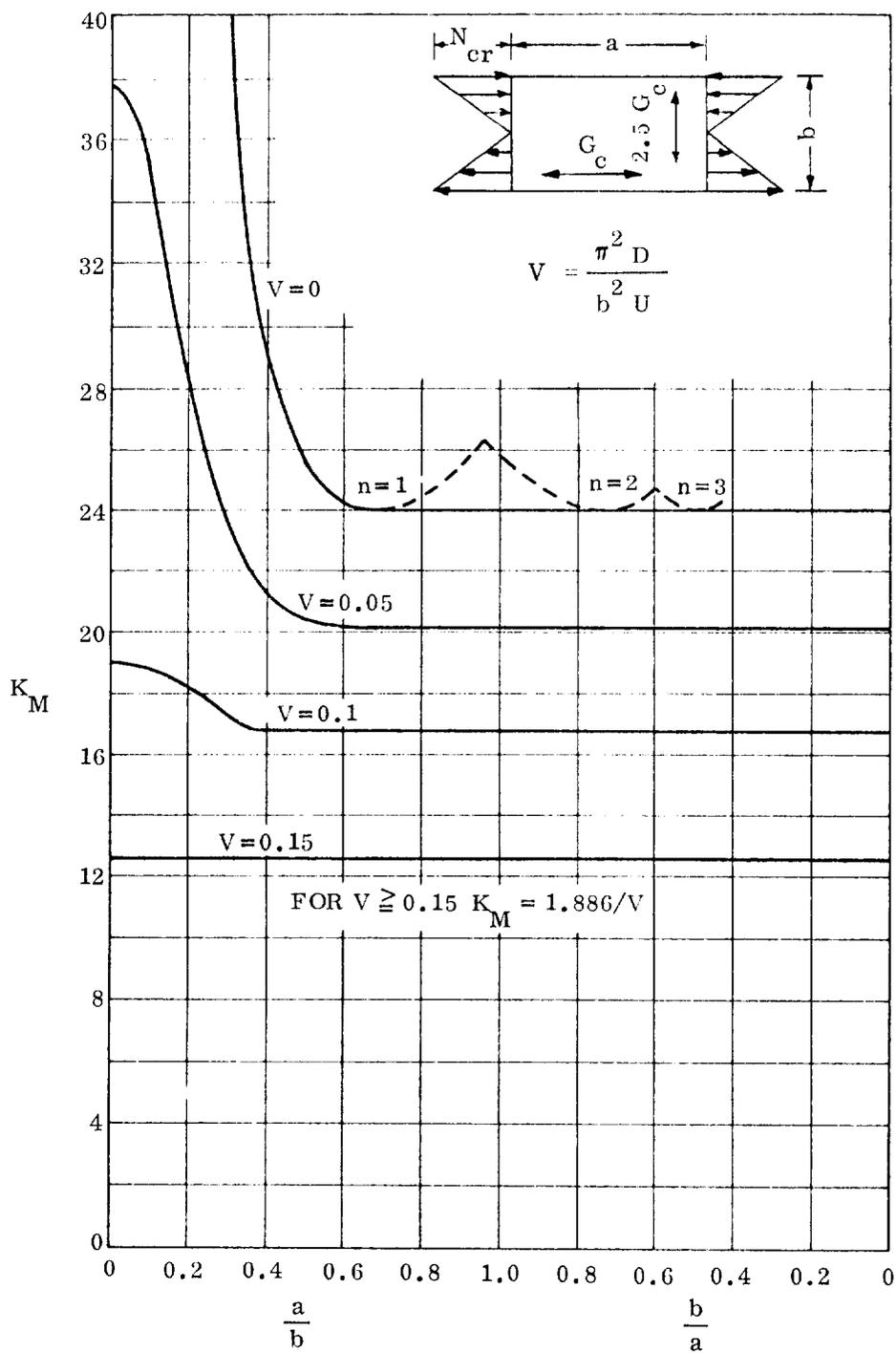
Figure 3.1-27. K_M for a Simply Supported Sandwich Panel with an Orthotropic Core, (R = 0.40)

$$W = \frac{\pi^2 t_c D}{b^2 h^2 G_{cb}}$$
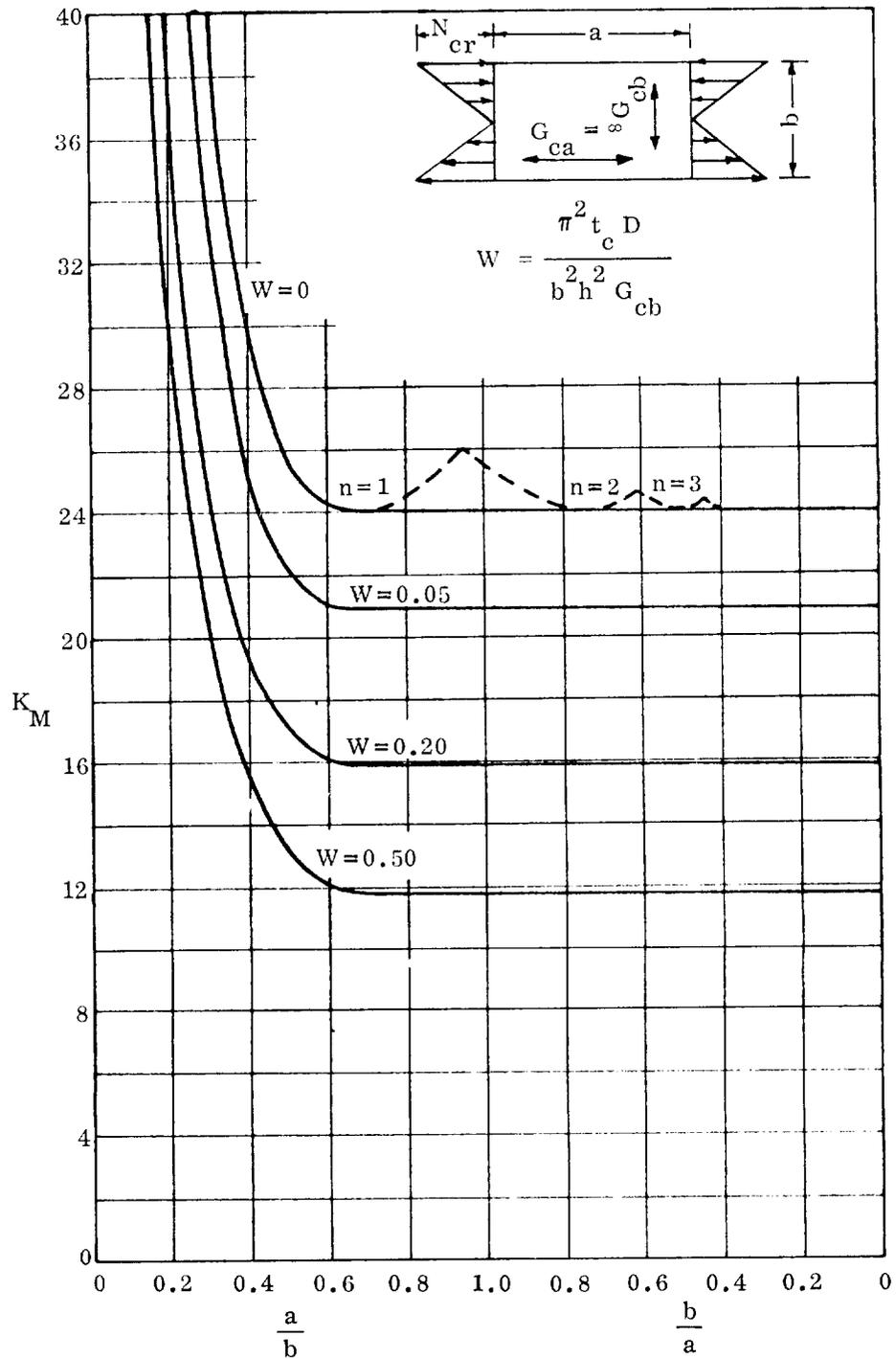
Figure 3.1-28. K_M for a Simply Supported Sandwich Panel with Corrugated Core. Core Corrugation Flutes Parallel to Side a

3.1.5   Other Single Loading Conditions

A search of the literature, as well as contacts with a number of people who have been active in the analytical methods field for this type of construction, revealed no other single loading conditions which might lead to panel instability problems. Consequently, the previously described loading conditions represent the extent of the flat panel stability data which will be given here for individual loading cases.

3.1.6   Combined Loading Conditions

3.1.6.1   Basic Principles

A study of the effects of combined loadings on the buckling of flat sandwich panels

requires the consideration of a number of factors. Some are:

   a.   The mode of failure of the panel under each of the applied loads.

   b.   The interaction between different modes for precipitation of panel

        buckling or failure.

   c.   The influence of variations in the core shear rigidity values on the

        interaction equations for panel instability failure under combined

        loadings.

Since little specific testing for biaxial instability modes has been accomplished for

flat sandwich panels, this part of the manual will provide analytically developed

equations for combination of the stress ratios which are conservative for most appli-

cations. Additionally, some discussion of the considerations involved is included

along with appropriate references in case more specific solutions or background is

needed.

The equations given on the following pages cover the interaction relationships between

the stress ratios, $(R_i = N_i/N_{i_{cr}})$, for each of the separate loadings which produce

failure by overall panel instability under the action of the combined loads. For the

stress ratio relationships which produce panel failure by local instability only, refer

to Section 2. These latter equations and pertinent discussion are not repeated here

although the specific equation number and report page are listed below for each of the local instability modes:

      a.   Intracellular Buckling: Equation (2.1-6), Page 2-7.

      b.   Face Wrinkling (Asymmetric): Equation (2.2-6), Page 2-26.

      c.   Face Wrinkling (Symmetric): Equation (2.2-15), Page 2-35.

It should be noted that there are no known data available for potential panel failures which might occur as a result of interaction between a local instability situation arising from the loading applied along one edge in conjunction with a general instability problem arising from the loading applied along the panel edge perpendicular to the first one. This situation might occur for panels having very high aspect ratios; however, most of these would also indicate a potential local instability failure under the action of the combined loads. In all cases, however, as has been previously noted, tests should be run to substantiate a final design in all cases where there is some question as to the structural adequacy of the sandwich component.

The effects of plasticity must be accounted for in calculating the stress ratios, R_i, to be used in the interaction equations which are given in later paragraphs. Reference is herewith made to the discussion and recommendations given in Section 9.2, COMBINED LOADING CONDITIONS, in this report and in particular to Equation (9.2-1) or (9.2-1a). Either of these equations define an effective uniaxial stress, σ_i, for use in determining an effective plasticity reduction factor which accounts for the effects of the biaxial stress field. Once the value of σ_i is known, the plasticity reduction factor, η, may be calculated by means of Equation (9.2-3).

3-48

3.1.6.2   Design Equations and Curves

The design equations and curves for combined loading conditions are separated into
those which should be used for sandwich panels having honeycomb cores and those to
be used with panels having corrugated cores. Supporting references are given for
each type and loading condition along with any limitations or restrictions on the use
of the interaction equation.

Sandwich Panels with Honeycomb Cores

The interaction relationships between the stress ratios which define the onset of general
instability buckling of honeycomb core panels under combined loadings are complex
functions of a number of factors. Some of these will be covered briefly here. One of
the prerequisites for the development of the interaction equation is the determination
of the number of half-waves in both the x and y directions for minimum energy plate
buckling. Since each of these is a function of not only its relationship with the other
but is also dependent upon the core shear rigidity parameter, V, the panel aspect
ratio, panel edge support considerations, etc., the establishment of general equations
covering all of these influences presents a formidable problem.

In view of the complexity involved in an exact definition of combined load interactions,
the writers of this manual propose the use of the following simplified stress ratio
relationships for panel buckling. These give somewhat conservative results over the
typical range of aerospace application and have been recommended for general use,
[3-1].

A. Biaxial Compression. The following formula is recommended for estimating buckling of a panel subjected to biaxial compression:

$$R_{cx} + R_{cy} = 1 \qquad (3.1\text{-}16)$$

where

$$R_c = N/N_{cr}$$

N = Loading along panel edge, lbs/inch.

N_{cr} = Critical loading along panel edge, lbs/inch. (See Equation 3.1-1.)

x, y = Subscripts denoting direction of loading. (See Figure 3.1-1.)

A plot of Equation (3.1-16) is given in Figure 3.1-29 to facilitiate its use in making design checks.

As noted in References 3-1 and 3-23, the above equation is correct for square, isotropic sandwich panels for which $V \approx 0$. It becomes appreciably conservative for panels of large aspect ratio, $(a/b \geq 3.0)$ and for panels bordering on the weak core regime $(V \geq 0.3)$. For panels with aspect ratios of 2.0 or less, and which have reasonably stiff honeycomb cores, Equation (3.1-16) provides a satisfactory method for prediction of the onset of panel buckling.

B. Bending and Compression. Equation (3.1-17) provides a sufficiently reliable method for the estimation of panel buckling under the action of combined bending and compression loads.

$$R_{cx} + (R_{Bx})^{3/2} = 1 \qquad (3.1\text{-}17)$$

where

R_c = N/N$_{cr}$ (See definition of Terms for Equation 3.1-16.)

R_B = (N/N$_{cr}$)$_{bending}$

N = Load per unit width of edge due to edgewise bending, lbs/in.

N$_{cr}$ = Critical edgewise loading on panel due to bending moment, lbs/in. (See Equation 3.1-13.)

Figure (3.1-30) plots the interaction relationship given by Equation (3.1-17) to enable its ready use.

References 3-19 and 3-23 are recommended, in case more accurate analysis of this loading combination is desired.

C.   Compression and Shear. The following interaction formula furnishes a dependable method for the prediction of panel buckling under this particular combination of loads:

$$R_c + (R_s)^2 = 1 \qquad\qquad (3.1-18)$$

where

R_c = N/N$_{cr}$ (See definition of terms for Equation 3.1-16.)

R_s = (N$_s$/N$_{scr}$)

N$_s$ = Shear loading per unit width of panel edge, lbs/in.

N$_{scr}$ = Critical edgewise shear loading, lbs/in. (See Equation 3.1-9.)

Equation (3.1-18) is plotted in Figure 3.1-31 to enable it to be more easily used in the solution of specific problems. References 3-21 and 3-23 develop this interaction relationship in greater depth for those needing this information.

D. Bending and Shear.   The following interaction equation represents a close

approximation of the buckling behavior of panels under combined edgewise

bending and shear loads.

$$(R_B)^2 + (R_s)^2 = 1 \qquad\qquad (3.1\text{-}19)$$

where

$R_B = (N/N_{cr})_{bending}$ These terms are defined as before for Equation (3.1-17).

$R_s = (N_s/N_{scr})$ As previously defined for Equation (3.1-18).

Again, as for the previous combined loadings, Equation (3.1-19) is plotted in

Figure 3.1-32 to make it more easily and readily usable. Reference 3-19 pro-

vides additional background information on the development of this interaction

equation.

Sandwich Panels with Corrugated Cores

The interaction equations for predicting the onset of general instability failure for

sandwich panels with corrugated cores involve the consideration of a number of com-

plex relationships also, as for the honeycomb core case. The same influences prevail

for fluted corrugations as before, with the additional consideration that the core shear

modulus normal to the direction of flute orientation is negligible in comparison to the

shear modulus measured parallel to the flutes. Also, the ability of the corrugations

to carry axial loading when it is applied along the axis of the flutes, further compli-

cates the problem since the distribution of this loading between the faceplates and the

flutes depends on the geometry and material thicknesses.

In view of the magnitude of the problem involved in developing specific equations for the interaction relationships, this manual will take advantage of the extensive studies in this area performed by Harris and Auelman, [3-14 and 3-16]. The latter reference presents interaction equations for the prediction of the onset of panel buckling in the form of curves relating the buckling coefficients to each other as a function of panel aspect ratio, the core bending-shear rigidity parameter, W, the relation between load direction and flute orientation, and the ratio of the loading carried by the flutes with respect to that carried by the faceplates. These interaction curves are repeated here in Figures 3.1-33 through 3.1-42 for several values of the shear rigidity parameter, W, and for the following additional relationships: 1) Panel aspect ratio, a/b = 1/2, 1.0, and 2.0, and 2) Amount of axial load carried by the core corrugations is negligible with respect to that carried by the faceplates, i.e., $D_c/D = 0$. (D_c = bending stiffness of corrugations, and D = bending stiffness of sandwich panel.)

A discussion of each of the sets of interaction curves follows.

A. Biaxial Compression. Interaction curves relating the buckling coefficients for this combined load condition are given in Figures 3.1-33 through 3.1-35. Buckling coefficients for other panel aspect ratios and different values of W may be obtained by interpolation.

The following example problem is offered to demonstrate how these curves may be used to predict the onset of panel buckling.

Given: Panel with N_x = 2000 lbs/in, N_y = 400 lbs/in, a = 30 in, b = 60 in, $D = 3.0 \times 10^5$ lbs/in^2, use W = 0 for example problem.

Figure 3.1-33 is used for this case since (a/b) = 1/2. The top line of this figure

applies since W = 0. The interaction equation takes the following general form:

$$R_{cx} + R_{cy} \le 1 \qquad\qquad (3.1\text{-}20)$$

or

$$\frac{N_x}{N_{xcr}} + \frac{N_y}{N_{ycr}} \le 1 \qquad\qquad (3.1\text{-}21)$$

where

R_{cx}, R_{cy} = Stress ratios for loads in subscript directions, dimensionless.

N_{xcr} = Critical panel loading for loading applied in the x direction, = $(\pi^2/b^2)\,(K_x)\,(D)$, lbs per inch.

N_{ycr} = Critical panel loading for the y direction, = $(\pi^2/b^2)\,(K_y)\,(D)$, lbs per inch.

K_x, K_y = Buckling coefficients for loading parallel to the subscript direction.

D = Sandwich bending stiffness = $\dfrac{E_f'\,(t_f)(t_c + t_f)^2}{2\,(1-\mu_f^2)}$ for equal facings.

W = $\pi^2\,(t_c)\,(E_f')\,(t_f)/2\,(1-\mu_f^2)\,(b^2)\,G_{cb}$ for equal facings.

E_f' = Effective Young's modulus for faces, psi.

G_{cb} = Core shear modulus in the direction parallel to the flutes, psi.

t_c = Thickness of core, inches.

t_f = Thickness of faceplates, inches.

μ_f = Poisson's ratio of faceplates.

a, b = Panel dimensions, inches.

Substituting in Equation (3.1-21):

$$\frac{N_x}{(K_x)(\pi^2)D/b^2)} + \frac{N_y}{(K_y)(\pi^2 D/b^2)} \leq 1.0 \qquad (3.1-22)$$

and, letting

$$r = N_y/N_x \qquad (3.1-23)$$

then

$$\left(\frac{N_x b^2}{\pi^2 D}\right)\left[\frac{1}{K_x} + \frac{r}{K_y}\right] \leq 1.0 \qquad (3.1-24)$$

Since D, b, N_x, and r will be known for the design in question, and K_x and K_y may be obtained from the appropriate curve, Equation (3.1-24) can be used in checking the panel stability on the basis that the panel margin of safety is the same for each loading direction. Thus,

$$(M.S.)_x = (M.S.)_y \qquad (3.1-25)$$

From which

$$\left(\frac{N_{xcr}}{N_x}\right) - 1.0 = \left(\frac{N_{ycr}}{N_y}\right) - 1.0$$

or

$$\left(\frac{N_{ycr}}{N_{xcr}}\right) = \left(\frac{N_y}{N_x}\right) = r \qquad (3.1-26)$$

then

$$\frac{(K_y)(\pi^2 D/b^2)}{(K_x)(\pi^2 D/b^2)} = r = \frac{K_y}{K_x} \qquad (3.1-27)$$

3-55

Returning to the data given for the example problem to demonstrate the method for checking panel stability:

$$r = N_y/N_x = (400/2000) = \underline{0.20}$$

$$K_y/K_x = 0.20, \text{ from Equation (3.1-27)}$$

Using Figure 3.1-33, erect a line passing through the origin and having a slope of $K_y/K_x = 0.20$ and extend it until it intersects the line for $W = 0$. The coordinates of this intersection point, as taken from the figure, are: $K_x = 6.0$, and $K_y = 1.2$.

Then,

$$N_{xcr} = K_x \, (\pi^2 D/b^2) = (6.0) \, (\pi^2 \times 3.0 \times 10^5/\overline{60}^2)$$

$$N_{xcr} = (6.0) \, (822.0) = \underline{4930} \text{ lbs/inch}$$

$$N_{ycr} = K_y \, (\pi^2 D/b^2) = (1.2) \, (822.0) = \underline{986} \text{ lbs/inch}$$

Solving Equation (3.1-21) for a panel stability check:

$$\frac{2000}{4930} + \frac{400}{986} = 0.406 + 0.406 = 0.812$$

Since the total is less than 1.0, the panel is stable under the applied loads. The margin of safety for panel buckling is: M.S. $= (1.0/0.812) - 1.0 = \underline{+0.232}$.

B.   Combined Compression Along Core Flutes and Shear.   Figures 3.1-36 through

3.1-38 give curves showing the interaction relationships between the buckling

coefficients for panels loaded in this manner.   Curves for other panel aspect

ratios and values of the shear rigidity parameter may be developed by inter-

polation from those given.   Panel stability checks for this combined loading

condition are made in the same manner as for the biaxial compression case.

This is accomplished by handling the calculations for the R_s term in the inter-

action equation in the same way as was done for the R_{cy} term in the example

given on page 3-53.

C.   Combined Compression Normal to Core Flutes and Shear.   Interaction curves

for the buckling coefficients covering this particular combination of loads are

given in Figures 3.1-39 through 3.1-41.   These curves may be interpolated to

obtain values for the specific design under study and the stability checks may

be made in a similar fashion to those for the biaxial compression case.   The

method to be used in performing design checks on panels loaded in this manner

is the same as that noted in item (B) above.

D.   Combined Biaxial Compression and Shear.   Figure 3.1-42 shows the relation-

ships for the compression and shear buckling coefficients for this loading con-

dition.   These curves are for a square panel only, however, as may be noted

from the small change in the values of K_y between the various values of the

shear rigidity parameter, W, approximate interpolations may be made on the

basis of ratios obtained from the curves of Figures 3.1-36 through 3.1-38.

Panel stability checks are made in basically the same manner as for the example problem given on page 3-53, except that the stress ratio, R_{cy}, is handled differently. The basic interaction equation for this condition takes the following general form:

$$R_{cx} + R_{cy} + R_s \leq 1$$

where

R_{cx} and R_{cy} are as defined on page 3-54.

$$R_s = (N_{xy}/N_{scr}) = [N_{xy}/(\pi^2/b^2)(K_s)(D)]$$

K_s = buckling coefficient for shear

Since, as may be seen in Figure 3.1-42, K_y is a function of W only for this case and is independent of the values of K_x and K_s, the value for R_{cy} may be calculated imm..diately and the interaction equation put in the following form:

$$R_{cx} + R_s = (1.0 - R_{cy}) \quad : \quad \text{Or,} \quad R_{cx} + R_s = C$$

The design check may now be performed in the same way as for the example problem on page 3-53, if the R_s term and calculations are handled in the same way as the R_{cy} term and calculations were handled for the example. It is to be noted, however, that the term on the right side of the equation, C, has a value which is less than 1.0 and this value should be used in place of the 1.0 used in the example. Thus, assuming R_{cy} = 0.10, then C = 1.0 – 0.1 = 0.9, and the margin of safety for panel buckling as calculated on page 3-57 for the example would now become:

$$M.S. = (0.90/0.812) - 1.0 = +0.109$$

$(R_{cx} + R_{cy} = 1.0)$
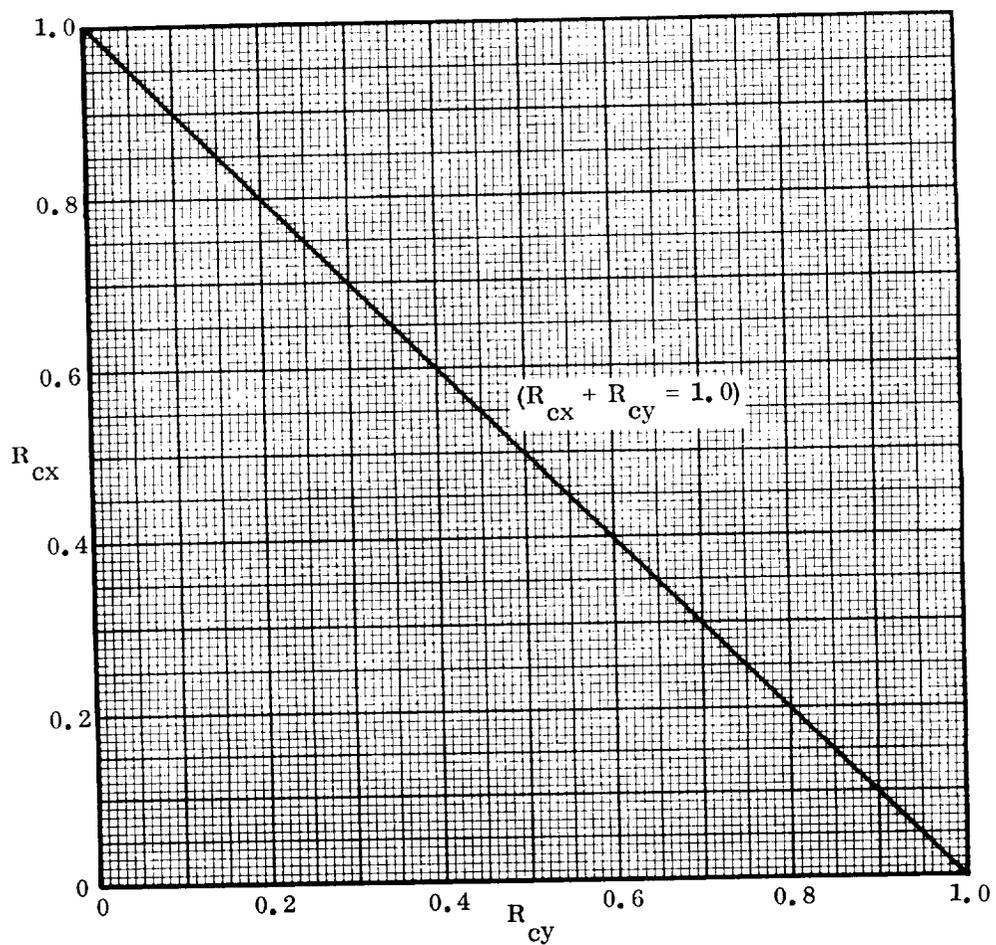
Figure 3.1-29. Interaction Curve for a Honeycomb Core Sandwich
Panel Subjected to Biaxial Compression
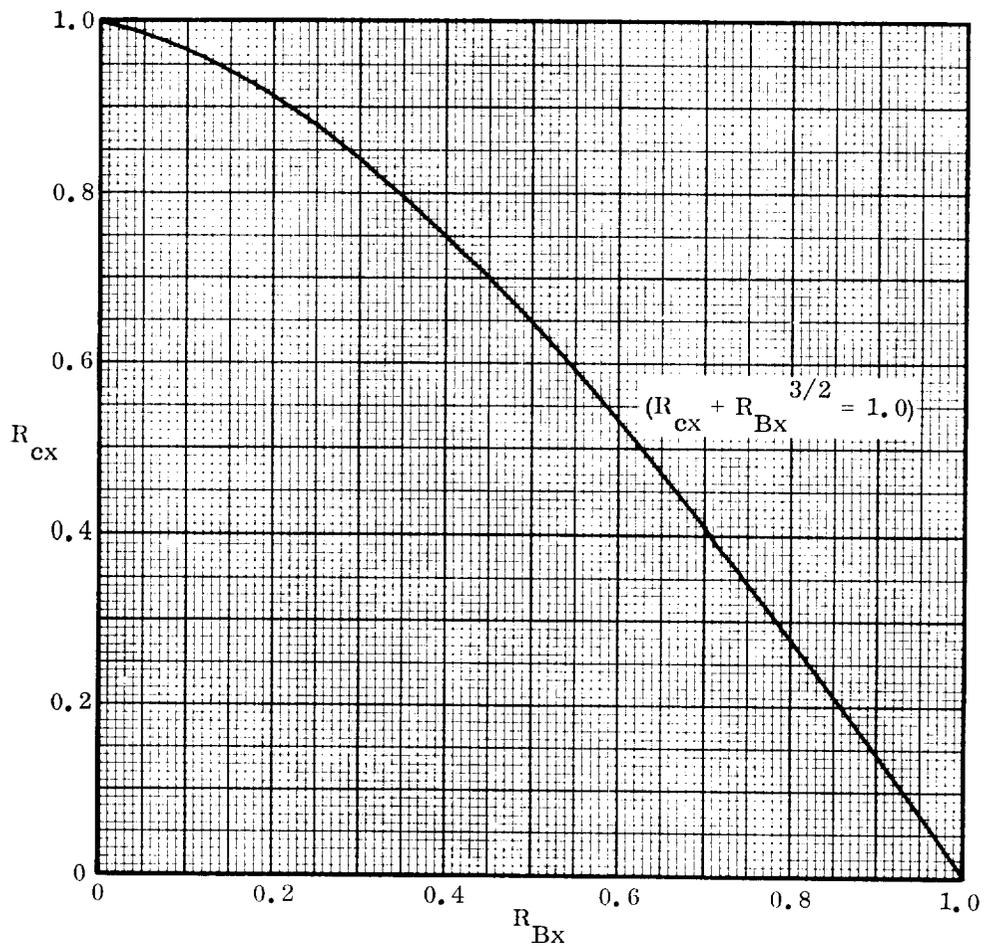
Figure 3.1-30. Interaction Curve for a Honeycomb Core Sandwich
Panel Subjected to Bending and Compression

The curve is labeled $(R_{cx} + R_{Bx}^{3/2} = 1.0)$. The vertical axis is R_{cx} and the horizontal axis is R_{Bx}.

3-60

$$(R_c + R_s^{\ 2} = 1.0)$$
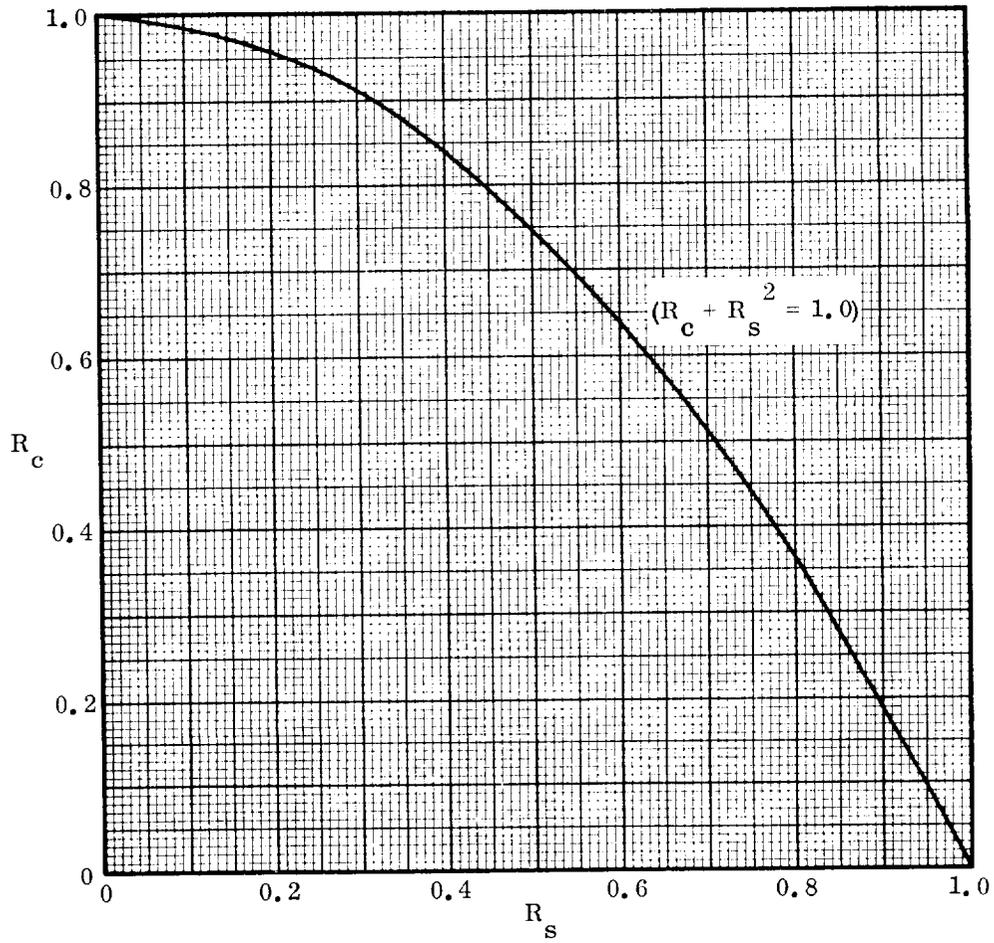
Figure 3.1-31. Interaction Curve for a Honeycomb Core Sandwich
Panel Subjected to Compression and Shear

3-61
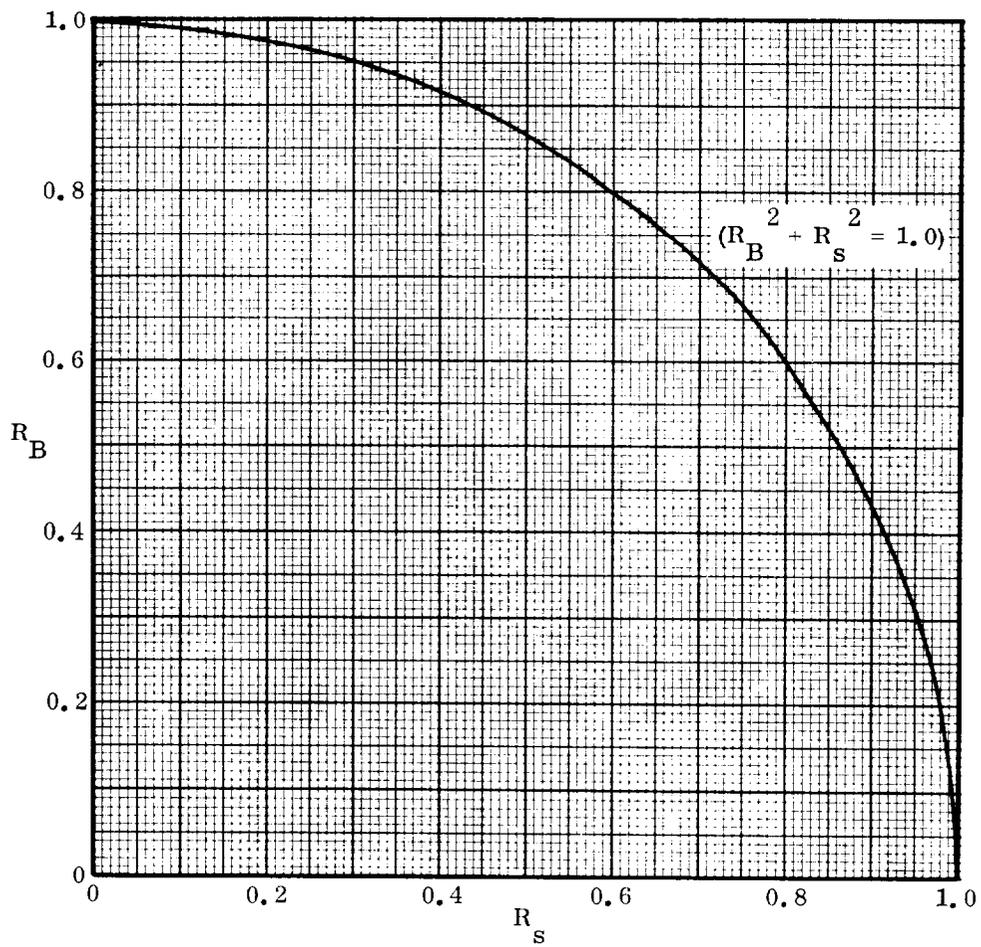
Figure 3.1-32. Interaction Curve for a Honeycomb Core Sandwich
Panel Subjected to Bending and Shear
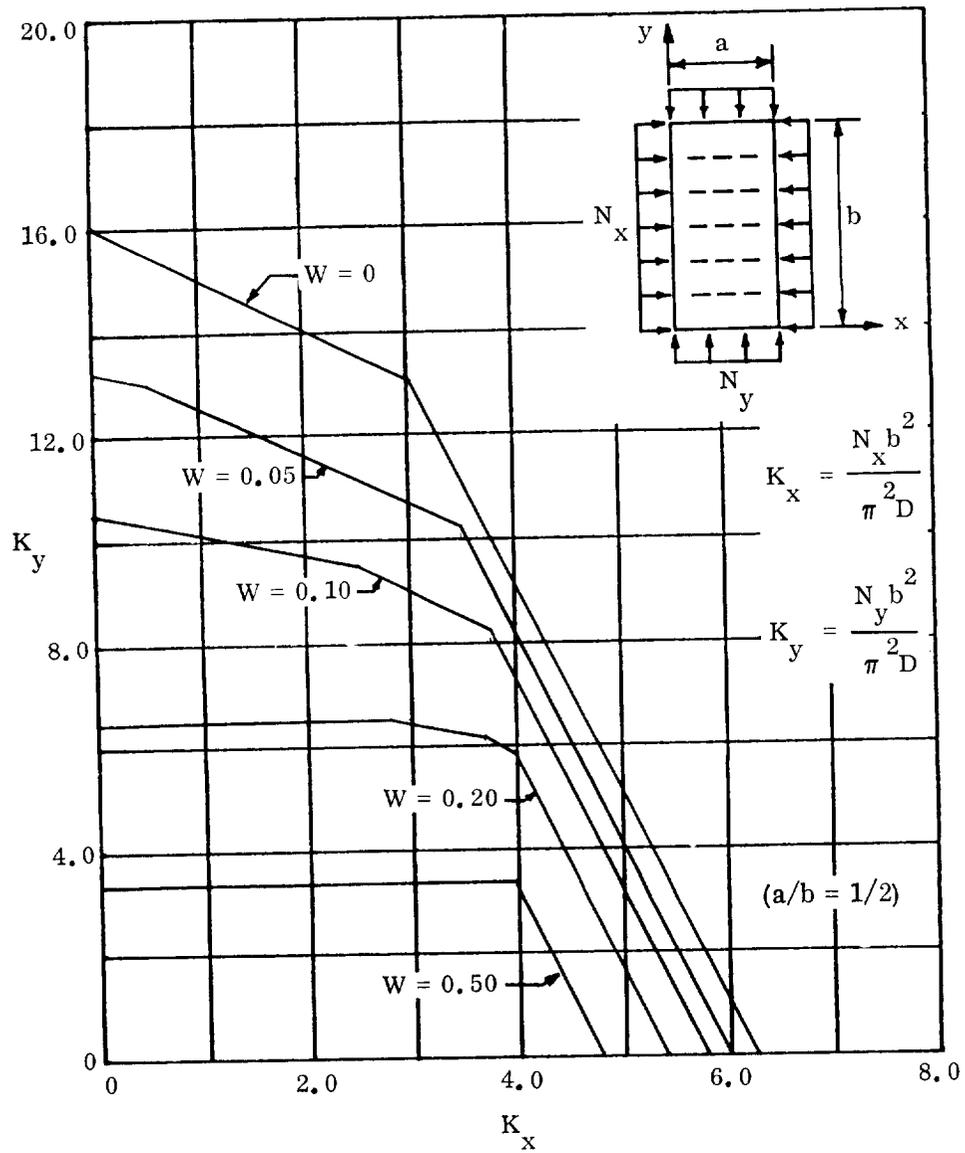
Figure 3.1-33. Buckling Coefficients for Corrugated Core Sandwich
Panels in Biaxial Compression (a/b = 1/2)
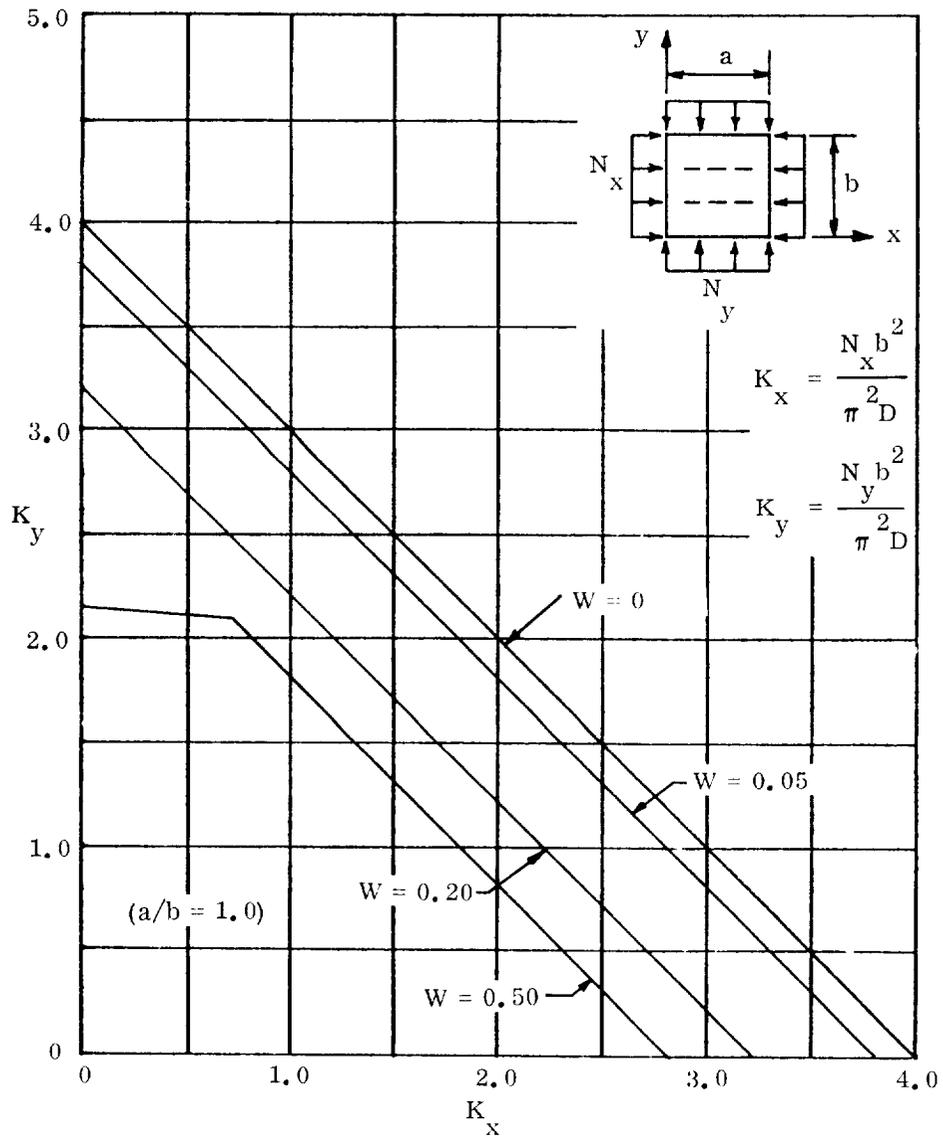
Figure 3.1-34. Buckling Coefficients for Corrugated Core Sandwich
Panels in Biaxial Compression (a/b = 1.0)

3-64
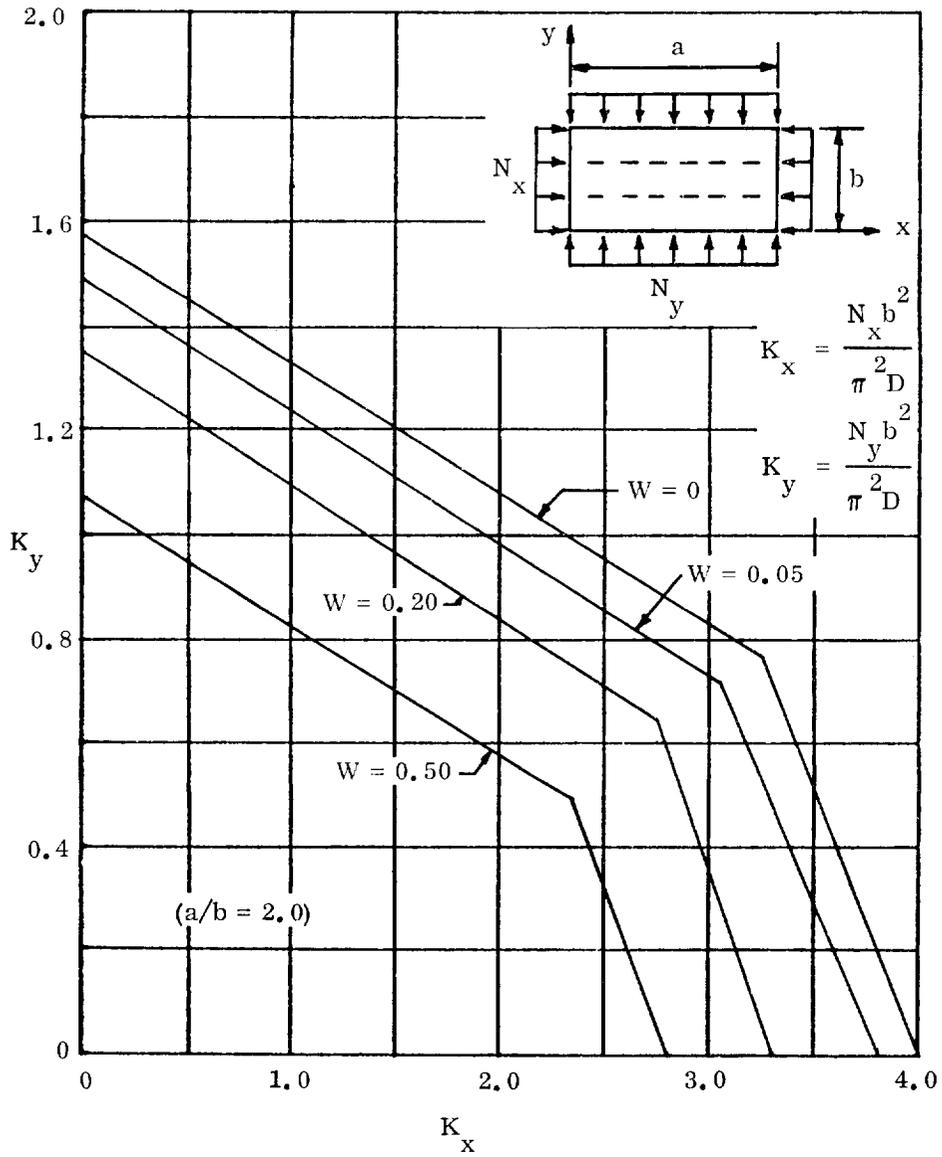
Figure 3.1-35. Buckling Coefficients for Corrugated Core Sandwich
Panels in Biaxial Compression (a/b = 2.0)
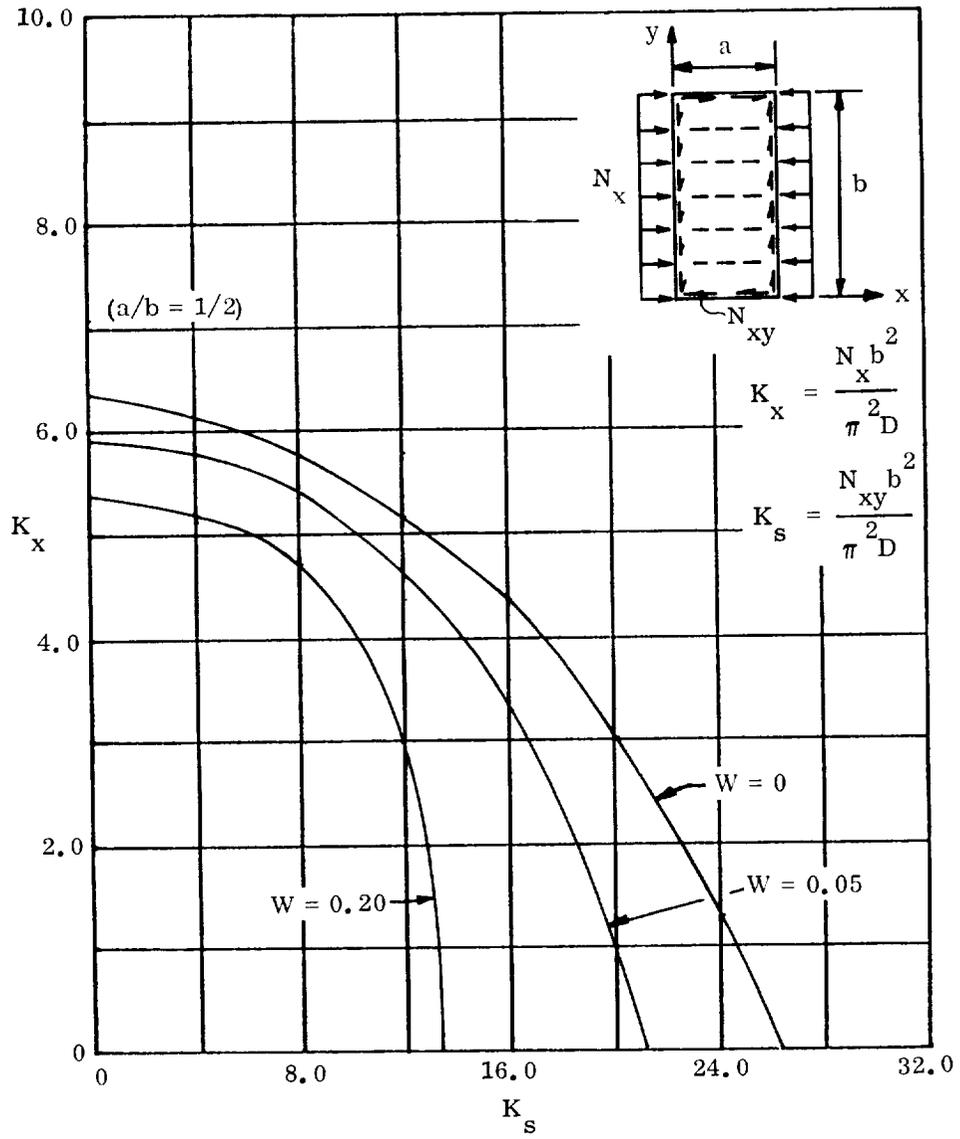
Figure 3.1-36. Buckling Coefficients for Corrugated Core Sandwich Panels Under Combined Longitudinal Compression and Shear with Longitudinal Core (a/b = 1/2)
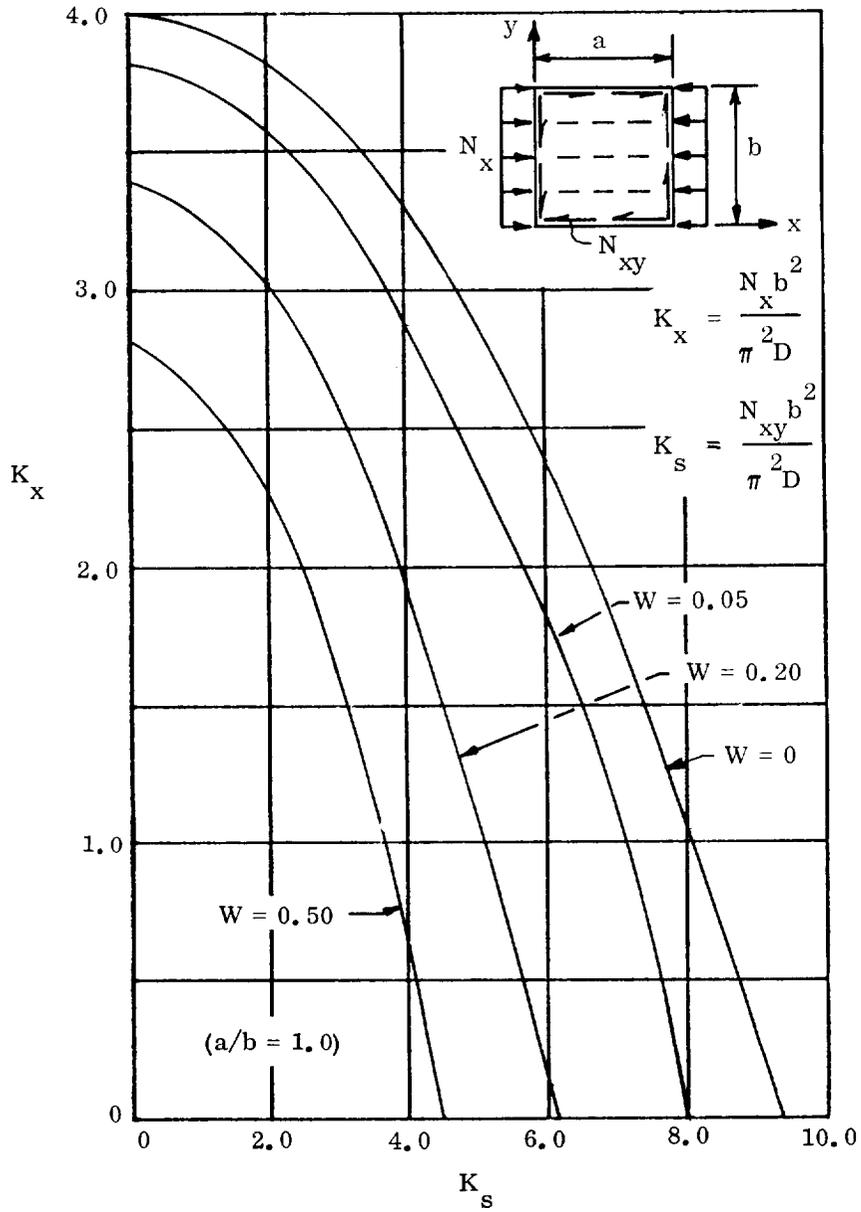
Figure 3.1-37. Buckling Coefficients for Corrugated Core Sandwich Panels Under Combined Longitudinal Compression and Shear with Longitudinal Core (a/b = 1.0)
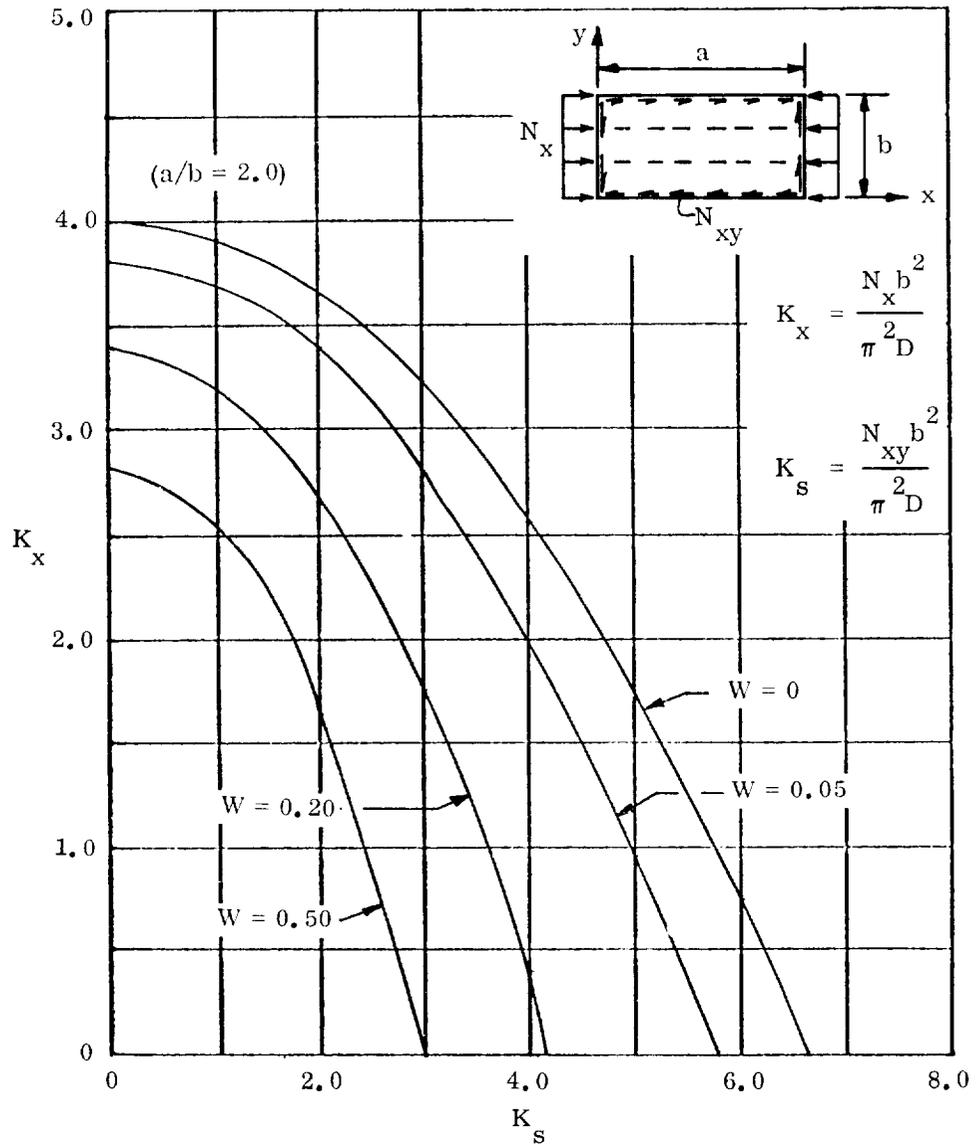
Figure 3.1-38. Buckling Coefficients for Corrugated Core Sandwich
Panels Under Combined Longitudinal Compression
and Shear with Longitudinal Core (a/b = 2.0)
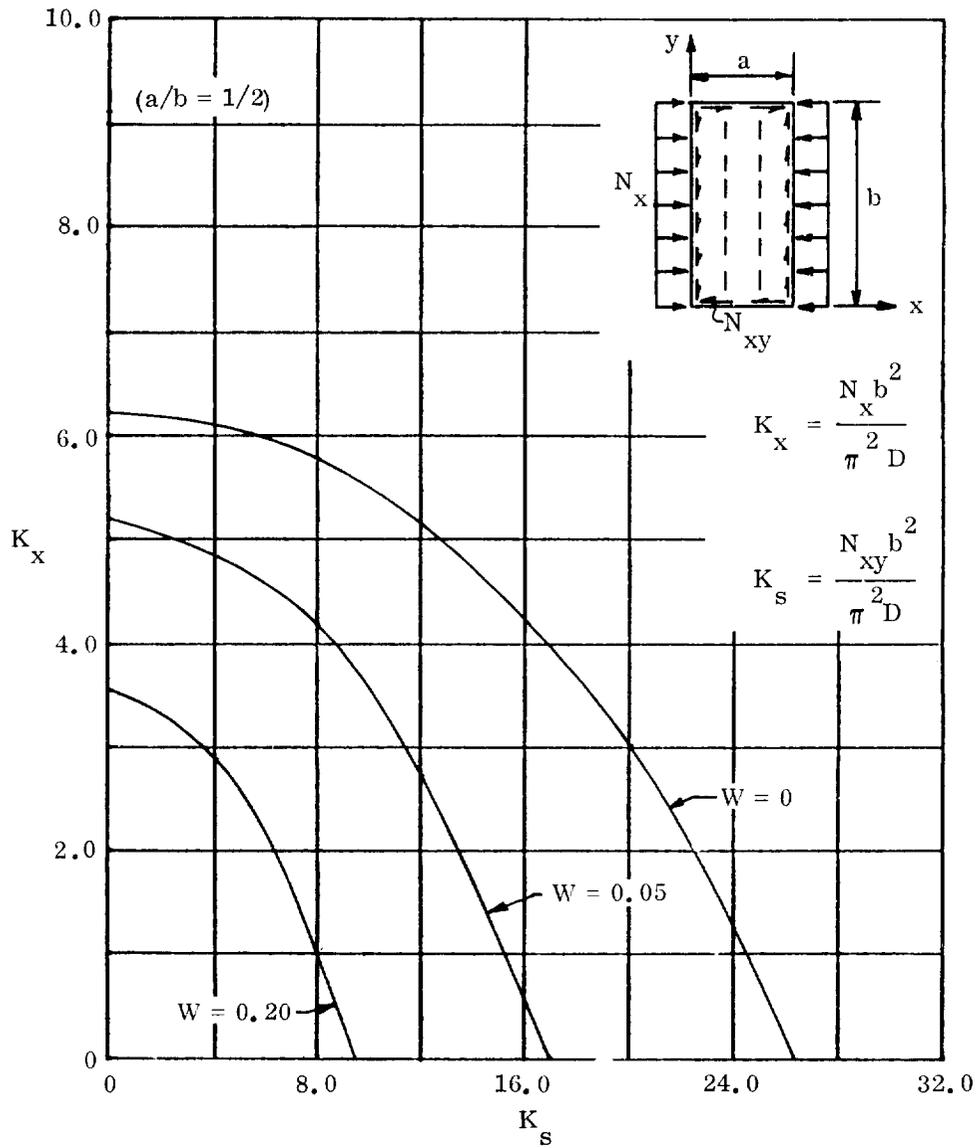
Figure 3.1-39. Buckling Coefficients for Corrugated Core Sandwich Panels Under Combined Longitudinal Compression and Shear with Transverse Core (a/b = 1/2)
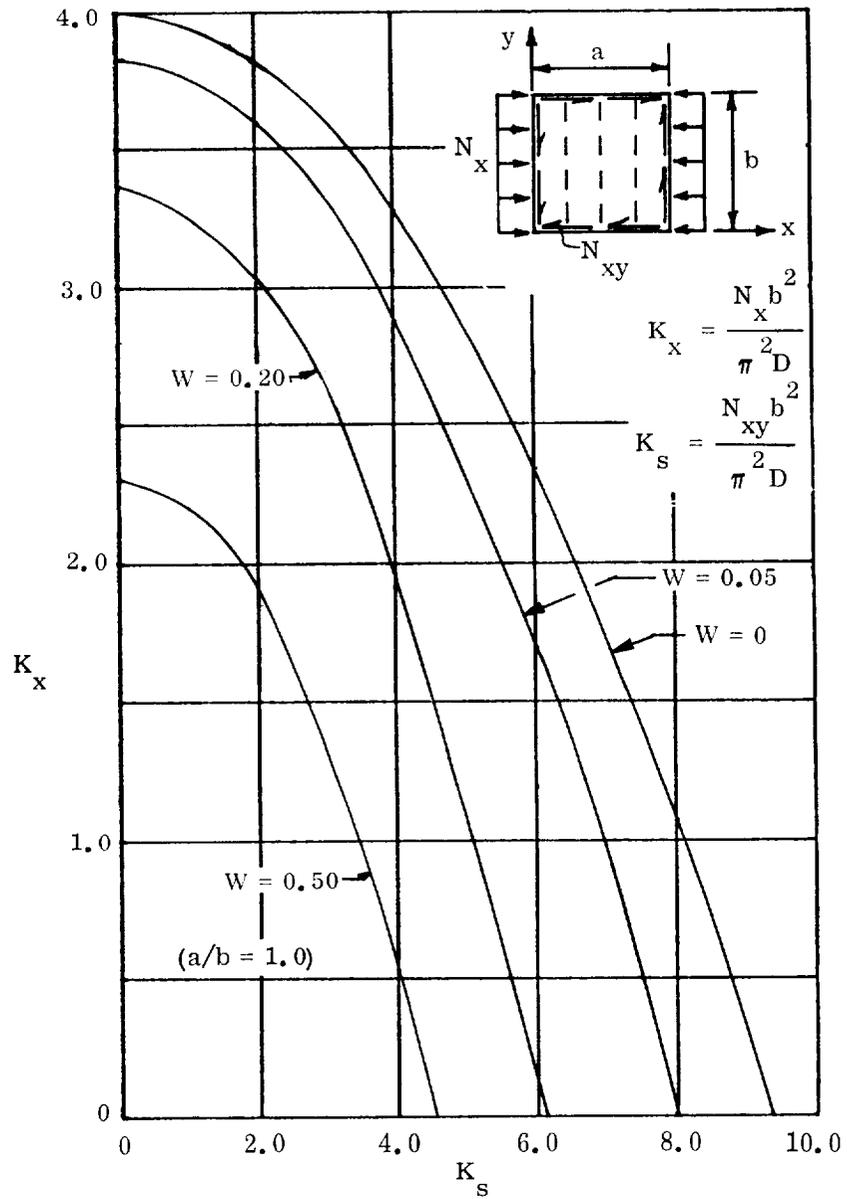
Figure 3.1-40. Buckling Coefficients for Corrugated Core Sandwich Panels Under Combined Longitudinal Compression and Shear with Transverse Core (a/b = 1.0)

$$K_x = \frac{N_x b^2}{\pi^2 D}$$

$$K_s = \frac{N_{xy} b^2}{\pi^2 D}$$
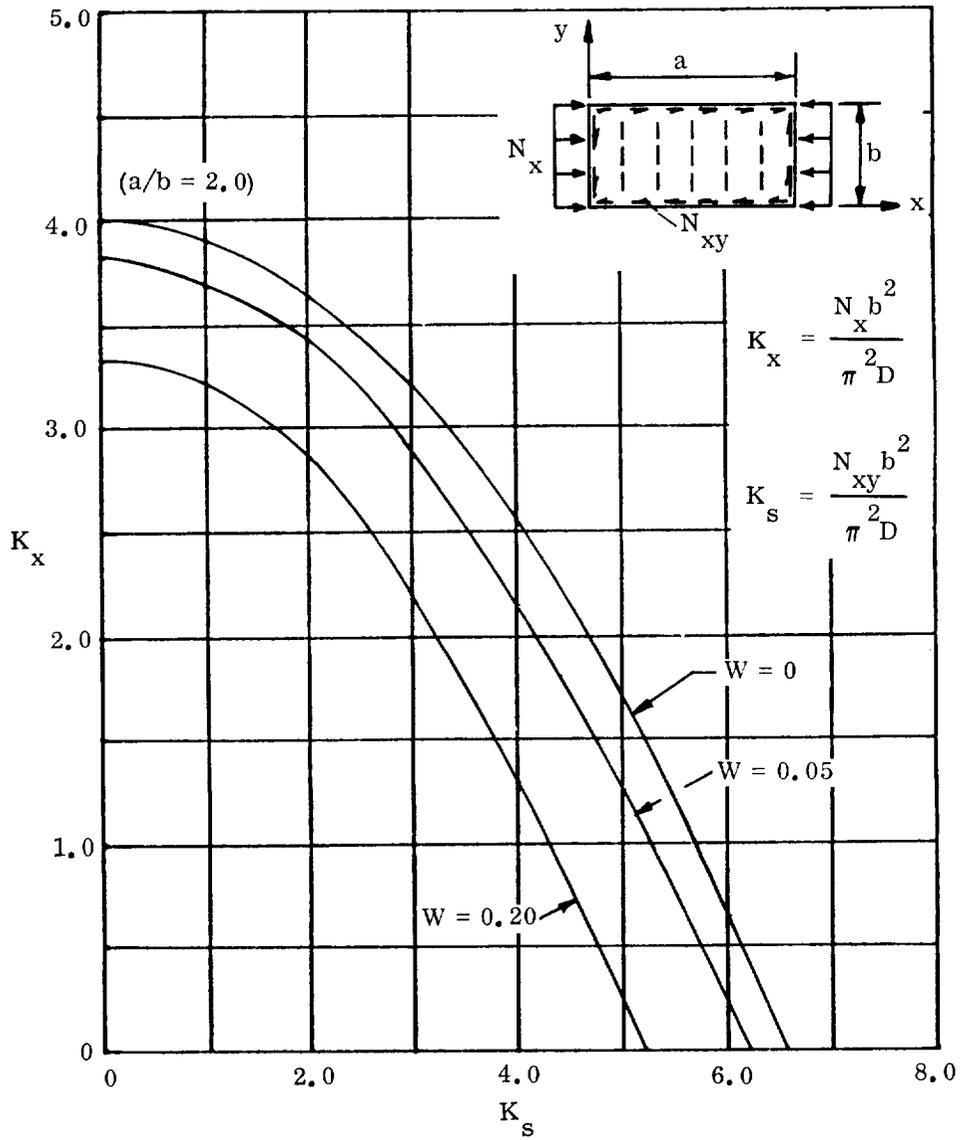
Figure 3.1-41. Buckling Coefficients for Corrugated Core Sandwich
Panels Under Combined Longitudinal Compression
and Shear with Transverse Core (a/b = 2.0)

K_X

2.5

2.0

(a/b = 1.0)

1.5

1.0

$K_y = 1.2$

$K_y = 1.7$

W = 0.20

0.5

W = 0.50

0

0   2.0   4.0   6.0   8.0

K_S

y

a

N_{xy}

N_x

b

x

N_y

$K_S = \dfrac{N_{xy} b^2}{\pi^2 D}$

$K_x = \dfrac{N_x b^2}{\pi^2 D}$

$K_y = \dfrac{N_y b^2}{\pi^2 D}$

W = 0
$K_y = 2.0$

W = 0.05
$K_y = 1.9$
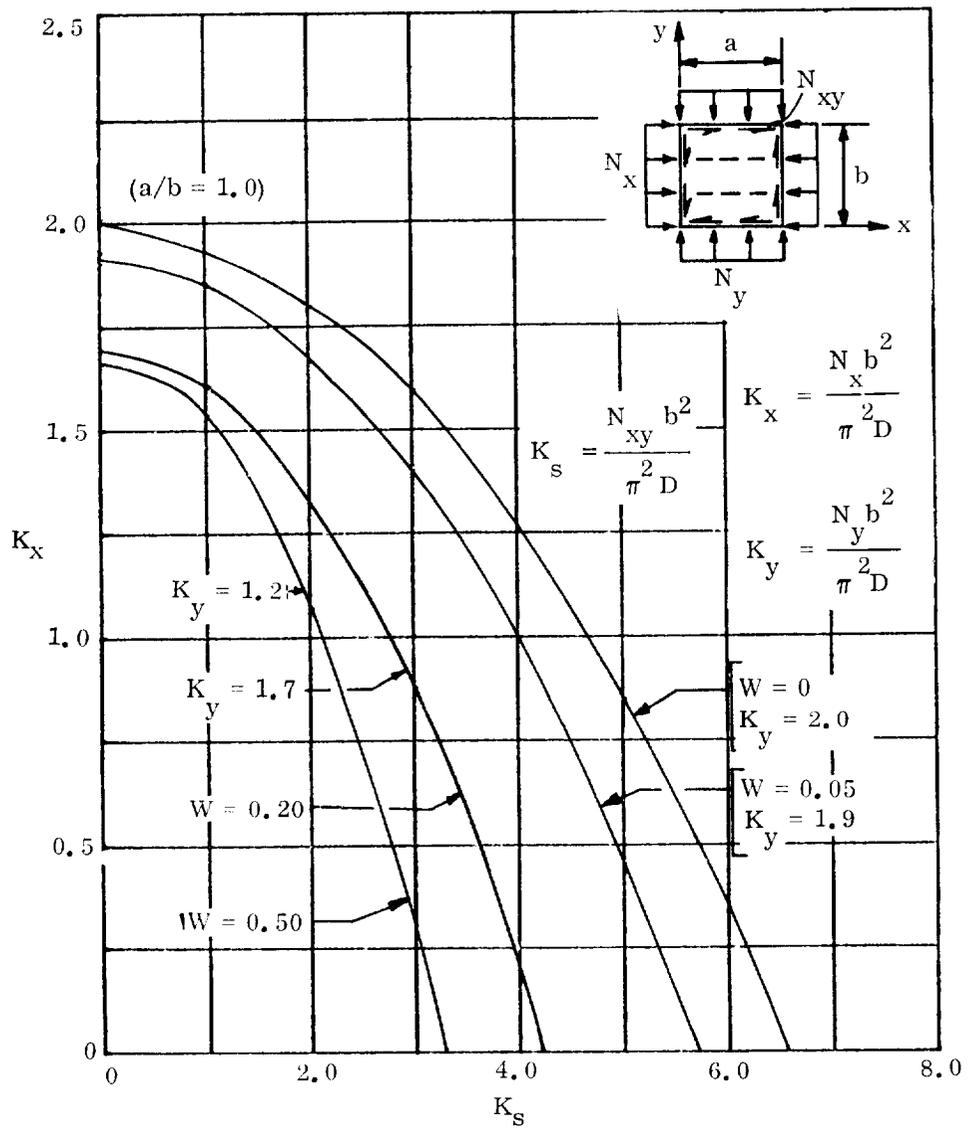
Figure 3.1-42. Buckling Coefficients for Corrugated Core Sandwich Panels
Under Combined Longitudinal Compression, Transverse
Compression, and Shear with Longitudinal Core

3-72

3.2   CIRCULAR PLATES

3.2.1   Available Single Loading Conditions

A search of the available literature as well as contacts with others who are familiar with sandwich panel stability references and studies in progress uncovered no stability solutions for any single loading condition. This result might have been anticipated since the flat, circular sandwich plate has very few applications in aerospace vehicle structures in which it must be stable under the applied loads. Consequently, this manual makes no recommendations for techniques to be used in design, and strongly suggests that all final configurations be tested as required to demonstrate their adequacy structurally.

3.2.2   Available Combined Loading Conditions

No panel stability solutions were found for any combined loading conditions applicable to flat, circular plates in the course of the literature search noted in Section 3.2.1. Consequently, this manual makes no recommendations for possible analytical approaches which would describe any stability limits for circular, flat sandwich plates.

3.3 PLATES WITH CUTOUTS

3.3.1 Framed Cutouts

While it is highly desirable to avoid cutouts in aerospace structures because of the attendant weight problems as well as uncertainties about load pile-up and redistribution, these are a practical necessity because of access and other requirements and every effort should be made to derive reliable design approaches which minimize these drawbacks.

Most generalized solutions for plates with cutouts employ framing members and base the analysis on the assumption of buckled skin panels which carry only shear loads. Obviously, the solution becomes much more complex when skin buckling does not occur, as would be the case for a framed cutout in a sandwich panel. Despite the increased complexity, however, solutions for the load distribution around the cutout can be obtained for various load applications away from the opening. Knowing the load distribution adjacent to the cutout does not necessarily provide an answer to all questions regarding the adequacy of the design, however, particularly in the case of sandwich construction.

In the case of monocoque or semi-monocoque panels, the lateral moments of inertia of the framing members are generally sufficiently greater than those of the skin such that they may be considered to provide lateral support for the panel edge. This is not necessarily the case for sandwich panels, thus setting up the case of a free, or nearly free, edge for the panel and for which condition no general stability solutions or data were found in the course of this study.

It may be possible for specific designs to be assessed, on the basis of good engineering

judgment, to be critical in local instability rather than for general instability. This

being the case, design checks may be made on the basis of the equations given in

Section 2. This manual makes no recommendations for those cases where the general

instability mode appears to control beyond the exercise of good judgment in the devel-

opment of the design, and sufficient testing as needed to insure its integrity.

3.3.2 Unframed Cutouts

Unframed cutouts in sandwich panels have all of the disadvantages noted for framed

cutouts and represent a much more serious design problem locally, insofar as the

free edge is concerned. The writers of this manual encountered no instances in which

such a design approach was used in primary or secondary structure and, in general,

recommend avoidance of this practice. This recommendation is based not only on the

lack of any analytical or test data but also on potential problems of faceplate-core bond

separation along the free edge due to damage while in use, adhesive deterioration,

load cycling, etc.

Table 3-1. Summary of Design Equations for General Instability of Flat Sandwich Panels

NOTATION: N = Edgewise loading (lbs./inch), F = Edgewise stress (psi), $K = (K_F + K_M)$ = Panel buckling coefficient (dimensionless), K_F = Theoretical buckling coefficient dependent on facing stiffness and panel aspect ratio (dimensionless), K_M = Theoretical coefficient dependent on sandwich bending and shear rigidities and panel aspect ratio (dimensionless), G_{ca} = Core shear modulus associated with the plane perpendicular to the facings and parallel to side a of panel (psi), G_{cb} = Core shear modulus associated with the plane perpendicular to the facings and parallel to side b of the panel (psi), E = Young's modulus for facing (psi), η = Plasticity reduction factor (dimensionless), E ' = Effective Young's modulus of facing $= \eta E$ (psi), μ = Poisson's ratio for facings (dimensionless), $\lambda = (1 - \mu^2)$ (dimensionless), D = Bending stiffness of sandwich panel (lbs.-inches), U = Transverse shear stiffness (lbs./inch), V = Bending and shear rigidity parameter for honeycomb core (dimensionless), W = Bending and shear rigidity parameter for panel with corrugated core (dimensionless), R = Degree of core orthotropicity $= (G_{ca}/G_{cb})$ (dimensionless), R_i = Stress or load ratio for the particular type of loading associated with the subscript i (dimensionless), h = Distance between middle surfaces of facings (inches), d = Total depth of sandwich (inches), t = Thickness (inches), $r = (N_y/N_x)$ (dimensionless), a, b = Panel dimensions — See figures below and next pages (inches).

SUBSCRIPTS: 1, 2 denote facing 1 or 2; f denotes facing when both are of equal thickness; B denotes bending; c designates core or compression, as applicable; cr denotes critical; x denotes acting along the x-axis; y denotes acting along the y-axis; cx denotes compression acting in the x-direction; cy denotes compression acting in the y-direction; Bx denotes bending acting in the x-direction; xy denotes shear loading which acts in both x and y-directions.

SANDWICH PANEL CORE CONFIGURATIONS AND DIMENSIONS:

Honeycomb

Single – Truss
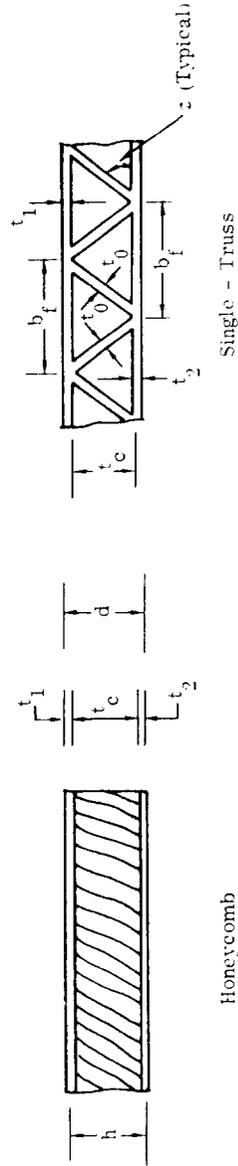
GENERAL EQUATIONS FOR SANDWICH PANEL PARAMETERS:

Panels with Faceplates of Different Materials and Thicknesses

$D = \eta(E_1 t_1)(E_2 t_2) h^2/(\lambda)(E_1 t_1 + E_2 t_2)$

$V = \eta(E_1 t_1)(E_2 t_2)(\pi^2) t_c/\lambda b^2(E_1 t_1 + E_2 t_2) G_{ca}$

$W = \eta(\pi^2) t_c (E_1 t_1)(E_2 t_2)/\lambda b^2(E_1 t_1 + E_2 t_2) G_{cb}$

$K_F = (E_1 t_1^3 + E_2 t_2^3)(E_1 t_1 + E_2 t_2) K_{M_o}/12(E_1 t_1)(E_2 t_2)(h^2)$

$K_{M_o} = K_M$ for case where V, or W, $= 0$

Panels with Faceplates of Same Material and Thickness

$D = \eta(E_f)(t_f) h^2/2\lambda$

$V = \eta(\pi^2) t_c (E_f) t_f/2\lambda(b^2) G_{ca}$

$W = \eta(\pi^2) t_c (E_f) t_f/2\lambda(b^2) G_{cb}$

$K_F = (t_f^2) K_{M_o}/2 (h^2)$

$K_{M_o} = K_M$ for case where V, or W, $= 0$

Loading Condition	Design Formulas for General Instability
1. UNIAXIAL IN-PLANE EDGEWISE COMPRESSION	$N_{cr} = (\pi^2/b^2)(K)(D)$

$$F_{c_{1,2}} = \pi^2 K \frac{(E_1' t_1)(E_2' t_2)}{(E_1' t_1 + E_2' t_2)^2} \frac{(h^2)}{(b^2)} \frac{(E_{1,2}')}{\lambda}$$

For equal facings:

$$F_c = \frac{\pi^2 K}{4} \frac{(h)^2}{(b)^2} \frac{E_f'}{\lambda}$$

where

$$K = K_F - K_M$$

K_F is as defined in the General Equations above. K_M is obtained from the curves given in Figures 3.1-2 through 3.1-13 for honeycomb cores for the appropriate boundary conditions and value of core orthotropicity, R. Figures 3.1-14 and 3.1-15 give K_M values for panels having corrugated cores. Figure 3.1-16 gives values of K_{M_o} for use in finding values of K_F.

(NOTE: Values required to obtain K_M from curves are (a/b) and V, or W in the case of corrugated cores.)

Table 3-1. Summary of Design Equations for General Instability of Flat Sandwich Panels, Cont'd.

Loading Condition	Design Formulas for General Instability
1. UNIAXIAL IN-PLANE EDGEWISE COMPRESSION, Cont'd.	Restrictions: $(F_{c_1}/E_{s_1}) \approx (F_{c_2}/E_{s_2})$ to avoid the overstressing of one facing with respect to the other. (E_s is the facing secant modulus of elasticity.) Faceplates are isotropic. Use $\eta = 1.0$ where behavior is elastic. Use Table 9-2 to find η for inelastic cases. For Combined Load cases use Equation 9.2-1 to find the effective stress for plasticity.
2. IN-PLANE EDGEWISE SHEAR	$$N_{scr} = (\pi^2/b^2)(K_s)(D)$$ $$F_{s1,2} = \pi^2 K_s \; \frac{(E'_1 t_1)(E'_2 t_2)(h^2) E'_{1,2}}{(E'_1 t_1 + E'_2 t_2)^2 (b^2)} \lambda$$ For equal facings: $$F_s = \frac{\pi^2 K_s (h^2) E'_f}{4(b^2) \lambda}$$ where $$K_s = K_F + K_M$$ K_F remains as previously defined in the General Equations. K_M is obtained from the curves given in Figures 3.1-17 through 3.1-19 for panels with all edges simply supported. Figures 3.1-22 through 3.1-24 cover the case for panels with all edges clamped. Figures 3.1-20 and 3.1-21 are for use with panels having corrugated cores. K_{M_o} values for use in calculating K_F are obtained from the appropriate curve using V, or W, = 0. (NOTE: Values required to obtain K_M from curves are (a/b) and V, or V, or W in the case of corrugated cores.)
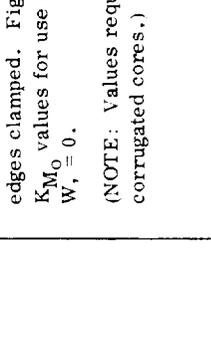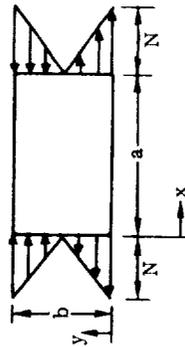
Restrictions: $(F_{S1}/G_{S1}) \approx (F_{S2}/G_{S2})$ to avoid the overstressing of one facing with respect to the other. (G_s is the secant shear modulus of the facing.)

Faceplates are isotropic

Use $\eta = 1.0$ where behavior is elastic. Use Table 9-2 to find η for inelastic cases.

For Combined Load cases use Equation 9.2-1 to find the effective stress for plasticity.

$$N_{cr} = (\pi^2/b^2)(K_b)(D)$$

$$F_{C1,2} = \pi^2 K_b \frac{(E_1 t_1)(E_2 t_2)}{(E_1 t_1 + E_2 t_2)^2} \frac{(h^2)}{(b^2)} \frac{(E_{1,2})}{\lambda}$$

For equal facings:

$$F_c = \frac{\pi^2 K_b}{4} \frac{(h^2)}{(b^2)} \frac{E}{\lambda}$$

where

$$K_b = K_F + K_M$$

K_F remains as previously defined in the General Equations.

K_M is obtained from the curves given in Figures 3.1-25 through 3.1-27 for panels with honeycomb cores. Figure 3.1-28 is for use with panels having corrugated cores. K_{M_O} values for use in calculating K_F are obtained from the appropriate curve using V, or W, $= 0$.

(NOTE: Values required to obtain K_M from curves are (a/b) and V, or W in the case of corrugated cores.)

Restrictions: The equations and curves given for this loading condition are good only for those cases where the panel behavior is elastic, thus, $\eta = 1.0$ for all applicable cases. $(F_{C1}/E_1) \approx (F_{C2}/E_2)$ to avoid the overstressing of one facing with respect to the other. (E is the elastic modulus of the facing.)

Faceplates are isotropic.

3. IN-PLANE EDGEWISE BENDING

Table 3-1. Summary of Design Equations for General Instability of Flat Sandwich Panels, Cont'd.

Combined Loading Condition	Design Formulas for General Instability
PANELS WITH HONEYCOMB CORES	
4. **BIAXIAL COMPRESSION**	For this case use the following interaction formula to estimate the onset of buckling: $$R_{cx} + R_{cy} = 1$$ where $$R_c = N/N_{cr} \quad \text{(See Loading Condition 1 - this table - for calculation of } N_{cr}.)$$ $x, y =$ subscripts denoting loading direction (See figure at the left.) A plot of the interaction equation above is given in Figure 3.1-29 for use in making design checks. When the value, $(R_{cx} + R_{cy})$, is less than 1.0 the panel is stable. When it reaches 1.0 buckling is imminent. The margin of safety, (M.S.), is given by the equation: $$M.S. = 1.0/(R_{cx} + R_{cy}) - 1.0$$
5. **BENDING AND COMPRESSION**	Use the following interaction formula to estimate buckling for this case: $$R_{cx} + (R_{Bx})^{3/2} = 1$$ where $$R_c = N/N_{cr} \quad \text{(See Loading Condition 1 - this table - for calculation of } N_{cr}.)$$ $$R_B = (N/N_{cr})_{bend.} \quad \text{(See Loading Condition 3 - this table - for calculation of } N_{cr\text{-bend.}})$$ This interaction equation is plotted in Figure 3.1-30 to facilitate its use for design checks. When the left side of the equation is less than 1.0 the panel is stable. When the value of the left hand terms reaches 1.0 buckling of the panel is imminent. The panel margin of safety is given by the equation: $$M.S. = \left[1.0 / R_{cx} + (R_{Bx})^{3/2} \right] - 1.0$$
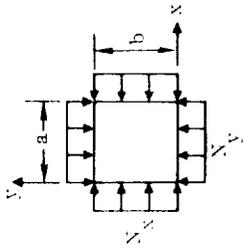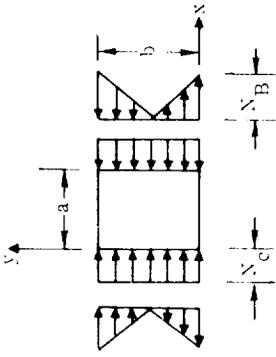
6. COMPRESSION AND SHEAR
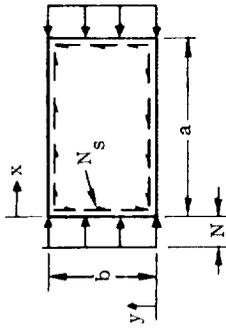
Use the following interaction formula to predict buckling for this loading condition:

$$R_c + (R_s)^2 = 1$$

where

$R_c = N/N_{cr}$ (See Loading Condition 1 - this table - for calculation of N_{cr}.)

$R_s = N_s/N_{scr}$ (See Loading Condition 2 - this table - for calculation of N_{scr}.)

This interaction curve is plotted in Figure 3.1-31 to facilitate its use in making design checks. When the sum of the terms on the left side of the interaction equation is less than 1.0 the panel is stable. When this value reaches 1.0 buckling of the panel is imminent. The panel margin of safety for buckling is given by the equation:

$$M.S. = [1.0/(R_c + R_s^2)] - 1.0$$

7. BENDING AND SHEAR
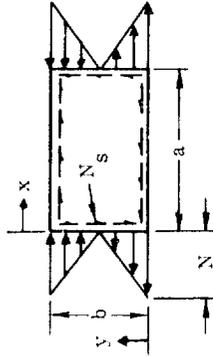
Use the following interaction equation to estimate the onset of buckling for this case:

$$(R_B)^2 + (R_s)^2 = 1$$

where

$R_B = (N/N_{cr})_{bend.}$ (See Loading Condition 3 - this table - for calculation of $N_{cr-bend.}$)

$R_s = N_s/N_{scr}$ (See Loading Condition 2 - this table - for calculation of N_{scr}.)

This interaction equation is plotted in Figure 3.1-32 to facilitate its use in making design checks. When the sum of the terms on the left side of the equation is less than 1.0 the panel is stable. When this value reaches 1.0 buckling of the panel is imminent. The panel margin of safety for buckling is given by the equation:

$$M.S. = [1.0/(R_B^2 + R_s^2)] - 1.0$$

Table 3-1. Summary of Design Equations for General Instability of Flat Sandwich Panels, Cont'd.

Combined Loading Conditions	Design Formulas for General Instability
PANELS WITH CORRUGATED CORES	
8. <u>BIAXIAL COMPRESSION</u> 	Figures 3.1-33 through 3.1-35 give the interaction relationships between the buckling coefficients, K_x and K_y, for this loading condition. This equation takes the general form: $$R_{cx} + R_{cy} = 1.0 = (N_x/N_{xcr}) + (N_y/N_{ycr})$$ where $$N_{xcr} = (\pi^2/b^2)(K_x)(D) \qquad N_{ycr} = (\pi^2/b^2)(K_y)(D)$$ K_x, K_y = buckling coefficients for loading along subscript direction Due to the complexity of the problem and assumptions required to make a design check, refer to the example given on page 3-53 for the approach to be taken and method used in calculating the margin of safety.
9. <u>COMPRESSION ALONG CORE FLUTES AND SHEAR</u> 	Figures 3.1-36 through 3.1-38 show the interaction relationships between the buckling coefficients, K_x and K_s, for this loading condition. This equation takes the general form: $$R_{cx} + R_s = 1.0 = (N_x/N_{xcr}) + (N_s/N_{scr})$$ where (using N_s and N_{xy} interchangeably to denote the shear loading.) $$N_{xcr} = (\pi^2/b^2)(K_x)(D) \qquad N_{scr} = (\pi^2/b^2)(K_s)(D)$$ K_s = buckling coefficient for shear K_x = coefficient for compression along x-axis Due to the complexity of the problem and assumptions required to make a design check, refer to the example given on page 3-53 for the approach to be taken and method used in calculating the margin of safety. (NOTE: Handle the R_s term in the same way as the R_{cy} term in the example.)
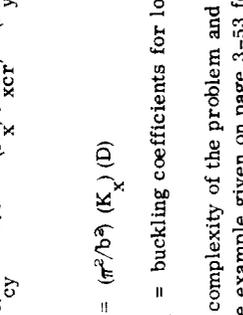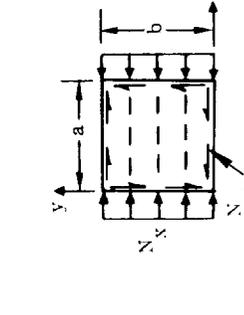
10. COMPRESSION NORMAL TO CORE FLUTES AND SHEAR
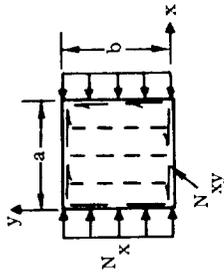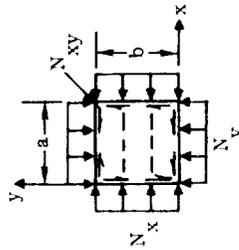
Figures 3.1-39 through 3.1-41 show the interaction relationships between the buckling coefficients, K_x and K_s, for this loading condition. This equation takes the general form:

$$R_{cx} + R_s = 1.0 = (N_x/N_{xcr}) + (N_s/N_{scr})$$

where (using N_s and N_{xy} interchangeably to denote the shear loading.)

$N_{xcr} = (\pi^2/b^2)(K_x)(D)$ $\qquad$ $N_{scr} = (\pi^2/b^2)(K_s)(D)$

K_s = buckling coefficient for shear $\qquad$ K_x = coefficient for compression along x-axis

Due to the complexity of the problem and assumptions required to make a design check, refer to the example given on page 3-53 for the approach to be taken and method used in calculating the margin of safety. (NOTE: Handle the R_s term in the same way as the R_{cy} term in the example.)

11. BIAXIAL COMPRESSION AND SHEAR

Figure 3.1-42 shows the interaction relationships between the buckling coefficients, K_x, K_y, and K_s, for this loading condition. This equation takes the general form:

$$R_{cx} + R_s = (1.0 - R_{cy}) = (N_x/N_{xcr}) + (N_s/N_{scr}) = \lceil 1.0 - (N_y/N_{ycr}) \rceil$$

where N_{xcr}, N_{ycr}, K_x, and K_y are as defined for Loading Condition 8 of this table.

N_{scr} and K_s are as defined for Loading Condition 10 of this table.

Due to the complexity of the problem and the assumptions required to make a design check, refer to the example given on page 3-53 for the approach to be taken and method used in calculating the margin of safety. (NOTE: Handle the R_{cx} term in the same manner as in the example and treat the R_s term in the same way as was done for the R_{cy} term in the example. Since K_y is a function of W only it may be found immediately for use in the above interaction equation, thus setting up an equality value for the left side of something less than 1.0. See the discussion on page 3-58 pertinent to this.)

REFERENCES

3-1   U. S. Department of Defense, "Structural Sandwich Composites," MIL-
        HDBK-23, 30 December 1968.

3-2   General Dynamics Fort Worth Division, Structures Manual - Volume 1,
        Methods of Analysis, November 1959.

3-3   Konishi, D., et al, Honeycomb Sandwich Structures Manual, North
        American Aviation Corp. Los Angeles Division, Report NA58-899.

3-4   Structures Manual - Section 11.00: Honeycomb Sandwich Structures,
        North American Aviation, Inc. Space and Information Systems Division,
        May 1964.

3-5   Lockheed-Georgia Company, A Division of Lockheed Aircraft Corp.,
        "Sandwich Panel Tests for C-5A Airplane," GELAC Report No. ER 8976,
        22 February 1967.

3-6   General Dynamics Corporation Forth Worth Division, "Design Allowables
        and Methods of Analysis, F-111 Airplane," Report No. FZS-12-141,
        1 August 1965.

3-7   Hexcel Corp., "Design Handbook for Honeycomb Sandwich Structures,"
        Report No. TSB 123, October 1967.

3-8   Ericksen, W. S. and March, H. W., "Effects of Shear Deformation in the
        Core of a Flat Rectangular Sandwich Panel - Compressive Buckling of
        Sandwich Panels Having Dissimilar Facings of Unequal Thickness," Forest
        Products Laboratory Report 1583-B, Revised 1958.

3-9   Norris, C. B., "Compressive Buckling Curves for Flat Sandwich Panels
        with Isotropic Facings and Isotropic or Orthotropic Cores," Forest
        Products Laboratory Report 1854, Revised 1958.

3-10   Norris, C. B., "Compressive Buckling Curves for Flat Sandwich Panels with Dissimilar Facings," Forest Products Laboratory Report 1875, September 1960.

3-11   Kuenzi, E. W., Norris, C. B. and Jenkinson, P. M., "Buckling Coefficients for Simply Supported and Clamped Flat, Rectangular Sandwich Panels Under Edgewise Compression," Forest Products Laboratory Research Note FPL-070, December 1964.

3-12   Jenkinson, P. M. and Kuenzi, E. W., "Buckling Coefficients for Flat, Rectangular Sandwich Panels with Corrugated Cores Under Edgewise Compression," Forest Products Laboratory Research Paper FPL 25, May 1965.

3-13   Kuenzi, E. W., and Ericksen, W. S., "Shear Stability of Flat Panels of Sandwich Construction," Forest Products Laboratory Report 1560, 1951.

3-14   Harris, L. A. and Auelman, R. R., "Stability of Flat, Simply Supported Corrugated Core Sandwich Plate Under Combined Longitudinal Compression and Bending, Transverse Compression and Bending, and Shear," North American Aviation, Inc., Missile Division, Report STR 67, 1959.

3-15   Kimel, W. R., "Elastic Buckling of a Simply Supported Rectangular Sandwich Panel Subjected to Combined Edgewise Bending and Compression," Forest Products Laboratory Report 1857A, 1956.

3-16   Harris, L. A., and Auelman, R. R., "Stability of Flat, Simply Supported Corrugated Core Sandwich Rectangular Plates Under Combined Loadings," Journal of Aerospace Sciences, Vol. 27, No. 7, p. 525-534, 1960.

3-17   Timoshenko, S. P., and Gere, J. M., Theory of Elastic Stability, McGraw-Hill Book Company, Inc., 1961, p. 373-379.

3-18   Gerard, G., and Becker, H., Handbook of Structural Stability, Part I - Buckling of Flat Plates, National Advisory Committee for Aeronautics Technical Note 3781, 1957.

3-19   Kimel, W. R., "Elastic Buckling of a Simply Supported Rectangular Sand-
        wich Panel Subjected to Combined Edgewise Bending, Compression, and
        Shear," Forest Products Laboratory Report 1859, 1956.

3-20   Noel, R. G., "Elastic Stability of Simply Supported Flat Rectangular Plates
        Under Critical Combinations of Longitudinal Bending, Longitudinal Com-
        pression, and Lateral Compression," Journal of the Aeronautical Sciences,
        Vol. 19, No. 12, p. 829-834, 1952.

3-21   Norris, C. B., and Kommers, W. J., "Critical Loads of a Rectangular,
        Flat Sandwich Panel Subjected to Two Direct Loads Combined with a Shear
        Load," Forest Products Laboratory Report 1833, 1952.

3-22   Norris, C. B., and Kommers, W. J., "Stresses within a Rectangular,
        Flat Sandwich Panel Subjected to a Uniformly Distributed Normal Load and
        Edgewise, Direct, and Shear Loads," Forest Products Laboratory Report
        1838, 1953.

3-23   Plantema, F. J., Sandwich Construction, John Wiley and Sons, Inc., New
        York, 1966.

3-24   U. S. Department of Defense, "Plastics for Flight Vehicles: Part I, Rein-
        forced Plastics," MIL-HDBK-17, Armed Forces Supply Support Center,
        1959, Available from U. S. Government Printing Office, Washington, D. C.

3-25   U. S. Department of Defense, "Metallic Materials and Elements for Aero-
        space Vehicle Structures," MIL-HDBK-5A, February 1966, Available from
        U. S. Government Printing Office, Washington, D. C.

4

GENERAL INSTABILITY OF CIRCULAR CYLINDERS

4.1 GENERAL

In the case of axially compressed, thin-walled, isotropic (non-sandwich) cylinders, it has long been recognized that test results usually fall far below the predictions from classical small-deflection theory [4-1]. These discrepancies are usually attributed primarily to

a. the shape of the post-buckling equilibrium path coupled with the presence of initial imperfections

and

b. the fact that classical small-deflection theory does not account for pre-buckling discontinuity distortions in the neighborhood of the boundaries.

Neglecting the discontinuity distortions, the equilibrium path for an axially compressed perfect cylinder is of the general shape shown by the solid curve in Figure 4.1-1. This path is linear until point A is reached and general instability occurs at a stress level σ_{CL} equal to the result from classical small-deflection theory $\left[\sigma_{CL} = \dfrac{E\,t}{R\sqrt{3(1-\nu_e^2)}} \text{ for elastic, isotropic (non-sandwich) cylinders} \right]$. However, if the cylinder is initially imperfect and the discontinuity distortions are considered, the behavior will be as shown by curve OB and buckling will occur at the stress σ_{cr}. The ratio $(\sigma_{cr}/\sigma_{CL})$ will be dependent upon the magnitude of the initial imperfections present in the cylinder. However, since this information is not normally available, one

usually finds it necessary to resort to either of the following practices to obtain practical design values:

a. Set the allowable compressive stress equal to the value σ_{MIN} shown in Figure 4.1-1.

b. Use the classical small-deflection value σ_{CL} in conjunction with a suitable knock-down factor γ_c which is based on the results from a large array of test data. The allowable compressive stress is then obtained from

$$\sigma_{cr} = \gamma_c \, \sigma_{CL} \qquad\qquad (4.1-1)$$
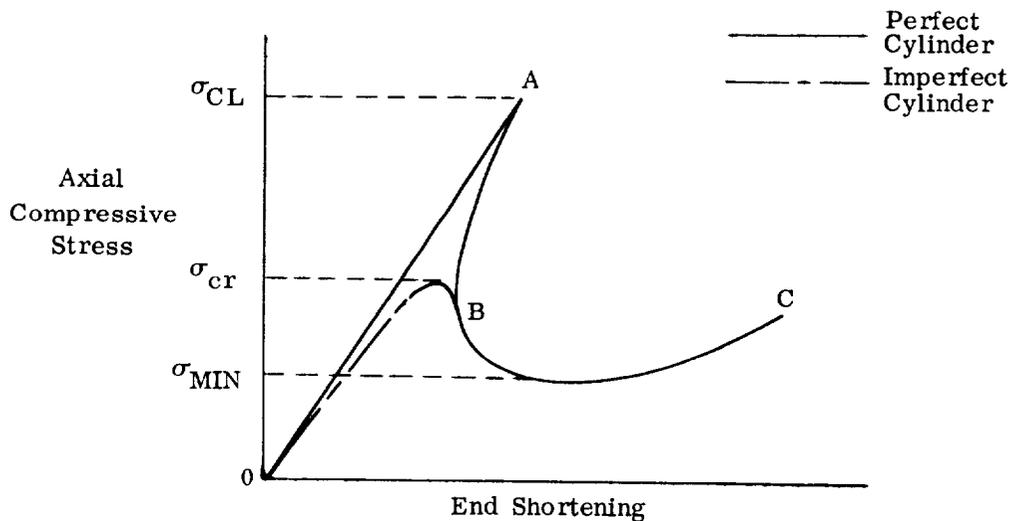
Figure 4.1-1. Equilibrium Paths for Axially
Compressed Circular Cylinders

For isotropic (non-sandwich) cylinders it is common practice to follow the second of these approaches and, for such cylinders, the test data shows that γ_c is a function of the radius-to-thickness ratio (R/t).

In the case of sandwich cylinders having relatively rigid cores, the behavior is similar to that of the isotropic (non-sandwich) cylinder and one can expect imperfections and boundary disturbances to precipitate general instability at compressive stresses below the predictions from classical small-deflection sandwich theory. However, in most practical applications, the sandwich wall will provide an effective relatively thick shell so that the discrepancies will not be as large as those normally encountered in thin-walled isotropic (non-sandwich) cylinders. In addition, as the core transverse shear rigidity decreases, the differences between test results and classical predictions will diminish. In the extreme case where shear crimping occurs, initial imperfections do not appear to have any influence.

One of the most prominent of the early design criteria developed for axially compressed circular sandwich cylinders is that of Reference 4-2. This solution employed large-deflection theory together with approach (a) cited above ($\sigma_{cr} = \sigma_{MIN}$). However, it is now rather generally agreed that this criterion often provides design values which are too conservative. In addition, the theoretical development of Reference 4-3 indicates that σ_{MIN} can be decreased to essentially zero by including a sufficient number of terms in the large-deflection displacement functions. Therefore, in recent years, it has become common practice to design sandwich cylinders by method (b) cited above [4-4 and 4-5]. This approach, which employs small-deflection theory in conjunction with an empirical knock-down factor, is likewise followed in this handbook.

In the treatment of various types of external loading, it is important to note that the characteristics of the equilibrium paths are not identical for cases of axial compression, torsion, or external radial pressure. For purposes of comparison, Figure 4.1-2

depicts the general shapes of these paths for each loading condition [4-6] assuming

that the cylinders are initially perfect and that no discontinuity distortions are present.

| Deflection | Deflection | Deflection |
| Axial Compression | Torsion | External Pressure |
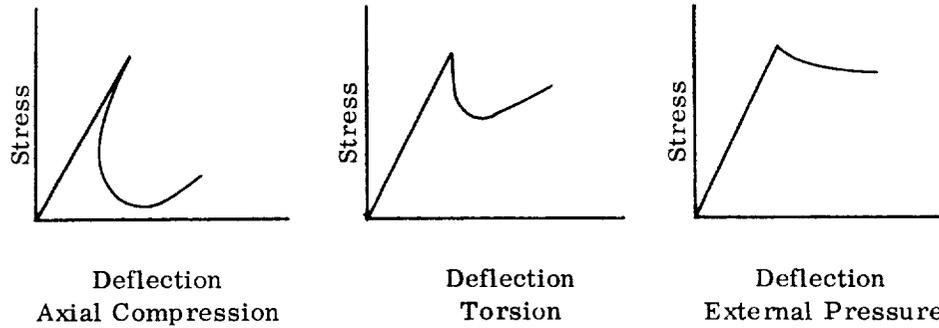
Figure 4.1-2. Typical Equilibrium Paths for Circular Cylinders

Based on the relative shapes of these curves, one would expect that, under torsion or

external pressure, the cylinders would be much less sensitive to initial imperfections

than in the case of axial compression. This has been borne out by the available test

data from thin-walled isotropic (non-sandwich) cylinders.

4.2 AXIAL COMPRESSION

4.2.1 Basic Principles

4.2.1.1 Theoretical Considerations

The theoretical basis used here is the classical small-deflection solution of Zahn and Kuenzi [4-7] which includes the following assumptions:

a. The facings are isotropic but the core may have orthotropic transverse shear properties.

b. Bending of the facings about their own middle surfaces can be neglected.

c. The core has infinite extensional stiffness in the direction normal to the facings.

d. The core extensional and shear rigidities are negligible in directions parallel to the facings.

e. The cylinder is not extremely short (a quantitative limit is specified in Section 4.2.2).

f. The approximations of Donnell [4-8] can be applied without introducing significant error.

In this handbook, the final equations of Reference 4-7 have been transformed into equivalent formulations which should be more meaningful to the user. For those cases where the core shear moduli satisfy the condition

$$\theta = \frac{G_{xz}}{G_{yz}} \leq 1 \qquad (4.2-1)$$

the following expression is obtained:

$$\sigma_{cr} = K_c \, \sigma_o \qquad (4.2-2)$$

where

$$\sigma_0 = \eta E_f \frac{h}{R} \frac{2\sqrt{t_1 t_2}}{\sqrt{1-\nu_e^2}\,(t_1 + t_2)} \qquad (4.2\text{-}3)$$

and

When $V_c \leq 2$
$$K_c = 1 - \frac{1}{4} V_c \qquad (4.2\text{-}4)$$

When $V_c \geq 2$
$$K_c = \frac{1}{V_c} \qquad (4.2\text{-}5)$$

where

$$V_c = \frac{\sigma_0}{\sigma_{crimp}} \qquad (4.2\text{-}6)$$

$$\sigma_{crimp} = \frac{h^2}{(t_1 + t_2) t_c} G_{xz} \qquad (4.2\text{-}7)$$

η = Plasticity reduction factor, dimensionless.

E_f = Young's modulus of facings, psi.

h = Distance between middle surfaces of facings, inches.

R = Radius to middle surface of cylindrical sandwich, inches.

t_1 and t_2 = Thicknesses of the facings (There is no preference as to which facing is denoted by the subscript 1 or 2.), inches.

ν_e = Elastic Poisson's ratio of facings, dimensionless.

t_c = Thickness of core, inches.

G_{xz} = Core shear modulus associated with the plane perpendicular to the facings and oriented in the axial direction, psi.

G_{yz} = Core shear modulus associated with the plane perpendicular to the axis of revolution, psi.

The relationship between K_c and V_c can be plotted as shown in Figure 4.2-1. It is important to note that the value $V_c = 2.0$ establishes a dividing line between two different types of behavior. The region where $V_c \leq 2.0$ covers the so-called stiff-core

4-6
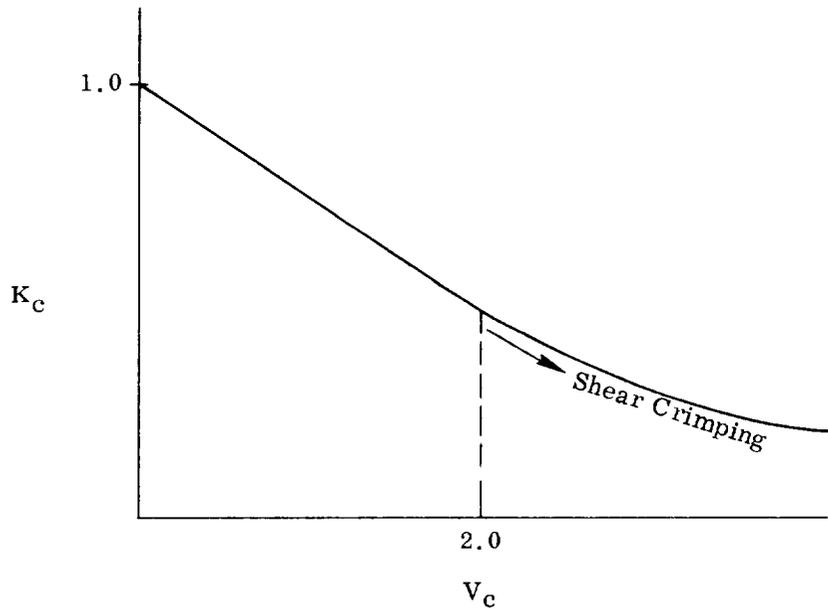
Figure 4.2-1. Schematic Representation of Relationship
Between K_c and V_c for $\theta \leq 1$

and moderately-stiff-core sandwich constructions. When V_c is in the neighborhood of zero, the core shear stiffness is high and the sandwich exhibits maximum sensitivity to initial imperfections. Hence, for any given radius-to-thickness ratio, the knock-down factors applicable to such constructions are of maximum severity. As V_c increases from zero to a value of 2.0, the sensitivity to imperfections becomes progressively less. The domain where $V_c \geq 2.0$ is the so-called weak-core region where shear crimping occurs. Sandwich constructions which fall within this category are not influenced by the presence of initial imperfections, and a knock-down factor of unity can be applied to such structures. It should be possible to develop a continuous transitional knock-down relationship which recognizes the variable influence of the core rigidity but this is beyond the scope of the present handbook.

4-7

4.2.1.2 Empirical Knock-Down Factor

As noted in Section 4.1, the allowable stress intensities for axially compressed, thin-walled, isotropic (non-sandwich) cylinders are usually computed using the following equation:

$$\sigma_{cr} = \gamma_c \, \sigma_{CL} \tag{4.2-8}$$

The quantity γ_c is referred to as the knock-down factor and this value is generally recognized to be a function of the radius-to-thickness ratio (R/t). Various investigators have proposed different relationships in this regard. The differences arise out of the chosen statistical criteria and/or out of the particular test data selected as the empirical basis. One of the most widely used of the relationships proposed to date is the lower-bound criterion of Seide, et al. [4-9] which can be expressed as follows:

$$\gamma_c = 1 - 0.901 \, (1 - e^{-\phi}) \tag{4.2-9}$$

where

$$\phi = \frac{1}{16} \sqrt{\frac{R}{t}} \tag{4.2-10}$$

This gives a knock-down curve of the general shape depicted in Figure 4.2-2. For the purposes of this handbook, it is desired that an empirical means of this type also be provided for the design of sandwich cylinders. One of the major obstacles to the achievement of this objective is the lack of sufficient sandwich test data for a thorough empirical determination. Faced with this deficiency, one finds it expedient to employ the data from isotropic (non-sandwich) cylinders in conjunction with an effective thickness concept and correction factors which are based on the few available sandwich test points. Toward this end, it is usually assumed that, when $V_c \leq 2.0$, equal sensitivity
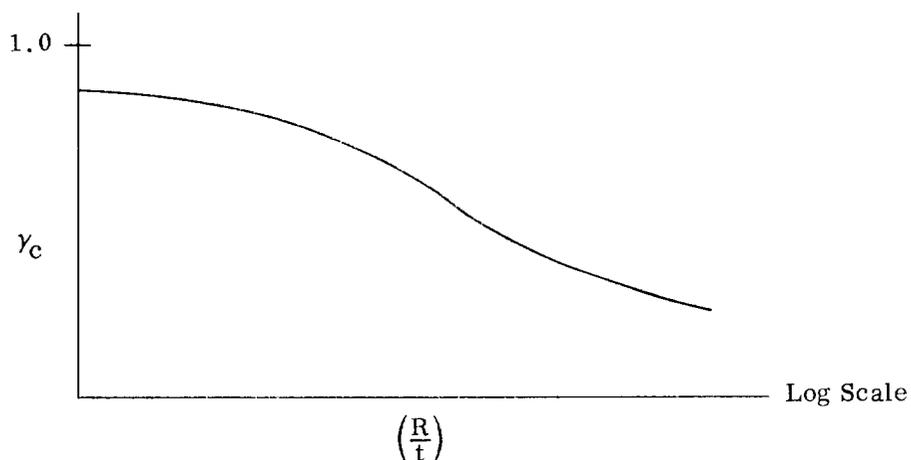
Figure 4.2-2. Semi-Logarithmic Plot of γ_c vs R/t for Isotropic (Non-Sandwich) Cylinders Under Axial Compression

to imperfections results from equivalence of the shell-wall radii of gyration ρ

($\approx \frac{h}{2}$ for sandwich constructions whose two facings are of equal thickness). There-

fore, the approach taken here is to rewrite Equations (4.2-9) and (4.2-10) in terms

of ρ. The revised formulations give the plot shown as a dashed curve in Figure

4.2-2. Also shown in this figure are the appropriate test points obtained from

axially compressed sandwich cylinders [4-2, 4-10, 4-28] which did not fall into

the weak-core category. Eleven such data points are shown. In addition, two

test points are shown for axially compressed conical sandwich constructions

[4-10] which likewise did not lie in the weak-core region. The conical data are

included in Figure 4.2-3 in view of the scarcity of available test results and

also because the cones were analyzed as equivalent cylinders whose radii were

taken equal to the R_2 (finite principal radius of curvature) values at the small end

of the specimens. Based on this limited amount of sandwich test data, it is recom-

mended that the solid curve of Figure 4.2-3 be used for design purposes. This

4-9
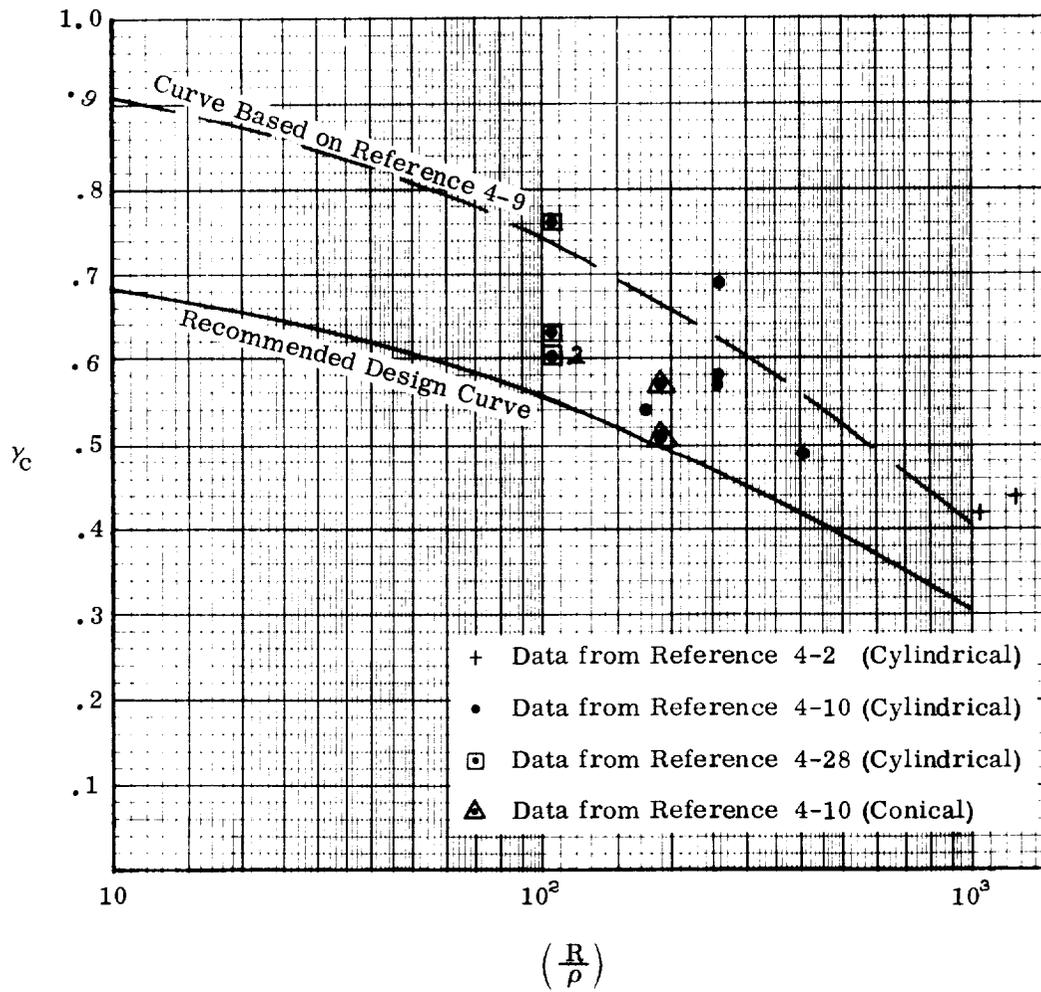
Figure 4.2-3. Knock-Down Factor γ_c for Circular Sandwich
Cylinders Subjected to Axial Compression

gives Y_c values that are 75 percent of those obtained from the dashed curve which was based on the empirical formula of Seide, et al. [4-9].

In addition to the test results described above, a considerable number of test points are available from cylindrical sandwich constructions which fall into the weak-core classification. As noted in Section 4.2.1.1, the methods recommended in this handbook are such that, in the weak-core region, no empirical reduction will be applied to the theoretical results of Reference 4-7. In order to explore the validity of this approach, plots are furnished in Figures 4.2-4 and 4.2-5 which compare the weak-core test results of References 4-2 and 4-11 against predictions from the recommended design criterion. It can be seen that all but one of the test results exceed the predicted strengths, and that the single exception failed at 86 percent of the predicted value. In many of the cases where $\left(\sigma_{cr_{Test}}/\sigma_{Predicted}\right) > 1.0$, although the discrepancies measured in units of psi were not very great, the percentage differences were quite large. This behavior can be explained by the fact that the theoretical basis [4-7] proposed in this handbook assumes that bending of the facings about their own middle surfaces can be neglected. As shown in Reference 4-12, this assumption can be very conservative in the weak-core region. However, in the interest of simplicity, the methods of this handbook retain this assumption especially since it is a conservative practice and most practical sandwich constructions will not be designed as weak-core structures.

In view of the meager compressive test data available from stiff-core and moderately-stiff-core sandwich cylinders, the method proposed here is not very reliable when

4-11

$V_c < 2.0$. Therefore, in such cases the method can only be considered as a "best-available" approach. On the other hand, where the failure is by shear crimping $(V_c \geq 2.0)$, the method is quite reliable and will, in fact, usually give conservative predictions.
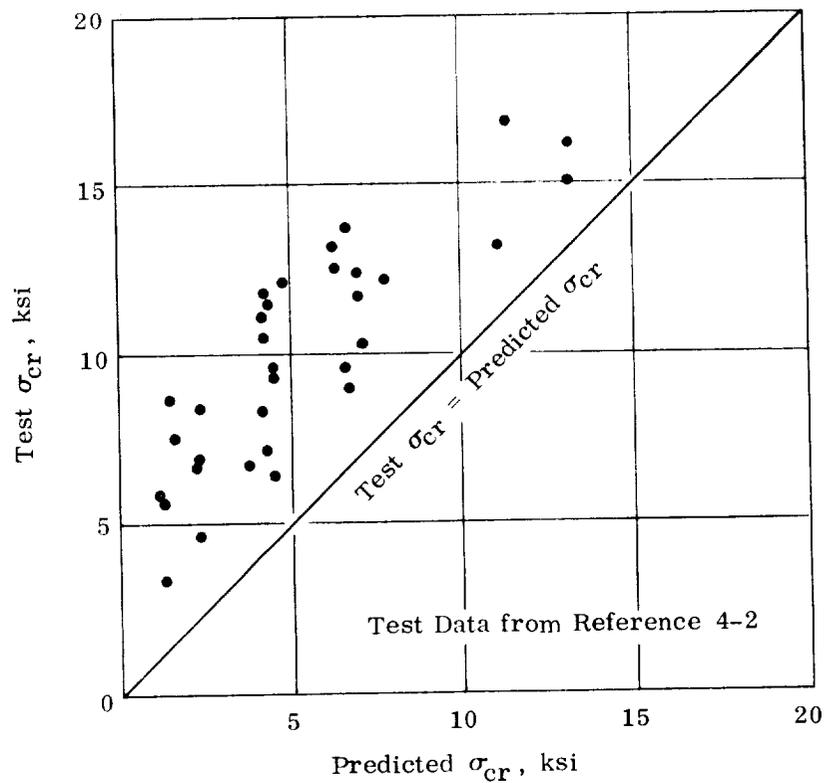
(Neglecting bending stiffness of individual facings)

Figure 4.2-4. Comparison of Proposed Design Criterion Against Test Data for Weak-Core Circular Sandwich Cylinders Subjected to Axial Compression

Figure 4.2-5. Comparison of Proposed Design Criterion Against
a Test Result for a Weak-Core Circular Sandwich
Cylinder Subjected to Axial Compression

4.2.1.2.1 Interpretation of Test Data

As indicated in the preceding paragraphs, appropriate test data must be used in order

to arrive at practical values for the knock-down factor. However, one can be easily

misled in this endeavor when the test data and/or the classical theoretical predictions

lie in the inelastic region. To demonstrate this point as simply as possible, the pre-

sent discussion is limited to the case of axially compressed circular sandwich cylin-

ders for which $V_c = 0$. Then the recommended design value for the critical stress

can be expressed as follows:

$$\sigma_{cr} = \gamma_c \, \eta \, E_f \, \frac{h}{R} \, \frac{2 \sqrt{t_1 \, t_2}}{\sqrt{1 - \nu_e^2} \, (t_1 + t_2)} \qquad (4.2-11)$$

For any particular test specimen, the related value for the knock-down factor should be computed from the following expression which is obtained by a simple transposition of Equation (4.2-11):

$$(\gamma_c)_{Test} = \frac{\left(\dfrac{\sigma_{cr_{Test}}}{\eta_{Test}}\right)}{\left[E_f \dfrac{h}{R} \dfrac{2\sqrt{t_1 \, t_2}}{\sqrt{1-\nu_e^2} \ (t_1 + t_2)}\right]} \qquad (4.2-12)$$

The plasticity reduction factor η_{Test} is evaluated at the actual experimental buckling stress. By inspection of the numerator and denominator of Equation (4.2-12), one can conclude that this formula may be rewritten in the following more meaningful form:

$$(\gamma_c)_{Test} = \frac{\left[\begin{array}{c}\text{Experimental critical stress value} \\ \text{which would have been attained had} \\ \text{the material remained elastic}\end{array}\right]}{\left[\begin{array}{c}\text{Classical theoretical critical} \\ \text{stress value assuming the} \\ \text{behavior to be elastic}\end{array}\right]} \qquad (4.2-13)$$

The example illustrated in Figure 4.2-6 should help to clarify this concept. In this figure, the solid line represents the stress-strain curve for the test specimen material. Suppose that this particular specimen buckled at a stress equal to $\sigma_{cr_{Test}}$. As indicated in the figure, it is assumed here that this stress lies in the inelastic region so that η_{Test} will be less than unity. For the purposes of this discussion, further assume that $\eta_{Test} = 0.80$. If the material had remained elastic, the experimental critical stress would have been somewhat higher than $\sigma_{cr_{Test}}$. This greater value will be denoted as $\sigma'_{cr_{Test}}$. Then it follows that

$$\sigma'_{cr_{Test}} = \frac{\sigma_{cr_{Test}}}{\eta_{Test}} = \frac{\sigma_{cr_{Test}}}{0.80} = 1.25 \ \sigma_{cr_{Test}} \qquad (4.2-14)$$
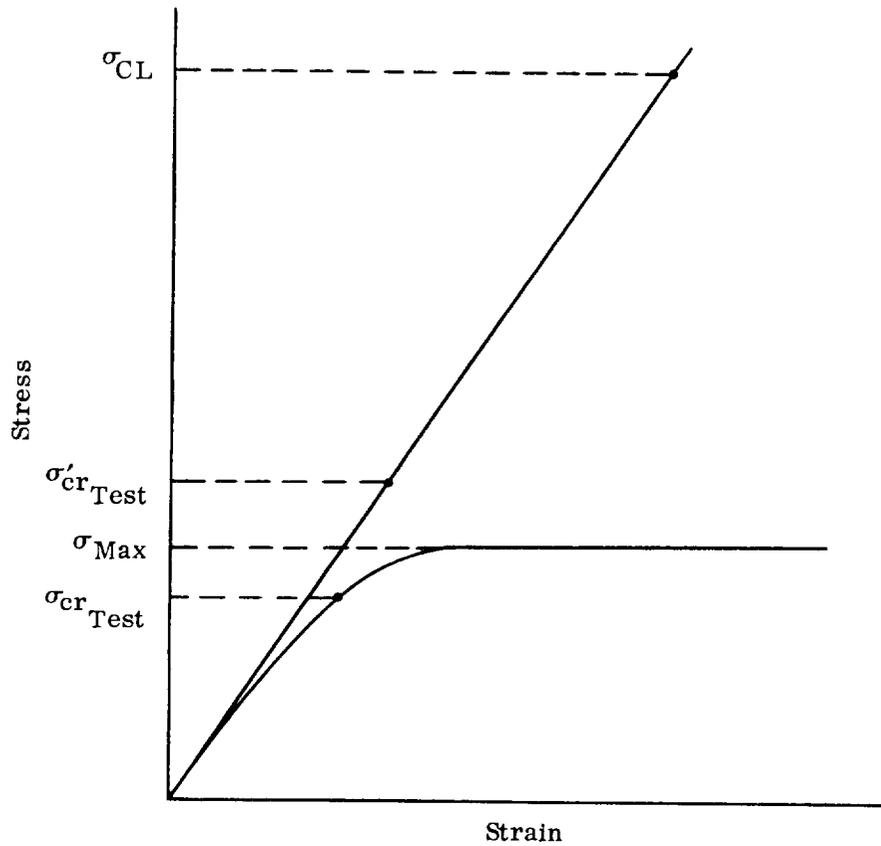
Figure 4.2-6. Stresses Involved in Interpretation of Test Data

Now let it also be assumed that, using elastic material properties, the classical theoretical critical stress equals the value σ_{CL} indicated in Figure 4.2-6. The following formula would then give the proper value for the experimental knock-down factor:

$$(\gamma_c)_{Test} = \frac{\sigma'_{cr_{Test}}}{\sigma_{CL}} = \frac{1.25\,\sigma_{cr_{Test}}}{\sigma_{CL}} \tag{4.2-15}$$

where

$$\sigma_{CL} = E_f\,\frac{h}{R}\,\frac{2\sqrt{t_1\,t_2}}{\sqrt{1-\nu_e^2}\,(t_1 + t_2)} \tag{4.2-16}$$

4-15

The above discussion is given here since some of the results presented in the literature can be quite misleading. That is, comparisons are often shown between the actual test value $\sigma_{cr_{Test}}$ (without regard as to whether elastic or not) and the inelastic classical theoretical prediction. For the case shown in Figure 4.2-6, the latter value cannot exceed σ_{Max} and this type of comparison might lead one to believe that the appropriate knock-down factor is very close to unity. However, use of the correct approach as expressed by Equations (4.2-13) and (4.2-15) gives a much lower γ_c value. For any given geometry, one could always show very close agreement between $\sigma_{cr_{Test}}$ and σ_{Max} simply by choosing a material with a sufficiently low yield strength and having a flat post-yield stress-strain curve.

4.2.2 Design Equations and Curves

For simply supported circular sandwich cylinders subjected to axial compression, the critical stresses may be computed from the relationships given on page 4-18 where the subscripts 1 and 2 refer to the separate facings. There is no preference as to which facing is denoted by either subscript. These equations were obtained by a simple extension of the formulas developed in Reference 4-7 which only considered the case where the behavior is elastic and the moduli of elasticity are identical for both facings. The extended versions given in this handbook were derived through the use of equivalent-thickness concepts based on the ratios of the moduli of the two facings. For cases where the two facings are not made of the same material, these equations are valid only when the behavior is elastic $(\eta = 1)$. Application to inelastic cases $(\eta \neq 1)$ can only be made when both facings are made of the same material. For such configurations, E_1 and E_2 will, of course, be equal.

The buckling coefficients K_c can be obtained from Figure 4.2-7. Curves are given there for both $\theta \leq 1$ and $\theta = 5$ where $\theta = \dfrac{G_{xz}}{G_{yz}}$. Since these two plots are not very different from each other, one may use Figure 4.2-7 to obtain rather accurate estimates of K_c when $1 < \theta < 5$.

Whenever $V_c < 2.0$, the knock-down factor γ_c can be obtained from Figure 4.2-8. When $V_c \geq 2.0$, use $\gamma_c = 1.0$.

For elastic cases, use $\eta = 1$. Whenever the behavior is inelastic, the methods of Section 9 must be employed.

4-17

Facing 1

$$\sigma_{cr_1} = \gamma_c\, K_{c_1}\, \sigma_{o_1} \qquad (4.2\text{-}17)$$

$$\sigma_{o_1} = \eta E_1\, C_o \qquad (4.2\text{-}19)$$

$$C_o = \frac{h}{R}\,\frac{2\sqrt{(E_1 t_1)(E_2 t_2)}}{\sqrt{1-\nu_e^2}\,\big[(E_1 t_1) + (E_2 t_2)\big]}$$

$$\sigma_{crimp_1} = \left[\frac{h^2}{t_1 + \left(\dfrac{E_2}{E_1}\right) t_2}\right]\frac{G_{xz}}{t_c} \qquad (4.2\text{-}22)$$

$$V_{c_1} = \frac{\sigma_{o_1}}{\sigma_{crimp_1}} = V_{c_2} \qquad (4.2\text{-}24)$$

Facing 2

$$\sigma_{cr_2} = \gamma_c\, K_{c_2}\, \sigma_{o_2} \qquad (4.2\text{-}18)$$

$$\sigma_{o_2} = \eta E_2\, C_o \qquad (4.2\text{-}20)$$

$$(4.2\text{-}21)$$

$$\sigma_{crimp_2} = \left[\frac{h^2}{\left(\dfrac{E_1}{E_2}\right) t_1 + t_2}\right]\frac{G_{xz}}{t_c} \qquad (4.2\text{-}23)$$

$$V_{c_2} = \frac{\sigma_{o_2}}{\sigma_{crimp_2}} = V_{c_1} \qquad (4.2\text{-}25)$$
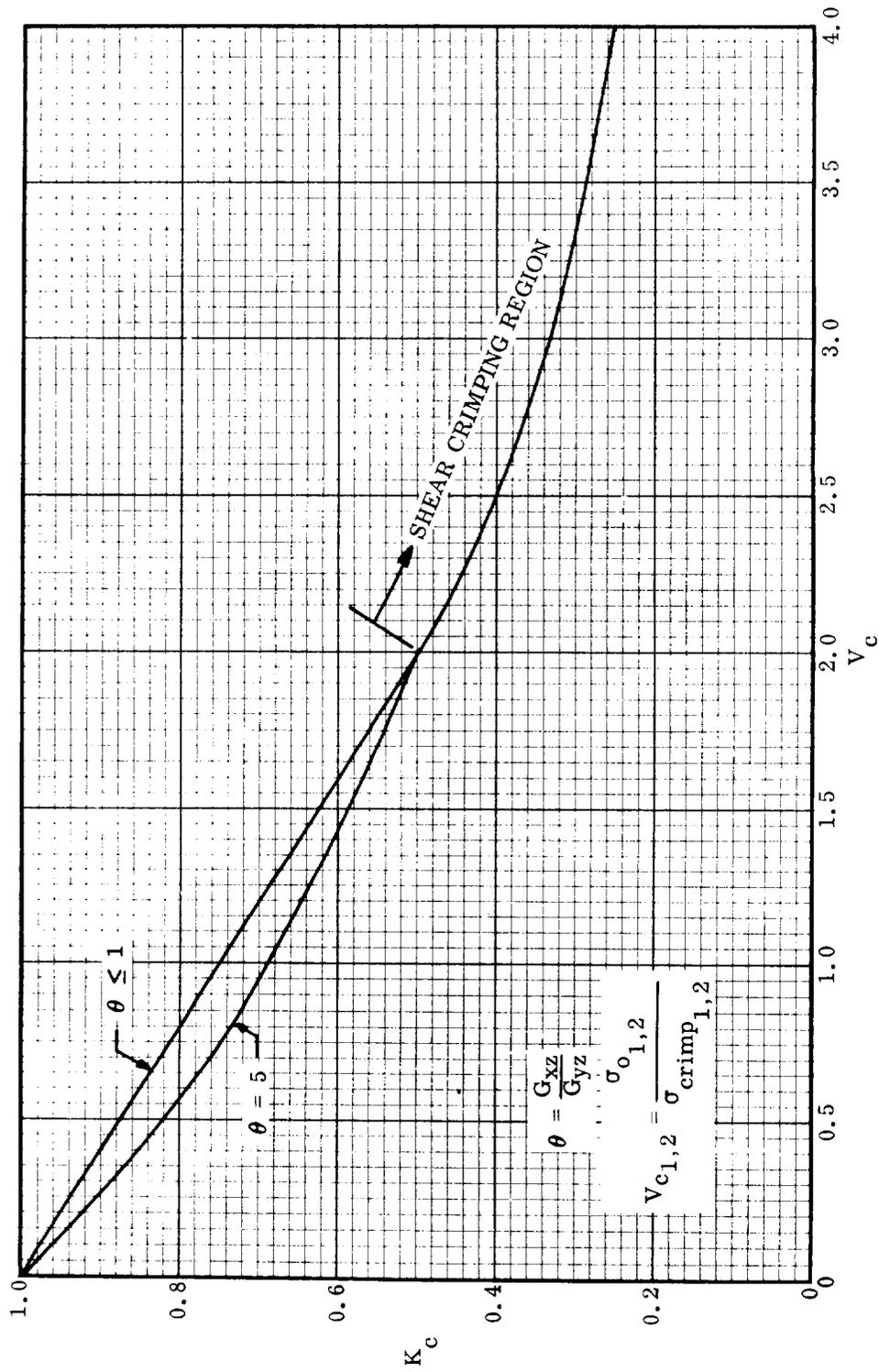
Figure 4.2-7. Buckling Coefficient for Axially Compressed Circular Sandwich Cylinders
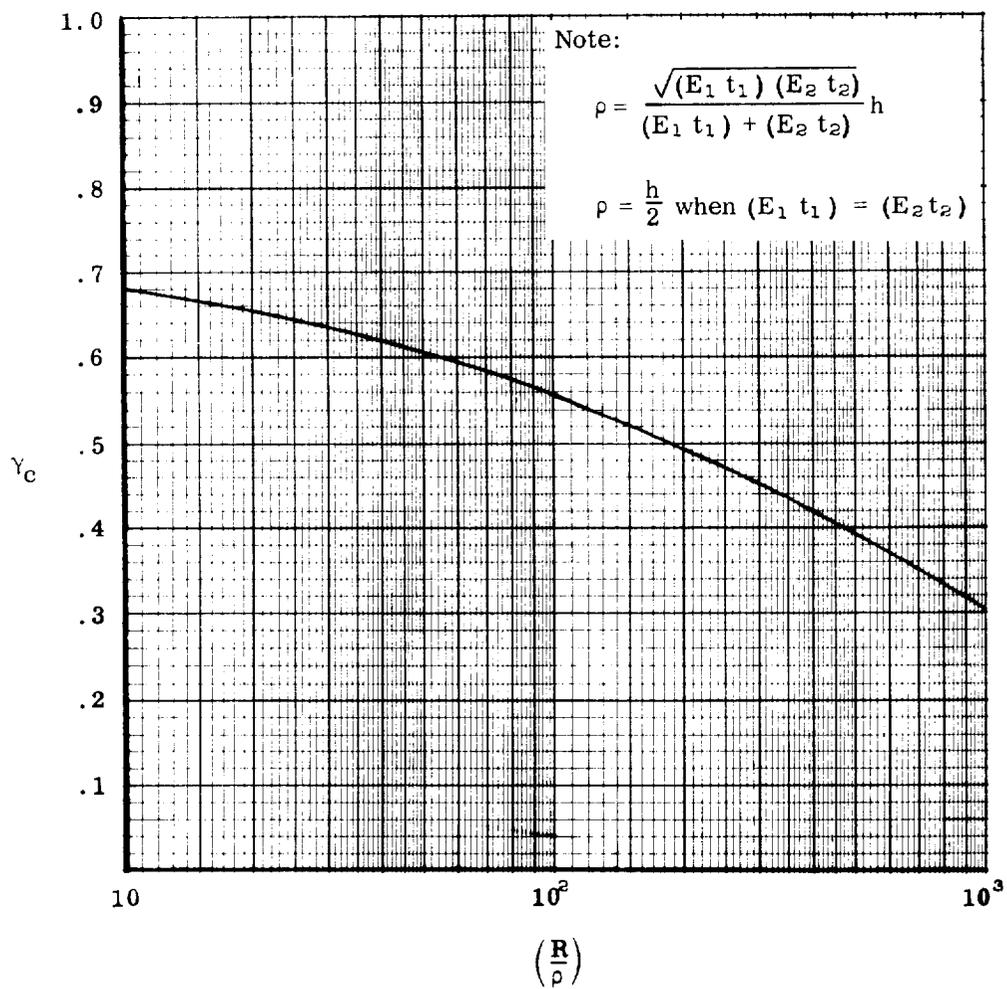
Figure 4.2-8. Design Knock-Down Factor for Circular Sandwich
Cylinders Subjected to Axial Compression

The chart shows γ_c on the vertical axis (from .1 to 1.0) and $\left(\dfrac{R}{\rho}\right)$ on the horizontal axis (from 10 to 10^3).

Note:

$$\rho = \frac{\sqrt{(E_1\, t_1)\,(E_2\, t_2)}}{(E_1\, t_1) + (E_2\, t_2)}\, h$$

$$\rho = \frac{h}{2} \text{ when } (E_1\, t_1) = (E_2\, t_2)$$

4-20

The critical axial load (in units of pounds) can be computed as follows:

$$P_{cr} = 2\pi R \left[\sigma_{cr_1} t_1 + \sigma_{cr_2} t_2 \right] \tag{4.2-26}$$

In the special case where $t_1 = t_2 \equiv t_f$ and both facings are made of the same material, Equations (4.2-17) through (4.2-26) can be simplified to the following:

$$\sigma_{cr} = \gamma_c K_c \sigma_0 \tag{4.2-27}$$

$$\sigma_0 = \frac{(\eta E_f)}{\sqrt{1-\nu_e^2}} \frac{h}{R} \tag{4.2-28}$$

$$\sigma_{crimp} = \frac{h^2}{2 t_f t_c} G_{xz} \tag{4.2-29}$$

$$V_c = \frac{\sigma_0}{\sigma_{crimp}} \tag{4.2-30}$$

$$P_{cr} = 4\pi R t_f \sigma_{cr} \tag{4.2-31}$$

Equations (4.2-17) through (4.2-31) and Figure 4.2-7 are valid only when the length L of the cylinder is greater than the length of a single axial half-wave in the buckle pattern for the corresponding infinite-length cylinder. For the case where $\theta = \dfrac{G_{xz}}{G_{yz}} = 1$, one can apply the following test to determine if the cylinder length is sufficiently large:

When $V_{c_1} < 2$	When $V_{c_1} \geq 2$
Equations (4.2-17) through (4.2-31) and Figure 4.2-7 are valid only where $$\left(\frac{L}{R}\right) \geq 1.57 \left[C_0 \left(2 - V_{c_1}\right) \right]^{\frac{1}{2}}$$	Equations (4.2-17) through (4.2-31) and Figure 4.2-7 are valid for any value of L.

4-21

For constructions where $\theta \neq 1$, no corresponding numerical criterion is presently available. In such cases, one can only use the above test in conjunction with engineering judgement. It is helpful to point out, however, that most practical sandwich cylinders for aerospace applications will be sufficiently long for Equations (4.2-17) through (4.2-31) and Figure 4.2-7 to be valid. In addition, it is comforting to note that the use of these relationships for shorter cylinders results in conservatism.

Cylinders which fail to meet the foregoing length requirement are usually referred to as short cylinders. The only means available for the analysis of such sandwich cylinders under axial compression is the solution of Stein and Mayers [4-13] which is only valid

     a.   when $\theta = 1$

and

     b.   when both ends of the cylinder are simply supported

and

     c.   when both facings are made of the same material

and

     d.   the thickness of one facing is not more than twice the thickness of the other facing.

For short sandwich cylinders which satisfy these conditions, one can use the design curves of Figure 4.2-9 which involves the following parameters:

$$Z = \frac{2L^2}{Rh} \sqrt{1-\nu_e^2} \qquad (4.2-32)$$

$$r_a = \frac{\pi^2 \, D}{L^2 \, D_q} \qquad\qquad (4.2\text{-}33)$$

$$K_c' = \frac{\sigma_{cr} \, (t_1 + t_2) \, L^2}{\gamma_c \, \pi^2 \, D} \qquad\qquad (4.2\text{-}34)$$

where

$$D = \eta \, \frac{(E_1 \, t_1)(E_2 \, t_2) \, h^2}{(1 - \nu_e^2) \left[(E_1 \, t_1) + (E_2 \, t_2) \right]} \qquad\qquad (4.2\text{-}35)$$

$$D_q = \frac{h^2}{t_c} \, G_{xz} \qquad\qquad (4.2\text{-}36)$$

and

L = Over-all length of cylinder, inches.

During the preparation of this handbook, no solutions were uncovered for axially com-
pressed sandwich cylinders having any degree of rotational restraint at the boundaries.
However, in most practical aerospace applications, the cylinders will be sufficiently
long for such fixity to have negligible effects on the buckling loads.
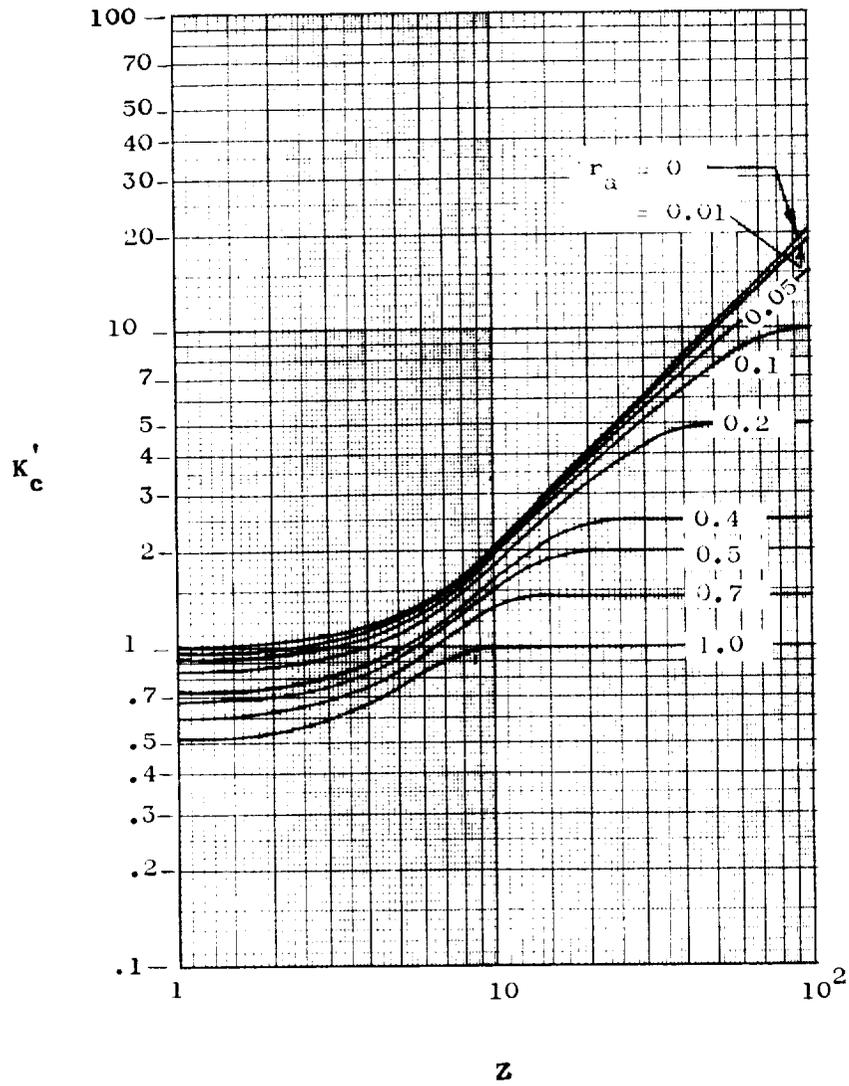
Figure 4.2-9. Buckling Coefficient for Short Simply-Supported Sandwich Cylinders Subjected to Axial Compression ($\theta = 1$)

4.3 PURE BENDING

4.3.1 Basic Principles

4.3.1.1 Theoretical Considerations

Based on small-deflection theory, investigations were made in References 4-14, 4-15, and 4-16 of elastic instability in thin-walled, isotropic (non-sandwich) cylinders subjected to axial compressive stresses which vary in the circumferential direction. From the results of these references, it can be concluded that, regardless of the nature of the circumferential stress distribution, classical instability is reached when the peak axial compressive stress satisfies the condition

$$\sigma \approx .6 \, \frac{Et}{R} \qquad\qquad (4.3-1)$$

It should be recalled that the value .6 Et/R is also obtained from the small-deflection solution for thin-walled, isotropic (non-sandwich) cylinders subjected to uniform axial compression. In view of this result, one might reasonably expect that small-deflection sandwich theory would also indicate that only the peak axial compressive stress need be considered in cases of pure bending or combined bending and axial compression. It has been shown in References 4-17, 4-18, and 4-19 that this is indeed the case. References 4-17 and 4-18 demonstrate this for weak-core sandwich cylinders while Reference 4-19 deals with infinitely long cylinders which fall in the stiff-core and moderately-stiff-core categories. Therefore, for the purposes of this handbook, it is assumed that the theoretical considerations of Section 4.2 (axial compression) apply equally well to sandwich cylinders which are subjected to pure bending if the analysis considers only the peak value of the applied compressive stress. The only differences lie in the empirical knock-down factors recommended for the two cases.

4-25

4.3.1.2 Empirical Knock-Down Factor

In the case of pure bending, only a relatively small portion of the cylinder's circumference experiences stress levels which initiate the buckling process. Because of the consequent reduced probability for peak stresses to coincide with the location of an imperfection, it is to be expected that the knock-down factors for pure bending will not be as severe as the corresponding factors for axial load. For thin-walled, isotropic (non-sandwich) cylinders under pure bending, Seide, et al. [4-9] have proposed the following lower-bound relationships:

$$\gamma_b = 1 - 0.731 \ (1 - e^{-\phi}) \qquad (4.3-2)$$

where

$$\phi = \frac{1}{16} \sqrt{\frac{R}{t}} \qquad (4.3-3)$$

Comparison against Equations (4.2-9) and (4.2-10) shows that this bending criterion does indeed give γ_b values of lesser severity than those which apply to the axially compressed cylinders. Following the same approach as that taken in Section 4.2, the above equations are rewritten in terms of the shell-wall radius of gyration $\rho \ (\approx \frac{h}{2}$ for sandwich constructions whose two facings are of equal thickness). The revised formulations then give the plot shown as a dashed curve in Figure 4.3-1. Also shown in this figure are the appropriate test points from stiff-core sandwich cylinders subjected to pure bending [4-20]. Since only three such data points are available, it was thought to be helpful to include the axial compression sandwich data points previously shown in Figure 4.2-3. To fully understand the information given in Figure 4.3-1, it is important for the reader to be aware of the data reduction techniques used here. For an

explanation of the procedures used in this handbook, reference should be made to the related discussion in Section 4.2.1.2.1.

Based on the limited amount of available test data, it is recommended here that the solid curve shown in Figure 4.3-1 be used for the design of sandwich cylinders subjected to pure bending. This gives γ_b values that are 75 percent of those obtained from the dashed curve which is based on the empirical formula of Seide, et al. [4-9]. This is consistent with the practice followed in Section 4.2 for the case of axial compression where the design knock-down factor was likewise taken to be 75 percent of the value obtained from the corresponding curve derived from Reference 4-9.

In view of the meager test data available from sandwich cylinders under pure bending, the method proposed in Section 4.3.2 is not very reliable when $V_c < 2.0$. Therefore, in such cases, the method can only be regarded as a "best-available" approach. On the other hand, when the failure is by shear crimping $(V_c \geq 2.0)$, the method is quite reliable and will, in fact, usually give conservative predictions.
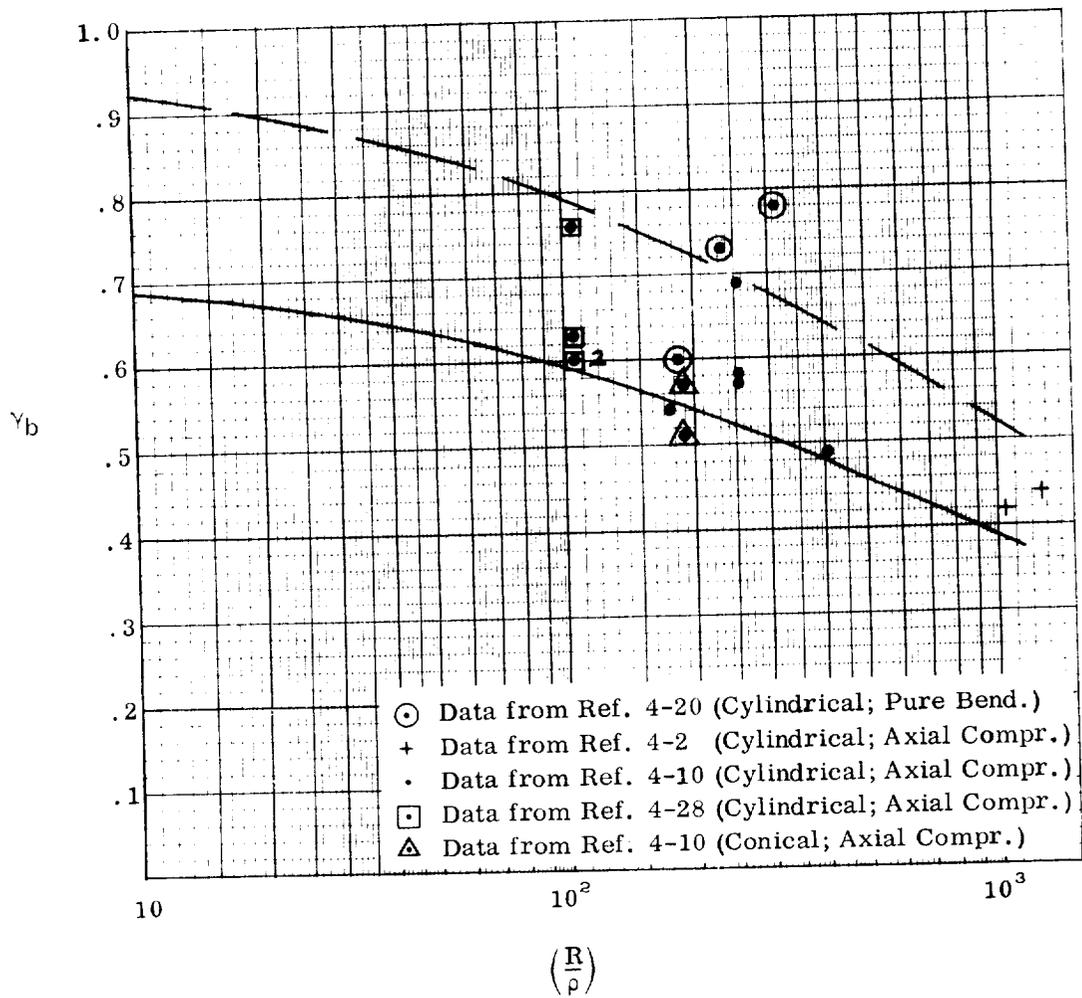
Figure 4.3-1. Knock-Down Factor γ_b for Circular Sandwich Cylinders Subjected to Pure Bending

The figure legend reads:

⊙ Data from Ref. 4-20 (Cylindrical; Pure Bend.)
+ Data from Ref. 4-2 (Cylindrical; Axial Compr.)
· Data from Ref. 4-10 (Cylindrical; Axial Compr.)
⊡ Data from Ref. 4-28 (Cylindrical; Axial Compr.)
△ Data from Ref. 4-10 (Conical; Axial Compr.)

4.3.2 Design Equations and Curves

For simply supported sandwich cylinders subjected to pure bending, one may use the same design equations and curves as are given in Section 4.2.2 (for axial compression) except for the following:

a.   For the case of pure bending, use Figure 4.3.2 to obtain the knock-down factor γ_b whenever $V_c < 2.0$ (When $V_c \geq 2.0$, use $\gamma_b = 1.0$).

b.   For the case of pure bending, the critical stresses obtained from the equations and curves of Section 4.2.2 correspond to the circumferential location which lies on the compressive side of the neutral axis and is furthest removed from that axis. Hence the computed stresses are the peak values within the variable circumferential distribution. Therefore, when the behavior is elastic, the critical bending moment M_{cr} can be computed from the following:

$$M_{cr} = \pi R^2 \left[\sigma_{cr_1} t_1 + \sigma_{cr_2} t_2 \right] \qquad (4.3-4)$$

where

M_{cr} = Critical bending moment, in.-lbs.

R = Radius to middle surface of sandwich cylinder, inches.

σ_{cr_1} and σ_{cr_2} = Critical compressive stresses in facings 1 and 2, respectively, which result in general instability of the cylinder, psi.

t_1 and t_2 = Thicknesses of the facings 1 and 2, respectively, inches.

Note: There is no preference as to which facing is denoted by the subscripts 1 and 2.

Note:

$$\rho = \frac{\sqrt{(E_1 \, t_1)(E_2 t_2)}}{(E_1 \, t_1) + (E_2 t_2)} h$$

$$\rho = \frac{h}{2} \text{ when } (E_1 \, t_1) = (E_2 t_2)$$
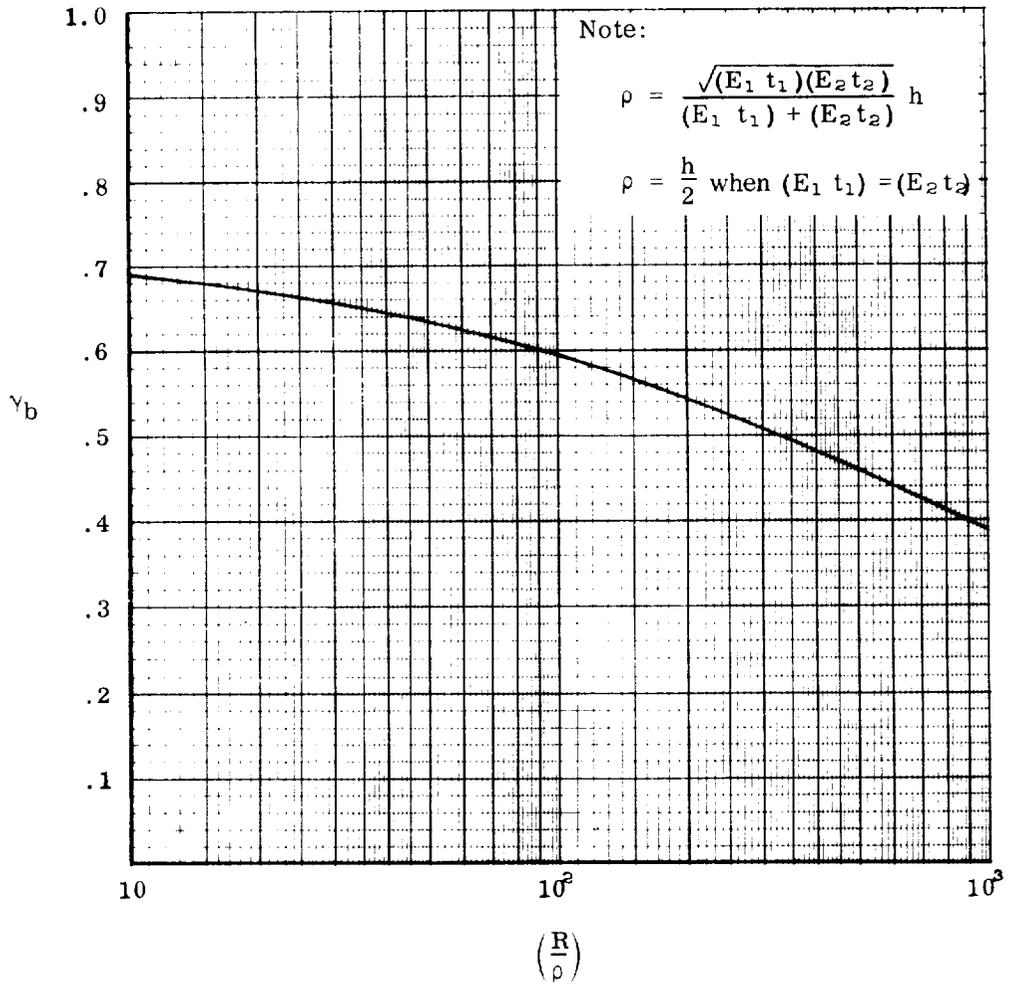
Figure 4.3-2. Design Knock-Down Factor γ_b for Circular Sandwich
Cylinders Subjected to Pure Bending

4-30

To compute M_{cr} when the behavior is inelastic, one must resort to numerical integration techniques.

Since the procedure recommended here makes use of the methods of Section 4.2.2, all of the limitations of that section are equally applicable to the present case. That is, only simply supported boundaries are considered and the primary solution is excessively conservative for the so-called short-cylinder constructions. In addition, only very limited means are available to facilitate a quantitative assessment of whether or not a particular construction falls within the short-cylinder classification. Furthermore, the computation of critical stresses for short-cylinder constructions can only be accomplished for rather special cases as cited in Section 4.2.2.

As noted in Section 4.2.2, during the preparation of this handbook, no solutions were uncovered for axially compressed sandwich cylinders having any degree of rotational restraint at the boundaries. However, it was also noted that, in most practical aerospace applications, the cylinders will be sufficiently long for such fixity to have negligible effects on the critical stresses. The same situation exists for the case of pure bending.

4.4 EXTERNAL LATERAL PRESSURE

4.4.1 Basic Principles

4.4.1.1 Theoretical Considerations

This section deals with the loading condition depicted in Figure 4.4-1. Note that the sandwich cylinder is subjected to external pressure only over the cylindrical surface. No axial loading is applied. In addition, it is specified that the ends are simply supported. That is, during buckling, both ends of the cylinder experience no radial displacements and no bending moments.
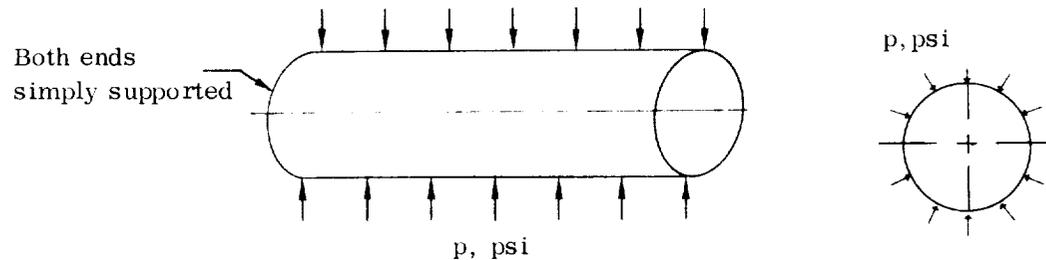
Figure 4.4-1. Circular Sandwich Cylinder Subjected to
External Lateral Pressure

The theoretical basis used here is the classical small-deflection solution of Kuenzi, et al. [4-21] which includes the following assumptions:

a. The facings are isotropic.

b. The facings may be of equal or unequal thicknesses.

c. The facings may be of the same or different materials.

d. Poisson's ratio is the same for both facings.

e. Bending of the facings about their own middle surfaces can be neglected.

f. The core has infinite extensional stiffness in the direction normal to the facings.

g. The core extensional and shear rigidities are negligible in directions parallel to the facings.

4-32

h. The transverse shear properties of the core may be either isotropic or orthotropic.

i. The inequality $\dfrac{2R}{h} \gg 1$ is satisfied.

j. Several additional order-of-magnitude assumptions are valid, as noted below in connection with Equation (4.4-2).

The solution of Kuenzi, et al. [4-21] draws upon the earlier groundwork laid by

Raville in References 4-22, 4-23, and 4-24. Norris and Zahn used these reports to

develop design curves which are published in References 4-25 and 4-26. The work of

Kuenzi, et al. [4-21] constitutes the latest revision to this series of reports and is

the most up-to-date treatment of the subject. However, the format of their results

has been slightly modified in Reference 4-5 in order to reduce the scope of interpola-

tion required in practical applications. The revised format is used here. However,

the need for interpolation has not been entirely eliminated since separate families are

still required for each of the selected values for V_p [see Equation (4.4-4)].

The final theoretical relationships used in this handbook are as follows:

$$P_{cr} = \frac{\eta \, C_p}{R\,(1-\nu_e^2)} \left[(E_1 t_1) + (E_2 t_2) \right] \qquad (4.4\text{-}1)$$

where

C_p = Minimum value (with respect to n) of K_p , dimensionless.

and

$$(4.4\text{-}2)$$

$$K_p = \frac{\psi^2\,(n^2-1)\left(3 + \frac{n^2\,L^2}{\pi^2 R^2}\right)\left[\left(\frac{n^2\,L^2}{\pi^2 R^2} - \frac{1}{3}\right)\left(n^2 - 1 + \frac{\pi^2 R^2}{L^2}\right) - \frac{2}{3}\right] + \frac{8}{9}\left[1 + \left(n^2 + \frac{\pi^2 R^2}{3L^2}\right)V_p\right]}{\left[\left(\frac{n^2\,L^2}{\pi^2 R^2} + 1\right)^2 (n^2-1) + \frac{1}{3}\right]\left[1 + \left(n^2 + \frac{\pi^2 R^2}{3L^2}\right)V_p\right]}$$

$$\nu^2 = \frac{(E_1 t_1)(E_2 t_2) h^2}{[(E_1 t_1) + (E_2 t_2)]^2 R^2} \tag{4.4-3}$$

$$V_p = \eta \frac{(E_1 t_1)(E_2 t_2) h}{[(E_1 t_1) + (E_2 t_2)](1-\nu_e^2) R^2 G_{yz}} \tag{4.4-4}$$

where

p_{cr} = Critical value of external lateral pressure, psi.

R = Radius to middle surface of cylindrical sandwich, inches.

ν_e = Elastic Poisson's ratio of facings, dimensionless.

η = Plasticity reduction factor, dimensionless.

E_1 and E_2 = Young's moduli of facings 1 and 2, respectively, psi.

t_1 and t_2 = Thicknesses of facings 1 and 2, respectively, inches.

n = Number of circumferential full-waves in the buckle pattern, dimensionless.

L = Over-all length of cylinder, inches.

h = Distance between middle surfaces of facings, inches.

G_{yz} = Core shear modulus associated with the plane perpendicular to the axis of revolution, psi.

Note: There is no preference as to which facing is denoted by the subscript 1 or 2.

For cases where the two facings are not made of the same material, the foregoing formulas are valid only when the behavior is elastic ($\eta = 1$). Application to inelastic cases ($\eta \neq 1$) can only be made when both facings are made of the same material. For such configurations, E_1 and E_2 will, of course, be equal.

Equation (4.4-2) constitutes an approximate expression for K_p since it embodies the assumptions cited earlier in this section in addition to the following:

a.   Terms containing K_p^2 and $\dfrac{K_p\, h^2}{4\, R^2}$ were neglected.

b.   It was assumed that $(1 \pm m\dfrac{h}{2R}) = 1$, where m is a small whole number.

By using Equation (4.4-2), plots can be generated of the form shown in Figure 4.4-2. The design curves of this handbook are of this type and were taken directly from Reference 4-5. It is helpful to note here that lower and upper limits exist for the coefficient C_p and these are identified in Figure 4.4-2. The lower limit is associated with long-cylinder behavior. Such configurations are unaffected by the end constraints and the related critical pressures are equal to those for rings which are subjected to external pressure. For portions of the cylinders that do not lie in the neighborhoods of the boundaries, the buckle patterns will be the same as are obtained from such rings. In this connection, it should be noted that application of the Donnell approximations [4-8] to non-sandwich rings leads to critical pressures which are 33 percent higher than the predictions from accurate ring formulations. This is due to the fact that the related number of circumferential full-waves (n = 2) is not sufficiently high to justify Donnell's [4-8] assumptions. It is important to observe that the theory of Reference 4-21 retains a sufficient number of terms to accurately predict the buckling of long cylinders. That is, when $G_{yz} \rightarrow \infty$ $(V_p \rightarrow 0)$ and L/R is large, the critical pressure is equal to the value obtained from that ring theory which is capable of properly describing the behavior where n = 2. The upper limit to the curve of Figure 4.4-2 is associated with the shear crimping mode of failure which involves extremely short

circumferential wavelengths $(n \to \infty)$. Specialization of Equations (4.4-1) through

(4.4-4) to this case gives the following formula for the critical compressive running

load N_{cr} measured in units of lbs/inch:

$$N_{cr} = h\, G_{yz} \qquad (4.4\text{-}5)$$

where

$$N_{cr} = p_{cr}\, R \qquad (4.4\text{-}6)$$

By using the approximation $h \approx t_c$, it can easily be shown that Equation (4.4-5) is

equivalent to the crimping formula presented earlier as Equation (2.3-9).
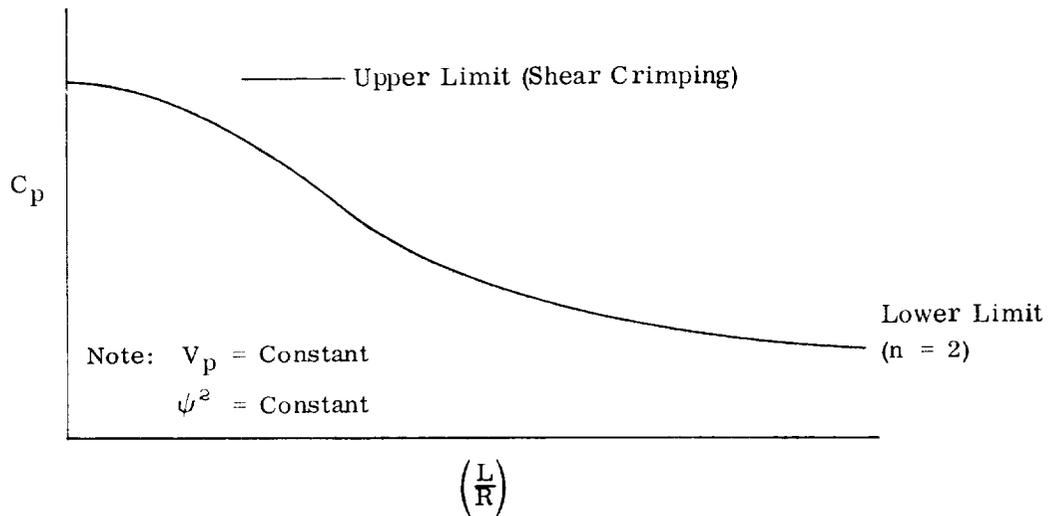
Figure 4.4-2. Schematic Representation of Log-Log Plot of C_p
Versus L/R for Circular Sandwich Cylinders
Subjected to External Lateral Pressure

Another important point which should be noted is that the approximate formula for K_p

[Equation (4.4-2)] does not contain the core shear modulus associated with the plane

perpendicular to the facings and oriented in the axial direction (G_{xz}). This modulus

has very little influence on cylinders longer than approximately one diameter and has

4-36

therefore disappeared through the approximations made in the development of Reference 4-21. Thus the theory and design curves presented in this section (Section 4.4) of the handbook can be considered applicable to sandwich cylinders having cores with either isotropic or orthotropic transverse shear moduli.

4.4.1.2 Empirical Knock-Down Factor

In Section 4.1 it is pointed out that, for circular cylinders subjected to external lateral pressure, the shape of the post-buckling equilibrium path is such that one would not expect strong sensitivity to the presence of initial imperfections. This has indeed been shown to be the case for isotropic (non-sandwich) cylinders where the available test data show rather good agreement with the predictions from classical small-deflection theory. In view of this, it has become widespread practice to either accept uncorrected small-deflection theoretical results as design values or to apply a uniform knock-down factor γ_p of 0.90 regardless of the radius-to-thickness ratio. In Reference 4-4 the latter practice is also recommended for sandwich cylinders and this approach has likewise been selected as the criterion for this handbook.

The only available test data for sandwich cylinders subjected to external lateral pressure are those given in References 4-27 and 4-28. In the first of these documents, Kazimi reports the results from two specimens which were identical except for the use of normal-expanded core in one cylinder while the other incorporated over-expanded core. The following results were obtained:

Comparison of Theoretical Predictions Versus Test Results of Kazimi [4-27]

①	②	③	④
Core Type	Test p_{cr} (psi)	Theoretical p_{cr} Based on Ref. 4-5 and $\gamma_p = 1.0$ (psi)	$(\gamma_p)_{Test}$ $= \dfrac{(Test\ p_{cr})}{(Theo.\ p_{cr})}$ $=$ ② $\div$ ③
Normal-Expanded	17	30.5	.56
Over-Expanded	27	30.5	.88

Kazimi [4-27] attributes the scatter in his test results to the circumstance whereby the over-expanded condition gives more uniform core properties than are obtained from normal-expanded honeycomb. The argument put forth on behalf of this viewpoint rests on the fact that the over-expanded core exhibits less anticlastic (saddle-type) deformation in forming the core to the shape of the cylinder.

In Reference 4-28 Jenkinson and Kuenzi report the results obtained from five test cylinders of nominally identical construction. These cylinders all had glass-reinforced plastic facings. Each facing was composed of three layers of glass fabric with their individual orientations controlled to provide a laminate having in-plane properties which were essentially isotropic. The following results were obtained from these cylinders:

<div align="center">

**Comparison of Theoretical Predictions Versus
Test Results of Reference 4-28**

</div>

①	②	③	④
Cylinder No.	Test p_{cr} (psi)	Theoretical p_{cr} Based on Ref. 4-5 and $\gamma_p = 1.0$ (psi)	$(\gamma_p)_{Test} = \dfrac{(Test\ p_{cr})}{(Theo.\ p_{cr})} = ② \div ③$
1	60	55.2	1.09
2	52.5	45.2	1.16
3	52.5	52.6	1.00
4	52.5	45.2	1.16
5	52.5	47.6	1.10

For specimens 2 through 5 it was reported that initial buckling occurred at external lateral pressures which ranged from 50 to 55 psi. Therefore, in the above tabulation

it was assumed that each of these four cylinders buckled at 52.5 psi. In general, the test values are somewhat higher than the theoretical predictions. This is probably due to

  a.   the absence of precise data on the material properties

  b.   inaccuracies due to interpolation between the theoretical curves

and

  c.   the fact that the facings were relatively thick in comparison with the sandwich thickness $\left(\dfrac{t_f}{h} \approx .25\right)$.

The foregoing test results from References 4-27 and 4-28 seem to provide added justification for the use of $\gamma_p = 0.90$ as a lower-bound knock-down factor. However, it would certainly be desirable to supplement these data with additional tests on specimens having small t_f/h ratios which would be truly representative of configurations usually found in realistic full-size sandwich cylinders.

An additional point of interest concerning the use of a uniform value of $\gamma_p = 0.90$ is the fact that shear crimping failures will be insensitive to the presence of initial imperfections. Hence, in the region where this mode of failure prevails, one could safely use the value $\gamma_p = 1.0$, especially since the theoretical basis used here neglects the bending stiffnesses of the facings about their own middle surfaces. However, inspection of the design curves of Section 4.4.2 shows that this type of failure will only occur for extremely low L/R values. This fact, coupled with considerations of simplicity and the moderate nature of the value $\gamma_p = 0.90$, led to the selection here of a uniform knock-down factor.

In view of the meager test data available from sandwich cylinders subjected to external lateral pressure, the method recommended here can presently be regarded as only a "best-available" approach. However, there appears to be little reason to doubt that further testing would show these procedures to be quite reliable.

4.4.2 Design Equations and Curves

For simply supported circular sandwich cylinders subjected to external lateral pressure, the critical pressure may be computed from the equation

$$P_{cr} = \frac{\gamma_p \, \eta \, C_p}{R(1-\nu_e^2)} \left[(E_1 t_1) + (E_2 t_2) \right] \qquad (4.4-7)$$

where

$$\gamma_p = 0.90$$

and C_p is obtained from Figures 4.4-3 through 4.4-5. In order to use these curves, one must compute the following values:

$$U^2 = \frac{(E_1 t_1)(E_2 t_2) \, h^2}{\left[(E_1 t_1) + (E_2 t_2) \right]^2 \, R^2} \qquad (4.4-8)$$

$$V_p = \eta \, \frac{(E_1 t_1)(E_2 t_2) \, h}{\left[(E_1 t_1) + (E_2 t_2) \right] (1-\nu_e^2) \, R^2 \, G_{yz}} \qquad (4.4-9)$$

For elastic cases, use $\eta = 1$. Whenever the behavior is inelastic, the methods of Section 9 must be employed.

For cases where the two facings are not made of the same material, the foregoing formulas are valid only when the behavior is elastic ($\eta = 1$). Application to inelastic cases ($\eta \neq 1$) can only be made when both facings are made of the same material. For such configurations, E_1 and E_2 will, of course, be equal.

Since separate families of design curves (C_p vs L/R) are provided for only three values of V_p, one will usually find it necessary to use graphical interpolation or extrapolation to establish C_p for the configuration of interest. Where desired,

4-42

improved accuracy can be obtained by minimizing Equation (4.4-2) with respect to n in order to obtain C_p.

The results given by the procedures specified here apply to sandwich cylinders having cores with either isotropic or orthotropic transverse shear moduli.
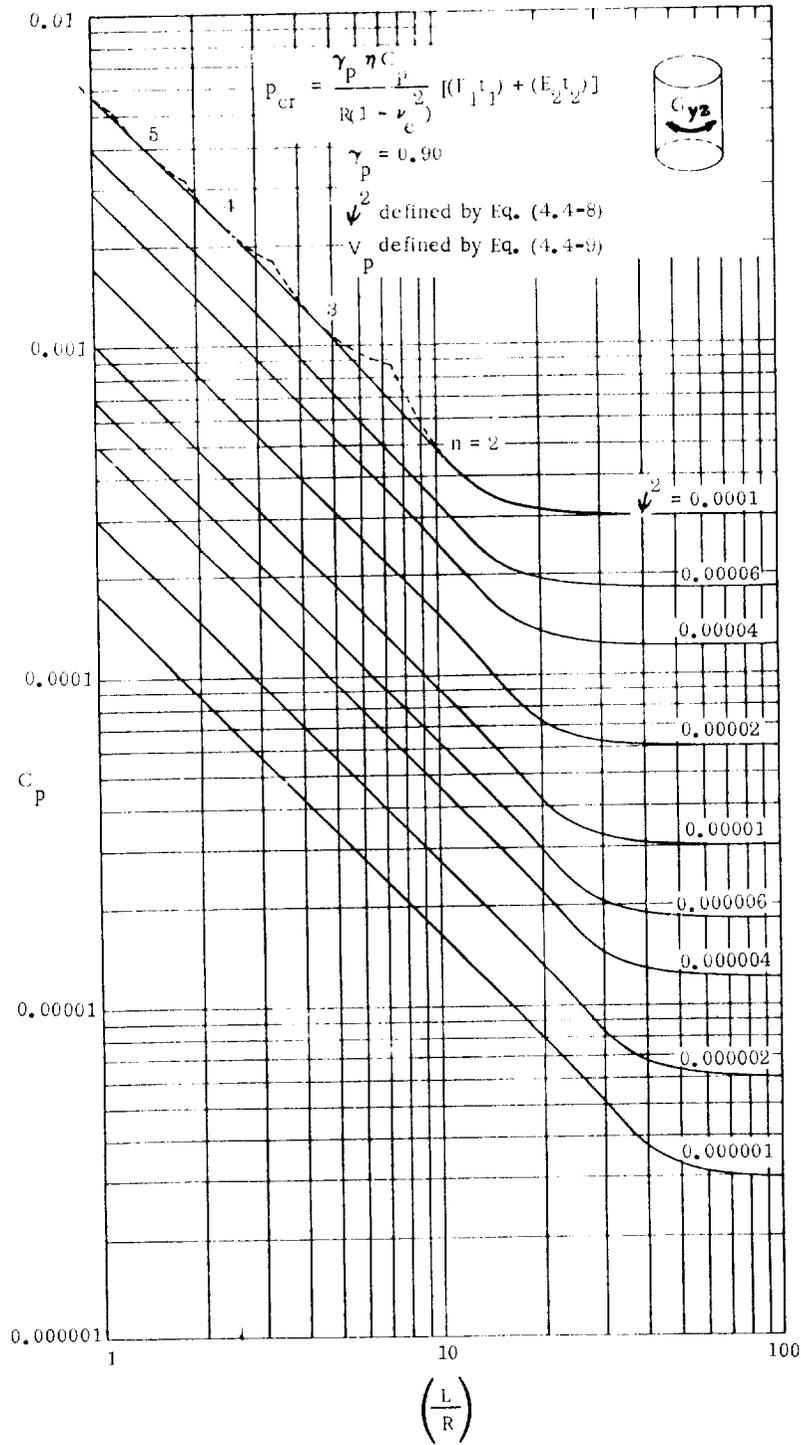
Figure 4.4-3. Buckling Coefficients C_p for Circular Sandwich Cylinders Subjected to External Lateral Pressure; Isotropic Facings; Transverse Shear Properties of Core Isotropic or Orthotropic; $V_p = 0$
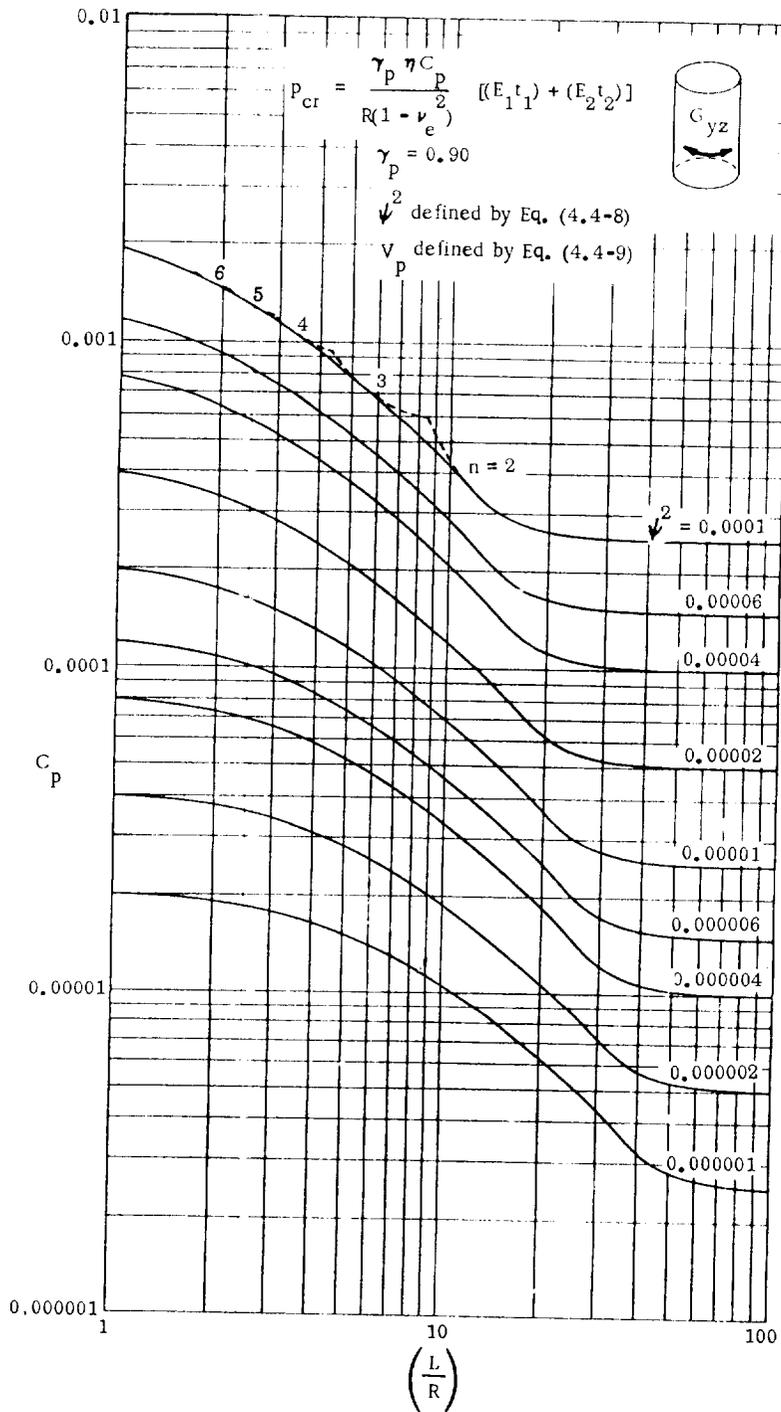
Figure 4.4-4. Buckling Coefficients C_p for Circular Sandwich Cylinders Subjected to External Lateral Pressure; Isotropic Facings; Transverse Shear Properties of Core Isotropic or Orthotropic; $V_p = 0.05$

4-45
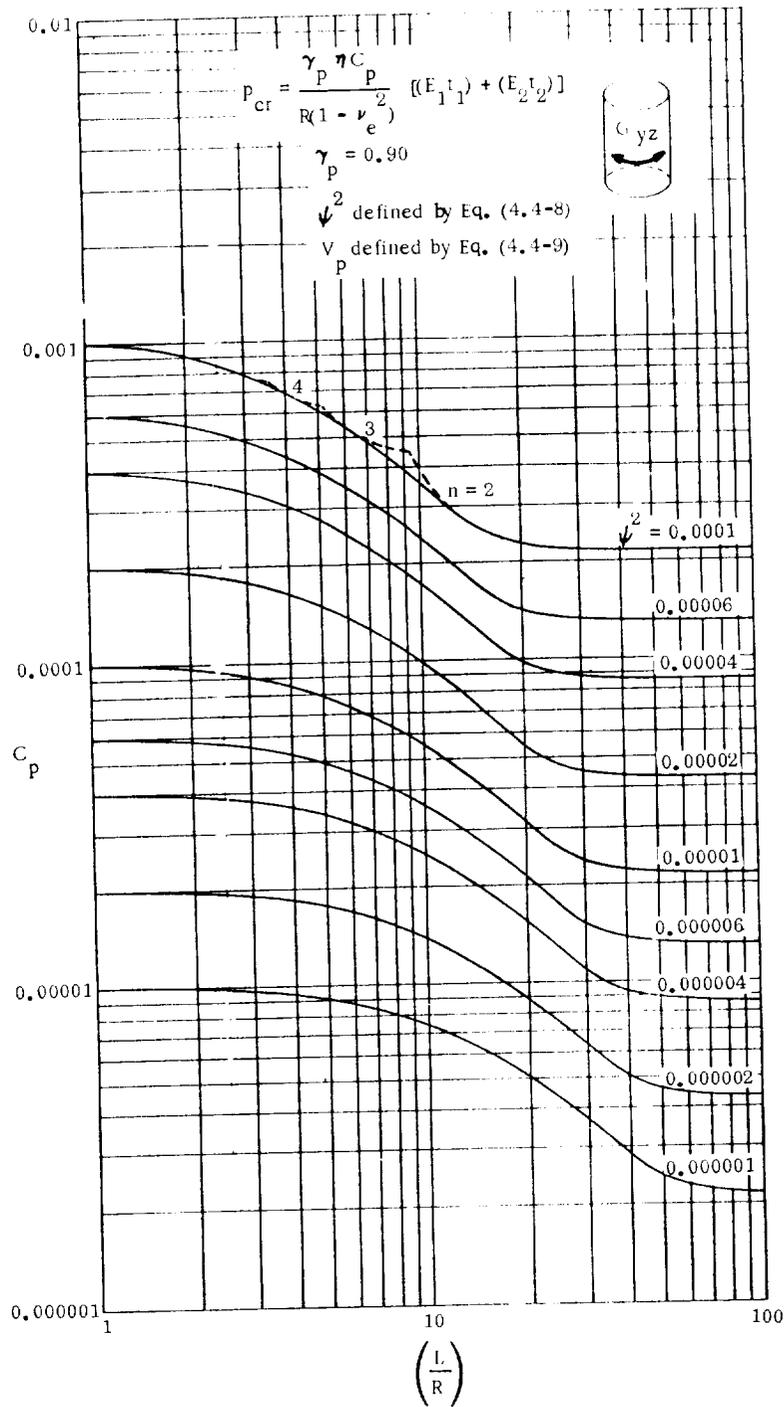
Figure 4.4-5. Buckling Coefficients C_p for Circular Sandwich Cylinders Subjected to External Lateral Pressure; Isotropic Facings; Transverse Shear Properties of Core Isotropic or Orthotropic; $V_p = 0.10$

4-46

4.5 TORSION

4.5.1 Basic Principles

4.5.1.1 Theoretical Considerations

This section deals with the loading condition depicted in Figure 4.5-1. Note that the only consideration given to boundary conditions is that, during buckling, it is assumed that no radial displacements occur at either end. Further conditions at these boundaries are completely disregarded. This approach should be sufficiently accurate for all simply supported cylinders except those which are very short.

T, In.-Lbs. Torque

T, In.-Lbs. Torque

It is assumed that, during buckling, no radial displacements occur at either end.
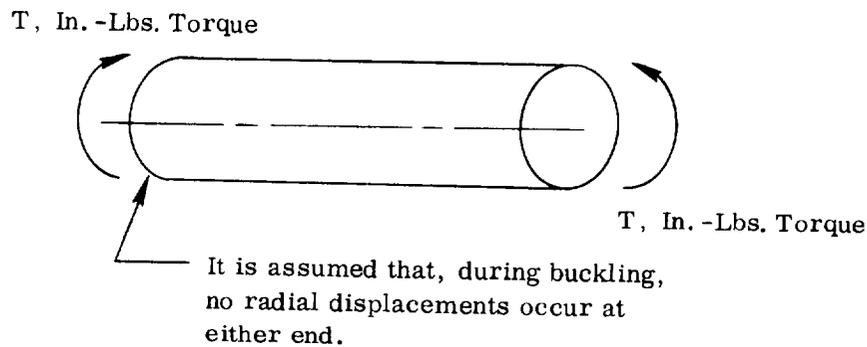
Figure 4.5-1. Circular Sandwich Cylinder Subjected to Torsion

The buckling of isotropic (non-sandwich), circular cylinders subjected to torsion was treated by Donnell in Reference 4-8 which has become a standard source of information concerning reasonable approximations which can be employed in practical thin-shell theory. Using the Donnell approximations, Gerard [4-29] has investigated the buckling of long circular sandwich cylinders subjected to torsion. This solution gives no consideration whatsoever to the boundary conditions. Such an approach is valid in

view of the assumed extremely long configuration. On the other hand, in Reference 4-30, March and Kuenzi develop small-deflection solutions for sandwich cylinders of both finite and infinite lengths. The boundary conditions taken for the finite-length cylinders are as indicated in Figure 4.5-1. For the purposes of this handbook, Reference 4-30 is considered to provide the most up-to-date treatment of the subject. The theoretical design curves given in Section 4.5.2 were taken directly from that report and embody the following assumptions:

a. The facings are isotropic.

b. The facings are of equal thickness. However, the curves are reasonably accurate for sandwich cylinders having unequal facings, provided that the thickness of one facing is not more than twice the other.

c. Young's modulus is the same for both facings.

d. Poisson's ratio is the same for both facings.

e. The core has infinite extensional stiffness in the direction normal to the facings.

f. The core extensional and shearing stiffnesses are negligible in directions parallel to the facings.

g. The transverse shear properties of the core may be either isotropic or orthotropic.

h. The approximations of Donnell [4-8] can be applied.

The design curves include separate families which respectively neglect and include bending of the facings about their own middle surfaces. However, for both of these situations, it is assumed that the facings are thin.

The theoretical buckling relationship used here is

$$\tau_{cr} = K_s \; \eta \; E_f \frac{d}{R} \tag{4.5-1}$$

which is based on the further assumption that both facings are made of the same material. The notation used here is as follows:

τ_{cr} = Critical value of facing shear stress, psi.

K_s = Torsional buckling coefficient, dimensionless.

η = Plasticity reduction factor, dimensionless.

E_f = Young's modulus of facings, psi.

d = Total thickness of sandwich wall.

$$d = t_c + t_1 + t_2 \tag{4.5-2}$$

t_c = Thickness of core, inches.

t_1 and t_2 = Thicknesses of the facings (There is no preference as to which facing is denoted by the subscript 1 or 2.), inches.

R = Radius to middle surface of sandwich cylinder, inches.

The buckling coefficient K_s is arrived at by the minimization of a complicated expression given in Reference 4-30. This formulation is not reproduced here. However, it should be noted that the indicated minimization leads to K_s values which can be plotted in the general form shown in Figure 4.5-2 where

$$Z_s = \frac{L^2}{dR} \tag{4.5-3}$$

$$V_s = \frac{16 \; t_c \; t_1 \; t_2 \; \eta \; E_f}{15 \; (t_1 + t_2) \; R \; d \; G_{xz}} \tag{4.5-4}$$

4-49

$$\theta \ - \ \frac{G_{xz}}{G_{yz}}$$

<div align="right">(4.5-5)</div>

and

L — Over-all length of cylinder, inches.

G_{xz} = Core shear modulus associated with the plane perpendicular to the facings and oriented in the axial direction, psi.

G_{yz} = Core shear modulus associated with the plane perpendicular to the axis of revolution, psi.

n — Number of circumferential full-waves in the buckle pattern, dimensionless.
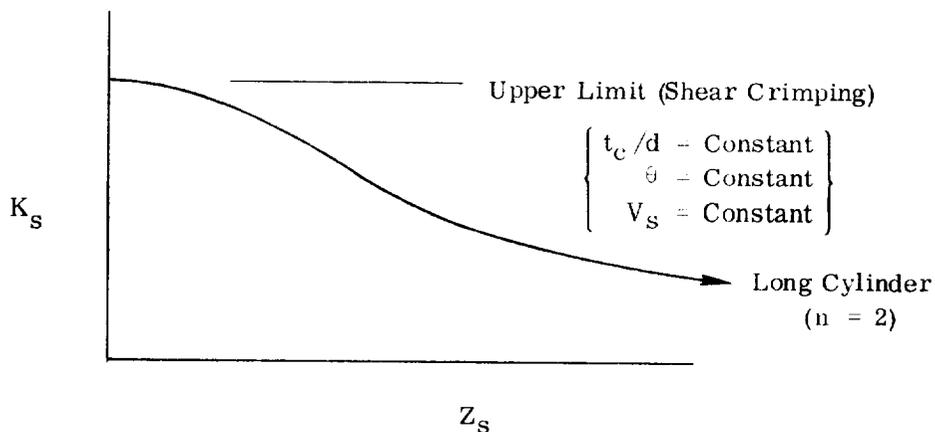
Figure 4.5-2. Typical Log-Log Plot of the Buckling Coefficient K_s for Circular Sandwich Cylinders Subjected to Torsion

The curves given in Section 4.5.2 are of this type. Note that the upper limit for the buckling coefficient K_s corresponds to the shear crimping mode of failure which involves extremely short circumferential wave-lengths ($n \to \infty$). Specialization of the buckling equations to this case leads to the following result when it is assumed that $t_c /d \approx 1$:

$$\tau_{cr} = \tau_{crimp} = \frac{h^2}{(t_1 + t_2) t_c} \sqrt{G_{xz} G_{yz}} \qquad (4.5\text{-}6)$$

where

h = Distance between middle surfaces of facings, inches.

In connection with sandwich constructions having large values for the parameter Z_s (long cylinders), it is pointed out that the cylinder will buckle into an oval shape (n = 2) for which the Donnell approximations [4-8] are no longer valid. To illustrate this point, attention is drawn to the results obtained for isotropic (non-sandwich), circular cylinders subjected to torsion. By using the Donnell approximations, Gerard [4-31] obtains the following result for the critical shear stress of such cylinders:

$$\tau_{cr} = \frac{0.272}{(1-\nu_e^2)^{3/4}} E \left(\frac{t}{R}\right)^{3/2} \qquad (4.5\text{-}7)$$

In Reference 4-32, Timoshenko presents the following result from a more rigorous solution which does not invoke the Donnell approximations:

$$\tau_{cr} = \frac{E}{3\sqrt{2}\,(1-\nu_e^2)^{3/4}} \left(\frac{t}{R}\right)^{3/2} \qquad (4.5\text{-}8)$$

The more exact result gives a critical stress which is only 87 percent of that given by the Donnell approach. This is similar to the situation encountered in the case of external lateral pressure (see Section 4.4) where the difference is even more pronounced. Since the torsional design curves of Section 4.5.2 incorporate the Donnell approximations, they must be used with caution in the case of long cylinders (n = 2).

4.5.1.2 Empirical Knock-Down Factor

In Section 4.1 it is pointed out that, for circular cylinders subjected to torsion, the shape of the post-buckling equilibrium path is such that one would not expect the sensitivity to initial imperfections to be as strong as that encountered in the case of axial compression. On the other hand, the sensitivity in torsion would be expected to be somewhat more severe than is exhibited by circular cylinders under external lateral pressure. In the case of isotropic (non-sandwich), circular cylinders loaded in torsion Reference 4-8 indicates that, over an enormous range of sizes, proportions, and materials, a lower-bound curve to the available test data can be obtained by taking 60 percent of the values obtained from classical small-deflection theory ($\gamma_s = 0.60$). Average values of the test data can be approximated by using 80 percent of the classical theoretical predictions ($\gamma_s = 0.80$).

To date, no test data has been published for sandwich cylinders which are of the types considered in this handbook and are subjected to torsion. Therefore, no empirical basis exists for the determination of reliable knock-down factors in such cases. Based on the moderate drop-off of the post-buckling equilibrium path, some sources [4-5] recommend that no reduction be employed ($\gamma_s = 1.0$). However, Reference 4-4 takes a more cautious approach in recommending the use of $\gamma_s = .80$ for the sandwich configuration. This selection was made largely on the basis of the isotropic (non-sandwich) data. Although this value did not furnish a lower-bound to the isotropic test points, it is reasonable to expect that the usually greater thicknesses of sandwich cylinders should lead to more moderate reductions than apply to the isotropic (non-

sandwich) configurations. In addition, it should be noted that cylinders under torsion will continue to support considerable torque well into the postbuckled region. Hence the torsional buckling mechanism should not be nearly so catastropic as the general instability of axially compressed cylinders. With these several factors in mind, the value $\gamma_S = 0.80$ has been selected for use in this handbook. In view of the lack of sandwich test data to substantiate this selection, the methods proposed here can only be regarded as a "best-available" approach.

4.5.2 Design Equations and Curves

For simply supported circular sandwich cylinders subjected to torsion, the critical shear stress may be computed from the equation

$$\tau_{cr} = \gamma_s \, K_s \, \eta \, E_f \, \frac{d}{R} \tag{4.5-9}$$

where

$$\gamma_s = 0.80 \tag{4.5-10}$$

$$d = t_c + t_1 + t_2 \tag{4.5-11}$$

and K_s is obtained from Figures 4.5-3 through 4.5-8. In order to use these curves, one must first compute each of the following values:

$$Z_s = \frac{L^2}{dR} \tag{4.5-12}$$

$$V_s = \frac{16 \, t_c \, t_1 \, t_2 \, \eta E_f}{15 \, (t_1 + t_2) \, R \, d \, G_{xz}} \tag{4.5-13}$$

$$\theta = \frac{G_{xz}}{G_{yz}} \tag{4.5-14}$$

It is required here that both facings be made of the same material.

For elastic cases, use $\eta = 1$. Whenever the behavior is inelastic, the methods of Section 9 must be employed.

The critical torque T_{cr}, measured in units of in.-lbs, can be computed from the following for both elastic and inelastic cases:

$$T_{cr} = 2\pi R^2 \, (t_1 + t_2) \, \tau_{cr} \tag{4.5-15}$$

4-54

Curves for K_s are given for values of $\theta = 0.4$; 1.0; and 2.5. Estimates of K_s for other values of θ can be obtained by interpolation.

In addition, curves for K_s are given for values of $t_c/d = 1.0$ and 0.7. The former neglect the contribution from bending of the facings about their own middle surfaces. The latter may be used to obtain numerical estimates of the conservatism introduced by neglecting these stiffnesses.

As noted in Section 4.5.1.1, the design curves are somewhat inaccurate in the region where Z_s is large (long cylinders). Some caution should be exercised in the application of the curves in this region.

Strictly speaking, Figures 4.5-3 through 4.5-8 apply only when the facings are equal. However, the curves are reasonably accurate for sandwich cylinders having unequal facings, provided that the thickness of one facing is not more than twice the other.

The equations shown on the figure:

$$\tau_{cr} = \gamma_s \, K_s \, \eta \, E_f \frac{d}{R}$$

$$Z_s = \frac{L^2}{dR}$$

$$V_s = \frac{16 \, t_c \, t_1 \, t_2 \, \eta \, E_f}{15(t_1 + t_2) \, R \, d \, G_{xz}}$$

$$\frac{t_c}{d} = 1$$

$$\eta = 0.4$$

Curve labels: $V_s = 0$, $V_s = 0.2$, $V_s = 0.4$, $V_s = 0.6$, $V_s = 0.8$, $V_s = 1.2$, $V_s = 1.6$, $V_s = 2.0$
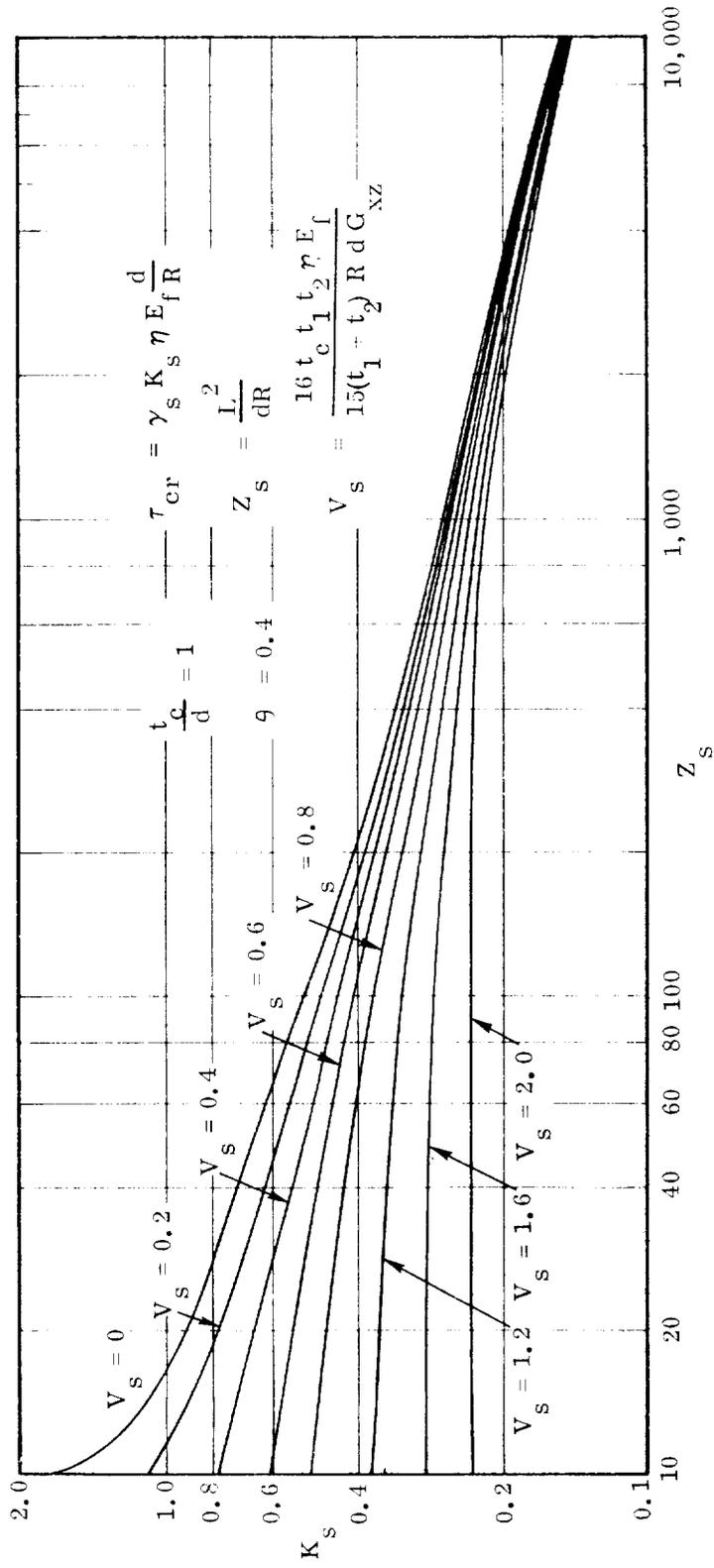
Figure 4.5-3. Buckling Coefficients for Circular Sandwich Cylinders Subjected to Torsion

4-56

$$\tau_{cr} = \gamma_s K_s \eta E_f \frac{d}{R}$$

$$\frac{t_c}{d} = 1$$

$$Z_s = \frac{L^2}{dR}$$

$$\theta = 1$$

$$V_s = \frac{16 t_c t_1 t_2 \eta E_f}{15(t_1 + t_2) R d G_{xz}}$$
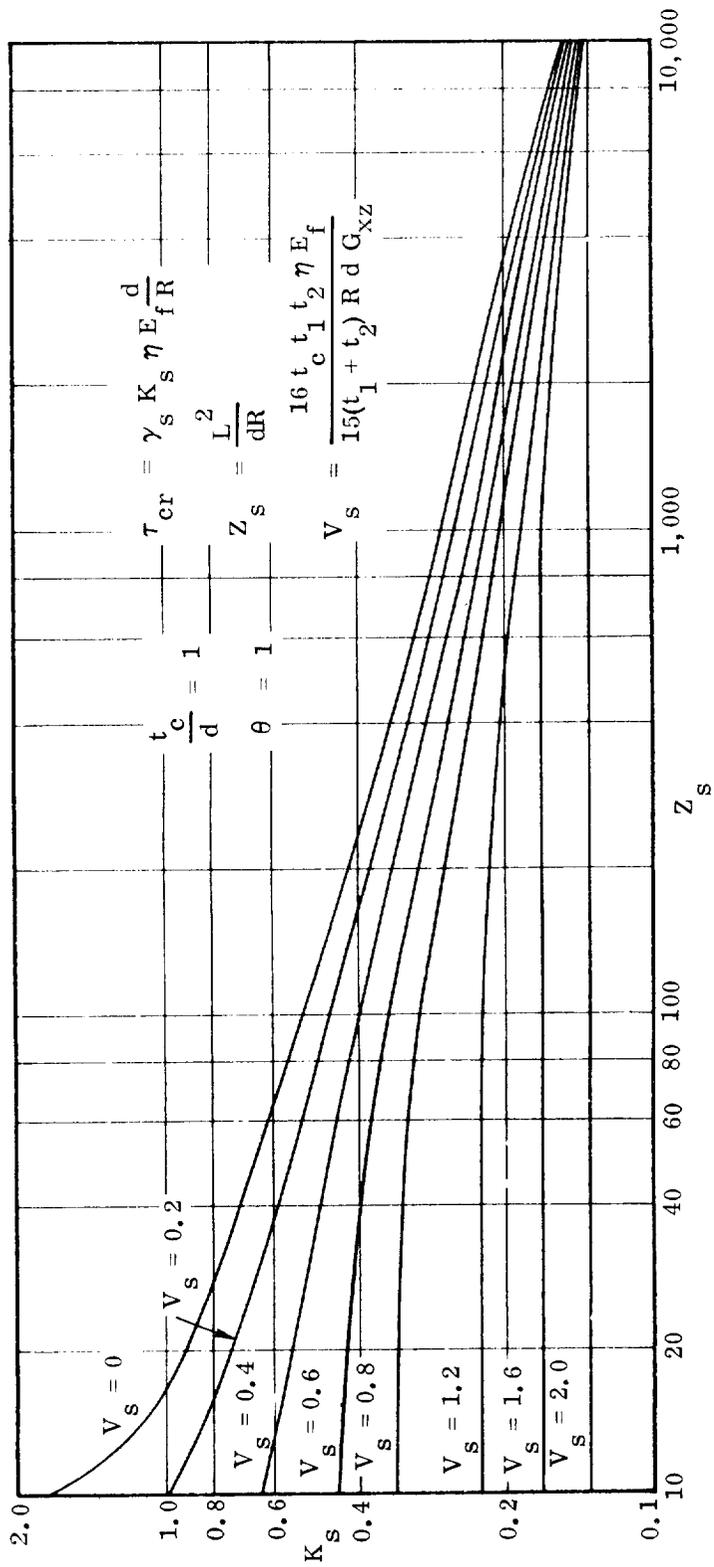
Figure 4.5-4. Buckling Coefficients for Circular Sandwich Cylinders Subjected to Torsion
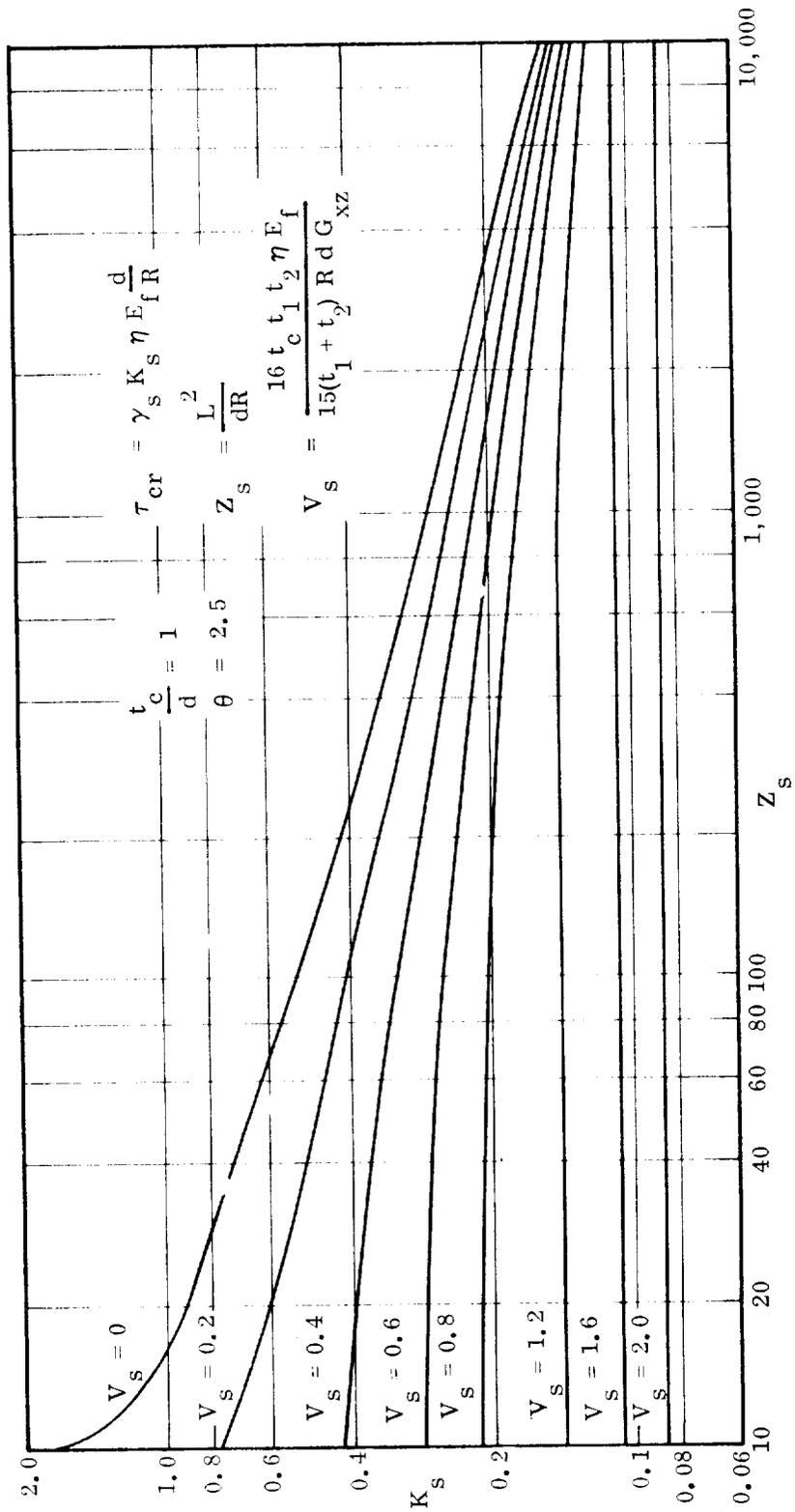
Figure 4.5-5. Buckling Coefficients for Circular Sandwich Cylinders Subjected to Torsion

The figure shows a plot of K_s versus Z_s with curves for various values of V_s ($V_s = 0$, 0.2, 0.4, 0.6, 0.8, 1.2, 1.6, 2.0).

$$\tau_{cr} = \gamma_s K_s \eta E_f \frac{d}{R}$$

$$Z_s = \frac{L^2}{dR}$$

$$V_s = \frac{16 t_c t_1 t_2 \eta E_f}{15(t_1 + t_2) R d G_{xz}}$$

$$\frac{t_c}{d} = 1$$

$$\theta = 2.5$$

$\tau_{cr} = \gamma_s K_s \eta E_f \dfrac{d}{R}$

$Z_s = \dfrac{L^2}{dR}$

$V_s = \dfrac{16 t_c t_1 t_2 \eta E_f}{15(t_1 + t_2) R d G_{xz}}$

$\dfrac{t_c}{d} = 0.7$

$\theta = 0.4$

$V_s = 0$

$V_s = 0.2$

$V_s = 0.4$

$V_s = 0.6$

$V_s = 0.8$

$V_s = 1.2$

$V_s = 1.6$

$V_s = 2.0$

Z_s

K_s
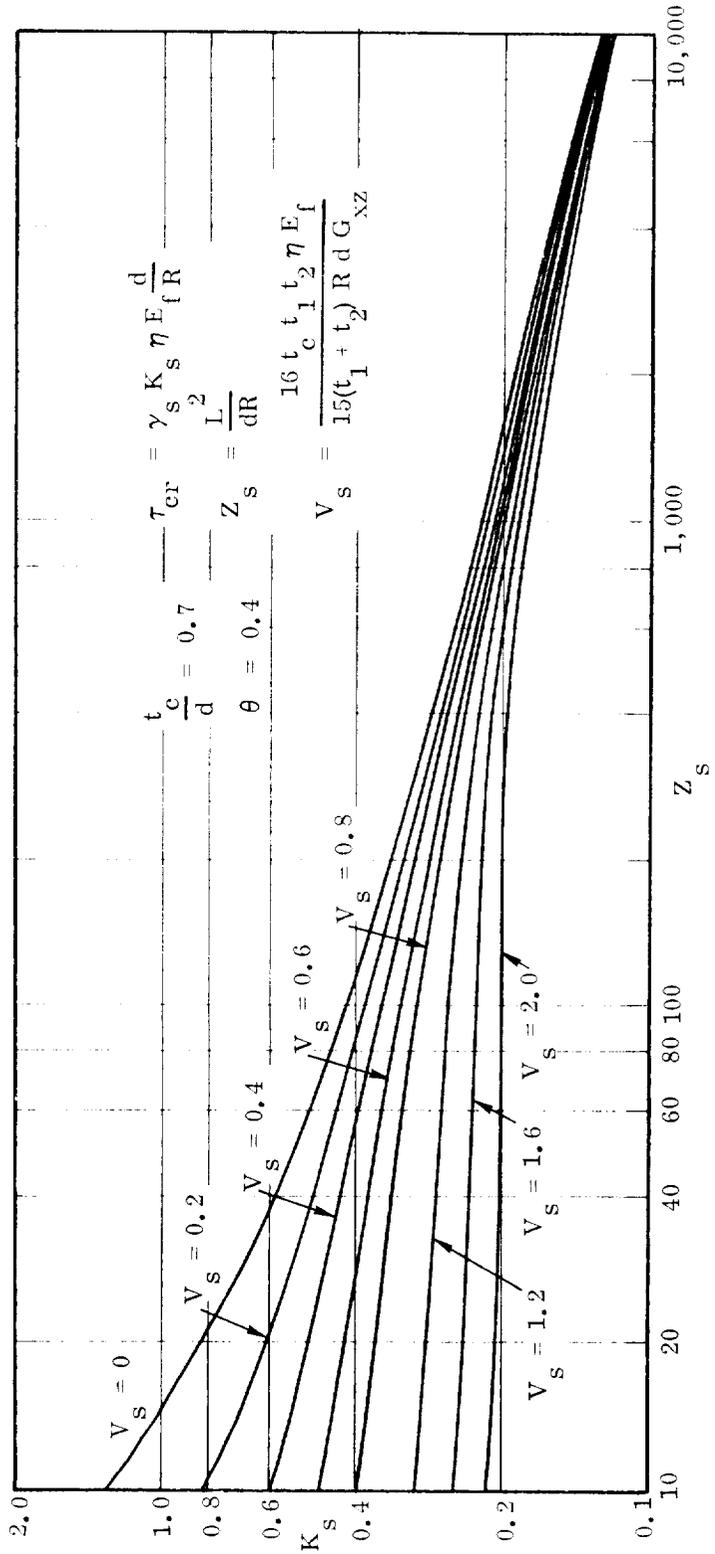
Figure 4.5-6. Buckling Coefficients for Circular Sandwich Cylinders Subjected to Torsion
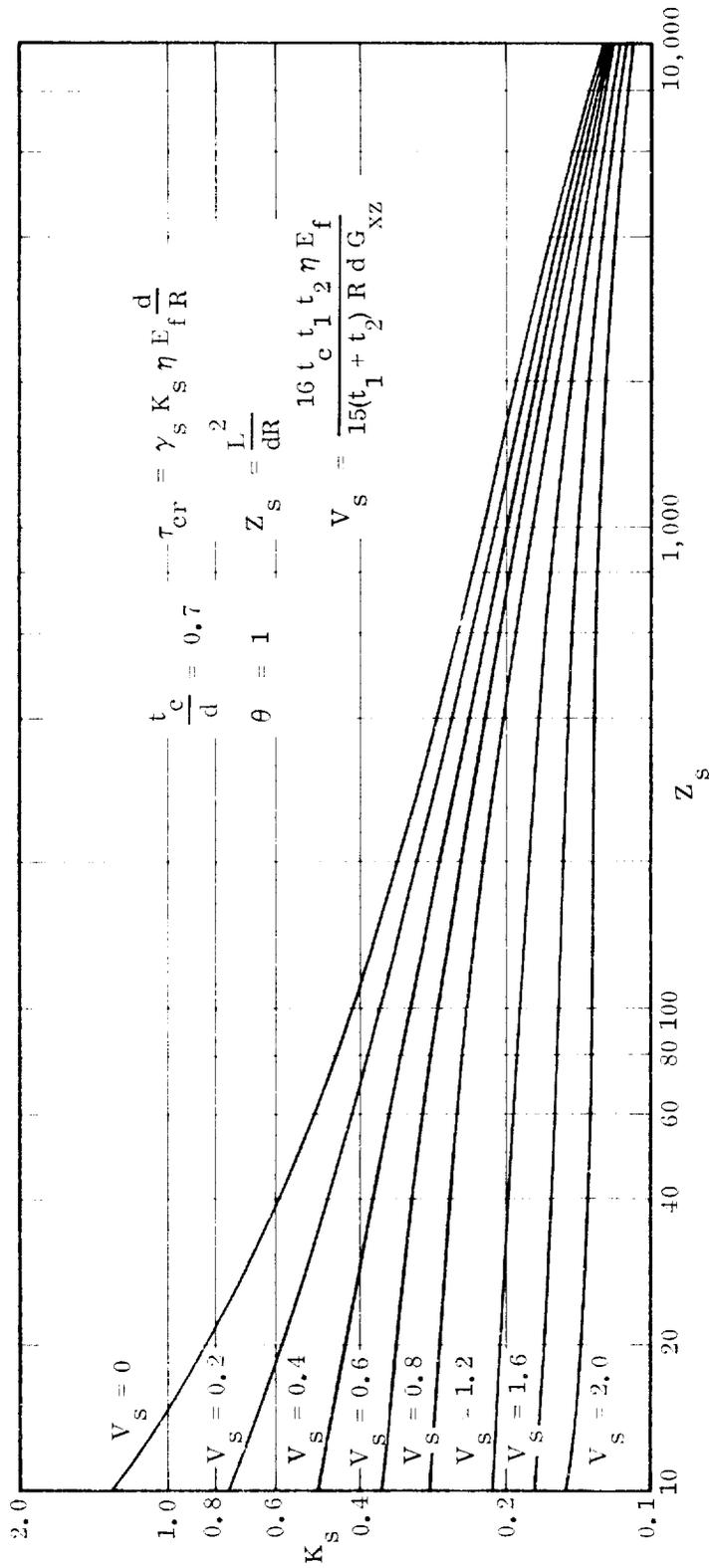
Figure 4.5-7. Buckling Coefficients for Circular Sandwich Cylinders Subjected to Torsion

The chart shows curves for $V_s = 0$, $V_s = 0.2$, $V_s = 0.4$, $V_s = 0.6$, $V_s = 0.8$, $V_s = 1.2$, $V_s = 1.6$, $V_s = 2.0$ plotted as K_s versus Z_s.

$$\frac{t_c}{d} = 0.7$$

$$\theta = 1$$

$$\tau_{cr} = \gamma_s K_s \eta E_f \frac{d}{R}$$

$$Z_s = \frac{L^2}{dR}$$

$$V_s = \frac{16 t_c t_1 t_2 \eta E_f}{15(t_1 + t_2) R d G_{xz}}$$

4-60

$$\dfrac{t_c}{d} = 0.7 \qquad \tau_{cr} = \gamma_s K_s \eta E_f \dfrac{d}{fR}$$

$$\theta = 2.5 \qquad Z_s = \dfrac{L^2}{dR}$$

$$V_s = \dfrac{16 t_c t_1 t_2 \eta E_f}{15(t_1 + t_2) R d G_{xz}}$$

$V_s = 0$

$V_s = 0.2$

$V_s = 0.4$

$V_s = 0.6$

$V_s = 0.8$

$V_s = 1.2$

$V_s = 1.6$

$V_s = 2.0$
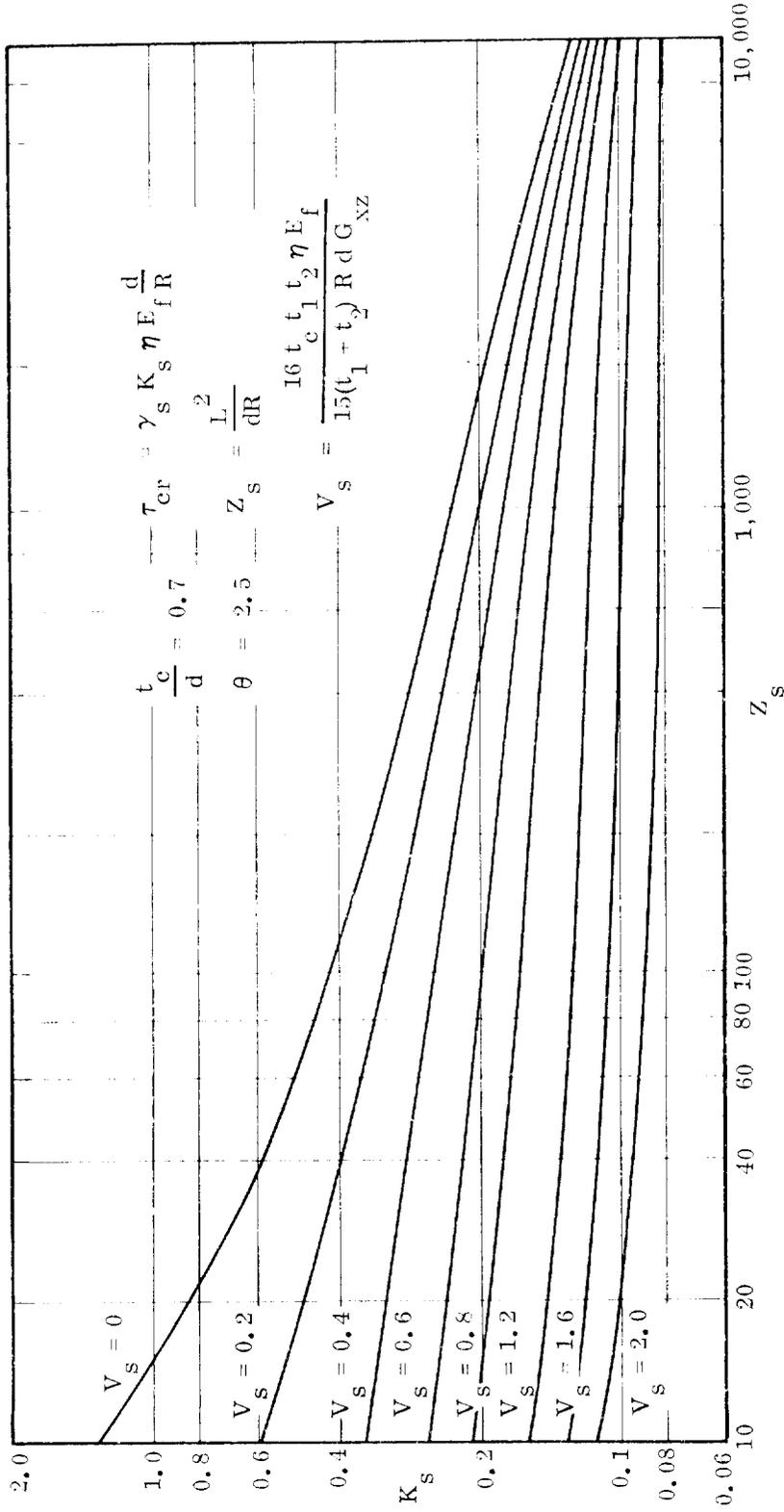
Figure 4.5-8. Buckling Coefficients for Circular Sandwich Cylinders Subjected to Torsion

4.6 TRANSVERSE SHEAR

4.6.1 Basic Principles

In Reference 4-33, Lundquist reports the results from a series of tests on isotropic (non-sandwich), circular cylinders subjected to combined transverse shear and bending. The same type of data is published in Reference 4-34 for elliptical cylinders. Both sets of data were obtained from cantilevered cylinders of varied lengths. Extrapolation of these results to the condition of zero bending stress permits a determination of critical stresses for pure transverse shear loading. It has proven useful to compare these stress values against the theoretical results obtained from small-deflection theory for isotropic (non-sandwich), circular cylinders loaded in torsion. Gerard and Becker [4-35] report that, for nominally identical specimens, such comparisons yield the following ratios where the theoretical predictions are obtained by using Reference 4-36:

$$\frac{\left[\begin{array}{l}\text{Average of } \tau_{cr} \text{ Test Values for} \\ \text{Transverse Shear Loading}\end{array}\right]}{\left[\begin{array}{l}\text{Small-Deflection Theoretical } \tau_{cr} \\ \text{Values for Torsional Loading}\end{array}\right]} \approx 1.6 \qquad (4.6-1)$$

$$\frac{\left[\begin{array}{l}\text{Lower-Bound} \tau_{cr} \text{ Test Values for} \\ \text{Transverse Shear Loading}\end{array}\right]}{\left[\begin{array}{l}\text{Small-Deflection Theoretical } \tau_{cr} \\ \text{Values for Torsional Loading}\end{array}\right]} \approx 1.25 \qquad (4.6-2)$$

To properly interpret these ratios, it is pointed out that, for torsional loading, the shear stress τ_{cr} is uniformly distributed around the circumference. On the other hand, under transverse shear loading, the shear stress is non-uniform and the value τ_{cr} then corresponds to the peak intensity which occurs at the neutral axis.

4-62

For the lack of a better approach, it is recommended that Equation (4.6-2) be used for the design and analysis of circular sandwich cylinders that are subjected to transverse shear forces. In such cases, the required small-deflection theoretical τ_{cr} values for torsional loading should be obtained as specified in Section 4.5 of this handbook with the exception that $\gamma_s = 1.0$ should be used here. No test data are available to substantiate the reliability of this practice. Until such data do become available, one can only regard this procedure as a "best-available" approach.

4.6.2 Design Equations and Curves

For simply supported circular sandwich cylinders subjected to a transverse shear force and having both facings made of the same material, the critical shear stress may be computed from the equation

$$\tau_{cr} = 1.25 \, K_s \, \eta \, E_f \, \frac{d}{R} \tag{4.6-3}$$

where the buckling coefficient K_s is obtained from Figures 4.5-3 through 4.5-8 and the notation is the same as that employed throughout Section 4.5. As noted in Section 4.5.1.1, these figures are somewhat inaccurate in the region where Z_s is large (long cylinders) and one should exercise some caution when dealing with such configurations.

Strictly speaking, Figures 4.5-3 through 4.5-8 apply only when the facings are of equal thickness. However, the curves are reasonably accurate for sandwich cylinders having unequal facings, provided that the thickness of one facing is not more than twice the other.

For elastic cases, use $\eta = 1$. Whenever the behavior is inelastic, the methods of Section 9 must be employed.

For elastic cylinders the critical transverse shear force $(F_v)_{cr}$, measured in units of pounds, can be computed from the following:

$$(F_v)_{cr} = \pi R \, (t_1 + t_2) \, \tau_{cr} \tag{4.6-4}$$

To compute $(F_v)_{cr}$ when the behavior is inelastic, one must resort to numerical integration techniques.

4.7 COMBINED LOADING CONDITIONS

4.7.1 General

For structural members subjected to combined loads, it is customary to represent critical loading conditions by means of so-called interaction curves. Figure 4.7-1 shows the graphic format usually used for this purpose. The quantity R_i is the ratio of an applied load or stress to the critical value for that type of loading when acting alone. The quantity R_j is similarly defined for a second type of loading. Curves of this form give a very clear picture as to the structural integrity of particular configurations. All computed points which fall within the area bounded by the interaction curve and the coordinate axes correspond to stable structures. All points lying on or outside of the interaction curve indicate that buckling will occur. Furthermore, as shown in Figure 4.7-1, a measure of the margin of safety is given by the ratio of distances from the actual loading point to the curve and to the origin. For example, assume that a particular structure is subjected to the combined loading condition corresponding to point B of Figure 4.7-1.

Then, for proportional increases in R_i and R_j, the margin of safety (M.S.) can be computed from the following:

$$M.S. = \frac{(R_j)_D}{(R_j)_B} - 1 \qquad (4.7-1)$$

As an alternative procedure, one might choose to compute a minimum margin of safety which is based on the assumption that loading beyond point B follows the path BM. Point M is located in such a position that BM is the shortest line that can be drawn

4-65

between point B and the interaction curve. The minimum margin of safety can then be calculated as follows:

$$\text{Minimum M.S.} = \frac{OB + BM}{OB} - 1 \qquad (4.7\text{-}2)$$
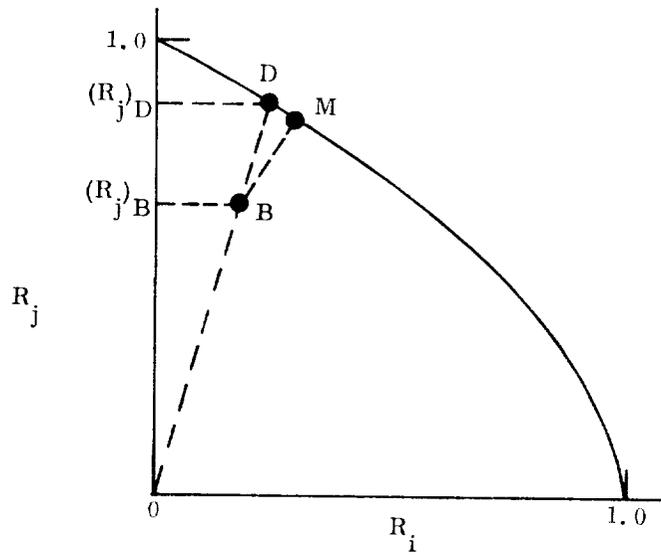
Figure 4.7-1. Sample Interaction Curve

4.7.2　Axial Compression Plus Bending

4.7.2.1　Basic Principles

In References 4-17, 4-18, and 4-19 it has been shown that, for circular sandwich

cylinders subjected to axial compression plus bending, the classical theoretical

interaction curve may be accurately described by the equation

$$(R_c)_{CL} + (R_b)_{CL} = 1 \tag{4.7-3}$$

where

$$(R_c)_{CL} = \frac{\sigma_c}{(\bar{\sigma}_c)_{CL}} \tag{4.7-4}$$

$$(R_b)_{CL} = \frac{\sigma_b}{(\bar{\sigma}_b)_{CL}} \tag{4.7-5}$$

$$(\bar{\sigma}_b)_{CL} = (\bar{\sigma}_c)_{CL} \tag{4.7-6}$$

and

σ_c = Uniform compressive stress due solely to applied axial load, psi.

σ_b = Peak compressive stress due solely to applied bending moment, psi.

$(\bar{\sigma}_c)_{CL}$ = Classical theoretical value for critical uniform compressive stress under an axial load acting alone, psi.

$(\bar{\sigma}_b)_{CL}$ = Classical theoretical value for critical peak compressive stress under a bending moment acting alone, psi.

References 4-17 and 4-18 develop the foregoing result for weak-core constructions

which fail in the shear crimping mode. On the other hand, Reference 4-19 deals

with infinitely long cylinders which fall in the stiff-core and the moderately-stiff-

core categories. Since Equation (4.7-3) is written in terms of classical theoretical

allowables, it does not include any consideration of the detrimental influences from
initial imperfections. For the purposes of this handbook, these influences are treated
by introducing the knock-down factors γ_c and γ_b (see Figures 4.2-8 and 4.3-2, re-
spectively) to obtain

$$R_c + R_b = 1 \qquad (4.7-7)$$

where

$$R_c = \frac{\sigma_c}{\gamma_c \, (\bar{\sigma}_c)_{CL}} \qquad (4.7-8)$$

$$R_b = \frac{\sigma_b}{\gamma_b \, (\bar{\sigma}_c)_{CL}} \qquad (4.7-9)$$

Therefore, the design interaction curve can be drawn as shown in Figure 4.7-2. Since
no test data is available for sandwich cylinders subjected to combined axial load and
bending, the general validity of this curve has not been experimentally verified. Some
degree of empirical correlation is inherent in the approach since the knock-down fac-
tors γ_c and γ_b were established, in part, from sandwich test data (see Sections 4.2
and 4.3). However, even these data were few in number. Therefore, until further
experimental substantiation is obtained, the recommended interaction relationship
can only be considered a "best-available" method.

Figure 4.7-2. Design Interaction Curve for Circular Sandwich Cylinders
Subjected to Axial Compression Plus Bending

4-68

4.7.2.2 Design Equations and Curves

For simply supported, circular, sandwich cylinders subjected to axial compression plus bending, the following interaction equation may be employed:

$$R_c + R_b = 1 \qquad (4.7\text{-}10)$$

where

$$R_c = \frac{\sigma_c}{\gamma_c \, (\bar{\sigma}_c)_{CL}} \qquad (4.7\text{-}11)$$

$$R_b = \frac{\sigma_b}{\gamma_b \, (\bar{\sigma}_c)_{CL}} \qquad (4.7\text{-}12)$$

A plot of Equation (4.7-10) is given in Figure 4.7-3.

In Equations (4.7-11) and (4.7-12), the knock-down factors γ_c and γ_b are those obtained from Figures 4.2-8 and 4.3-2, respectively.

The quantity $(\bar{\sigma}_c)_{CL}$ is simply the result obtained by using $\gamma_c = 1.0$ in the method of Section 4.2.2.

Plasticity considerations should be handled as specified in Section 9.2 except that, in this case, one may use

a. $\quad \eta = \left[\dfrac{1 - \nu_e^{\,2}}{1 - \nu^2}\right] \dfrac{E_t}{E_f}$ for short cylinders, and

b. $\quad \eta = \left[\dfrac{1 - \nu_e^{\,2}}{1 - \nu^2}\right]^{\frac{1}{2}} \dfrac{\sqrt{E_t E_s}}{E_f}$ for moderate-length through long cylinders.

Equation (4.7-10) may be applied to sandwich cylinders of any length. However, length considerations should be included in the computation of $(\bar{\sigma}_c)_{CL}$ when the structure falls into the short-cylinder range (see Section 4.2.2).
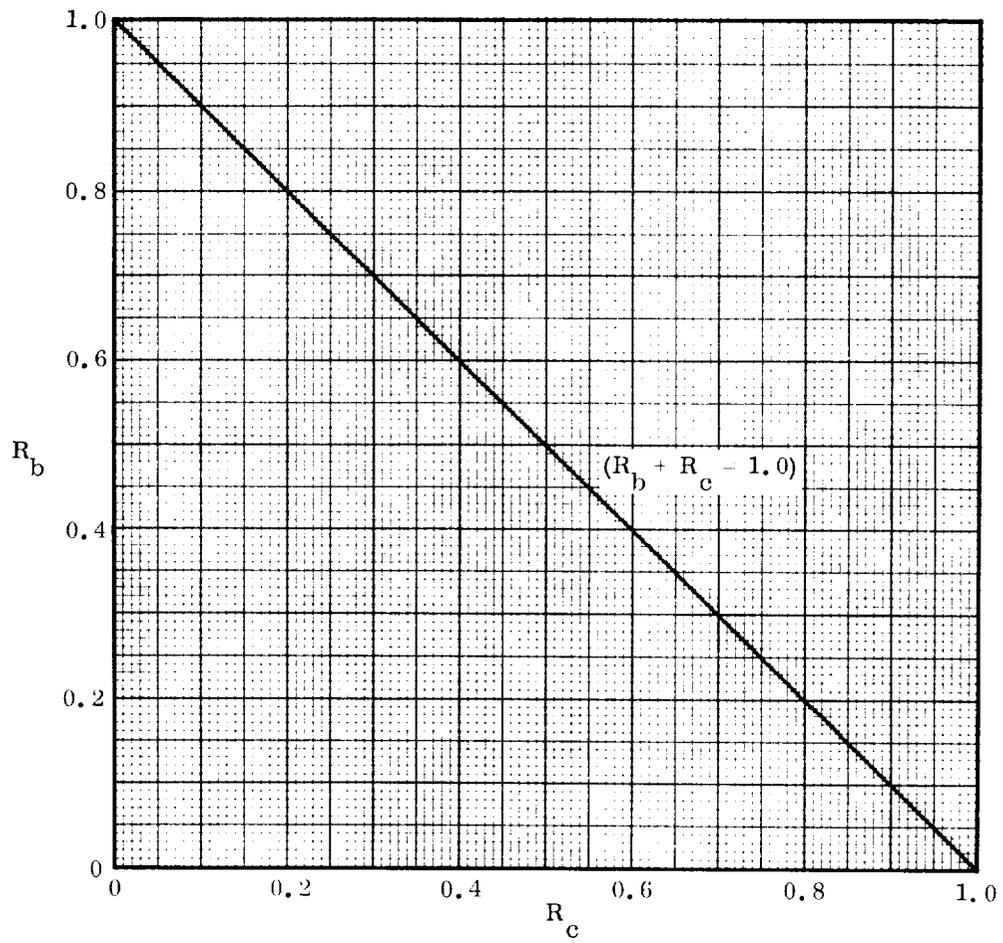
Figure 4.7-3. Design Interaction Curve for Circular Sandwich Cylinders
Subjected to Axial Compression Plus Bending

4.7.3 Axial Compression Plus External Lateral Pressure

4.7.3.1 Basic Principles

This section deals with the loading condition depicted in Figure 4.7-4. The sandwich cylinder is subjected to uniform external pressure over the cylindrical surface. Axial loading is imposed as indicated by the forces P. These forces can originate from any source including external pressures which are uniformly distributed over the end closures. In addition, it is specified that the ends of the cylinder are simply supported. This is, during buckling, the ends are constrained such that they experience no radial or circumferential displacements and they are free of bending moments.
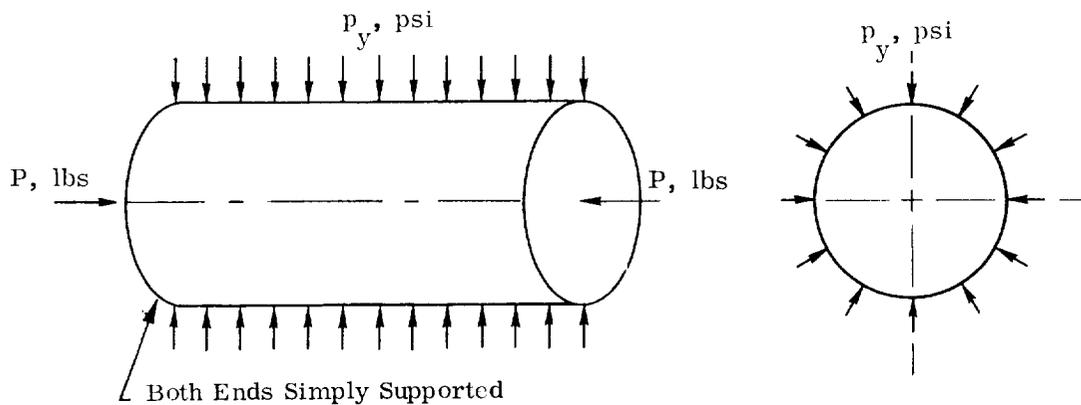
Figure 4.7-4. Circular Sandwich Cylinder Subjected to Axial Compression Plus External Lateral Pressure

The theoretical basis used here is the classical small-deflection solution of Maki [4-37]. The design curves given in this handbook were taken directly from that source and embody the following assumptions:

a. The facings are isotropic.

b. Both facings are of the same thickness.

c. Both facings have identical material properties.

4-71

d.   Poisson's ratio for the facings is equal to 0.33.

e.   Bending of the facings about their own middle surfaces can be neglected.

f.   The core has infinite extensional stiffness in the direction normal to the facings.

g.   The core extensional and shear rigidities are negligible in directions parallel to the facings.

h.   The transverse shear moduli of the core are the same in the circumferential and longitudinal directions ($G_{xz} = G_{yz}$).

i.   The mean radius of the cylinder is large in comparison with the sandwich thickness.

The theoretical relationship derived by Maki [4-37] is in the form of a complicated sixth order determinant and no significant advantage would be gained by reproducing that formulation in this handbook. However, it is important to note that a sufficient number of terms were retained throughout the derivation to obtain accurate results when the number of circumferential full-waves equals two (n = 2). If the derivation had been based on the well-known Donnell approximations [4-8], the results would not be applicable to structures which buckle in this manner.

The interaction curves given in Reference 4-37 are of the two different types depicted in Figure 4.7-5 where

$$V_{xz} = \frac{E_f t_f h}{2(1 - .33^2) R^2 G_{xz}}$$ (4.7-13)

$$V_{yz} = \frac{E_f t_f h}{2(1 - .33^2) R^2 G_{yz}}$$ (4.7-14)

$$(R_p)_{CL} = \frac{p_y}{(\bar{p}_y)_{CL}}$$ (4.7-15)

4-72

$$(R_c)_{CL} = \frac{\sigma_x}{(\bar{\sigma}_x)_{CL}} \qquad (4.7\text{-}16)$$

and

E_f = Young's modulus of facings, psi.

t_f = Thickness of single facing, inches.

h = Distance between middle surfaces of facings, inches.

R = Radius to middle surface of cylindrical sandwich, inches.

G_{xz} = Core shear modulus associated with the plane perpendicular to the facings and oriented in the axial direction, psi.

G_{yz} = Core shear modulus associated with the plane perpendicular to the axis of revolution, psi.

p_y = Applied external lateral pressure, psi.

$(\bar{p}_y)_{CL}$ = Classical theoretical value for critical external lateral pressure when acting alone, psi.

σ_x = Uniform axial compressive stress due to applied axial load, psi.

$(\bar{\sigma}_x)_{CL}$ = Classical theoretical value for critical uniform axial compressive stress when acting alone, psi.

L = Over-all length of cylinder, inches.

Note: The value .33 appearing in Equations (4.7-13) and (4.7-14) is an assumed representative value for the elastic Poisson's ratio of the facings.

Since the curves of Reference 4-37 were developed from a classical, small-deflection approach, they do not include any consideration of the detrimental effects from initial imperfections. This is evident from the fact that classical theoretical allowables are used in the ratios $(R_p)_{CL}$ and $(R_c)_{CL}$. For the purposes of this handbook, the effects

Figure 4.7-5. Typical Interaction Curves for Circular Sandwich Cylinders Subjected to Axial Compression Plus External Lateral Pressure

from initial imperfections are introduced through the replacement of $(R_p)_{CL}$ and

$(R_c)_{CL}$ by the ratios R_p and R_c which are defined as follows:

$$R_p = \frac{P_y}{\gamma_p (\bar{P}_y)_{CL}}$$ (4.7-17)

$$R_c = \frac{\sigma_x}{\gamma_c (\bar{\sigma}_x)_{CL}}$$ (4.7-18)

The quantities γ_p and γ_c are the knock-down factors discussed in Sections 4.4 and 4.2, respectively. Values for γ_c can be obtained from Figure 4.2-8 while γ_p may be taken equal to 0.90.

No test data are available for sandwich cylinders which are of the types considered here and are subjected to axial compression plus external lateral pressure. Therefore, the general validity of the design curves recommended here has not been experimentally verified. Some degree of empirical correlation is inherent in the approach since the

knock-down factors γ_c and γ_p were established, in part, from sandwich test data (see Sections 4.2 and 4.4). However, even these data were few in number. Therefore, until further experimental substantiation is obtained, the recommended interaction curves can only be considered as "best-available" criteria.
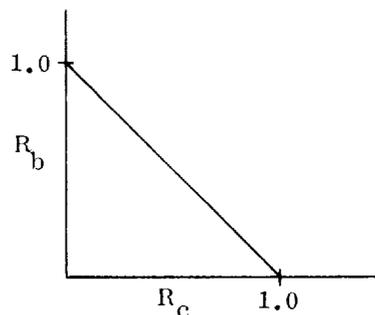
4.7.3.2 Design Equations and Curves

For simply supported, circular, sandwich cylinders subjected to axial compression plus external lateral pressure, one may employ the interaction curves of Figures 4.7-6 through 4.7-15 where

$$V_{xz} = \frac{E_f t_f h}{2(1 - .33^2) R^2 G_{xz}} \tag{4.7-19}$$

$$V_{yz} = \frac{E_f t_f h}{2(1 - .33^2) R^2 G_{yz}} \tag{4.7-20}$$

$$R_p = \frac{p_y}{\gamma_p (\bar{p}_y)_{CL}} \tag{4.7-21}$$

$$R_c = \frac{\sigma_x}{\gamma_c (\bar{\sigma}_x)_{CL}} \tag{4.7-22}$$

In Equations (4.7-21) and (4.7-22), the knock-down factor γ_c is that obtained from Figure 4.2-8 while γ_p may be taken equal to 0.90.

The quantity $(\bar{p}_y)_{CL}$ is simply the result obtained by using $\gamma_p = 1.0$ in the methods of Section 4.4.

The quantity $(\bar{\sigma}_x)_{CL}$ is simply the result obtained by using $\gamma_c = 1.0$ in the methods of Section 4.2.

Plasticity considerations should be handled as specified in Section 9.2.

Figures 4.7-6 through 4.7-12 give interaction curves only for cases where $V_{xz} = V_{yz} = 0$ ($G_{xz} = G_{yz} \to \infty$). Separate families are provided for each of three selected values for the parameter $\frac{R}{h}$ $\left(\frac{R}{h} = 50; 160; \text{ and } 500\right)$. Graphical interpolation may be

used to obtain results for intermediate values of this parameter. Each family includes

separate curves for ten different values of the ratio $\frac{\pi R}{L}$ $\left(\frac{\pi R}{L} = 0.1; 0.2; \text{---} 1.0\right)$. In

view of the restrictions on V_{xz} and V_{yz}, these curves can only be used to describe the

behavior of stiff-core constructions. For the purposes of practical design and analysis,

it is proposed here that Figures 4.7-6 through 4.7-12 be considered applicable only

when

$$\frac{R t_c}{h^2} V_{xz} \leq 0.05 \qquad (4.7-23)$$

$$\frac{R t_c}{h^2} V_{yz} \leq 0.05 \qquad (4.7-24)$$

where

t_c = Thickness of core, inches.

It is expected that many realistic sandwich configurations will satisfy these requirements.

Figures 4.7-13 through 4.7-15 present a partial picture of the effects which variations

in V_{xz} (= V_{yz}) will have on the interaction relationships. These figures only treat

cases for which $\frac{\pi R}{L} = 0.1$. However, the trends displayed furnish some basis for one

to conjecture that the curves given for $V_{xz} = V_{yz} = 0$ would result in conservative pre-

dictions if they were applied to sandwich configurations which do not satisfy the In-

equalities (4.7-23) and (4.7-24). However, one should be cautioned against making

sweeping application of this observation in view of the limited scope of the information

shown in Figures 4.7-13 through 4.7-15.

It should be kept in mind that the interaction curves given in Figures 4.7-6 through

4.7-12 include C_L values ranging only from 0.1 through 1.0. Since

$$C_L = \frac{\pi R}{L} \qquad (4.7\text{-}25)$$

it follows that these curves only embrace the range where

$$3.14 \leq \frac{L}{R} \leq 31.4 \qquad (4.7\text{-}26)$$
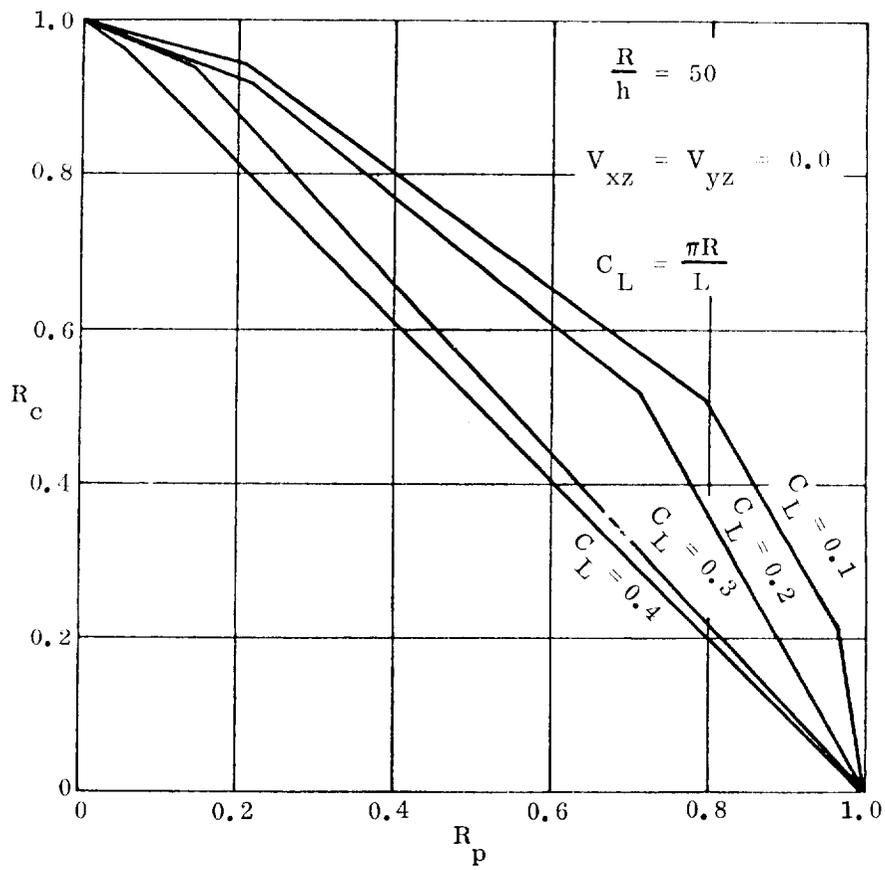
Figure 4.7-6. Interaction Curves for Circular Sandwich Cylinders
Subjected to Axial Compression Plus External
Lateral Pressure

4-79
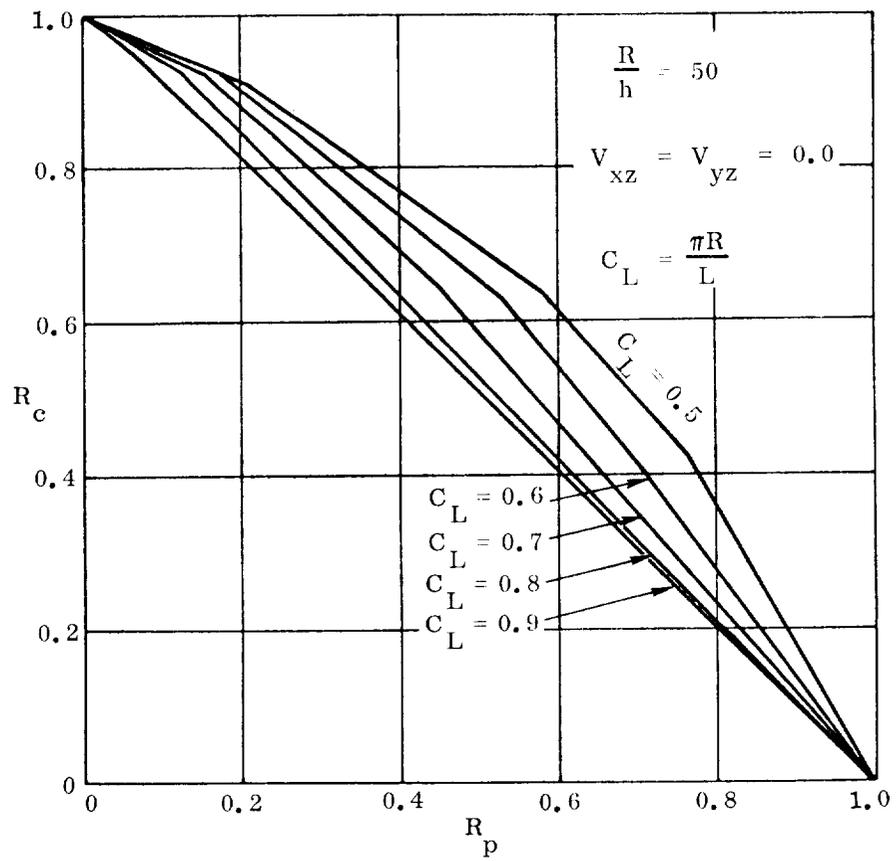
Figure 4.7-7. Interaction Curves for Circular Sandwich Cylinders
Subjected to Axial Compression Plus External
Lateral Pressure

4-80
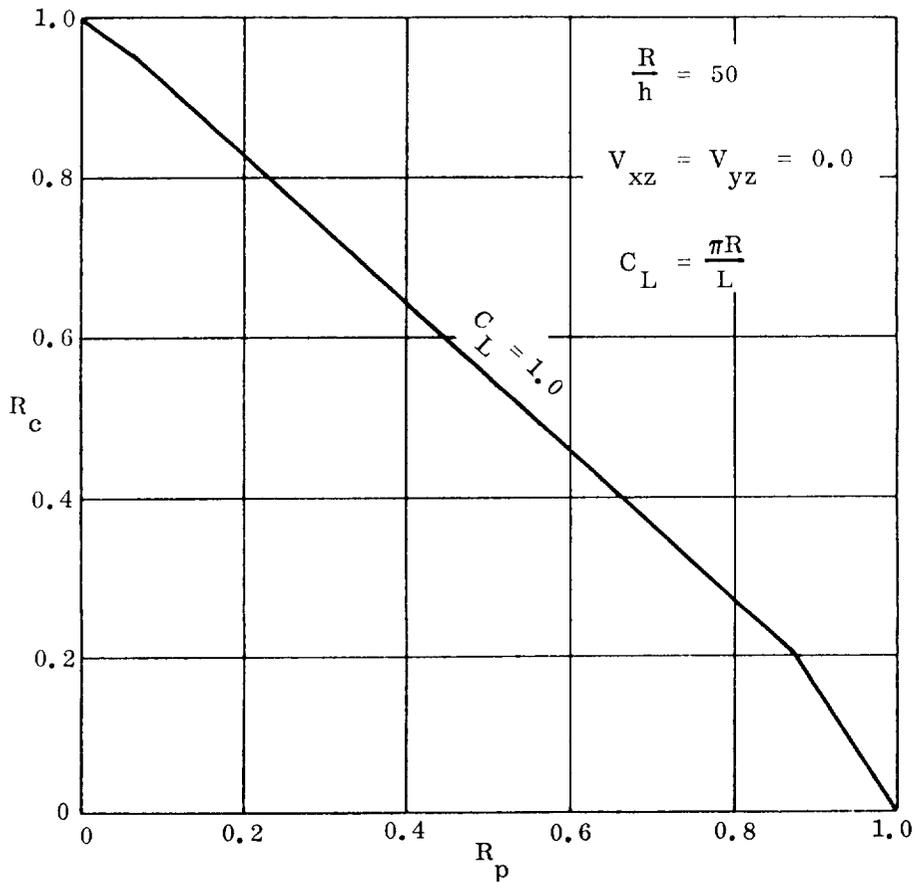
Figure 4.7-8. Interaction Curve for Circular Sandwich Cylinders
Subjected to Axial Compression Plus External
Lateral Pressure
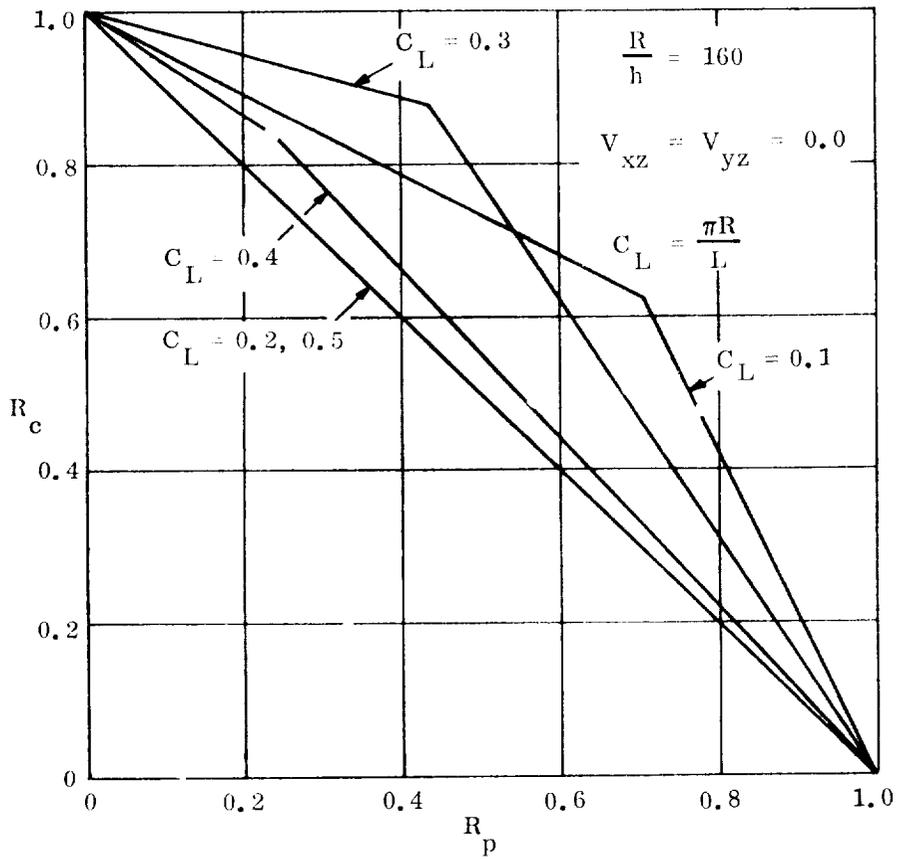
Figure 4.7-9. Interaction Curves for Circular Sandwich Cylinders
Subjected to Axial Compression Plus External
Lateral Pressure

4-82
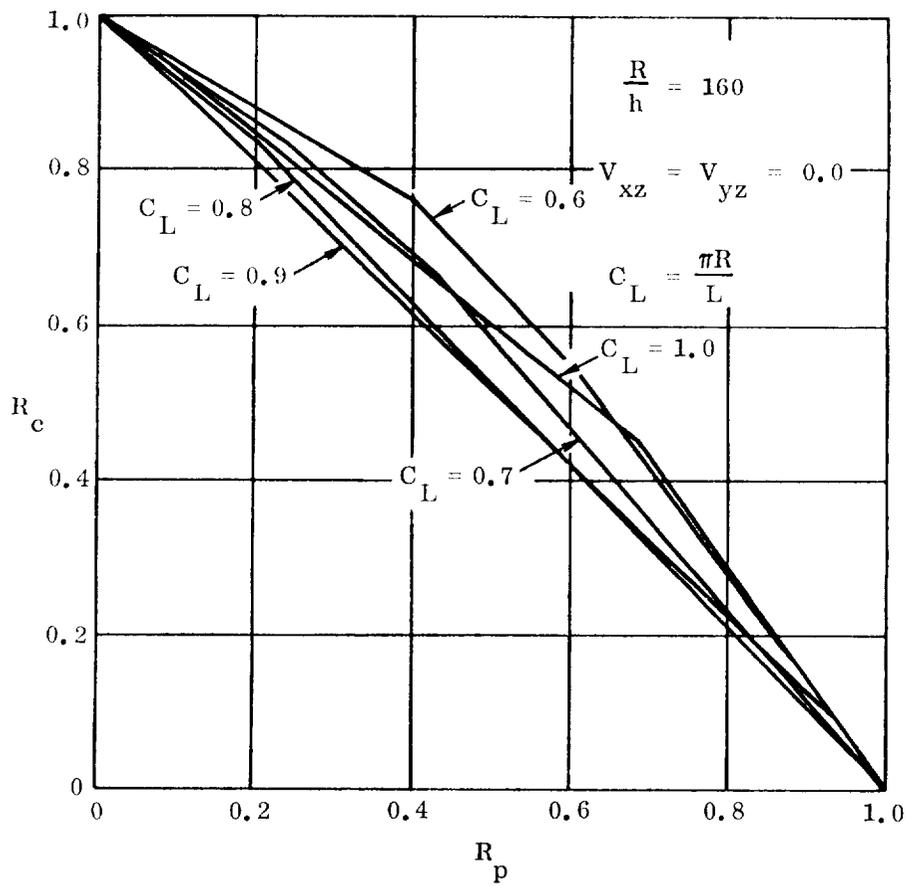
Figure 4.7-10. Interaction Curves for Circular Sandwich
Cylinders Subjected to Axial Compression
Plus External Lateral Pressure
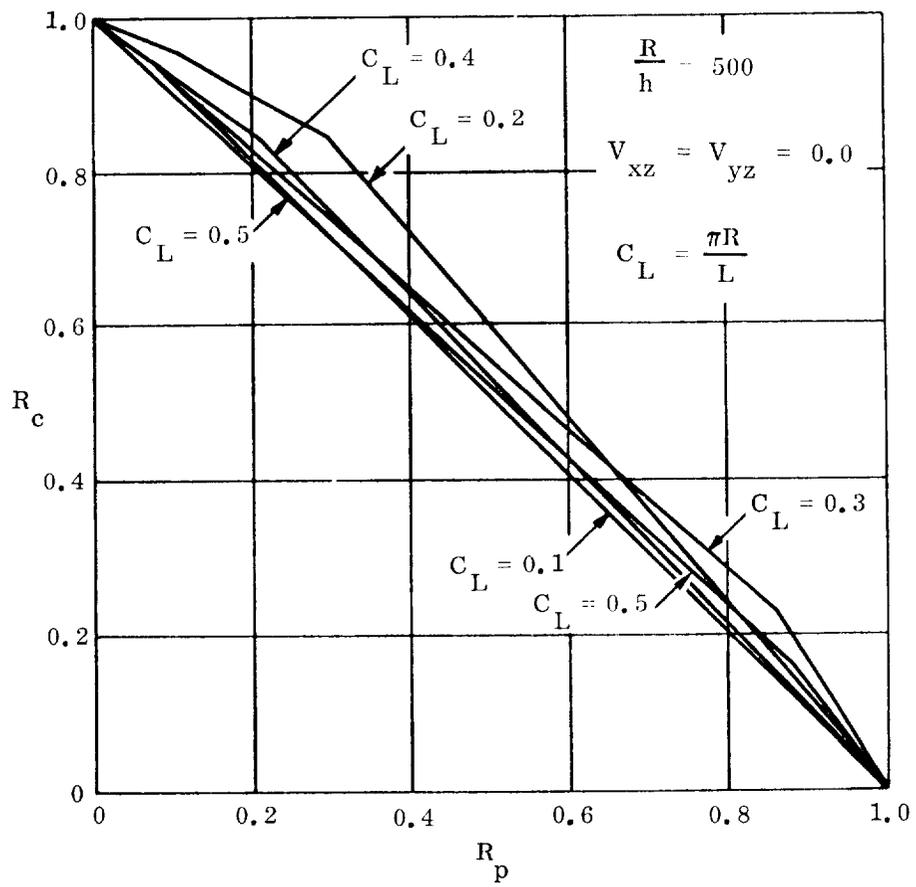
Figure 4.7-11. Interaction Curves for Circular Sandwich Cylinders
Subjected to Axial Compression Plus External
Lateral Pressure

4-84
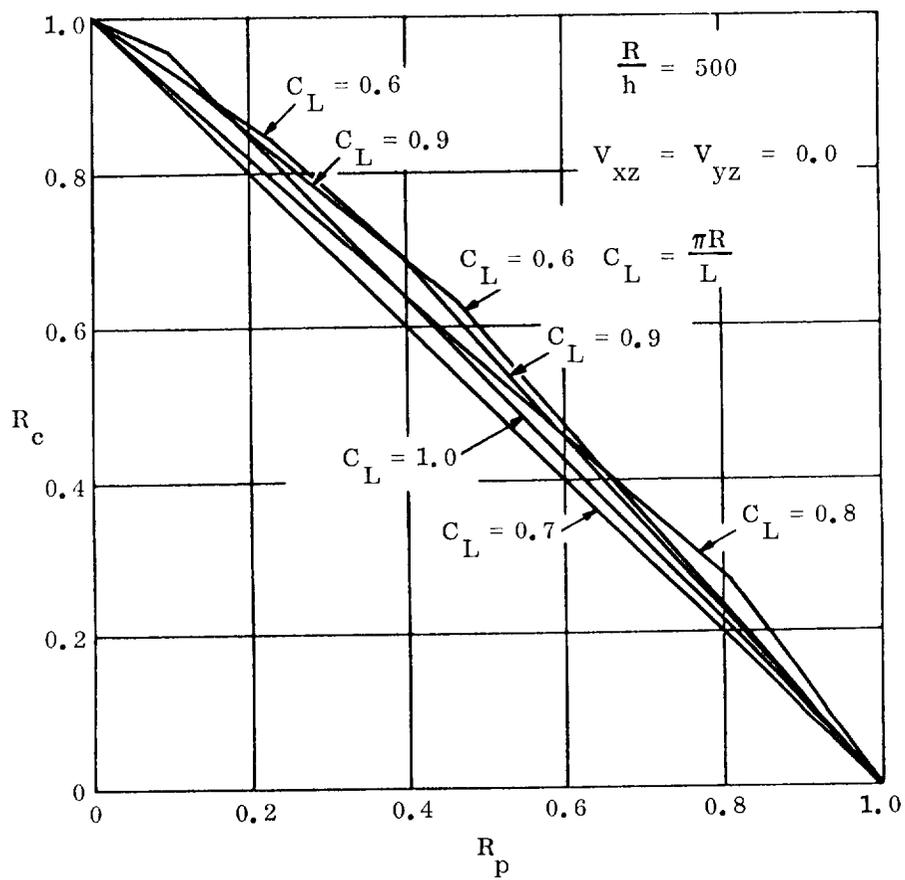
Figure 4.7-12. Interaction Curves for Circular Sandwich Cylinders
Subjected to Axial Compression Plus External
Lateral Pressure

4-85
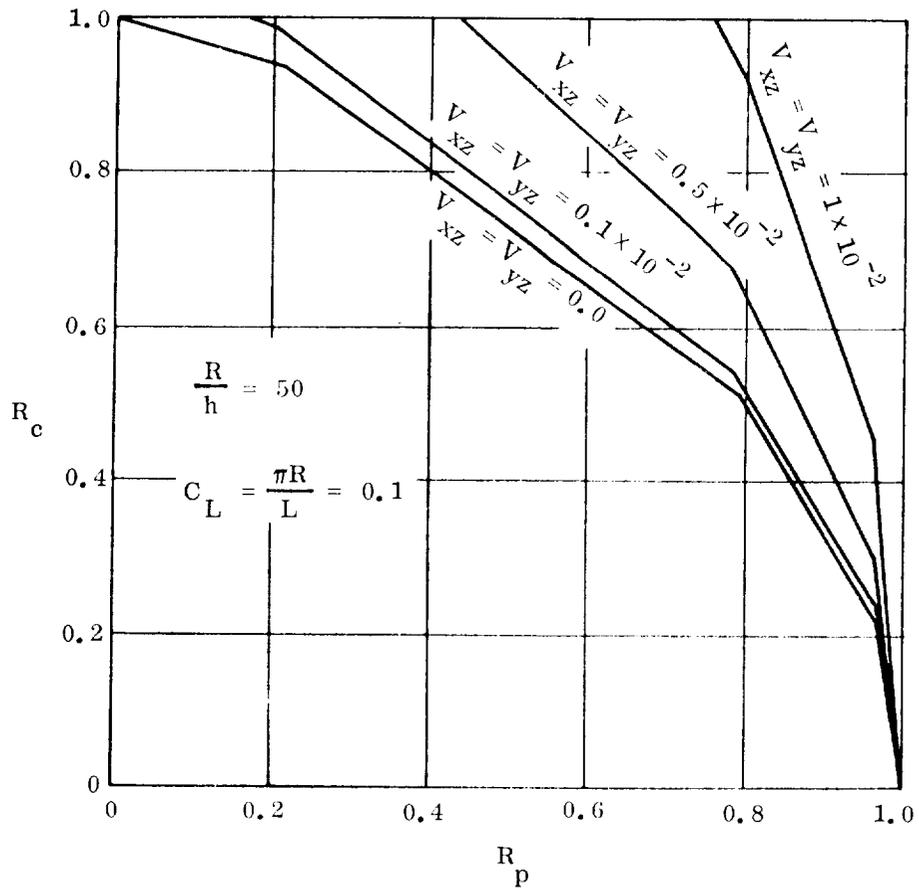
Figure 4.7-13. Interaction Curves for Circular Sandwich Cylinders
Subjected to Axial Compression Plus External
Lateral Pressure

4-86
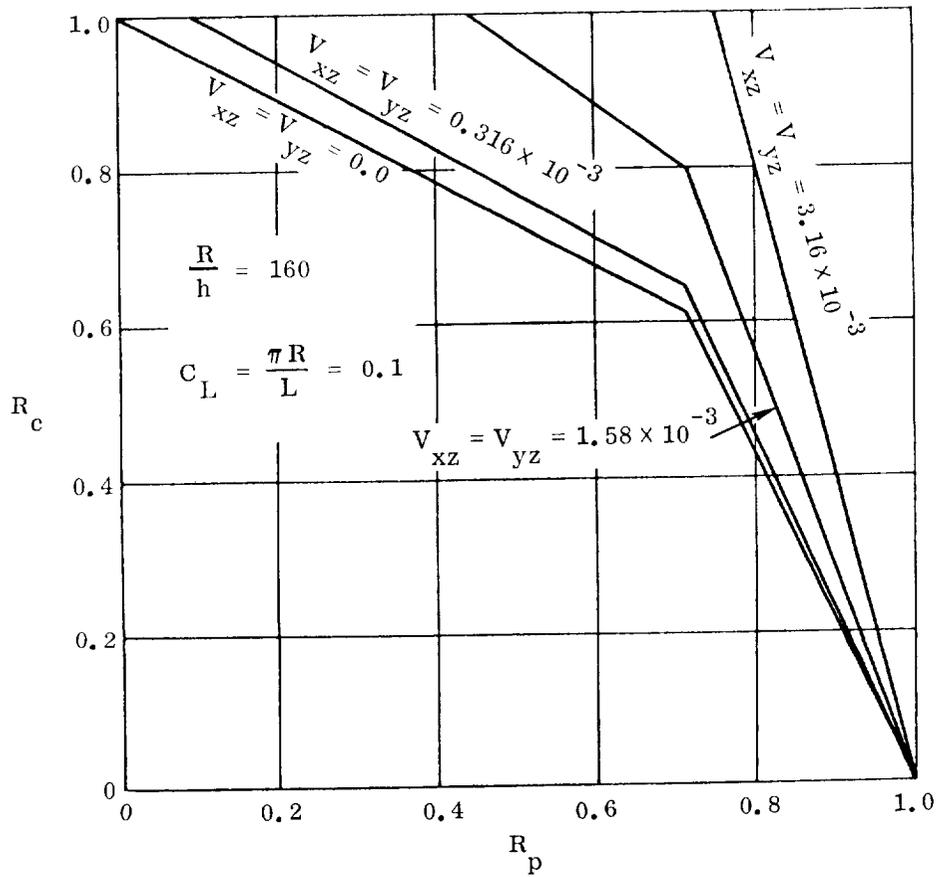
Figure 4.7-14. Interaction Curves for Circular Sandwich Cylinders Subjected to Axial Compression Plus External Lateral Pressure

4-87
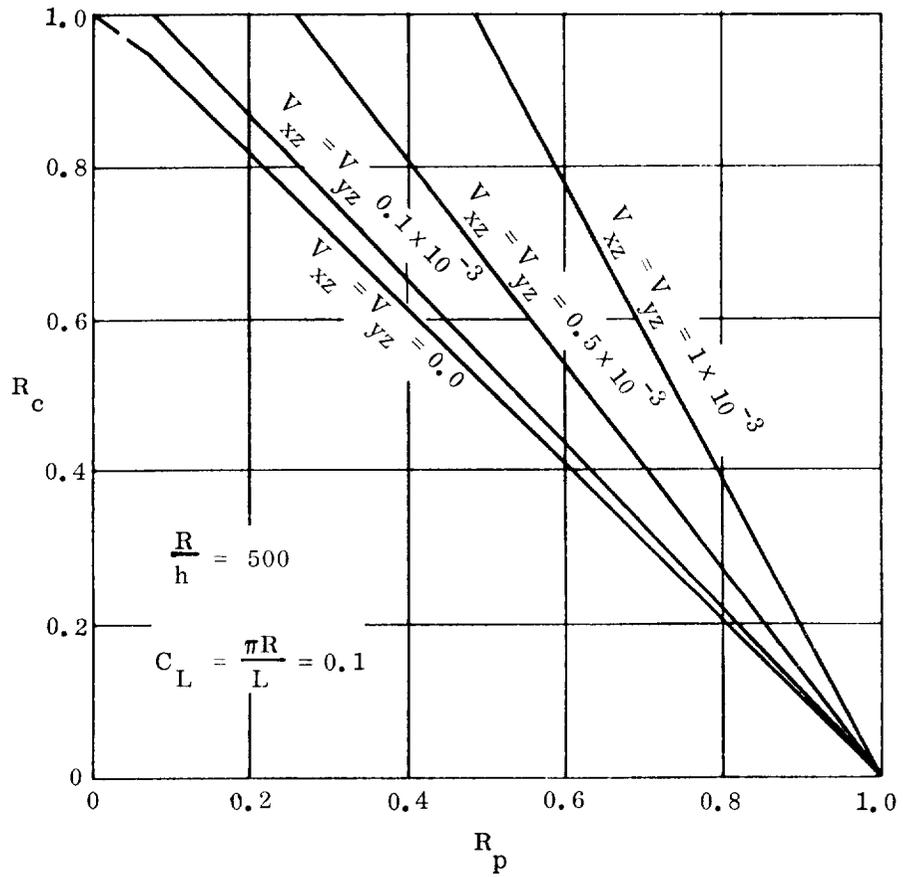
Figure 4.7-15. Interaction Curves for Circular Sandwich Cylinders
Subjected to Axial Compression Plus External
Lateral Pressure

4.7.4 Axial Compression Plus Torsion

4.7.4.1 Basic Principles

This section deals with the loading condition depicted in Figure 4.7-16. The sandwich

cylinder is subjected to end torque T plus axial loading indicated by the forces P.
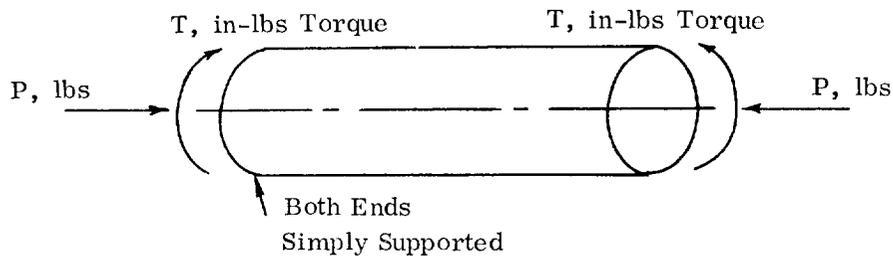
Figure 4.7-16. Circular Sandwich Cylinder Subjected to
Axial Compression Plus Torsion

In Reference 4-18 Wang, et al. treat this type of problem but only consider the case

of weak-core configurations which fail in the shear crimping mode. In addition they

assume that the cylinder is long so that the boundary conditions can be ignored. This

small-deflection analysis makes use of the Donnell approximations [4-8] to arrive at

the following interaction relationship:

$$(R_c)_{CL} + (R_s)^2_{CL} = 1 \qquad (4.7\text{-}27)$$

where

$$(R_c)_{CL} = \frac{\sigma_c}{(\bar{\sigma}_c)_{CL}} \qquad (4.7\text{-}28)$$

4-89

$$(R_s)_{CL} = \frac{\tau}{(\bar{\tau})_{CL}} \qquad\qquad (4.7\text{-}29)$$

and

σ_c = Uniform axial compressive stress due to applied axial load, psi.

$(\bar{\sigma}_c)_{CL}$ = Classical theoretical value for critical uniform axial compressive stress when acting alone, psi.

τ = Uniform shear stress due to applied torque, psi.

$(\bar{\tau})_{CL}$ = Classical theoretical value for critical uniform shear stress due to torque acting alone, psi.

Because Equation (4.7-27) was developed from a classical, small-deflection approach, it does not include any consideration of the detrimental effects from initial imperfections. That is evident from the fact that classical theoretical allowables are used in the ratios $(R_c)_{CL}$ and $(R_s)_{CL}$. For th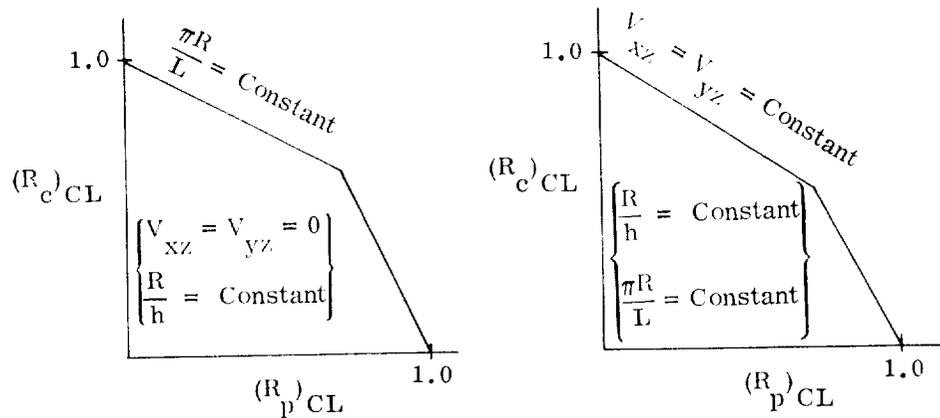e purposes of this handbook, the effects from initial imperfections are introduced through the replacement of $(R_c)_{CL}$ and $(R_s)_{CL}$ by the ratios R_c and R_s which are defined as follows:

$$R_c = \frac{\sigma_c}{\gamma_c (\bar{\sigma}_c)_{CL}} \qquad\qquad (4.7\text{-}30)$$

$$R_s = \frac{\tau}{\gamma_s (\bar{\tau})_{CL}} \qquad\qquad (4.7\text{-}31)$$

The quantities γ_c and γ_s are the knock-down factors discussed in Sections 4.2 and 4.5, respectively. Values for γ_c can be obtained from Figure 4.2-8 while γ_s may be taken equal to 0.80. Incorporation of the foregoing substitutions into Equation (4.7-27) then gives the following interaction relationship for weak-core constructions:

$$R_c + R_s^2 = 1 \qquad\qquad (4.7\text{-}32)$$

4-90

In Reference 4-38, Batdorf, et al. deal with the subject loading condition for thin-walled, isotropic (non-sandwich), circular cylinders. Since, for such constructions, transverse shear deformations of the shell wall are of negligible importance, one might conjecture that this work could be applied to sandwich cylinders which fall into the stiff-core category. Based on theoretical considerations modified by test results, Batdorf, et al. ⌐4-38⌐ arrived at the same interaction expression as that given above as Equation (4.7-32). In view of this, one might choose to view Equation (4.7-32) as a comprehensive interaction formula for sandwich cylinders. However, some caution should be observed in implementing this viewpoint, partially because of the fact that only the extremes of transverse shear stiffness of the core have been considered. In addition, although the interaction relationship for the subject loading condition should probably be dependent upon a length parameter, no investigations were made to establish the sandwich cylinder lengths over which Equation (4.7-32) is a reasonable representation of the actual behavior. Furthermore, no test data are available for sandwich cylinders which are of the types considered in this handbook and are subjected to axial compression plus torsion. Therefore the general validity of Equation (4.7-32) has not been experimentally verified. Some degree of empirical correlation is inherent in the approach since the knock-down factor γ_c was established, in part, from sandwich test data (see Section 4.2). However, even these data were few in number. Therefore, until further theoretical and experimental investigations are accomplished, the interaction relationship cited here can only be considered as a "best-available" criterion.

4.7.4.2 Design Equations and Curves

For simply supported, circular, sandwich cylinders subjected to axial compression plus torsion, one might choose to employ the interaction formula

$$R_c + R_s^2 = 1 \qquad (4.7-33)$$

which is plotted in Figure 4.7-17 and where

$$R_c = \frac{\sigma_c}{\gamma_c \, (\bar{\sigma}_c)_{CL}} \qquad (4.7-34)$$

$$R_s = \frac{\tau}{\gamma_s \, (\bar{\tau})_{CL}} \qquad (4.7-35)$$

In Equations (4.7-34) and (4.7-35), the knock-down factor γ_c is that obtained from Figure 4.2-8 while γ_s may be taken equal to 0.80.

The quantity $(\bar{\sigma}_c)_{CL}$ is simply the result obtained by using $\gamma_c = 1.0$ in the methods of Section 4.2.

The quantity $(\bar{\tau})_{CL}$ is simply the result obtained by using $\gamma_s = 1.0$ in the methods of Section 4.5.

Plasticity considerations should be handled as specified in Section 9.2.

Attention is drawn to the fact that, in Section 4.7.4.1, several factors are cited which shed considerable doubt upon the reliability of results obtained from the indiscriminate use of Equation (4.7-33) and Figure 4.7-17. In view of these uncertainties, one might often choose to employ the straight-line interaction formula

$$R_c + R_s = 1 \qquad (4.7-36)$$

which is plotted in Figure 4.7-18. This relationship can be used with confidence for any length of cylinder and for any region of transverse shear rigidity of the core since experience has shown that the linear interaction formula is never unconservative for shell stability problems. However, in many cases it will, of course, introduce excessive conservatism.

$$R_c + R_s^2 = 1$$
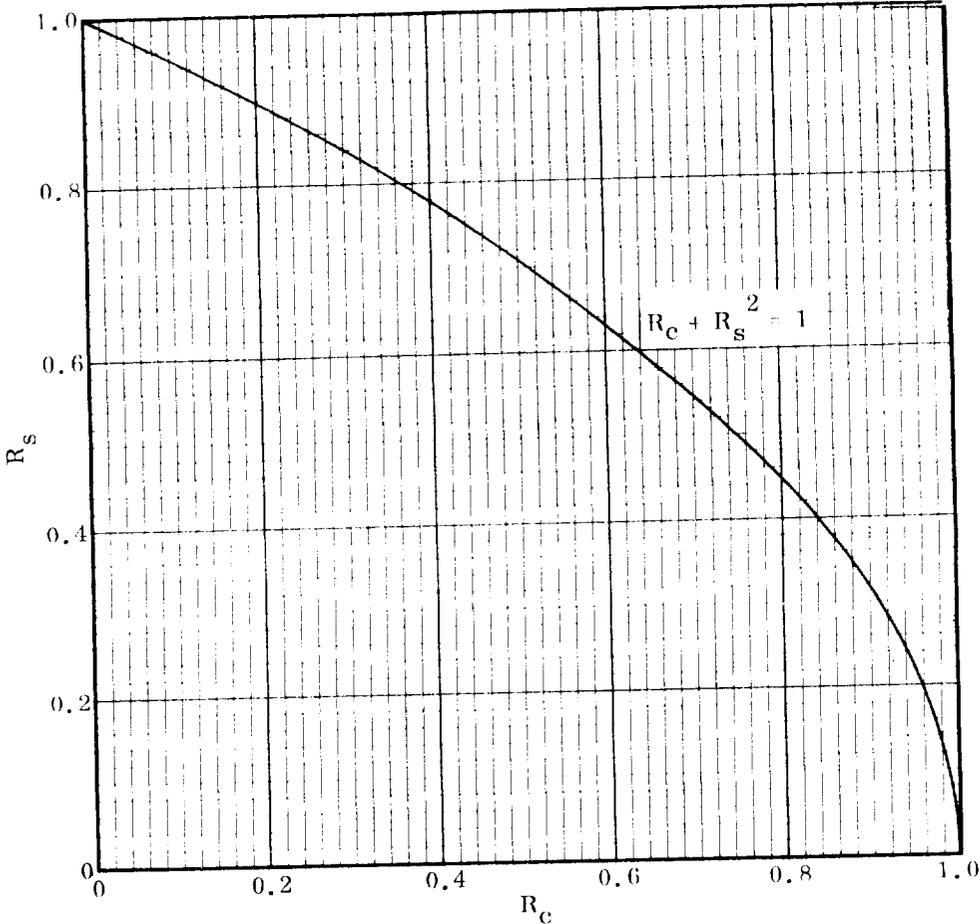
Figure 4.7-17. Conditional Interaction Curve for Circular Sandwich Cylinders Subjected to Axial Compression Plus Torsion
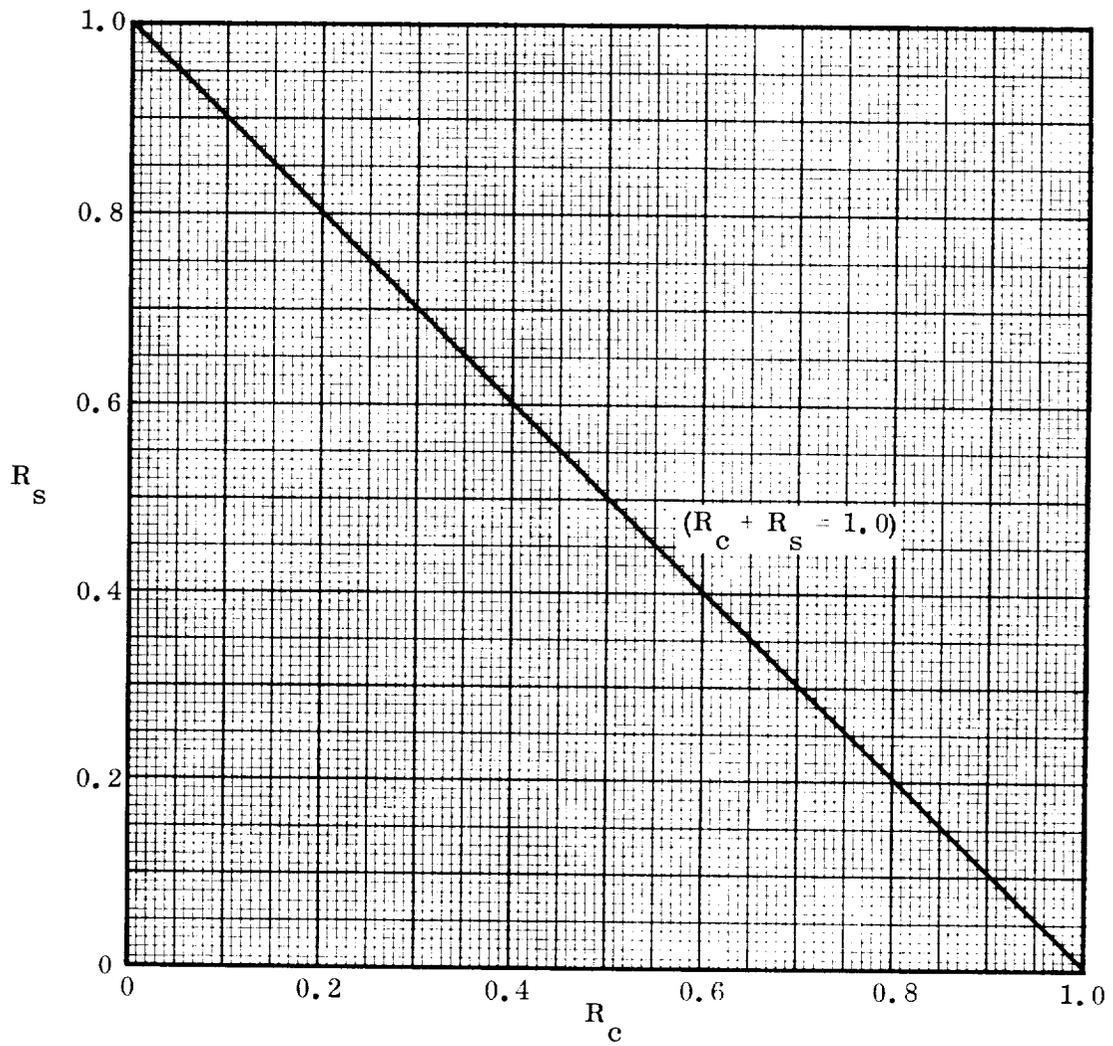
Figure 4.7-18. Conservative Interaction Curve for Circular Sandwich Cylinders Subjected to Axial Compression Plus Torsion

4.7.5   Other Loading Combinations

4.7.5.1   Basic Principles

In Sections 4.7.3 and 4.7.4 the following combined loading conditions are treated:

a.   Axial Compression plus External Lateral Pressure.

b.   Axial Compression plus Torsion.

The corresponding interaction relationships can be used for certain additional combinations by recognizing that

a.   the peak axial stress due to an applied bending moment can be converted into an equivalent uniform axial stress, and

b.   the peak shear stress due to a transverse shear force can be converted into an equivalent uniform torsional shear stress.

With this in mind, the design equations and curves of Section 4.7.3.2 can be used for the combination of AXIAL COMPRESSION PLUS BENDING PLUS EXTERNAL LATERAL PRESSURE if one simply substitutes the quantity σ'_x for σ_x where

$$\sigma'_x = (\sigma_x)_c + \left(\frac{\gamma_c}{\gamma_b}\right)(\sigma_x)_b \qquad (4.7\text{-}37)$$

and

$(\sigma_x)_c$ = Uniform axial compressive stress due solely to applied axial load, psi.

$(\sigma_x)_b$ = Peak axial compressive stress due solely to applied bending moment, psi.

γ_c = Knock-down factor associated with axial compression and as given in Figure 4.2-8, dimensionless.

γ_b = Knock-down factor associated with pure bending and as given in Figure 4.3-2, dimensionless.

4-95

This formula is based on the findings reported in Section 4.3.

In addition, the design equations and curves of Section 4.7.4.2 can be used for the combination of AXIAL COMPRESSION PLUS BENDING PLUS TORSION PLUS TRANSVERSE SHEAR FORCE if one simply substitutes the quantities σ_c' and τ' for σ_c and τ, respectively, where

$$\sigma_c' = (\sigma_c)_c + \left(\frac{\gamma_c}{\gamma_b}\right)(\sigma_c)_b \tag{4.7-38}$$

$$\tau' = \tau_T + \frac{0.80}{1.25}\tau_V = \tau_T + 0.64\tau_V \tag{4.7-39}$$

and

$(\sigma_c)_c$ = Uniform axial compressive stress due solely to applied axial load, psi.

$(\sigma_c)_b$ = Peak axial compressive stress due solely to applied bending moment, psi.

τ_T = Uniform shear stress due solely to applied torque, psi.

τ_V = Peak shear stress due solely to applied transverse shear force, psi.

γ_c and γ_b = Knock-down factors specified above.

Equation (4.7-38) is based on the findings reported in Section 4.3 while Equation (4.7-39) stems from a comparison of Equations (4.5-9) and (4.6-3).

Since no sandwich test data are available to substantiate the foregoing procedures, they can only be regarded as "best-available" criteria.

4.7.5.2 Design Equations and Curves

For the combination of AXIAL COMPRESSION PLUS BENDING PLUS EXTERNAL LATERAL PRESSURE, substitute σ'_x for σ_x and use the design equations and curves given in Section 4.7.3.2. The quantity σ'_x is defined as follows:

$$\sigma'_x = (\sigma_x)_c + \left(\frac{\gamma_c}{\gamma_b}\right)(\sigma_x)_b \tag{4.7-40}$$

However, the quantity $(\bar{\sigma}_x)_{CL}$ used in Section 4.7.3.2 remains as defined in that section.

For the combination of AXIAL COMPRESSION PLUS BENDING PLUS TORSION PLUS TRANSVERSE SHEAR FORCE, substitute σ'_c for σ_c and τ' for τ in the design equations and curves given in Section 4.7.4.2. The quantities σ'_c and τ' are defined as follows:

$$\sigma'_c = (\sigma_c)_c + \left(\frac{\gamma_c}{\gamma_b}\right)(\sigma_c)_b \tag{4.7-41}$$

$$\tau' = \tau_T + \frac{0.80}{1.25}\tau_V = \tau_T + 0.64\tau_V \tag{4.7-42}$$

However, the quantities $(\bar{\sigma}_c)_{CL}$ and $(\bar{\tau})_{CL}$ used in Section 4.7.4.2 remain as defined in that section.

The foregoing criteria will still apply, of course, where one or more of the specified applied loads equal zero.

Table 4-1. Summary of Design Equations for Instability of Circular Cylinders

NOTATION: σ = Normal stress (psi), η = Plasticity reduction factor (dimensionless), E = Young's modulus (psi), h = Distance between middle surfaces of facings (inches), R = Radius to the middle surface of sandwich cylinder (inches), t = Thickness (inches), ν = Poisson's ratio (dimensionless), G = Transverse shear modulus of core (psi), p = External pressure (psi), τ = Facing shear stress (psi), γ = Knock-down factor (dimensionless).

SUBSCRIPTS: 1, 2 denote facing 1 or 2, c denotes core or compression as applicable, f denotes facing, e denotes elastic property, cr denotes critical value for buckling, xz denotes the plane perpendicular to the facings and oriented in the axial direction, yz denotes the plane perpendicular to the axis of revolution.

Loading Condition	Design Formulas for General Instability
1. **AXIAL COMPRESSION** **MODE A:** Length L is greater than the length of a single axial half-wave. That is, for cases where $$\theta = \frac{G_{xz}}{G_{yz}} = 1,$$ (1) and $V_{c_1} < 2$, this mode is applicable to cylinders for which $$\left(\frac{L}{R}\right) \ge 1.57\left[C_0(2 - V_{c_1})\right]^{\frac{1}{2}},$$ (2) and when $V_{c_1} \ge 2$, this mode is applicable for all values of L.	(a) $\sigma_{cr_{1,2}} = \gamma_c K_{c_{1,2}} \sigma_{o_{1,2}}$ where $K_{c_{1,2}}$ may be obtained from Figure 4.2-7. When $V_{c_1} < 2.0$, the value for γ_c may be obtained from Figure 4.2-8. When $V_{c_1} \ge 2.0$, use $\gamma_c = 1.0$. $$\sigma_{o_{1,2}} = \eta E_{1,2} C_0$$ $$C_0 = \frac{h}{R}\sqrt{1 - \nu_e^2\left[(E_1 t_1) + (E_2 t_2)\right]}$$ $$\sigma_{crimp_1} = \frac{h^2 G_{xz}}{\left[t_1 + \left(\frac{E_2}{E_1}\right)t_2\right]t_c}$$ $$\sigma_{crimp_2} = \frac{h^2 G_{xz}}{\left[\left(\frac{E_1}{E_2}\right)t_1 + t_2\right]t_c}$$ $$V_{c_1} = V_{c_2} = \frac{\sigma_{o_{1,2}}}{\sigma_{crimp_{1,2}}}$$ $(V_{c_{1,2}}$ are used in obtaining $K_{c_{1,2}}$ from Figure 4.2-7) For cases where the two facings are not made of the same material, the foregoing equations are valid only when the behavior is elastic. Application to inelastic cases can only be made when both facings are made of the same material. Use $\eta = 1.0$ for elastic cases. Refer to Section 9 for inelastic cases.

4-98

(b) In the special case where $t_1 = t_2 \equiv t_f$ and both facings are made of the same material

$\sigma_{cr} = \gamma_c K_c \sigma_o$ where K_c may be obtained from Figure 4.2-7.

When $V_c < 2.0$, the value for γ_c may be obtained from Figure 4.2-8.

When $V_c \geq 2.0$, use $\gamma_c = 1.0$.

$$\sigma_o = \frac{(\eta E_f)}{\sqrt{1-\nu_e^2}} \frac{h}{R}$$

$$\sigma_{crimp} = \frac{h^2 G_{xz}}{2 t_f t_c}$$

$$V_c = \frac{\sigma_o}{\sigma_{crimp}}$$

(V_c is used in obtaining K_c from Figure 4.2-7)

In this case, V_{c_1} is used in place of V_{c_1} in the length criteria given in the LOADING CONDITION column.

Use $\eta = 1.0$ for elastic cases. Refer to Section 9 for inelastic cases.

Restrictions: $\theta = \dfrac{G_{xz}}{G_{yz}} = 1$, $t_1, t_2 \leq t_1 \leq 2 t_2$, and both facings must be made of the same material.

$$\sigma_{cr} = \frac{\gamma_c K_c' \pi^2 D}{(t_1 + t_2) L^2}$$ where K_c' may be obtained from Figure 4.2-9.

When $K_c' < \left(\dfrac{1}{r_a}\right)$, obtain γ_c from Figure 4.2-8.

When $K_c' = \left(\dfrac{1}{r_a}\right)$, use $\gamma_c = 1.0$.

$$Z = \frac{2 L^2}{Rh} \sqrt{1-\nu_e^2} \quad \text{and} \quad r_a = \frac{\pi^2 D}{L^2 D_q} \quad \text{where}$$

Both Ends
Simply Supported

MODE B: (Short Cylinder) Buckle pattern has only 1 axial half-wave. That is, for cases where

$$\theta = \frac{G_{xz}}{G_{yz}} = 1,$$

(1) and $V_{c_1} < 2$, this mode is applicable to cylinders for which

$$\left(\frac{L}{R}\right) < 1.57 \left[C_o (2 - V_{c_1})\right]^{\frac{1}{2}},$$

(2) and when $V_{c_1} \geq 2$, this mode is never applicable.

Table 4-1. Summary of Design Equations for Instability of Circular Cylinders, Cont'd.

Loading Condition	Design Formulas for General Instability
Both Ends Simply Supported **2. PURE BENDING** MODE A: Length L is greater than the length of a single axial half-wave. That is, for cases where $\theta = \dfrac{G_{xz}}{G_{yz}} = 1,$ (1) and $V_{c_1} < 2$, this mode is applicable to cylinders for which $\left(\dfrac{L}{R}\right) \geq 1.57\left[C_o\,(2 - V_{c_1})\right]^{\frac{1}{2}},$ (2) and when $V_{c_1} \geq 2$, this mode is applicable for all values of L.	$D = \eta\,\dfrac{(E_1 t_1)(E_2 t_2)\,h^2}{(1-\nu_e^2)\left[(E_1 t_1)+(E_2 t_2)\right]}$ $D_q = \dfrac{h^2\,G_{xz}}{t_c}$ (Z and r_a are used in obtaining K'_c from Figure 4.2-9.) Use $\eta = 1.0$ for elastic cases. Refer to Section 9 for inelastic cases. (a) $\sigma_{cr_{1,2}} = \gamma_b K_{c_{1,2}}\,\sigma_{o_{1,2}}$ where $K_{c_{1,2}}$ may be obtained from Figure 4.2-7. When $V_{c_1} < 2.0$, the value for γ_b may be obtained from Figure 4.3-2. When $V_{c_1} \geq 2.0$, use $\gamma_b = 1.0$. $\sigma_{o_{1,2}} = \eta E_{1,2}\,C_o$ $\sigma_{crimp_1} = \dfrac{h^2 G_{xz}}{\left[t_1 + \left(\dfrac{E_2}{E_1}\right)t_2\right]t_c}$ $V_{c_1} = V_{c_2} = \dfrac{\sigma_o}{\sigma_{crimp_{1,2}}}$ $C_o = \dfrac{h}{R}\,\dfrac{2\sqrt{(E_1 t_1)(E_2 t_2)}}{\sqrt{1-\nu_e^2}\,(E_1 t_1)-(E_2 t_2)}$ $\sigma_{crimp_2} = \dfrac{h^2 G_{xz}}{\left[\left(\dfrac{E_1}{E_2}\right)t_1 + t_2\right]t_c}$ ($V_{c_{1,2}}$ are used in obtaining $K_{c_{1,2}}$ from Figure 4.2-7) For cases where the two facings are not made of the same material, the foregoing equations are valid only when the behavior is elastic. Application to inelastic cases can only be made when both facings are made of the same material.

Use $\eta = 1.0$ for elastic cases. Refer to Section 9 for inelastic cases.

Base the entire design and analysis on the peak compressive stress due to the applied bending moment.

(b) In the special case where $t_1 = t_2 = t_f$ and both facings are made of the same material

$$\sigma_{cr} = \gamma_b K_c \sigma_o \text{ where } K_c \text{ may be obtained from Figure 4.2-7.}$$

When $V_c < 2.0$, the value for γ_b may be obtained from Figure 4.3-2.

When $V_c \geq 2.0$, use $\gamma_b = 1.0$.

$$\sigma_o = \frac{(\eta E_f)}{\sqrt{1-\nu_e^2}} \frac{h}{R}$$

$$\sigma_{crimp} = \frac{h^2 G_{xz}}{2 t_f t_c}$$

$$V_c = \frac{\sigma_o}{\sigma_{crimp}}$$

(V_c is used in obtaining K_c from Figure 4.2-7)

In this case, V_c is used in place of V_{c_1} in the length criteria given in the LOADING CONDITION column.

Use $\eta = 1.0$ for elastic cases. Refer to Section 9 for inelastic cases.

Base the entire design and analysis on the peak compressive stress due to the applied bending moment.

Restrictions: $\theta = \dfrac{G_{xz}}{G_{yz}} = 1$, $t_2 \leq t_1 \leq 2t_2$, and both facings must be made of the same material.

$$\sigma_{cr} = \frac{\gamma_b K_c' \pi^2 D}{(t_1 + t_2) L^2} \text{ where } K_c' \text{ may be obtained from Figure 4.2-9.}$$

When $K_c' < \left(\dfrac{1}{r_a}\right)$, obtain γ_b from Figure 4.3-2.

When $K_c' = \left(\dfrac{1}{r_a}\right)$, use $\gamma_b = 1.0$.

Both Ends Simply Supported

M, in-lbs — M, in-lbs — L — G_{yz} — G_{xz} — Axis of Revolution — Buckle Pattern

MODE B: (Short Cylinder) Buckle pattern has only 1 axial half-wave. That is, for cases where

$$\theta = \frac{G_{xz}}{G_{yz}} = 1,$$

(1) and $V_{c_1} < 2$, this mode is applicable to cylinders for which

$$\left(\frac{L}{R}\right) < 1.57 \left[C_o (2 - V_{c_1})\right]^{\frac{1}{4}},$$

(2) and when $V_{c_1} \geq 2$, this mode is never applicable

4-101

Table 4-1. Summary of Design Equations for Instability of Circular Cylinders, Cont'd.

Loading Condition	Design Formulas for General Instability
  Buckle Pattern Both Ends Simply Supported	$Z = \dfrac{2L^2}{Rh}\sqrt{1-\nu_e^2}$ and $r_a = \dfrac{\pi^2 D}{L^2 D_q}$ where $D = \eta \dfrac{(E_1 t_1)(E_2 t_2) h^2}{(1-\nu_e^2)[(E_1 t_1)+(E_2 t_2)]}$ $D_q = \dfrac{h^2 G_{xz}}{t_c}$ (Z and r_a are used in obtaining K_c' from Figure 4.2-9.) Use $\eta = 1.0$ for elastic cases. Refer to Section 9 for inelastic cases. Base the entire design and analysis on the peak compressive stress due to the applied bending moment.
3. <u>UNIFORM EXTERNAL LATERAL PRESSURE</u> Both Ends Simply Supported	$p_{cr} = \dfrac{\gamma_p \,\eta\, C_p}{R(1-\nu_e^2)}\,[(E_1 t_1)+(E_2 t_2)]$ where $\gamma_p = 0.90$ and C_p may be obtained from Figures 4.4-3 through 4.4-5 for appropriate values of $\phi^2 = \dfrac{(E_1 t_1)(E_2 t_2) h^2}{[(E_1 t_1)+(E_2 t_2)]^{-2} R^2}$ $V_p = \eta \dfrac{(E_1 t_1)(E_2 t_2) h}{[(E_1 t_1)+(E_2 t_2)]\,(1-\nu_e^2)\, R^2\, G_{yz}}$ For cases where the two facings are not made of the same material, the foregoing equations are valid only when the behavior is elastic. Application to inelastic cases can only be made when both facings are made of the same material. Use $\eta = 1.0$ for elastic cases. Refer to Section 9 for inelastic cases.
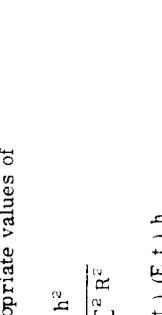
4. TORSION

$$\tau_{cr} = \gamma_s K_s \eta E_f \frac{d}{R} \quad \text{where } \gamma_s = 0.30 \text{ and } K_s \text{ may be obtained from Figures 4.5-3 through 4.5-8.}$$

$$d = t_c + t_1 + t_2$$

To use Figures 4.5-3 through 4.5-8, the following values must first be computed:

$$Z_s = \frac{L^2}{dR} \qquad V_s = \frac{16 t_c t_1 t_2 \eta E_f}{15 (t_1 + t_2) Rd G_{xz}} \qquad \theta = \frac{G_{xz}}{G_{yz}}$$

This criterion is valid only where $t_2 \le t_1 \le 2 t_2$ and both facings are made of the same material. In addition, the results will be somewhat inaccurate for very long cylinders (large values of Z_s).

Use $\eta = 1.0$ for elastic cases. Refer to Section 9 for inelastic cases.

T, in-lbs

Axis of Revolution

G_{xz}
G_{yz}

T, in-lbs

L

Both Ends Simply Supported

5. TRANSVERSE SHEAR

$$\tau_{cr} = 1.25 K_s \eta E_f \frac{d}{R} \quad \text{where } K_s \text{ may be obtained from Figures 4.5-3 through 4.5-8.}$$

$$d = t_c + t_1 + t_2$$

To use Figures 4.5-3 through 4.5-8, the following values must first be computed:

$$Z_s = \frac{L^2}{dR} \qquad V_s = \frac{16 t_c t_1 t_2 \eta E_f}{15 (t_1 + t_2) Rd G_{xz}} \qquad \theta = \frac{G_{xz}}{G_{yz}}$$

This criterion is valid only where $t_2 \le t_1 \le 2 t_2$ and both facings are made of the same material. In addition, the results will be somewhat inaccurate for very long cylinders (large values of Z_s).

Use $\eta = 1.0$ for elastic cases. Refer to Section 9 for inelastic cases.

F_v, lbs

L

G_{yz}
G_{xz}

Axis of Revolution

Both Ends Simply Supported

4-103

Loading Condition	Design Formulas for General Instability
6. COMBINED AXIAL COMPRESSION AND BENDING Both Ends Simply Supported	Interaction Formula $R_c + R_b = 1$ (See Figure 4.7-3) where $$R_c = \frac{\sigma_c}{\gamma_c (\bar{\sigma}_c)_{CL}} \qquad R_b = \frac{\sigma_b}{\gamma_b (\bar{\sigma}_c)_{CL}}$$ σ_c = Uniform compressive stress due solely to applied axial load, psi. σ_b = Peak compressive stress due solely to applied bending moment, psi. γ_c and γ_b may be obtained as specified for Loading Conditions 1 and 2, respectively, with due consideration as to whether Mode A or Mode B is applicable. $(\bar{\sigma}_c)_{CL}$ is the result obtained by using $\gamma_c = 1.0$ in the equations of Loading Condition 1 (Axial Compression). The equations for the appropriate mode (A or B) should be used as determined by the length L of the cylinder. Plasticity considerations should be handled as specified in Section 9 except that, in this case, one may use (1) $\eta = \left[\dfrac{1-\nu_e^2}{1-\nu^2}\right] \dfrac{E_t}{E_f}$ for short cylinders (Mode B). (2) $\eta = \left[\dfrac{1-\nu_e^2}{1-\nu^2}\right]^{\frac{1}{2}} \sqrt{\dfrac{E_t E_s}{E_f}}$ for constructions which buckle in Mode A. For elastic cases, use $\eta = 1.0$.

7. COMBINED AXIAL COMPRESSION AND EXTERNAL LATERAL PRESSURE
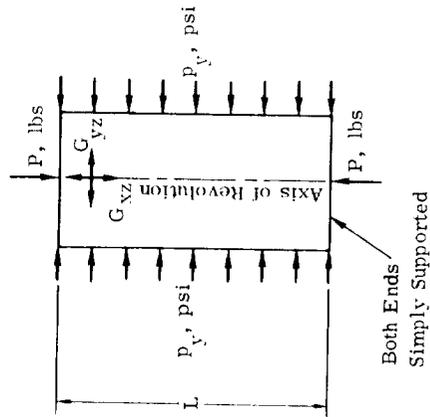
Both Ends Simply Supported

Use the interaction curves of Figures 4.7-6 through 4.7-15 where

$$V_{xz} = \frac{E_f t_f h}{2(1-.33^2) R^2 G_{xz}}$$

$$V_{yz} = \frac{E_f t_f h}{2(1-.33^2) R^2 G_{yz}}$$

$$R_p = \frac{p_y}{\gamma_p (\bar{p}_y)_{CL}}$$

$$R_c = \frac{\sigma_x}{\gamma_c (\bar{\sigma}_x)_{CL}}$$

$$\gamma_p = 0.90$$

γ_c may be obtained as specified for Loading Condition 1 with due consideration as to whether Mode A or Mode B is applicable.

p_y = Applied external lateral pressure, psi.

σ_x = Uniform axial compressive stress due solely to the applied axial load, psi.

$(\bar{p}_y)_{CL}$ = Classical theoretical value for critical external lateral pressure when acting alone, psi. This value may be computed by setting $\gamma_p = 1.0$ in the equations of Loading Condition 3.

$(\bar{\sigma}_x)_{CL}$ = Classical theoretical value for critical uniform axial compressive stress when acting alone, psi. This value may be computed by setting $\gamma_c = 1.0$ in the equations of Loading Condition 1. The equations for the appropriate mode (A or B) should be used as determined by the length L of the cylinder.

This criterion is valid only where both facings are made of the same material and are of the same thickness ($t_1 = t_2 = t_f$). Figures 4.7-6 through 4.7-12 are subject to the added restrictions that they can be used only where

$$\frac{R t_c}{h^2} V_{xz} \le 0.05 \text{ and } \frac{R t_c}{h^2} V_{yz} \le 0.05$$

For inelastic cases, refer to Section 9.

Table 4-1. Summary of Design Equations for Instability of Circular Cylinders, Cont'd.

Loading Condition	Design Formulas for General Instability
8. COMBINED AXIAL COMPRESSION AND TORSION T, in-lbs P, lbs Axis of Revolution G_{xz} G_{yz} L P, lbs T, in-lbs Both Ends Simply Supported	Interaction Formula: $R_c + R_s = 1$, (See Figure 4.7-18) where $$R_c = \frac{\sigma_c}{\gamma_c (\bar{\sigma}_c)_{CL}} \qquad R_s = \frac{\tau}{\gamma_s (\bar{\tau})_{CL}}$$ σ_c = Uniform compressive stress due solely to applied axial load, psi. τ = Uniform shear stress due solely to applied torque, psi. γ_c may be obtained as specified for Loading Condition 1 with due consideration as to whether Mode A or Mode B is applicable. $\gamma_s = 0.80$ $(\bar{\sigma}_c')_{CL}$ = Classical theoretical value for critical uniform axial compressive stress when acting alone, psi. This value may be obtained by setting $\gamma_c = 1.0$ in the equations of Loading Condition 1. The equations for the appropriate mode (A or B) should be used as determined by the length L of the cylinder. $(\bar{\tau})_{CL}$ = Classical theoretical value for critical uniform shear stress due to torque acting alone, psi. This value may be obtained by setting $\gamma_s = 1.0$ in the equations of Loading Condition 4.
9. COMBINED AXIAL COMPRESSION PLUS BENDING PLUS EXTERNAL LATERAL PRESSURE	For inelastic cases, refer to Section 9. Use interaction curves and equations for Loading Condition 7 except substitute σ_x' for σ_x where $$\sigma_x' = (\sigma_x)_c + \left(\frac{\gamma_c}{\gamma_b}\right)(\sigma_x)_b$$ $(\sigma_x)_c$ = Uniform axial compressive stress due solely to applied axial load, psi.

4-106

$(\sigma_x)_b$ = Peak axial compressive stress due solely to applied bending moment, psi.

γ_c and γ_b may be obtained as specified for Loading Conditions 1 and 2, respectively, with due consideration as to whether Mode A or Mode B is applicable.

For inelastic cases, refer to Section 9.

Both Ends
Simply Supported

---

10. COMBINED AXIAL COMPRESSION PLUS BENDING PLUS TORSION PLUS TRANSVERSE SHEAR

Use interaction relationship for Loading Condition 9 except substitute σ_c' and τ' for σ_c and τ, respectively, where

$$\sigma_c' = (\sigma_c)_c - \left(\frac{\gamma_c}{\gamma_b}\right)(\sigma_c)_b \qquad \tau' = \tau_T + 0.64\,\tau_v$$

$(\sigma_c)_c$ = Uniform axial compressive stress due solely to applied axial load, psi.

$(\sigma_c)_b$ = Peak axial compressive stress due solely to applied bending moment, psi.

τ_T = Uniform shear stress due solely to applied torque, psi.

τ_v = Peak shear stress due solely to applied transverse shear force, psi.

γ_c and γ_b may be obtained as specified for Loading Conditions 1 and 2, respectively, with due consideration as to whether Mode A or Mode B is applicable.

For inelastic cases, refer to Section 9.

Both Ends
Simply Supported

4-107

REFERENCES

4-1   Donnell, L. H. and Wan, C. C., "Effect of Imperfections on Buckling of Thin Cylinders and Columns Under Axial Compression," Journal of Applied Mechanics, March 1950.

4-2   March, H. W. and Kuenzi, E. W., "Buckling of Cylinders of Sandwich Construction in Axial Compression," FPL Report No. 1830, Revised December 1957.

4-3   Hoff, N. J., Madsen, W. A., and Mayers, J., "The Postbuckling Equilibrium of Axially Compressed Circular Cylindrical Shells," Stanford University Department of Aeronautics and Astronautics, Report SUDAER No. 221, February 1965.

4-4   Anonymous, "Buckling of Thin-Walled Circular Cylinders," NASA Space Vehicle Design Criteria, NASA SP-8007, September 1965.

4-5   U. S. Department of Defense, Structural Sandwich Composites, MIL-HDBK-23, 30 December 1968.

4-6   Thielemann, W. F., "New Developments in the Nonlinear Theories of the Buckling of Thin Cylindrical Shells," Proceedings of the Durand Centennial Conference, Held at Stanford University, 5-8 August 1969, Pergamon Press, New York, Copyright 1960.

4-7   Zahn, J. J. and Kuenzi, E. W., "Classical Buckling of Cylinders of Sandwich Construction in Axial Compression --- Orthotropic Cores," U. S. Forest Service Research Note, FPL-018, November 1963.

4-8   Donnell, L. H., "Stability of Thin-Walled Tubes Under Torsion," NACA Technical Report No. 479, 1934.

4-9   Seide, P., Weingarten, V. I., and Morgan, E. J., "Final Report on the Development of Design Criteria for Elastic Stability of Thin Shell Structures," STL-TR-60-0000-19425, 31 December 1960.

4-10   Baker, E. H., "Experimental Investigation of Sandwich Cylinders and Cones Subjected to Axial Compression," AIAA Journal, Volume 6, No. 9, September 1968.

4-11   Anonymous, "Status Summary Report for R&D Project 6002," Hexcel Products, Inc., Advanced Structures Group, 25 July 1963.

4-12   Plantema, F. J., Sandwich Construction, John Wiley & Sons, Inc., New York, Copyright 1966.

4-13   Stein, M. and Mayers, J., "Compressive Buckling of Simply Supported Curved Plates and Cylinders of Sandwich Construction," NACA Technical Note 2601, January 1952.

4-14   Bijlaard, P. P. and Gallagher, R. H., "Elastic Instability of a Cylindrical Shell Under Arbitrary Circumferential Variation of Axial Stress," Journal of the Aerospace Sciences, Vol. 27, 1960.

4-15   Abir, D. and Nardo, S. V., "Thermal Buckling of Circular Cylindrical Shells Under Circumferential Temperature Gradients," Journal of the Aerospace Sciences, Vol. 26, 1959.

4-16   Seide, P. and Weingarten, V. I., "On the Buckling of Circular Cylindrical Shells Under Pure Bending," Transactions of the A.S.M.E., Journal of Applied Mechanics, March 1961.

4-17   Wang, C. T. and Sullivan, D. P., "Buckling of Sandwich Cylinders Under Bending and Combined Bending and Axial Compression," Journal of the Aeronautical Sciences, Vol. 19, July 1952.

4-18   Wang, C. T., Vaccaro, R. J., and DeSanto, D. F., "Buckling of Sandwich Cylinders Under Combined Compression, Torsion, and Bending Loads," Journal of Applied Mechanics, Vol. 22, September 1955.

4-19   Gellatly, R. A. and Gallagher, R. H., "Sandwich Cylinder Instability Under Nonuniform Axial Stress," AIAA Journal, February 1964.

4-20   Peterson, J. P. and Anderson, J. K., "Structural Behavior and Buckling Strength of Honeycomb Sandwich Cylinders Subjected to Bending," NASA TN D-2926, August 1965.

4-21   Kuenzi, E. W., Bohannan, B., and Stevens, G. H., "Buckling Coefficients for Sandwich Cylinders of Finite Length Under Uniform External Lateral Pressure," U. S. Forest Service Research Note FPL-0104, September 1965.

4-22   Raville, M. E., "Analysis of Long Cylinders of Sandwich Construction Under Uniform External Lateral Pressure," FPL Report No. 1844, November 1954.

4-23   Raville, M. E., "Supplement to Analysis of Long Cylinders of Sandwich Construction Under Uniform External Lateral Pressure," FPL Report No. 1844-A, February 1955.

4-24   Raville, M. E., "Buckling of Sandwich Cylinders of Finite Length Under Uniform External Lateral Pressure," FPL Report No. 1844-B, May 1955.

4-25   Norris, C. B. and Zahn, J. J., "Design Curves for the Buckling of Sandwich Cylinders of Finite Length Under Uniform External Lateral Pressure," FPL Report No. 1869, May 1959.

4-26   Norris, C. B. and Zahn, J. J., "Design Curves for the Buckling of Sandwich Cylinders of Finite Length Under Uniform External Lateral Pressure," U. S. Forest Service Research Note FPL-07, 1963.

4-27   Kazimi, M. I., "Sandwich Cylinders Part II - Uniformity of the Mechanical Properties of the Core," Aerospace Engineering, September 1960.

4-28   Jenkinson, P. M. and Kuenzi, E. W., "The Buckling Under External Radial Pressure and Buckling Under Axial Compression of Sandwich Cylindrical Shells," FPL Report PE-227, January 1962.

4-29   Gerard, G., "Torsional Instability of a Long Sandwich Cylinder," Proc. 1st U. S. Natl. Congr. Appl. Mech., Copyright 1951.

4-30   March, H. W. and Kuenzi, E. W., "Buckling of Sandwich Cylinders in Torsion," FPL Report No. 1840 Revised, January 1958.

4-31   Gerard, G., Introduction to Structural Stability Theory, McGraw-Hill Book Company, Inc., New York, Copyright 1962.

4-32   Timoshenko, S. P. and Gere, J. M., Theory of Elastic Stability, McGraw-Hill Book Company, Inc., New York, Copyright 1961.

4-33   Lundquist, E. E., "Strength Tests of Thin-Walled Duralumin Cylinders in Combined Transverse Shear and Bending," NACA TN 523, 1935.

4-34   Lundquist, E. E. and Burke, W. F., "Strength Tests of Thin-Walled Duralumin Cylinders of Elliptic Section," NACA TN 527, 1935.

4-35   Gerard, G. and Becker, H., "Handbook of Structural Stability, Part III - Buckling of Curved Plates and Shells," NACA TN 3783, August 1957.

4-36   Batdorf, S. B., Stein, M., and Schildcrout, M., "Critical Stress of Thin-Walled Cylinders in Torsion," NACA TN 1344, 1947.

4-37   Maki, A. C., "Elastic Stability of Cylindrical Sandwich Shells Under Axial and Lateral Load," U. S. Forest Service Research Note FPL-0173, October 1967.

4-38   Batdorf, S. B., Stein, M., and Schildcrout, M., "Critical Combinations of Torsion and Direct Axial Stress for Thin-Walled Cylinders," NACA Technical Note 1345, June 1947.

5

GENERAL INSTABILITY OF TRUNCATED CIRCULAR CONES

5.1 AXIAL COMPRESSION

5.1.1 Basic Principles

It appears that no significant theoretical solutions have been published for axially compressed sandwich cones. Therefore, for the purposes of this handbook, the equivalent-cylinder concept of Seide, et al. [5-1] has been adopted as a practical expediency. Based on a large array of test data from thin-walled, isotropic (non-sandwich), truncated cones, Seide, et al. concluded that the critical stresses for such cones can be taken equal to the values for circular cylinders which satisfy the following conditions:

    a.   The wall thickness of the equivalent cylinder is equal to that of the cone. In the case of sandwich constructions, the logical extension of this condition is that the equivalent cylinder have the same facing and core thicknesses found in the cone.

    b.   The radius of the equivalent cylinder is equal to the finite principal radius of curvature at the small end of the cone.

    c.   The length of the equivalent cylinder is equal to the slant length of the cone.

In Reference 5-2, Baker presents test data from two axially compressed, truncated sandwich cones having vertex half-angles equal to 15 degrees. These data were used in conjunction with the foregoing equivalent-cylinder concept to arrive at knock-down factors γ_c. The results are shown in Figure 5.1-1, along with data obtained from

Figure 5.1-1. Empirical Knock-Down Factors

△ DATA FROM REFERENCE 5-2 (CONICAL)
● DATA FROM REFERENCE 5-2 (CYLINDRICAL)
◇ DATA FROM REFERENCE 4-2 (CYLINDRICAL)
☐ DATA FROM REFERENCE 4-28 (CYLINDRICAL)

DESIGN CURVE RECOMMENDED FOR CYLINDERS

$\left(\dfrac{R}{\rho}\right)$

γ_c

axially compressed sandwich cylinders. This figure also includes the design curve recommended in Section 4.2.2 for such cylinders. It can be seen that the data from the cones are in favorable agreement with the results obtained from cylinders. This provides at least a small degree of experimental substantiation for application of the equivalent-cylinder approach to sandwich cones. However, in view of the scarcity of test points from conical specimens, this method can presently be considered as only a "best-available" criterion.

5.1.2 Design Equations and Curves

For simply supported, truncated, right-circular, sandwich cones subjected to axial compression, the critical stresses σ_{cr_1} and σ_{cr_2} (for facings 1 and 2, respectively) may be computed from the equations and curves of Section 4.2.2, provided that the following substitutions are made:

a. The values t_1, t_2, t_c, and h are measured as shown in Figure 5.1-2. (There is no preference as to which facing is denoted by the subscripts 1 or 2.)

b. The radius R is replaced by the effective radius R_e shown in Figure 5.1-2.

c. The length L is replaced by the effective length L_e shown in Figure 5.1-2.
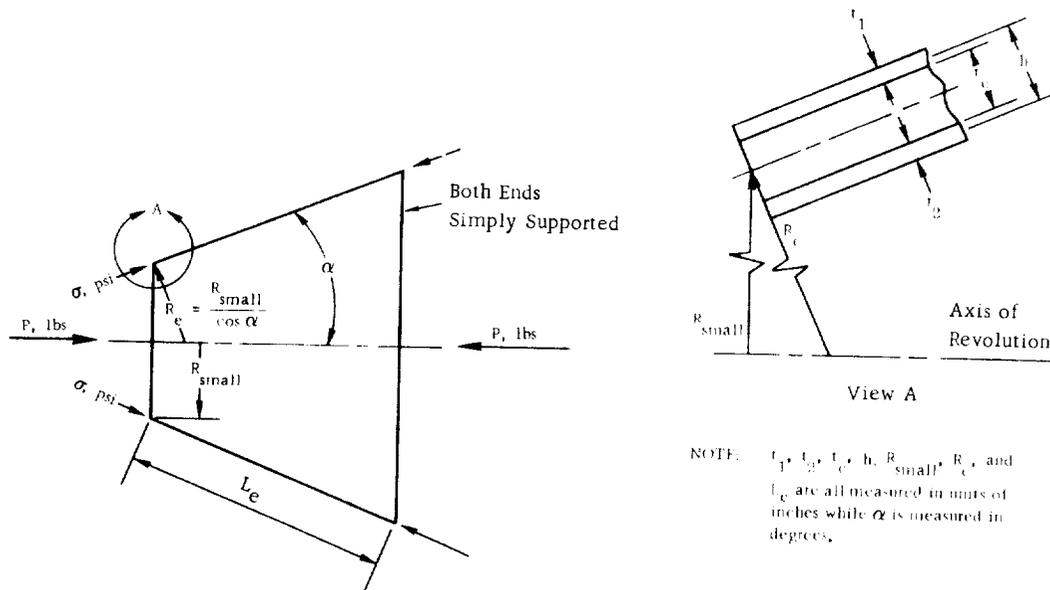
Figure 5.1-2. Truncated Sandwich Cone Subjected to Axial Compression

The applied axial load P and the computed stresses are associated with the directions indicated in Figure 5.1-2. In addition, since the maximum stresses occur at the small end of the cone, the critical values are associated with this location. For both elastic and inelastic cases, one can therefore write

$$P_{cr} = 2\pi R_e \left(\sigma_{cr_1} t_1 + \sigma_{cr_2} t_2 \right) \cos^2 \alpha \qquad (5.1\text{-}1)$$

where

$$R_e = \frac{R_{small}}{\cos \alpha} \qquad (5.1\text{-}2)$$

It is recommended that the approach specified here be applied only to cases where $\alpha \le 30$ degrees.

Plasticity reduction factors should always be based on the stress at the small end of the cone (see Section 9).

5.2 PURE BENDING

5.2.1 Basic Principles

It appears that no significant theoretical solutions have been published for sandwich cones subjected to pure bending. Therefore, for the purposes of this handbook, the equivalent-cylinder concept of Seide, et al. has been adopted as a practical expediency. Based on a large array of test data from thin-walled, isotropic (non-sandwich), truncated cones, Seide, et al. concluded that the critical peak stresses for such cones can be taken equal to the corresponding values for circular cylinders which satisfy the following conditions:

a. The wall thickness of the equivalent cylinder is equal to that of the cone. In the case of sandwich constructions, the logical extension of this condition is that the equivalent cylinder have the same facing and core thicknesses as are found in the cone.

b. The radius of the equivalent cylinder is equal to the finite principal radius of curvature at the small end of the cone.

c. The length of the equivalent cylinder is equal to the slant length of the cone.

No test data are available for sandwich cones which are of the types considered in this handbook and are subjected to pure bending. Therefore, the validity of the method recommended here has not been experimentally verified and can only be considered as a "best-available" approach.

5.2.2 Design Equations and Curves

For simply supported, truncated, right-circular, sandwich cones subjected to pure

bending, the critical peak stresses σ_{cr_1} and σ_{cr_2} (for facings 1 and 2, respectively)

may be computed from the equations and curves of Section 4.3.2, provided that the

following substitutions are made:

a. The values t_1, t_2, t_c, and h are measured as shown in Figure 5.2-1.
(There is no preference as to which facing is denoted by the subscripts 1 or 2.)

b. The radius R is replaced by the effective radius R_e shown in Figure 5.2-1.

c. The length L is replaced by the effective length L_e shown in Figure 5.2-1.

Note: t_1, t_2, t_c, h, R_{small}, R_e, and l_e
are all measured in units of inches
while α is measured in degrees.
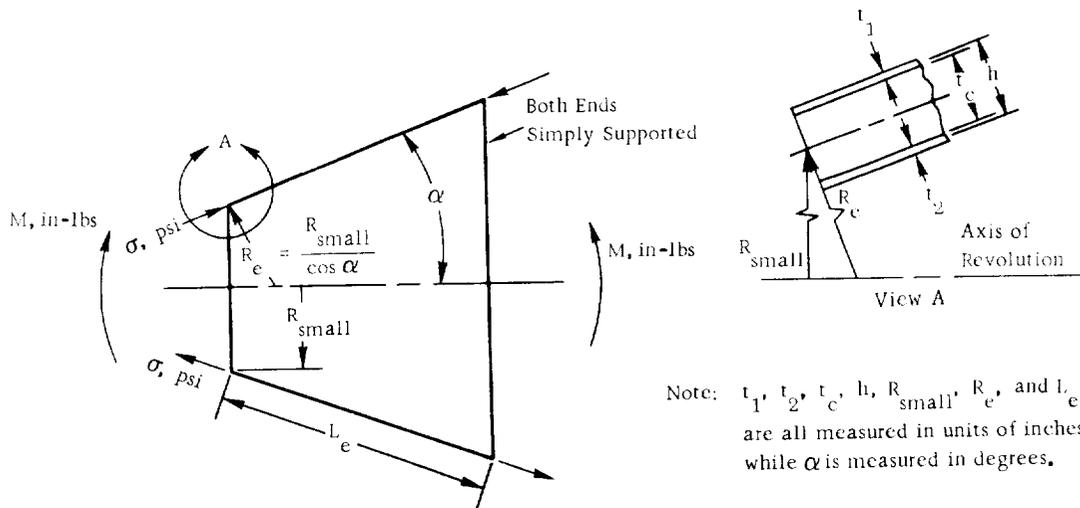
Figure 5.2-1. Truncated Sandwich Cone Subjected to Pure Bending

The applied bending moment M and the computed stresses are associated with the directions indicated in Figure 5.2-1. In addition, since the maximum stresses occur at the small end of the cone, the critical values are associated with this location. When the behavior is elastic, one can therefore write

$$M_{cr} = \pi R_e^2 \left(\sigma_{cr_1} t_1 + \sigma_{cr_2} t_2 \right) \cos^3 \alpha \qquad (5.2\text{-}1)$$

where

$$R_e = \frac{R_{small}}{\cos \alpha} \qquad (5.2\text{-}2)$$

To compute M_{cr} when the behavior is inelastic, one must resort to numerical integration techniques.

It is recommended that the approach specified here be applied only to cases where $\alpha \leq 30$ degrees.

Plasticity reduction factors should always be based on the peak compressive stress at the small end of the cone (see Section 9).

5.3 EXTERNAL LATERAL PRESSURE

5.3.1 Basic Principles

The loading condition considered here is depicted in Figure 5.3-1. As shown, the cone

is subjected to a uniform external lateral pressure. The axial component of this loading
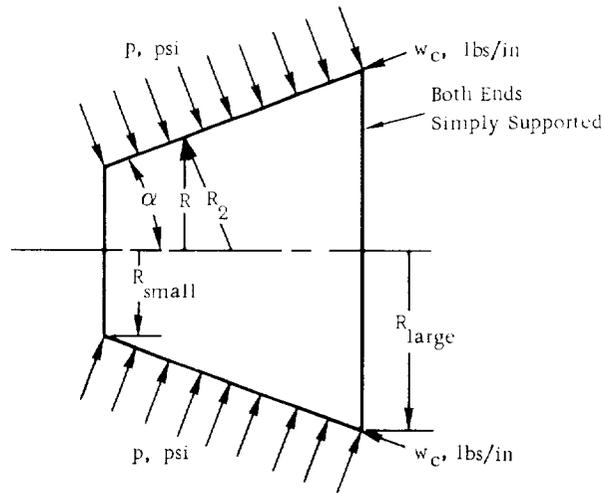
Figure 5.3-1. Truncated Cone Subjected to Uniform External Lateral Pressure

is reacted by a uniform compressive running load at the large end of the cone. This

results in principal membrane stresses which may be computed as follows, when the

core has a relatively high extensional stiffness in the direction normal to the facings:

$$\sigma_H = \frac{p\, R_2}{(t_1 + t_2)} \qquad (5.3-1)$$

$$\sigma_M = \frac{p}{(t_1 + t_2)} \frac{\left(R + R_{small}\right)}{2 \cos \alpha} \left(1 - \frac{R_{small}}{R}\right) \qquad (5.3-2)$$

where

$$R_2 = \frac{R}{\cos \alpha} \qquad\qquad (5.3\text{-}3)$$

and

σ_H = Hoop membrane stress, psi.

σ_M = Meridional membrane stress, psi.

p = Uniform external lateral pressure, psi.

R_2 = Finite principal radius of curvature of middle surface, inches.

t_1 and t_2 = Thicknesses of the facings, inches. (There is no preference as to which facing is denoted by the subscripts 1 or 2.)

R = Radius of middle surface measured perpendicular to the axis of revolution, inches.

R_{small} = Radius of middle surface, at small end of cone, measured perpendicular to the axis of revolution, inches.

R_{large} = Radius of middle surface, at large end of cone, measured perpendicular to the axis of revolution, inches.

α = Vertex half-angle of cone, degrees.

Since the radii R and R_2 vary with the axial location, the stresses σ_H and σ_M are non-uniform over the conical surface. The maximum values for each of these quantities occur at the large end of the cone.

It appears that no significant theoretical solutions have been published for the stability of truncated sandwich cones which are subjected to uniform external hydrostatic pressure. Therefore, for the purposes of this handbook, the equivalent-cylinder approach suggested in Reference 5-11 has been adopted as a practical expediency. Based on this method, the critical lateral pressure for the truncated cone may be taken equal

to that for an equivalent circular sandwich cylinder which satisfies the following conditions:

a.   The facing and core thicknesses of the equivalent cylinder are the same as those found in the cone.

b.   The length of the equivalent cylinder is equal to the slant length of the cone.

c.   The radius of the equivalent cylinder is equal to the average finite principal radius of curvature of the cone. That is,

$$R_e = \frac{R_{small} + R_{large}}{2 \cos \alpha} \tag{5.3-4}$$

The critical lateral pressure for the equivalent cylinder can be obtained by using the equations and curves of Section 4.4.2.

Since no test data are available from truncated sandwich cones subjected to external lateral pressure, the reliability of the foregoing approach has not been experimentally verified and can only be considered as a "best-available" technique.

5.3.2 Design Equations and Curves

For a simply supported, truncated, right-circular, sandwich cone subjected to uniform, external, lateral pressure, the critical pressure may be taken equal to the critical lateral pressure for an equivalent sandwich cylinder which satisfies the following:

a.   The values t_1, t_2, t_c, and h are measured as shown in Figure 5.3-2.

b.   The length is taken equal to the slant length L_e.

c.   The radius is denoted R_e and is computed from the formula

$$R_e = \frac{R_{small} + R_{large}}{2 \cos \alpha} \qquad (5.3-5)$$

where R_{small}, R_{large}, and α are as shown in Figure 5.3-2.

NOTE: t_1, t_2, t_c, h, R, R_2, R_{small}, R_{large}, and L_e are all measured in units of inches while α is measured in degrees.
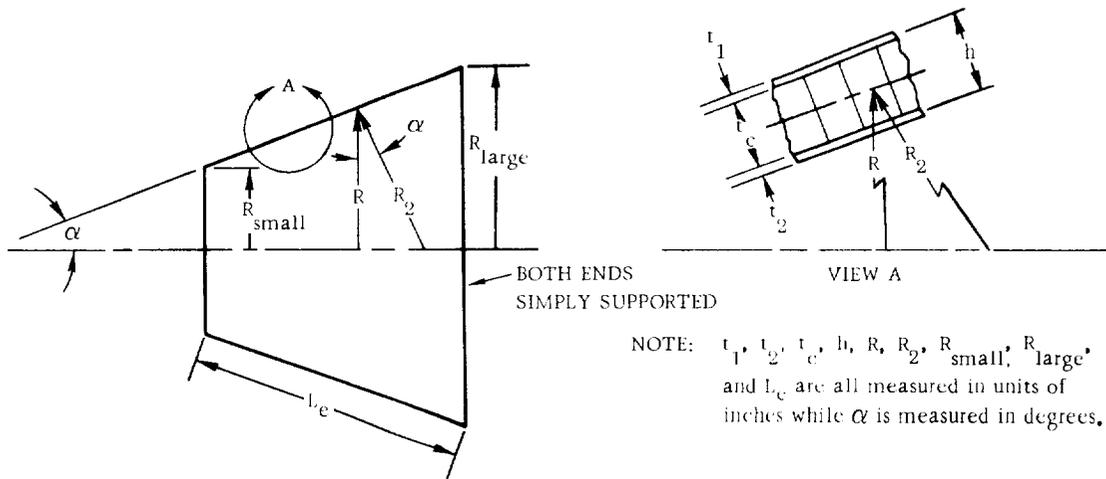
Figure 5.3-2. Truncated Sandwich Cone

The critical lateral pressure for the equivalent sandwich cylinder can be obtained by using the equations and curves of Section 4.4.2.

Plasticity considerations should be handled as specified in Section 9.2. The plasticity reduction factor η should always be based on the principal membrane stresses at the large end of the cone where

$$\sigma_H = \frac{p\,R_{large}}{(t_1 + t_2)\cos\alpha} \tag{5.3-6}$$

$$\sigma_M = \frac{p\,R_e}{(t_1 + t_2)} \left(1 - \frac{R_{small}}{R_{large}}\right) \tag{5.3-7}$$

It is recommended that the approach specified here be applied only to cases where $\alpha \leq 30$ degrees.

5.4 TORSION

5.4.1 Basic Principles

It appears that no significant theoretical solutions have been published for sandwich cones subjected to torsion. Therefore, for the purposes of this handbook, the equivalent-cylinder concept of Seide [5-3] has been adopted as a practical expediency. Based on the analysis of his numerical computations for thin-walled, isotropic (non-sandwich), truncated cones, Seide concluded that the critical torques for such shells can be taken equal to the values for circular cylinders which satisfy the following conditions:

a. The wall thickness of the equivalent cylinder is equal to that of the cone. In the case of sandwich constructions, the logical extension of this condition is that the equivalent cylinder have the same facing and core thicknesses as are found in the cone.

b. The length of the equivalent cylinder is equal to the axial length of the cone.

c. The radius of the equivalent cylinder is computed from the relationship

$$R_c = \left(R_{small} \cos\alpha \right) \left\{ 1 + \left[\frac{1}{2} \left(1 + \frac{R_{large}}{R_{small}} \right) \right]^{\frac{1}{2}} - \left[\frac{1}{2} \left(1 + \frac{R_{large}}{R_{small}} \right) \right]^{-\frac{1}{2}} \right\} \quad (5.4-1)$$

where

R_c = Radius of equivalent cylinder, inches.

R_{small} = Radius at small end of cone, inches (measured perpendicular to the axis of revolution).

R_{large} = Radius at large end of cone, inches (measured perpendicular to the axis of revolution).

α = Vertex half-angle of cone, degrees.

In Reference 5-1, Seide, et al. present test results from ten isotropic (non-sandwich), truncated cones which were subjected to torsion. These tests included specimens having vertex half-angles (α) of both 30 and 60 degrees. The agreement of these results with equivalent-cylinder predictions was similar to that obtained from comparisons of test data from isotropic (non-sandwich) cylinders against the corresponding small-deflection theoretical solutions. For conical sandwich constructions it was therefore decided to use the same knock-down factor ($\gamma_s = 0.80$) as was selected in Section 4.5 for sandwich cylinders under torsion.

No test data are available for sandwich cones which are of the types considered in this handbook and are subjected to torsion. Therefore the method recommended here has not been experimentally verified and can only be considered as a "best-available" approach.

5.4.2 Design Equations and Curves

For simply supported, truncated, right-circular sandwich cones subjected to torsion, the critical torque may be computed from the equation

$$T_{cr} = 2\pi R_e^2 (t_1 + t_2) \tau'_{cr} \qquad (5.4\text{-}2)$$

where

T_{cr} = Critical torque for sandwich cone subjected to torsion, in-lbs.

R_e = Radius of equivalent sandwich cylinder, inches [see Equation (5.4-3)].

t_1 and t_2 = Thicknesses of the facings, inches. (There is no preference as to which facing is denoted by the subscript 1 or 2.)

τ'_{cr} = Critical shear stress for equivalent sandwich cylinder when subjected to torsion, psi. (It should be noted that this value is not equal to the critical shear stress of the conical sandwich construction.)

The radius R_e is computed from

$$R_e = \left(R_{small}\cos\alpha\right)\left\{1 + \left[\frac{1}{2}\left(1 + \frac{R_{large}}{R_{small}}\right)\right]^{\frac{1}{2}} - \left[\frac{1}{2}\left(1 + \frac{R_{large}}{R_{small}}\right)\right]^{-\frac{1}{2}}\right\} \qquad (5.4\text{-}3)$$

where R_{small}, R_{large}, and α are as shown in Figure 5.4-1.

The stress τ'_{cr} may be computed from the equations and curves of Section 4.5.2 provided that

a.   The values t_1, t_2, t_c, and d are measured as shown in Figure 5.4-1.

b.   The radius R is replaced by the effective radius R_e.

c.   The length L is taken equal to the axial length of the cone (see Figure 5.4-1).

5-16
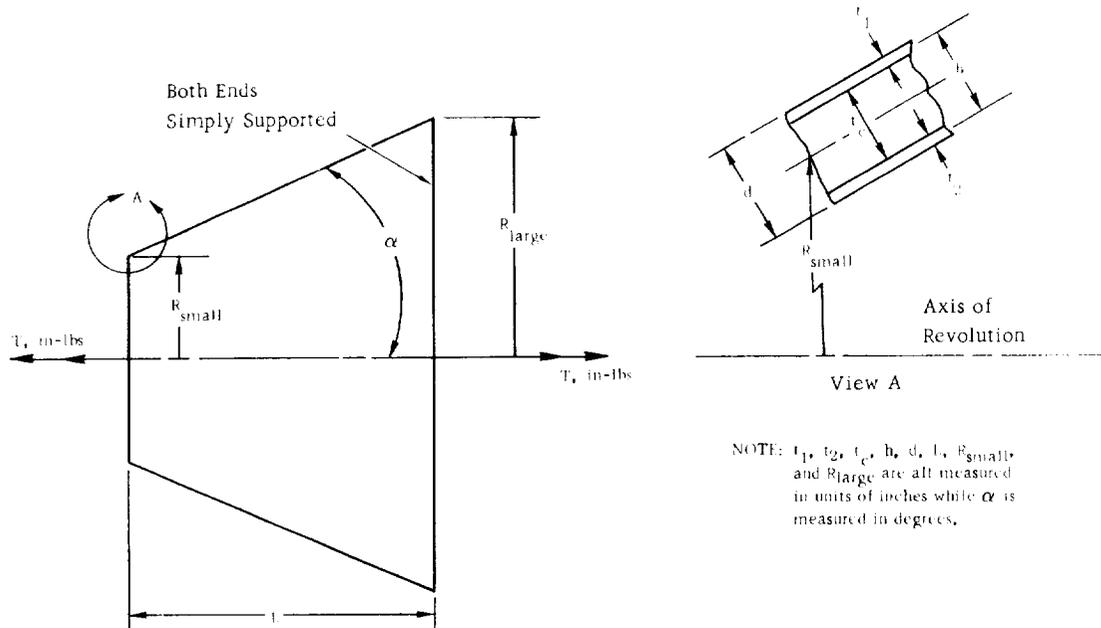
Figure 5.4-1. Truncated Sandwich Cone Subjected to Torsion

In a truncated cone which is subjected to torsion, the maximum shear stress will occur at the small end. Hence, for sandwich constructions of this type, the critical stress value is associated with that same location. One can therefore write

$$\tau_{cr} = \frac{T_{cr}}{2\pi R_{small}^2 (t_1 + t_2)}$$

(5.4-4)

where

τ_{cr} = Critical shear stress for truncated sandwich cone when subjected to torsion, psi.

It is recommended that the approach specified here be applied only to cases where $\alpha \leq 30$ degrees.

Plasticity reduction factors should always be based on the stress at the small end of the cone (see Section 9).

5.5 TRANSVERSE SHEAR

5.5.1 Basic Principles

The case considered here is that of a truncated sandwich cone which is subjected only to transverse shear forces as shown in Figure 5.5-1. Note that all transverse sections, such as A-A, are subjected to the same magnitude of shear load.
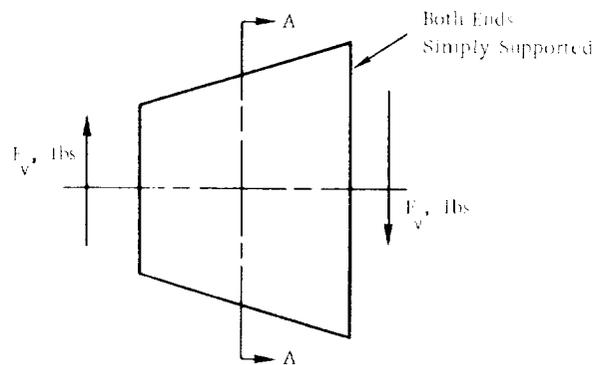
Figure 5.5-1. Truncated Cone Subjected to Transverse Shear

This, of course, is a purely hypothetical loading condition since it does not result in over-all static equilibrium of the structure. To obtain the necessary balance of forces and moments, it is required that an external bending moment also be present. Nevertheless, the hypothetical unbalanced loading system does prove to be of interest since the combined effects of transverse shear and its associated bending are usually analyzed by using an interaction equation. Such a relationship involves both the critical peak meridional stress under a bending moment acting alone and the critical peak shear stress corresponding to the subject artificial loading condition.

It appears that no significant theoretical solutions have been published for sandwich cones subjected to transverse shear. Therefore, for the purposes of this handbook,

the concept used for sandwich cylinders (see Section 4.6) will also be adopted here as a practical expediency. As noted in Section 4.6, the results from a series of tests [5-4 and 5-5] on isotropic (non-sandwich), circular and elliptic cylinders led to the conclusion [5-6] that

$$\frac{\left[\begin{array}{l}\text{Lower-Bound } \tau_{cr} \text{ Test Values for} \\ \text{Transverse Shear Loading}\end{array}\right]}{\left[\begin{array}{l}\text{Small-Deflection Theoretical} \\ \tau_{cr} \text{ Values for Torsional Loading}\end{array}\right]} \approx 1.25 \qquad (5.5-1)$$

To properly understand this ratio, it should be observed that for torsional loading of a thin-walled circular cross section the shear stress τ_{cr} is uniformly distributed around the circumference. On the other hand, under transverse shear loading, the shear stress is nonuniform and the value τ_{cr} then corresponds to the peak intensity which occurs at the neutral axis.

For the lack of a better approach, it was recommended in Section 4.6 that Equation (5.5-1) be used for the design and analysis of sandwich cylinders that are subjected to transverse shear forces. For the same reason, it is recommended here that Equation (5.5-1) also be used for truncated sandwich cones. In the latter case, the required small-deflection theoretical τ_{cr} values for torsional loading should be obtained as specified in Section 5.4, with the exception that γ_s must now be taken equal to unity. No sandwich test data are available to substantiate the reliability of this practice. Until such data do become available, one can only regard this procedure as a "best-available" approach.

5.5.2 Design Equations and Curves

For simply supported, right-circular, truncated sandwich cones subjected to transverse shear forces, the critical peak shear stress may be computed from the equation

$$\tau_{cr} = 1.25 \; (\tau_{cr})_{\substack{\text{Torsion} \\ \gamma_s = 1.0}} \tag{5.5-2}$$

where

$(\tau_{cr})_{\substack{\text{Torsion} \\ \gamma_s = 1.0}}$ = The critical torsional shear stress obtained by substituting $\gamma_s = 1.0$ throughout the methods cited in Section 5.4, psi.

In a truncated cone which is subjected to transverse shear, the maximum shear stress will occur at the small end. Hence, the critical stress value is associated with that location.

Plasticity reduction factors should always be based on the stress at the small end of the cone (see Section 9).

When the behavior is elastic, the critical transverse shear force $(F_v)_{cr}$ can be computed from the following:

$$(F_v)_{cr} = \pi \, R_{small} \, (t_1 + t_2) \, \tau_{cr} \tag{5.5-3}$$

To compute $(F_v)_{cr}$ when the behavior is inelastic, one must resort to numerical integration techniques.

5.6 COMBINED LOADING CONDITIONS

5.6.1 General

For structural members subjected to combined loads, it is customary to represent critical loading conditions by means of so-called interaction curves. Figure 5.6-1 shows the graphic format usually used for this purpose. The quantity R_i is the ratio of an applied load or stress to the critical value for that type of loading when acting alone. The quantity R_j is similarly defined for a second type of loading. Curves of this form give a very clear picture as to the structural integrity of particular configurations. All computed points which fall within the area bounded by the interaction curve and the coordinate axes correspond to stable structures. All points lying on or outside of the interaction curve indicate that buckling will occur. Furthermore, as shown in Figure 5.6-1, a measure of the margin of safety is given by the ratio of distances from the actual loading point to the curve and to the origin. For example, assume that a particular structure is subjected to the combined loading condition corresponding to point B of Figure 5.6-1.
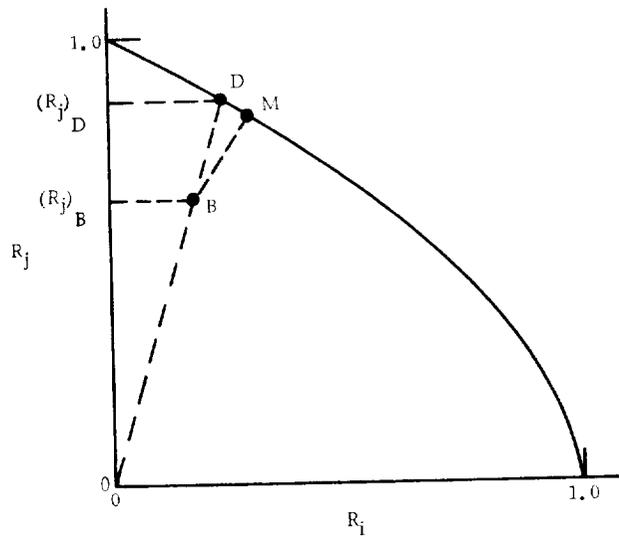
Figure 5.6-1. Sample Interaction Curve

5-21

Then, for proportional increases in R_i and R_j, the margin of safety (MS) can be computed from the following:

$$MS = \frac{(R_j)_D}{(R_j)_B} - 1 \qquad (5.6\text{-}1)$$

As an alternative procedure, one might choose to compute a minimum margin of safety which is based on the assumption that loading beyond point B follows the path BM. Point M is located in such a position that BM is the shortest line that can be drawn between point B and the interaction curve. The minimum margin of safety can then be calculated as follows:

$$\text{Minimum MS} = \frac{OB + BM}{OB} - 1 \qquad (5.6\text{-}2)$$

5-22

5.6.2 Axial Compression Plus Bending

5.6.2.1 Basic Principles

In Section 4.7.2 this loading condition is treated for the case of circular sandwich cylinders. For such configurations, it was concluded that one may use the following interaction relationship:

$$R_c + R_b = 1 \qquad (5.6-3)$$

where

$$R_c = \frac{\sigma_c}{\gamma_c \, (\bar{\sigma}_c)_{CL}} \qquad (5.6-4)$$

$$R_b = \frac{\sigma_b}{\gamma_b \, (\bar{\sigma}_c)_{CL}} \qquad (5.6-5)$$

and

σ_c = Uniform compressive stress due solely to applied axial load, psi.

σ_b = Peak compressive stress due solely to applied bending moment, psi.

$(\bar{\sigma}_c)_{CL}$ = Classical theoretical value for critical uniform compressive stress under an axial load acting alone, psi.

γ_c = Knock-down factor given by Figure 4.2-8, dimensionless.

γ_b = Knock-down factor given by Figure 4.3-2, dimensionless.

In this handbook it is proposed that for truncated sandwich cones the cases of pure bending and of axial load acting alone both be treated by means of an equivalent-cylinder concept (see Sections 5.1 and 5.2). For both types of loading, the radius of the equivalent cylinder is taken equal to the finite principal radius of curvature at the small end of the cone. It should be noted that the maximum stresses from both

bending and axial compression occur at this same location. In view of these several

considerations, it is assumed here that Equations (5.6-3) through (5.6-5) can be

applied to truncated sandwich cones if

a. σ_c and σ_b are both computed for the meridional direction and at the small
     end of the cone, and

b.   the values for γ_c, and γ_b, and $(\bar{\sigma}_c)_{CL}$ are those which apply to the equivalent
     sandwich cylinder described in Sections 5.1 and 5.2. (It is important to
     keep in mind that γ_c must be taken equal to 1.0 when computing the value
     $(\bar{\sigma}_c)_{CL}$.)

Since no test data have been published for truncated, sandwich cones subjected to axial

compression plus bending, the recommended approach has not been experimentally

verified and can only be regarded as a "best-available" method.

5.6.2.2 Design Equations and Curves

For simply supported, truncated, right-circular sandwich cones subjected to axial compression plus bending, the following interaction equation may be employed:

$$R_c + R_b = 1 \qquad (5.6-6)$$

where

$$R_c = \frac{\sigma_c}{\gamma_c \, (\bar{\sigma}_c)_{CL}} \qquad (5.6-7)$$

$$R_b = \frac{\sigma_b}{\gamma_b \, (\bar{\sigma}_c)_{CL}} \qquad (5.6-8)$$

Equation (5.6-6) may be used for cones of any length. A plot of this equation is given in Figure 5.6-2.

The quantity σ_c is the uniform meridional compressive stress, at the small end of the cone, due to the axial force acting alone.

The quantity σ_b is the peak meridional compressive stress, at the small end of the cone, due to the bending moment acting alone.

The quantities γ_c, γ_b, and $(\bar{\sigma}_c)_{CL}$ are those which apply to the equivalent sandwich cylinder described in Sections 5.1 and 5.2.

In Equations (5.6-7) and (5.6-8), the knock-down factors γ_c and γ_b are those obtained from Figures 4.2-8 and 4.3-2, respectively.

The quantity $(\bar{\sigma}_c)_{CL}$ is simply the result obtained by using $\gamma_c = 1.0$ in the method of Section 4.2.2.

Plasticity considerations should be handled as specified in Section 9.2 except, that in

this case, one may use

$$\text{(a)} \quad \eta = \left[\frac{1-\nu_e^{\,2}}{1-\nu^2}\right] \frac{E_t}{E_f} \quad \text{for short cones, and}$$

$$\text{(b)} \quad \eta = \left[\frac{1-\nu_e^{\,2}}{1-\nu^2}\right]^{\frac{1}{2}} \frac{\sqrt{E_t E_s}}{E_f} \quad \text{for moderate-length through long cones.}$$

The plasticity reduction factor η should always be based on the peak compressive stress

at the small end of the cone.
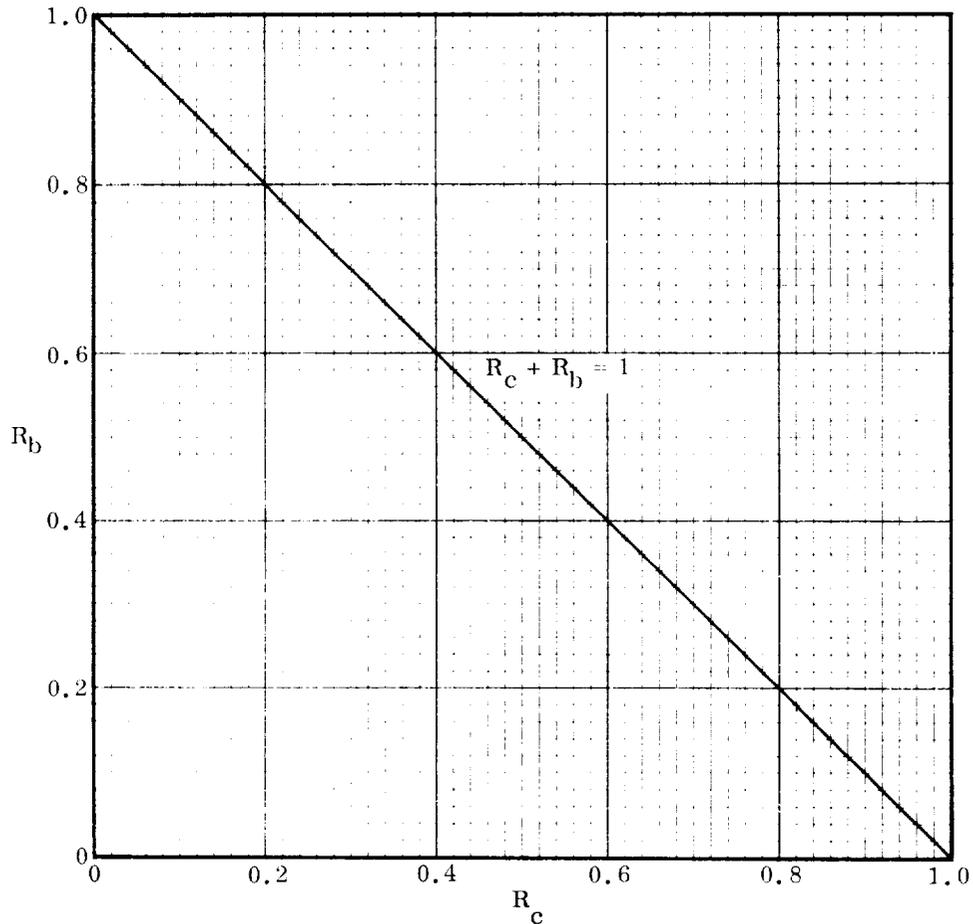
Figure 5.6-2. Design Interaction Curve for Truncated Sandwich Cones
Subjected to Axial Compression Plus Bending

5.6.3 Uniform External Hydrostatic Pressure

5.6.3.1 Basic Principles

The loading condition considered here is depicted in Figure 5.6-3. As shown, the cone

is subjected to a uniform external pressure over the lateral surface and both end closures.
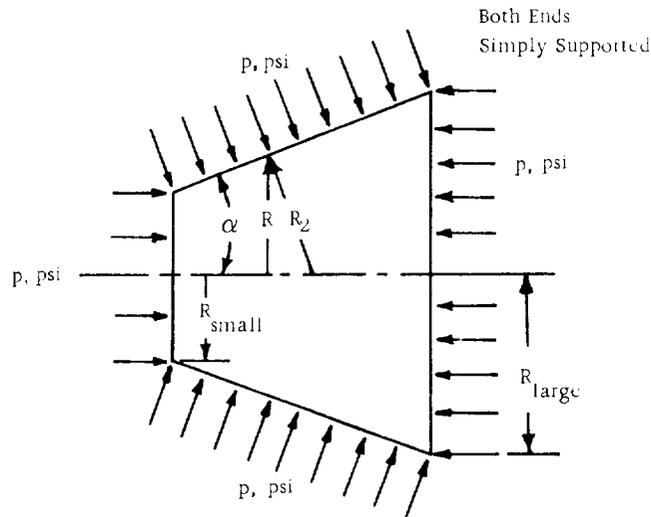
Figure 5.6-3. Truncated Cone Subjected to Uniform
External Hydrostatic Pressure

This results in principal membrane stresses which may be computed as follows when

the core has a relatively high extensional stiffness in the direction normal to the

facings:

$$\sigma_H = \frac{p\,R_2}{(t_1 + t_2)} \qquad (5.6\text{-}9)$$

$$\sigma_M = \frac{p\,R_2}{2\,(t_1 + t_2)} \qquad (5.6\text{-}10)$$

where

$$R_2 = \frac{R}{\cos\alpha} \qquad (5.6\text{-}11)$$

and

σ_H = Hoop membrane stress, psi.

σ_M = Meridional membrane stress, psi.

p = Uniform external hydrostatic pressure, psi.

R_2 = Finite principal radius of curvature of middle surface, inches.

t_1 and t_2 = Thicknesses of the facings, inches. (There is no preference as to which facing is denoted by the subscripts 1 or 2.)

R = Radius of middle surface measured perpendicular to the axis of revolution, inches.

α = Vertex half-angle of cone, degrees.

Since the radii R and R_2 vary with the axial location, the stresses σ_H and σ_M are non-uniform over the conical surface. The maximum values for each of these quantities occur at the large end of the cone.

It appears that no significant theoretical solutions have been published for the stability of truncated sandwich cones which are subjected to uniform external hydrostatic pressure. Therefore, for the purposes of this handbook, the equivalent-cylinder approach of Seide, et al. [5-1] has been adopted as a practical expediency. Based on a large array of test data from thin-walled, isotropic (non-sandwich), cylinders and truncated cones, Seide, et al. concluded that the critical hydrostatic pressures for such cones can be taken equal to the values for equivalent circular cylinders which satisfy the following conditions:

a. The wall thickness of the equivalent cylinder is equal to that of the cone. In the case of sandwich constructions, the logical extension of this condition is that the equivalent cylinder have the same facing and core thicknesses as are found in the cone.

5-28

b. The length of the equivalent cylinder is equal to the slant length of the cone.

c. The radius of the equivalent cylinder is equal to the average finite principal radius of curvature of the cone. That is,

$$R_c = \frac{R_{small} + R_{large}}{2 \cos \alpha} \qquad (5.6\text{-}12)$$

where

R_c = Radius of middle surface for equivalent cylinder, inches.

R_{small} = Radius of middle surface at small end of cone (measured perpendicular to the axis of revolution), inches.

R_{large} = Radius of middle surface at large end of cone (measured perpendicular to the axis of revolution), inches.

The critical hydrostatic pressure for the equivalent cylinder can be obtained by using the equations and curves of Section 4.7.3.

The only available experimental results for conical sandwich shells under uniform external hydrostatic pressure are the data from two tests conducted by North American Rockwell, Corp. [5-7 and 5-8] in conjunction with the Navajo missile program. To assist in the preparation of this handbook, an analysis was made of the result published in Reference 5-7. The other specimen was not studied since it was stressed too deeply into the plastic region. The specimen of Reference 5-7 was also inelastic but the stresses in this instance were low enough to permit reliable computations. Using the approach of the present section in conjunction with the plasticity reduction criteria of Section 9, the design critical pressure was computed to be 36.4 psi. This is in satis-factory agreement with the experimental value of 43.6 psi.

The foregoing substantiates, to a very small degree, the reliability of the equivalent-cylinder concept recommended here. However, in view of the lack of a sufficient number of test results, this approach can presently be considered as only a "best-available" method.

5.6.3.2 Design Equations and Curves

For a simply supported, truncated, right-circular sandwich cone subjected to uniform, external, hydrostatic pressure, the critical pressure may be taken equal to that for an equivalent sandwich cylinder for which

a. The values t_1, t_2, t_c, and h are measured as shown in Figure 5.6-4.

b. The length is taken equal to the slant length L_c of the cone as shown in Figure 5.6-4.

c. The radius is denoted R_e and is computed from the formula

$$R_e = \frac{R_{small} + R_{large}}{2 \cos \alpha} \qquad (5.6-13)$$

where R_{small}, R_{large}, and α are as shown in Figure 5.6-4.

VIEW A

BOTH ENDS
SIMPLY SUPPORTED

NOTE: t_1, t_2, t_c, h, R, R_2, R_{small}, R_{large}, and L_e are all measured in units of inches while α is measured in degrees.
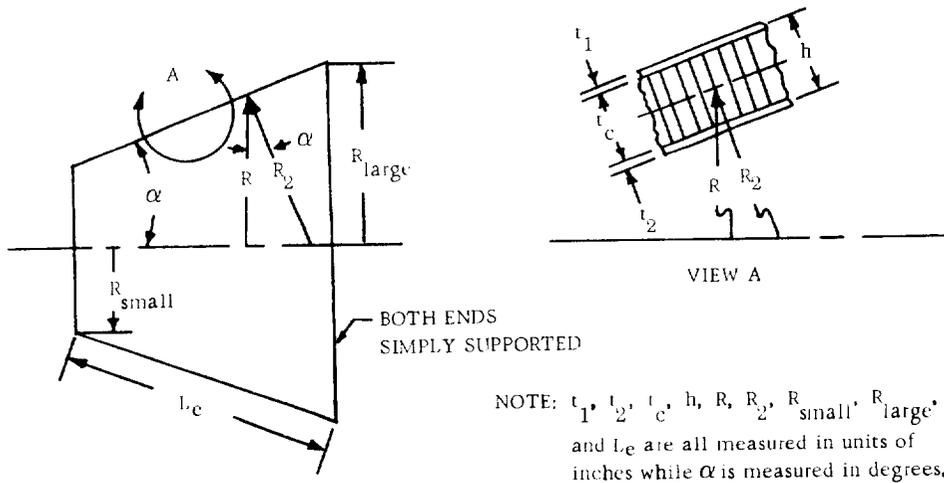
Figure 5.6-4. Truncated Sandwich Cone

The critical hydrostatic pressure for the equivalent sandwich cylinder can be obtained from the equations and curves of Section 4.7.3 if the ratios R_c and R_p are now defined as follows:

$$R_c = \frac{p}{\gamma_c \, (\bar{p}_x)_{CL}} \qquad\qquad (5.6\text{-}14)$$

$$R_p = \frac{p}{\gamma_p \, (\bar{p}_y)_{CL}} \qquad\qquad (5.6\text{-}15)$$

where

p = Uniform, external, hydrostatic pressure applied to lateral surfaces and end closures of the equivalent sandwich cylinder, psi.

In Equations (5.6-14) and (5.6-15), the knock-down factor γ_c is that obtained from Figure 4.2-8, while γ_p may be taken equal to 0.90.

It should be noted that

$$(\bar{\sigma}_x)_{CL} = \frac{(\bar{p}_x)_{CL} \, R_c}{2 \, (t_1 + t_2)} \qquad\qquad (5.6\text{-}16)$$

or

$$(\bar{p}_x)_{CL} = \frac{2 \, (\bar{\sigma}_x)_{CL} \, (t_1 + t_2)}{R_e} \qquad\qquad (5.6\text{-}17)$$

where

$(\bar{\sigma}_x)_{CL}$ = Classical theoretical value for critical uniform axial compressive stress when acting alone on the equivalent sandwich cylinder. This value can be obtained by using $\gamma_c = 1.0$ in the equations and curves of Section 4.2.

The value $(\bar{p}_y)_{CL}$ can be obtained by using $\gamma_p = 1.0$ in the equations and curves of Section 4.4.

Plasticity considerations should be handled as specified in Section 9.2. The plasticity reduction factor η should always be based on the principal membrane stresses at the large end of the cone where,

$$\sigma_H = \frac{p \, R_{large}}{(t_1 + t_2) \, (\cos \alpha)} \qquad (5.6\text{-}18)$$

$$\sigma_M = \frac{p \, R_{large}}{2 \, (t_1 + t_2) \, (\cos \alpha)} \qquad (5.6\text{-}19)$$

It is recommended that the approach specified here be applied only to cases where $\alpha \leq 30$ degrees.

5.6.4 Axial Compression Plus Torsion

5.6.4.1 Basic Principles

The loading condition considered here is depicted in Figure 5.6-5. The axial load P

can originate from any source including external pressures which are distributed

uniformly over the end closures.
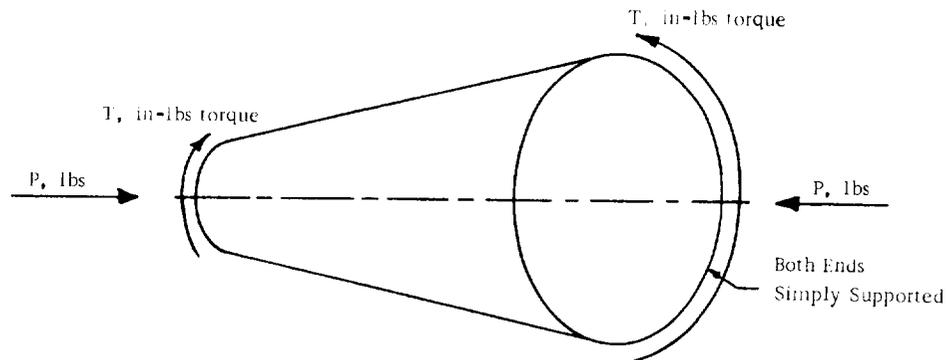
Figure 5.6-5. Truncated Cone Subjected to Axial
Compression Plus Torsion

It appears that no significant theoretical solutions have been published for the stability

of truncated sandwich cones under this combination of loads. However, MacCalden

and Matthiesen [5-9] have arrived at certain conclusions for non-sandwich shells under

such loading and, for the purposes of this handbook, these results provide the basis for

an expedient engineering approach to the case of conical sandwich constructions. Based

on a large array of test data from Mylar specimens, MacCalden and Matthiesen con-

cluded that the following interaction relationship could be applied to thin-walled, iso-

tropic (non-sandwich), truncated cones:

$$R_c + R_s^2 = 1 \qquad\qquad (5.6\text{-}20)$$

where

$$R_c = \frac{P}{(\bar{P}_{cr})_{Empirical}} \qquad (5.6\text{-}21)$$

$$R_s = \frac{T}{(\bar{T}_{cr})_{Empirical}} \qquad (5.6\text{-}22)$$

and

$(\bar{P}_{cr})_{Empirical}$ = Empirical lower-bound value for the critical axial load when acting alone, lbs.

$(\bar{T}_{cr})_{Empirical}$ = Empirical lower-bound value for the critical torque when acting alone, in-lbs.

This result is identical to that given in Reference 5-10 for thin-walled, isotropic (non-sandwich) cylinders subjected to axial compression plus torsion. One might, therefore, conjecture that in the case of sandwich constructions the interaction curves for truncated cones under the subject loading condition are of the same shape as those presented in Section 4.7.4.2 for circular cylinders. The design equations and curves recommended here are based on this premise. That is, one might choose to view the formula,

$$R_c + R_s^2 = 1 \qquad (5.6\text{-}23)$$

as a comprehensive interaction equation for truncated cones of both isotropic (non-sandwich) and sandwich construction. However, it is important to note here that MacCalden and Matthiesen observed that the presence of even a very small axial load made the torsionally-loaded conical shell much more sensitive to imperfections than was the case when no axial load was applied at all. They, therefore, recommended that whenever R_c is non-zero, the same knock-down factor be employed in computing

$(\bar{T}_{cr})_{\text{Empirical}}$ as is used in the calculation of $(\bar{P}_{cr})_{\text{Empirical}}$. It was further specified that this single knock-down factor should be taken equal to that which applies for the case of axial compression acting alone. The same practice is adopted here.

Caution should be exercised in implementing the foregoing recommendations, partially because only the extremes of transverse shear rigidity of the core have been considered (see Section 4.7.4.1). In addition, although the interaction relationship for the subject loading condition should probably be dependent upon a length parameter, no investigations were made to establish the sandwich lengths over which Equation (5.6-23) is a reasonable representation of the actual behavior. Furthermore, no test data have been obtained for sandwich cones subjected to axial compression plus torsion. Therefore, the general validity of Equation (5.6-23) has not been experimentally verified and can only be regarded as a "best-available" approach.

5.6.4.2 Design Equations and Curves

For simply supported, truncated, right-circular sandwich cones subjected to axial compression plus torsion, one might choose to employ the interaction formula,

$$R_c + R_s^2 = 1 \qquad (5.6\text{-}24)$$

which is plotted in Figure 5.6-6 and where,

$$R_c = \frac{P}{(\bar{P}_{cr})_{Empirical}} \qquad (5.6\text{-}25)$$

$$R_s = \frac{T}{\left(\frac{\gamma_c}{0.80}\right)(\bar{T}_{cr})_{Empirical}} \qquad (5.6\text{-}26)$$

P = Applied axial load, lbs.

T = Applied torque, in-lbs.

$(\bar{P}_{cr})_{Empirical}$ = Lower-bound value for the critical axial load when acting alone. This value can be obtained by using the equations and curves of Section 5.1.2, lbs.

$(\bar{T}_{cr})_{Empirical}$ = Lower-bound value for the critical torque when acting alone. This value can be obtained by using the equations and curves of Section 5.4.2, in-lbs.

γ_c = The knock-down factor obtained from Figure 4.2-8 (dimensionless). For the purposes of the present case, the quantity R (see Figure 4.2-8) must be set equal to the equivalent radius R_e which is computed as follows:

$$R_e = \frac{R_{small}}{\cos \alpha} \qquad (5.6\text{-}27)$$

R_{small} = Radius at small end of cone, inches (measured perpendicular to the axis of revolution).

α = Vertex half-angle of cone, degrees.

5-37
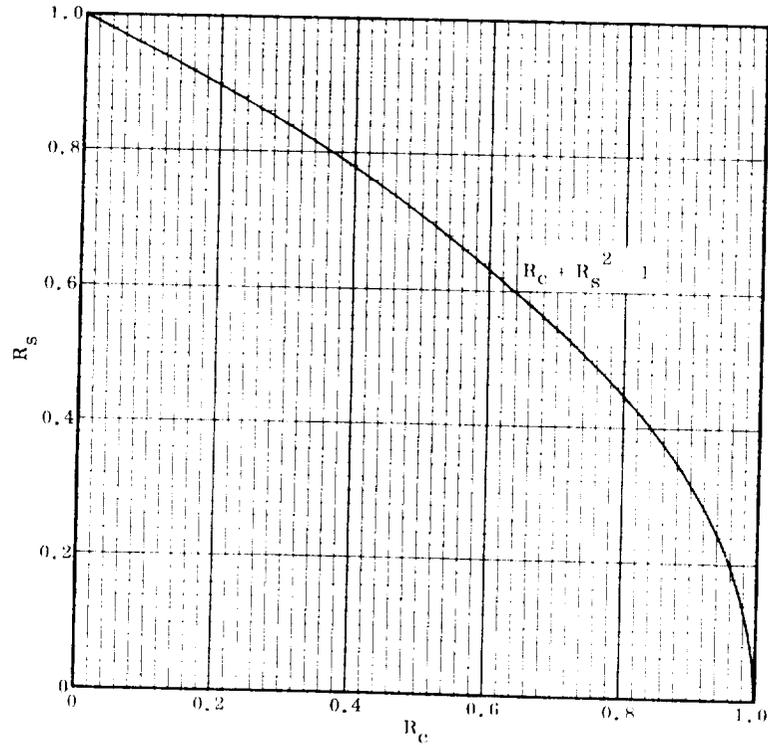
Figure 5.6-6. Conditional Interaction Curve for Truncated Sandwich Cones
Subjected to Axial Compression Plus Torsion

The factor $\left(\dfrac{\gamma_c}{0.80}\right)$ should be introduced into the demoninator of the ratio R_s only when

R_c is non-zero. For the special case where no axial load is present $(R_c = 0)$, R_s

should be taken equal to $T \div (\bar{T}_{cr})_{\text{Empirical}}$.

Attention is drawn to the fact that in Section 5.6.4.1, several factors are cited which

shed considerable doubt upon the reliability of results obtained from the indiscriminate

use of Equation (5.6-24) and Figure 5.6-6. In view of these uncertainties, one might

often choose to employ the straight-line interaction formula,

$$R_c + R_s = 1 \qquad\qquad (5.6\text{-}28)$$

which is plotted in Figure 5.6-7. This relationship can be used with confidence for

any length of cone and for any region of transverse shear rigidity of the core, since

experience has shown that the linear interaction formula is never unconservative for

shell stability problems. However, in many cases it will, of course, introduce

excessive conservatism.

Plasticity considerations should be handled as specified in Section 9.2. The plasticity

reduction factor η should always be based on the stresses at the small end of the cone.
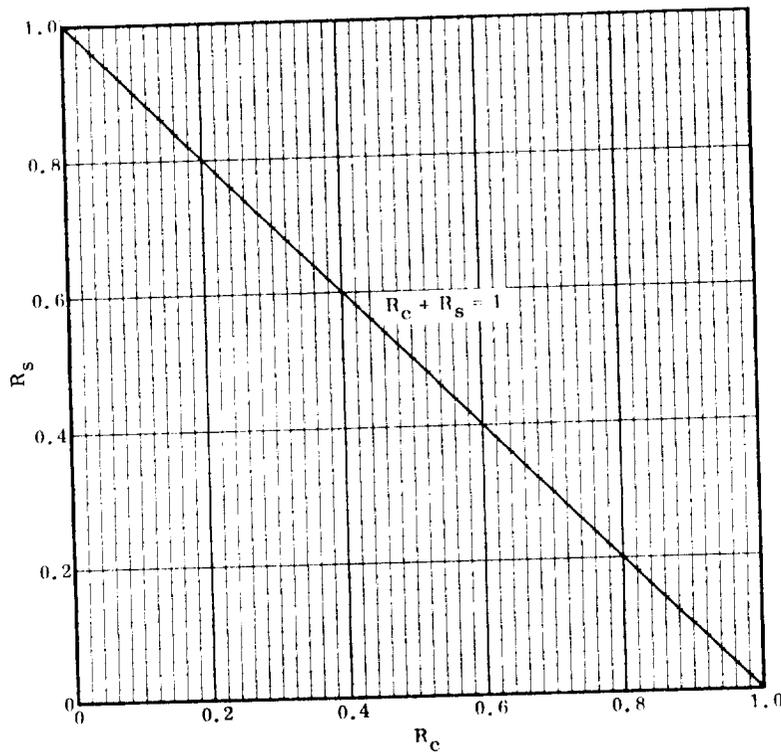
Figure 5.6-7. Conservative Interaction Curve for Truncated Sandwich Cones Subjected to Axial Compression Plus Torsion

5.6.5 Other Loading Combinations

5.6.5.1 Basic Principles

In Section 5.6.4, the combined loading condition of axial compression plus torsion is

treated. The interaction relationships presented there can be used for an additional

loading combination by recognizing that at any given axial location on the cone the peak meridional stress due to an applied bending moment can be converted into an equivalent uniform meridional stress. With this in mind, the design equations and curves of Section 5.6.4.2 can be used for the combination of axial compression plus bending plus torsion which is depicted in Figure 5.6-8.
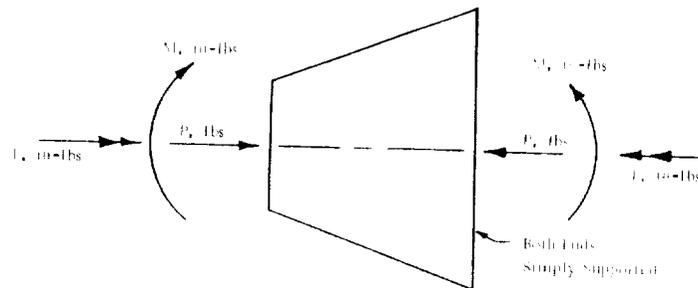
Figure 5.6-8. Truncated Cone Subjected to Axial Compression Plus Bending Plus Torsion

To accomplish this it is simply required that the quantity R_c be redefined as follows:

$$R_c = \frac{P'}{(\bar{P}_{cr})_{Empirical}}$$

(5.6-29)

where

$$P' = P + \left(\frac{\gamma_c}{\gamma_b}\right) \left(\frac{2M}{R_{small}}\right)$$

(5.6-30)

and

P - Applied axial load, lbs.

M - Applied bending moment, in-lbs.

γ_c - Axial compression knock-down factor from Figure 4.2-8, dimensionless.

Note: For the purposes of the present case, the quantity R (see Figure 4.2-8) must be set equal to the equivalent radius R_e which is computed as follows:

5-40

$$R_e = \frac{R_{small}}{\cos\alpha} \qquad (5.6\text{-}31)$$

γ_b = Bending knock-down factor from Figure 4.3-2, dimensionless.

Note: For the purposes of the present case, the quantity R (see Figure 4.3-2) must be set equal to the equivalent radius R_e which is computed as follows:

$$R_e = \frac{R_{small}}{\cos\alpha} \qquad (5.6\text{-}32)$$

R_{small} = Radius at small end of cone (measured perpendicular to the axis of revolution), inches.

α = Vertex half-angle of cone, degrees.

The foregoing formula for P' is based on the principles cited in Section 5.2

Since no sandwich test data are available to substantiate the recommendations made here, they can only be regarded as a "best-available" criterion.

5.6.5.2 Design Equations and Curves

For simply supported, truncated, right-circular sandwich cones subjected to the loading condition depicted in Figure 5.6-8, one may use the design equations and curves of Section 5.6.4.2, except that the quantity R_c must now be defined as follows:

$$R_c = \frac{P'}{(\overline{P}_{cr})_{Empirical}} \qquad (5.6\text{-}33)$$

where

$$P' = P + \left(\frac{\gamma_c}{\gamma_b}\right)\left(\frac{2M}{R_{small}}\right) \qquad (5.6\text{-}34)$$

Table 5-1. Summary of Design Equations for Instability of Truncated Circular Cones

NOTATION: σ = Facing normal stress (psi), η = Plasticity reduction factor (dimensionless), E = Young's modulus (psi), h = Distance between middle surfaces of facings (inches), d = Total depth of sandwich (inches), R_{small} = Radius to middle surface at the small end of truncated conical shell measured perpendicular to the axis of revolution (inches), R_{large} = Radius to middle surface at the large end of truncated conical shell measured perpendicular to the axis of revolution (inches), R_e = Effective middle surface radius (inches), R_2 = Middle surface radius of curvature in the plane perpendicular to the meridian (inches), t = Thickness (inches), p = External pressure (psi), ν = Poisson's ratio (dimensionless), G = Transverse shear modulus of core (psi), τ = Facing shear stress (psi), γ = Knock-down factor (dimensionless), α = Vertex half-angle of cone (degrees).

SUBSCRIPTS: 1, 2 denote facing 1 or 2; in addition, as applicable, 2 denotes a specific principal radius of curvature; c denotes core or compression as applicable; f denotes facing; e denotes elastic property or effective value as applicable; cr denotes critical value for buckling; xz denotes the plane perpendicular to the facings and oriented in the meridional direction; yz denotes the plane perpendicular to the facings and oriented perpendicular to a meridian.

Loading Condition	Design Formulas for General Instability
1. AXIAL COMPRESSION MODE A: Length L_e is greater than the length of a single axial half-wave. That is, for cases where $\hat{g} = \dfrac{G_{xy}}{G_{yz}} = 1,$ (1) and $V_c < 2$, this mode is applicable to cones for which $\left(\dfrac{L_e}{R_c}\right) \ge 1.57 \left[C_o(2 - V_c)\right]^{\frac{1}{4}}.$ (2) and when $V_c \ge 2$, this mode is applicable for all values of L_e.	(a) $\sigma_{cr,c} = \gamma_c K_c \, \sigma_{o,c}$ where K_c may be obtained from Figure 4.2-7. $\sigma_{cr,c}$ occurs at small end of cone. When $V_c \ge 2.0$, the value for γ_c may be obtained from Figure 4.2-8 for $\dfrac{R}{o} = \dfrac{R_c}{o}$ where $R_c = \dfrac{R_{small}}{\cos\alpha}.$ When $V_c < 2.0$, use $\gamma_c = 1.0.$ $\sigma_{o,c} = \eta\, E_{c,c}\, C_o$ $C_o = \dfrac{h}{R_c} \cdot \dfrac{2\sqrt{(E_{1c})(E_{2c})}}{\sqrt{1 - \nu_e^2}\sqrt{(E_{1c}) + (E_{2c})}}$ $\sigma_{crimp} = \dfrac{h^2 G_{xz}}{\left[t - \left(\dfrac{E_1}{E_2}\right)t\right]_c}$ $\sigma_{crimp} = \dfrac{\sigma_{o,c}}{\sqrt{t - \left(\dfrac{E_1}{E_2}\right)t}\,}_c$ $V_c = V_{c,f} = \dfrac{\sigma_{o,c}}{\sigma_{crimp,c}}$ $(V_c$ are used in obtaining K_c from Figure 4.2-7)

5-42

$$P_{cr} = 2\pi R_e (\sigma_{cr_1} t_1 + \sigma_{cr_2} t_2) \cos^2 \alpha$$

For cases where the two facings are not made of the same material, the foregoing equations are valid only when the behavior is elastic. Application to inelastic cases can only be made when both facings are made of the same material.

Use $\eta = 1.0$ for elastic cases. Refer to Section 9 for inelastic cases. Plasticity reduction factor should always be based on stress at small end of the cone.

(b) In the special case where $t_1 = t_2 = t_f$ and both facings are made of the same material, $\sigma_{cr} = \gamma_c K_c \sigma_o$ where K_c may be obtained from Figure 4.2-7. (σ_{cr} occurs at small end of cone.)

When $V_{c_1} < 2.0$, the value for γ_c may be obtained from Figure 4.2-8 for $\dfrac{R}{\rho} = \dfrac{R_e}{\rho}$ where $R_e = \dfrac{R_{small}}{\cos \alpha}$.

When $V_{c_1} \geq 2.0$, use $\gamma_c = 1.0$.

$$\sigma_o = \frac{(\eta E_f)}{\sqrt{1-\nu_e^2}} \frac{h}{R_e}$$

$$\sigma_{crimp} = \frac{h^2 G_{xz}}{2 t_f t_c}$$

$$V_c = \frac{\sigma_o}{\sigma_{crimp}}$$

(V_c is used in obtaining K_c from Figure 4.2-7)

$$P_{cr} = 4\pi R_e \sigma_{cr} t_f \cos^2 \alpha$$

In this case, V_c is used in place of V_{c_1} in the length criteria given in the LOADING CONDITION column.

Use $\eta = 1.0$ for elastic cases. Refer to Section 9 for inelastic cases. Plasticity reduction factor should always be based on stress at small end of cone.

Both Ends Simply Supported

P, lbs

Axis of Revolution

$R_e = \dfrac{R_{small}}{\cos \alpha}$

σ, psi

τ, psi

VIEW A

Limitation: $\alpha \leq 30°$

Table 5-1. Summary of Design Equations for Instability of Truncated Circular Cones, Cont'd.

Loading Condition	Design Formulas for General Instability
1. AXIAL COMPRESSION, Cont'd. MODE B: (Short Cone) Buckle pattern has only 1 axial half-wave. That is for cases where $$\theta = \frac{G_{xz}}{G_{yz}} = 1,$$ (1) and $V_{c_1} < 2$, this mode is applicable to cones for which $$\left(\frac{L_e}{R_e}\right) < 1.57 \left[C_0 (2-V_{c_1})\right]^{\frac{1}{2}}.$$ (2) and when $V_{c_1} \geq 2$, this mode is never applicable. Limitation: $\alpha \leq 30°$	Restrictions: $\theta = \dfrac{G_{xz}}{G_{yz}} = 1$, $t_3 \leq t_1 \leq 2t_3$, and both facings must be made of the same material. $$\sigma_{cr} = \frac{\gamma_c K_c' \pi^2 D}{(t_1+t_2)L_e^2}$$ where K_c' may be obtained from Figure 4.2-9. (σ_{cr} occurs at small end of cone.) When $K_c' < \left(\dfrac{1}{r_a}\right)$, obtain γ_c from Figure 4.2-8 for $\dfrac{R}{\rho} = \dfrac{R_e}{\rho}$ where $R_e = \dfrac{R_{small}}{\cos\alpha}$. When $K_c' \geq \left(\dfrac{1}{r_a}\right)$, use $\gamma_c = 1.0$. $$Z = \frac{2 L_e^2}{R_e h}\sqrt{1-\nu_e^2} \quad \text{and} \quad r_a = \frac{\pi^2 D}{L_e^2 D_q} \quad \text{where}$$ $$D = \eta \frac{(E_1 t_1)(E_2 t_2) h^2}{(1-\nu_e^2)[(E_1 t_1)+(E_2 t_2)]}$$ $$D_q = \frac{h^2 G_{xz}}{t_c}$$ (Z and r_a are used in obtaining K_c' from Figure 4.2-9.) $$P_{cr} = 2\pi R_e \sigma_{cr}(t_1-t_2)\cos^2\alpha$$ Use $\eta = 1.0$ for elastic cases. Refer to Section 9 for inelastic cases. Plasticity reduction factor should always be based on stress at small end of cone.

2. PURE BENDING

MODE A: Length L_e is greater than the length of a single axial half-wave. That is, for cases where

$$\theta = \frac{G_{xz}}{G_{yz}} = 1,$$

(1) and $V_{c_1} < 2$, this mode is applicable to cones for which

$$\left(\frac{L_e}{R_e}\right) \geq 1.57 \left[C_o (2 - V_{c_1})\right]^{\frac{1}{2}},$$

(2) and when $V_{c_1} \geq 2$, this mode is applicable for all values of L_e.

Both Ends Simply Supported

Axis of Revolution
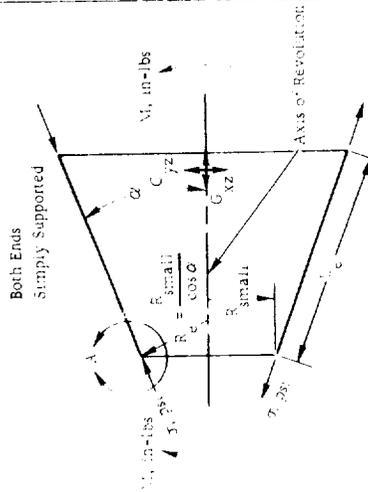
(a) $\sigma_{cr_{1,2}} = \gamma_b K_{c_{1,2}} \sigma_{o_{1,2}}$ where $K_{c_{1,2}}$ may be obtained from Figure 4.2-7. ($\sigma_{cr_{1,2}}$ occurs at small end of cone.)

When $V_{c_1} < 2.0$, the value for γ_b may be obtained from Figure 4.3-2 for $\frac{R}{\rho} = \frac{R_e}{\rho}$ where

$$R_e = \frac{R_{small}}{\cos \alpha}.$$

When $V_{c_1} \geq 2.0$, use $\gamma_b = 1.0$.

$$\sigma_{o_{1,2}} = \eta E_{1,2} C_o$$

$$C_o = \frac{h}{R_e} \frac{2}{\sqrt{1 - \nu_e^2}} \frac{\sqrt{(E_1 t_1)(E_2 t_2)}}{[(E_1 t_1) + (E_2 t_2)]}$$

$$\sigma_{crimp_1} = \frac{h^2 G_{xz}}{\left[t_1 + \left(\frac{E_2}{E_1}\right) t_2\right] t_c}$$

$$\sigma_{crimp_2} = \frac{h^2 G_{xz}}{\left[\left(\frac{E_1}{E_2}\right) t_1 + t_2\right] t_c}$$

$$V_{c_1} = V_{c_2} = \frac{\sigma_{o_{1,2}}}{\sigma_{crimp_{1,2}}}$$

($V_{c_{1,2}}$ are used in obtaining $K_{c_{1,2}}$ from Figure 4.2-7.)

For cases where the two facings are not made of the same material, the foregoing equations are valid only when the behavior is elastic. Application to inelastic cases can only be made when both facings are made of the same material.

For elastic cases, $M_{cr} = \pi R_e^2 (\sigma_{cr_1} t_1 + \sigma_{cr_2} t_2) \cos^3 \alpha$

Use $\eta = 1.0$ for elastic cases. Refer to Section 9 for inelastic cases.

The entire design and analysis, including plasticity reduction factors, should be based on the peak meridional compressive stress at the small end of the cone.

(b) In the special case where $t_1 = t_2 = t_f$ and both facings are made of the same material, $\sigma_{cr} = \gamma_b K_c \sigma_o$ where K_c may be obtained from Figure 4.2-7. (σ_{cr} occurs at small end of cone.)
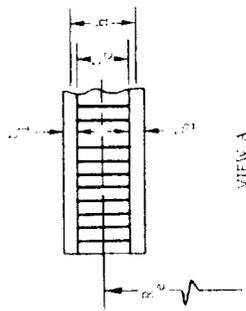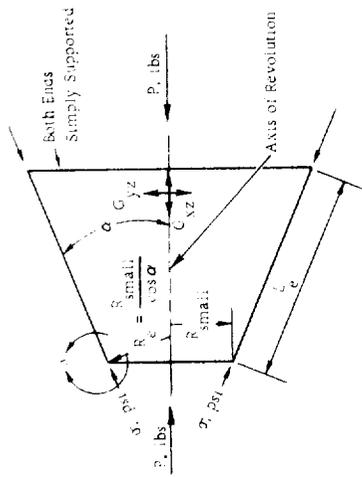
Table 5-1. Summary of Design Equations for Instability of Truncated Circular Cones, Cont'd.

Loading Condition	Design Formulas for General Instability
2. PURE BENDING, Cont'd. VIEW A Limitation: $\alpha \leq 30°$ **MODE B:** (Short Cone) Buckle pattern has only 1 axial half-wave. That is, for cases where $$\theta = \frac{G_{Nz}}{G_{yz}} = 1,$$ (1) and $V_c < 2$ this mode is applicable to cones for which $$\left(\frac{L_e}{R_e}\right)\left(\frac{1}{r_a}\right) < 1.5\left[C_o(2-V_c)\right]^{\frac{1}{2}}.$$	When $V_c > 2.0$, the value for γ_b may be obtained from Figure 4.3-2 for $\frac{R}{\rho} = \frac{R_e}{\rho}$ where $$R_e = \frac{R_{small}}{\cos\alpha}.$$ When $V_c < 2.0$, use $\gamma_b = 1.0$. $$\sigma_o = \frac{\eta E_f}{\sqrt{1-\nu_e^2}} \cdot \frac{h}{R_e}$$ $$\sigma_{crimp} = \frac{h^2 G_{xz}}{2t_f t_c}$$ $$V_c = \frac{\sigma_o}{\sigma_{crimp}}$$ (V_c is used in obtaining κ_c from Figure 4.2-7.) In this case, V_c is used in place of V_c in the length criteria given in the LOADING CONDITION column. For elastic cases, $M_{cr} = 2\pi R_e^2 \sigma_{cr} t_f \cos^3\alpha$ Use $\eta = 1.0$ for elastic cases. Refer to Section 9 for inelastic cases. The entire design and analysis, including plasticity reduction factors, should be based on the peak meridional compressive stress at the small end of the cone. Restrictions: $\theta = \frac{G_{Nz}}{G_{yz}} = 1$, $t_2 = t_1 = 2t_z$, and both facings must be made of the same material. $$\sigma_{cr} = \frac{\gamma_b K_c' \pi^2 D}{(t+t_c)L_e^2}$$ where K_c' may be obtained from Figure 4.2-9. σ_{cr} occurs at small end of cone. When $K_c'\left(\frac{1}{r_a}\right)$ obtain γ_b from Figure 4.3-2 for $\frac{R}{\rho} = \frac{R_c}{\rho}$ where $R_c = \frac{R_{small}}{\cos\alpha}$

(2) and when $V_{c_2} \geq 2$, this mode is never applicable

Limitation: $\alpha \leq 30°$

When $K'_c = \left(\frac{1}{r_a}\right)$, use $\gamma_b = 1.0$.

$$Z = \frac{2 L_e^2}{R_e h} \sqrt{1 - \nu_e^2} \quad \text{and} \quad r_a = \frac{\pi^2 D}{L_e^2 D_q} \text{ where}$$

$$D = \eta \frac{(E_1 t_1)(E_2 t_2) h^2}{(1-\nu_e^2)[(E_1 t_1)+(E_2 t_2)]}$$

$$D_q = \frac{h^2 G_{xz}}{t_c}$$

(Z and r_a are used in obtaining K'_c from Figure 4.2-9.)

For elastic cases, $M_{cr} = \pi R_e^2 \sigma_{cr} (t_1 + t_2) \cos^3\alpha$

Use $\eta = 1.0$ for elastic cases. Refer to Section 9 for inelastic cases.

The entire design and analysis, including plasticity reduction factors, should be based on the peak meridional compressive stress at the small end of the cone.
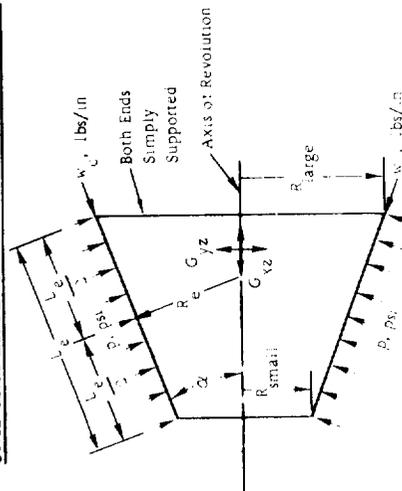
$$p_{cr} = \frac{\gamma_p \eta C_p}{R_e (1-\nu_e^2)} [(E_1 t_1) + (E_2 t_2)]$$

where $\gamma_p = 0.90$ and C_p may be obtained from Figures 4.4-3 through 4.4-5 for appropriate values of $\frac{L}{R} = \frac{L_e}{R_e}$ and

$$\omega^2 = \frac{(E_1 t_1)(E_2 t_2) h^2}{[(E_1 t_1) + (E_2 t_2)]^2 R_e^2}$$

$$V_p = \eta \frac{(E_1 t_1)(E_2 t_2) h}{[(E_1 t_1) + (E_2 t_2)] (1 - \nu_e^2) R_e^2 G_{yz}}$$

For cases where the two facings are not made of the same material, the foregoing equations are valid only when the behavior is elastic. Application to inelastic cases can only be made when both facings are made of the same material.
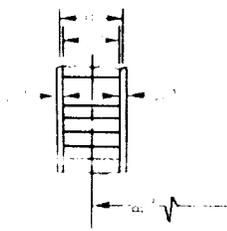
3. **UNIFORM EXTERNAL LATERAL PRESSURE**

$$R_e = \frac{R_{small} + R_{large}}{2 \cos \alpha}$$

Table 5-1. Summary of Design Equations for Instability of Truncated Circular Cones, Cont'd.

Loading Condition	Design Formulas for General Instability
3. UNIFORM EXTERNAL LATERAL PRESSURE, Cont'd. Limitation: $\alpha \leq 30°$	Use $\eta = 1.0$ for elastic cases. Refer to Section 9 for inelastic cases. The plasticity reduction factor should always be based on the stresses at the large end of the cone where $$\text{Hoop Stress} = \frac{p\,R_{large}}{(t_s + t_r)\cos\alpha}$$ $$\text{Meridional Stress} = \frac{p\,R_e}{(t_s + t_r)}\left(1 - \frac{R_{small}}{R_{large}}\right)$$
4. TORSION 	$$T_{cr} = 2\pi R_e^2 (t_s + t_r)\,\tau'_{cr}$$ $$\tau'_{cr} = \gamma_s K_s \eta E_f \frac{d}{R_e}$$ where $\gamma_s = 0.80$ and K_s may be obtained from Figures 4.5-3 through 4.5-5 for appropriate values of $$\phi = \frac{G_{xz}}{G_{yz}}$$ $$Z_s = \frac{L^2}{d R_e}$$ $$\nu_s = \frac{16 t_s t_r t \eta E_f}{15 (t_s + t_r) R_e\, d\, G_{xz}}$$
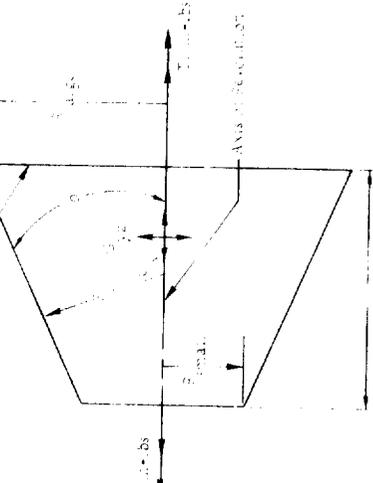
5-48

τ'_{cr} = Critical shear stress for equivalent sandwich cylinder when subjected to torsion, psi. (It should be noted that this value is not equal to the critical shear stress of the conical sandwich construction.)

This criterion is valid only where $t_2 \leq t_1 \leq 2t_2$ and both facings are made of the same material. In addition, the results will be somewhat inaccurate for very long cones (large values of Z_s).

Use $\eta = 1.0$ for elastic cases. Refer to Section 9 for inelastic cases.

The plasticity reduction factor should always be based on the stress at the small end of the cone where

$$\tau = \frac{T}{2\pi\, R^2_{small}\, (t_1 + t_2)}$$

Use the equations of Loading Condition 4 to obtain the appropriate value for T_{cr}.

Then the critical peak shear stress due to the transverse shear force F_V is computed from

$$\tau_{cr} = \frac{1.56\, T_{cr}}{2\pi\, R^2_{small}\, (t_1 + t_2)}$$

This critical stress occurs at the small end of the cone.

This criterion is valid only where $t_2 \leq t_1 \leq 2t_2$ and both facings are made of the same material. In addition, the results will be somewhat inaccurate for very long cones (large values of $Z_s = \dfrac{L^2}{dR_e}$).

For elastic cases, $(F_V)_{cr} = \pi R_{small}\,(t_1 + t_2)\,\tau_{cr}$.

$$R_e = (R_{small}\cos\alpha)\left\{\left[1 + \left[\frac{1}{2}\left(1 + \frac{R_{large}}{R_{small}}\right)\right]^{-\frac{1}{2}} - \left[\frac{1}{2}\left(1 + \frac{R_{large}}{R_{small}}\right)\right]^{-\frac{1}{2}}\right]\right\}^{\frac{1}{2}}$$

Limitation: $\alpha \leq 30°$

---

5. TRANSVERSE SHEAR

Both Ends
Simply Supported

Table 5-1. Summary of Design Equations for Instability of Truncated Circular Cones, Cont'd.

Loading Condition	Design Formulas for General Instability
5. TRANSVERSE SHEAR, Cont'd Limitation: $\alpha \leq 30°$	
6. COMBINED AXIAL COMPRESSION AND BENDING Both Ends Simply Supported $$R_e = \frac{R \text{ small}}{\cos \alpha}$$	Interaction Formula: $R_c - R_b = 1$ (See Figure 5.6-2) where $$R_c = \frac{\sigma_c}{\gamma_c (\overline{\sigma}_c)_{CL}}$$ $$R_b = \frac{\sigma_b}{\gamma_b (\overline{\sigma}_c)_{CL}}$$ σ_c = Uniform meridional compressive stress, at the small end of the cone, due to the axial force acting alone, psi. σ_b = Peak meridional compressive stress, at the small end of the cone, due to the bending moment acting alone, psi. γ_c and γ_b may be obtained as specified for Loading Conditions 1 and 2, respectively, with due consideration as to whether Mode A or Mode B is applicable. $(\overline{\sigma}_c)_{CL}$ is the result obtained by using $\gamma_c = 1.0$ in the equations of Loading Condition 1 (Axial Compression). The equations for the appropriate mode (A or B) should be used as determined by the length L_e.

Plasticity considerations should be handled as specified in Section 9 except that, in this case, one may use

(a) $\eta = \left[\frac{1-\nu_e^2}{1-\nu^2}\right]\frac{E_t}{E_f}$ for short cones (Mode B).

(b) $\eta = \left[\frac{1-\nu_e^2}{1-\nu^2}\right]^{\frac{1}{2}}\sqrt{\frac{E_t E_s}{E_f}}$ for constructions which buckle in Mode A.

The plasticity reduction factor should always be based on the peak stress at the small end of the cone.

For elastic cases, use $\eta = 1.0$.

Use the interaction curves of Figures 4.7-6 through 4.7-15 where

$$V_{xz} = \frac{E_f t_f h}{2(1-.33^2)R_e^2 G_{xz}}$$

$$V_{yz} = \frac{E_f t_f h}{2(1-.33^2)R_e^2 G_{yz}}$$

$$R_p = \frac{p}{\gamma_p (\bar{p}_y)CL}$$

$$R_c = \frac{p}{\gamma_c (\bar{p}_x)CL}$$

$$\gamma_p = 0.90$$

γ_c may be obtained as specified for Loading Condition 1 (Axial Compression) except R_e is now computed as indicated for the present loading condition $\left(R_e = \frac{R_{small} + R_{large}}{2\cos\alpha}\right)$. Due regard should be given as to whether Mode A or Mode B is applicable.

$(\bar{p}_y)CL$ = Classical theoretical value for critical uniform external lateral pressure when acting alone, psi. This value may be computed by setting $\gamma_p = 1.0$ in the equations of Loading Condition 3.

$$(\bar{p}_x)CL = \frac{4\bar{\sigma}_x CL t_f}{R_e}$$
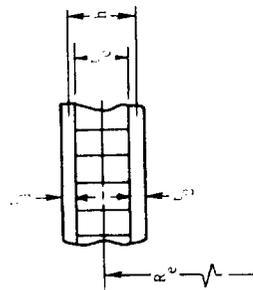
Limitation: $\alpha \le 30°$

7. UNIFORM EXTERNAL HYDROSTATIC PRESSURE

$$R_e = \frac{R_{small} + R_{large}}{2\cos\alpha}$$

Table 5-1. Summary of Design Equations for Instability of Truncated Circular Cones, Cont'd.

Loading Condition	Design Formulas for General Instability
7. UNIFORM EXTERNAL HYDROSTATIC PRESSURE, Cont'd. Limitation: $\alpha \le 30°$	where $(\bar{\sigma}_x)_{CL}$ = Classical theoretical value for critical uniform axial compressive stress when acting alone on the equivalent sandwich cylinder, psi. This value can be obtained by setting $\gamma_c = 1.0$, $R = R_e$, and $L = L_e$ in the equations for Loading Condition 1 (Axial Compression) of Section 4 (General Instability of Circular Cylinders). This criterion is valid only where both facings are made of the same material and are of the same thickness ($t_1 = t_2 = t_f$). Figures 4.7-6 through 4.7-12 are subject to the added restrictions that they can be used only where $$\frac{R_e t_c}{h^2} V_{xz} \le 0.05 \quad \text{and} \quad \frac{R_e t_c}{h^2} V_{yz} \le 0.05$$ Plasticity considerations should be handled as specified in Section 9. The plasticity reduction factor should always be based on the stresses at the large end of the cone where Hoop Stress = $\dfrac{p R_{large}}{(2 t_f)(\cos \alpha)}$ Meridional Stress = $\dfrac{p R_{large}}{(4 t_f)(\cos \alpha)}$
8. COMBINED AXIAL COMPRESSION AND TORSION	For elastic cases, use $\eta = 1.0$ Interaction Formula: $R_c + R_s = 1$ (See Figure 5.6-7) where $R_c = \dfrac{P}{(\bar{P}_{cr})_{Empirical}}$ $R_s = \dfrac{T}{\left(\dfrac{\gamma_c}{0.80}\right)(\bar{T}_{cr})_{Empirical}}$

P = Applied axial load, lbs.

T = Applied Torque, in-lbs.

$(\bar{P}_{cr})$ = Lower-bound value for the critical axial load when acting alone, lbs. This value can be obtained by using the equations for Loading Condition 1 (Axial Compression) with due regard as to whether Mode A or Mode B is applicable.

γ_c may be obtained as specified for Loading Condition 1 (Axial Compression) with due consideration as to whether Mode A or Mode B is applicable.

$(\bar{T}_{cr})_{Empirical}$ = Lower-bound value for the critical torque when acting alone, lbs. This value can be obtained by using the equations for Loading Condition 4 (Torsion).

The factor $\left(\dfrac{\gamma_c}{0.80}\right)$ should be introduced into the denominator of the ratio R_s only when R_c is non-zero. For the special case where no axial load is present ($R_c = 0$), R_s should be taken equal to $T \div (\bar{T}_{cr})_{Empirical}$.

Plasticity considerations should be handled as specified in Section 9.

The plasticity reduction factor should always be based on the stresses at the small end of the cone.

For elastic cases, use $\eta = 1.0$.

Both Ends
Simply Supported

Limitation: $\alpha \leq 30°$

Table 5-1. Summary of Design Equations for Instability of Truncated Circular Cones, Cont'd.

Loading Condition	Design Formulas for General Instability
9. COMBINED AXIAL COMPRESSION PLUS BENDING PLUS TORSION Both Ends Simply Supported Limitation: $\alpha \leq 30°$	Use interaction curves and equations for Loading Condition 8 except substitute P' for P where $$P'_c = P + \left(\frac{\gamma_c}{\gamma_b}\right)\left(\frac{2M}{R_{small}}\right)$$ P = Applied axial load, lbs. M = Applied bending moment, in-lbs. γ_c and γ_b may be obtained as specified for Loading Conditions 1 and 2, respectively, with due consideration as to whether Mode A or Mode B is applicable. For inelastic cases, refer to Section 9.
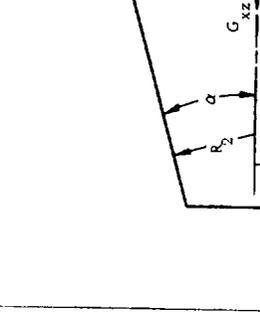
REFERENCES

5-1 Seide, P., Weingarten, V. I., and Morgan, E. J., "Final Report on the Development of Design Criteria for Elastic Stability of Thin Shell Structures", STL-TR-60-0000-19425, 31 December 1960.

5-2 Baker, E. H., "Experimental Investigation of Sandwich Cylinders and Cones Subjected to Axial Compression", AIAA Journal, Volume 6, No. 9, September 1968.

5-3 Seide, P., "On the Buckling of Truncated Conical Shells in Torsion", Journal of Applied Mechanics, June 1962.

5-4 Lundquist, E. E., "Strength Tests of Thin-Walled Duralumin Cylinders in Combined Transverse Shear and Bending", NACA TN 523, 1935.

5-5 Lundquist, E. E. and Burke, W. F., "Strength Tests of Thin-Walled Duralumin Cylinders of Elliptic Section", NACA TN 527, 1935.

5-6 Gerard, G. and Becker, H., "Handbook of Structural Stability, Part III - Buckling of Curved Plates and Shells", NACA TN 3783, August 1957.

5-7 Anonymous, "Test of XSM-64A Booster Fuel Tank Conical Bulkhead No. 3," North American Rockwell, Corp. Report No. AL-2622, 15 September 1957.

5-8 Anonymous, "Test of XSM-64A Booster Fuel Tank Conical Bulkhead No. 4," North American Rockwell, Corp. Report No. AL-2623, 16 September 1957.

5-9 MacCalden, P. B. and Matthiesen, R. B., "Combination Torsion and Axial Compression Tests of Conical Shells", AIAA Journal, February 1967.

5-10 Batdorf, S. B., Stein, M., and Schildcrout, M., "Critical Combinations of Torsion and Direct Axial Stress for Thin-Walled Cylinders," NACA Technical Note 1345, June 1947.

5-11 Baker, E. H., Cappelli, A. P., Kovalevsky, L., Rish, F. L., and Verette, R. M., <u>Shell Analysis Manual</u>, Prepared by North American Rockwell Corp. for the National Aeronautics and Space Administration, Manned Spacecraft Center, Houston, Texas, June 1966.

6

GENERAL INSTABILITY OF DOME-SHAPED SHELLS

6.1 GENERAL

This section deals with dome-shaped shells whose contours are surfaces of revolution.

Figure 6.1-1 shows the shapes considered here, all of which are truncated at the equator. Note that the torispherical shape consists of a lower toroidal segment which

blends into a spherical cap. It is expected that the configurations shown here will

cover the large majority of the dome structures likely to be encountered in aerospace

applications. One should observe that for each of

(a) Hemispherical (b) Ellipsoidal (c) Torispherical
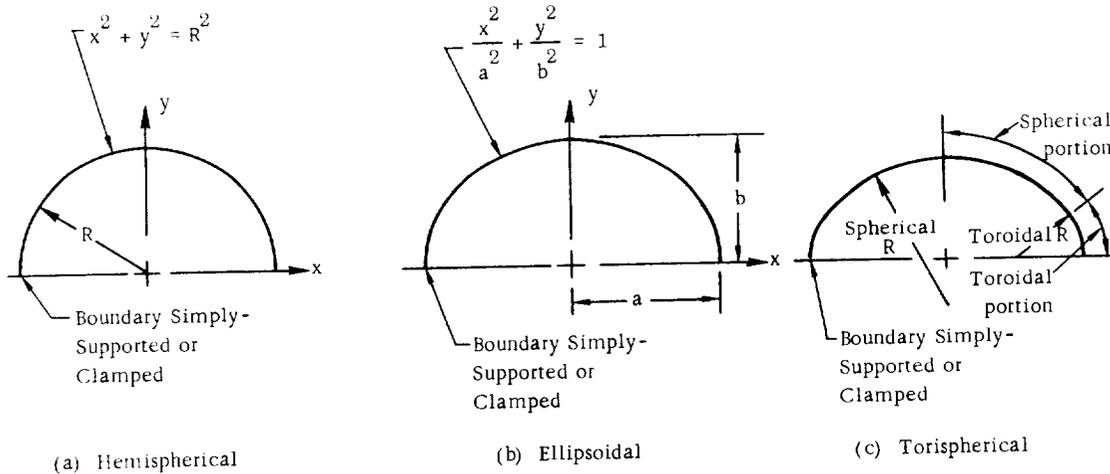
Figure 6.1-1. Structural Dome Shapes

these domes the maximum radius of curvature R_{Max} occurs at the apex. As a practical engineering expediency, analysis of all the illustrated configurations will be based

on this radius.

In the case of externally pressurized, thin-walled, isotropic (non-sandwich) domes, it has long been recognized that the test results normally fall far below the predictions from classical small-deflection theory for the axisymmetric buckling of complete spheres. The discrepancies are usually attributed to,

a. the shape of the postbuckling equilibrium path coupled with the presence of initial imperfections,

b. the fact that large-deflection analyses of asymmetric behavior yield critical stresses approximately 20 percent lower than the small-deflection axisymmetric values, and

c. the fact that classical small-deflection theory does not account for pre-buckling discontinuity distortions in the neighborhood of the boundary.

This is analogous to the situation described earlier in this handbook (see Section 4.1) for the case of circular cylinders. For the latter, it has become common practice to base stability analyses and design procedures on the use of classical small-deflection theory modified by empirical knock-down factors. This approach was selected in Section 4.1 for sandwich cylinders and is also adopted here for sandwich domes.

6.2 EXTERNAL PRESSURE

6.2.1 Basic Principles

6.2.1.1 Theoretical Considerations

This section deals with the loading condition depicted in Figure 6.2-1. That is, a uniform external pressure acts over the entire surface of the sandwich dome. The net
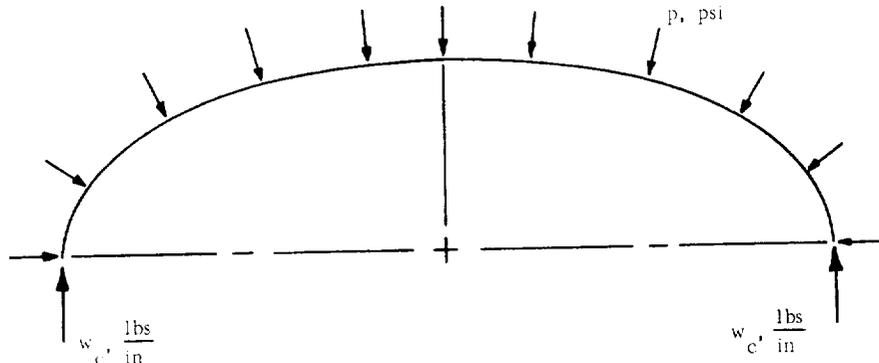
Figure 6.2-1. Sandwich Dome Subjected to External Pressure

vertical component of this loading is reacted by a uniform running load on the boundary.

From Figure 6.1-1, note that the domes can have either simply-supported or clamped edges. That is, during buckling the boundary is constrained such that no radial displacements occur. In the simply-supported case, the shell wall is free to rotate along the boundary whereas for clamped edges such rotations are completely suppressed. It follows, of course, that intermediate restraints to edge rotation are also acceptable.

The theoretical basis used here is the classical, small-deflection solution by Yao [6-1] as reformulated by Plantema [6-2]. This result embodies the following assumptions:

    a.   The facings are isotropic.

    b.   Both facings are of the same thickness.

    c.   Both facings have identical material properties.

d. Bending of the facings about their own middle surfaces can be neglected.

e. The core has infinite extensional stiffness in the direction normal to the facings.

f. The core extensional and shear stiffnesses are negligible in directions parallel to the facings.

g. The transverse shear properties of the core are isotropic.

h. The inequality $\dfrac{R}{t_c} \gg 1$ is satisfied,

where

R = Radius to middle surface of sandwich sphere, inches.

t_c = Thickness of core, inches.

i. Approximations equivalent to those of Donnell [6-3] can be applied.

Strictly speaking, this solution was derived for complete sandwich spheres which exhibit small buckles that are axisymmetric with respect to a radius of the sphere. The development isolated one such buckle as a free body so that shallow-shell theory could then be employed. Yao presented his results in a form which is not conducive to a ready physical interpretation of the phenomena involved. Therefore, Plantema undertook to express the final relationships in a manner which would foster some insight in this regard. He was able to show that, when the core has isotropic transverse shear stiffness, Yao's solution is identical to the equations given earlier in this handbook for axially compressed circular sandwich cylinders [see Equations (4.2-27) through (4.2-30) and Equations (4.2-4) and (4.2-5)]. That is, when the knock-down factor, γ_d, is included,

$$\sigma_{cr} = \gamma_d K_c \sigma_o \qquad (6.2-1)$$

6-4

where

$$\sigma_o = \frac{\eta E_f}{\sqrt{1 - \nu_c^2}} \frac{h}{R} \qquad (6.2\text{-}2)$$

and

When $V_c \leq 2$

$$K_c = 1 - \frac{1}{4} V_c \qquad (6.2\text{-}3)$$

When $V_c \geq 2$

$$K_c = \frac{1}{V_c} \qquad (6.2\text{-}4)$$

where

$$V_c = \frac{\sigma_o}{\sigma_{crimp}} \qquad (6.2\text{-}5)$$

$$\sigma_{crimp} = \frac{h^2}{2 t_f t_c} G_c \qquad (6.2\text{-}6)$$

σ_{cr} = Critical compressive stress for sandwich sphere, psi.

η = Plasticity reduction factor, dimensionless.

E_f = Young's modulus of facings, psi.

h = Distance between middle surfaces of facings, inches.

ν_e = Elastic Poisson's ratio of facings, dimensionless.

R = Radius to middle surface of sandwich sphere, inches.

t_f = Thickness of a single facing, inches.

t_c = Thickness of core, inches.

G_c = Transverse shear modulus of core, psi.

6-5

The equivalence between an axially compressed sandwich cylinder and an externally pressurized sandwich sphere has been analytically demonstrated only for the case where the two facings have identical material properties and are of the same thickness. If one assumes that this equivalence still holds true when the facings are of different thicknesses, Equations (4.2-2) through (4.2-7) can then be used here if G_{xz} is replaced by G_c so that, when the knock-down factor γ_d is included,

$$\sigma_{cr} = \gamma_d K_c \sigma_o \qquad (6.2-7)$$

where

$$\sigma_o = \eta E_f \frac{h}{R} \frac{2\sqrt{t_1 t_2}}{\sqrt{1 - \nu_e^2}\,(t_1 + t_2)} \qquad (6.2-8)$$

and

When $V_c \leq 2$

$$K_c = 1 - \frac{1}{4} V_c \qquad (6.2-9)$$

When $V_c > 2$

$$K_c = \frac{1}{V_c} \qquad (6.2-10)$$

where

$$V_c = \frac{\sigma_o}{\sigma_{crimp}} \qquad (6.2-11)$$

$$\sigma_{crimp} = \frac{h^2}{(t_1 + t_2)\,t_c}\, G_c \qquad (6.2-12)$$

t_1 and t_2 = Thicknesses of the facings (There is no preference as to which facing is denoted by the subscript 1 or 2.), inches.

The relationship between K_c and V_c can be plotted as shown in Figure 6.2-2. It is important to note that the value $V_c = 2.0$ establishes a dividing line between two different types of behavior. The region where $V_c < 2.0$ covers the so-called stiff-core and moderately-stiff-core sandwich constructions. When V_c is in the neighborhood of zero, the core transverse shear stiffness is high and the sandwich exhibits maximum sensitivity to initial imperfections. As V_c increases from
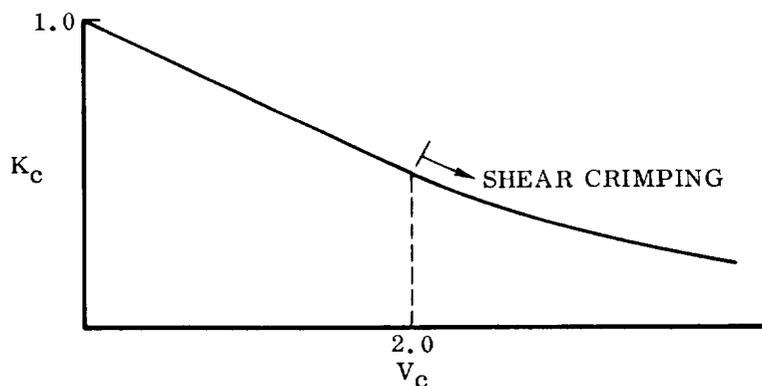
Figure 6.2-2. Schematic Representation of Relationship Between K_c and V_c

zero to a value of 2.0, this sensitivity becomes progressively less. The domain where $V_c \geq 2.0$ is the so-called weak-core region where shear crimping occurs. Sandwich constructions which fall within this category are not influenced by the presence of initial imperfections and a knock-down factor of unity can be applied to such structures. It should be possible to develop a continuous transitional knock-down relationship which recognizes the variable influence of the core rigidity but this is beyond the scope of the present handbook.

6.2.1.2   Empirical Knock-Down Factor

As noted in Section 6.1, for the purposes of this handbook, the allowable stresses for externally pressurized sandwich domes are established by applying an empirical knock-down factor (γ_d) to the results from classical small-deflection theory. However, since the available test data from sandwich dome constructions are very scarce, one cannot yet determine γ_d values with a high degree of reliability. The only useful data uncovered during the preparation of this handbook are those which were obtained by North American Rockwell [6-4] in conjunction with the Saturn S-II development program. These results give the γ_d values shown in Figure 6.2-3 which includes two data points from hemispheres and six data points from domes that were approximately ellipsoidal. Reference 6-4 includes specimens whose membrane stresses at failure ranged all the way from the elastic to the deeply plastic zones. In three cases it was felt that these stresses were too high to permit the computation of reliable plasticity reduction factors. Therefore, these particular data were discarded and they do not appear in Figure 6.2-3. Still another experimental point was discarded because of a faulty edge condition in the test. In addition, as noted in Figure 6.2-3, two specimens were subjected to a thermal gradient along with the external pressure. For each of these domes, the inner facing was at roughly +280°F while the outer facing was at approximately +10°F. This gradient was completely neglected in the analysis performed to arrive at the related γ_d values. Nevertheless, these results are retained in Figure 6.2-3 since they fall within the scatter band displayed by the other specimens having the same basic contour.
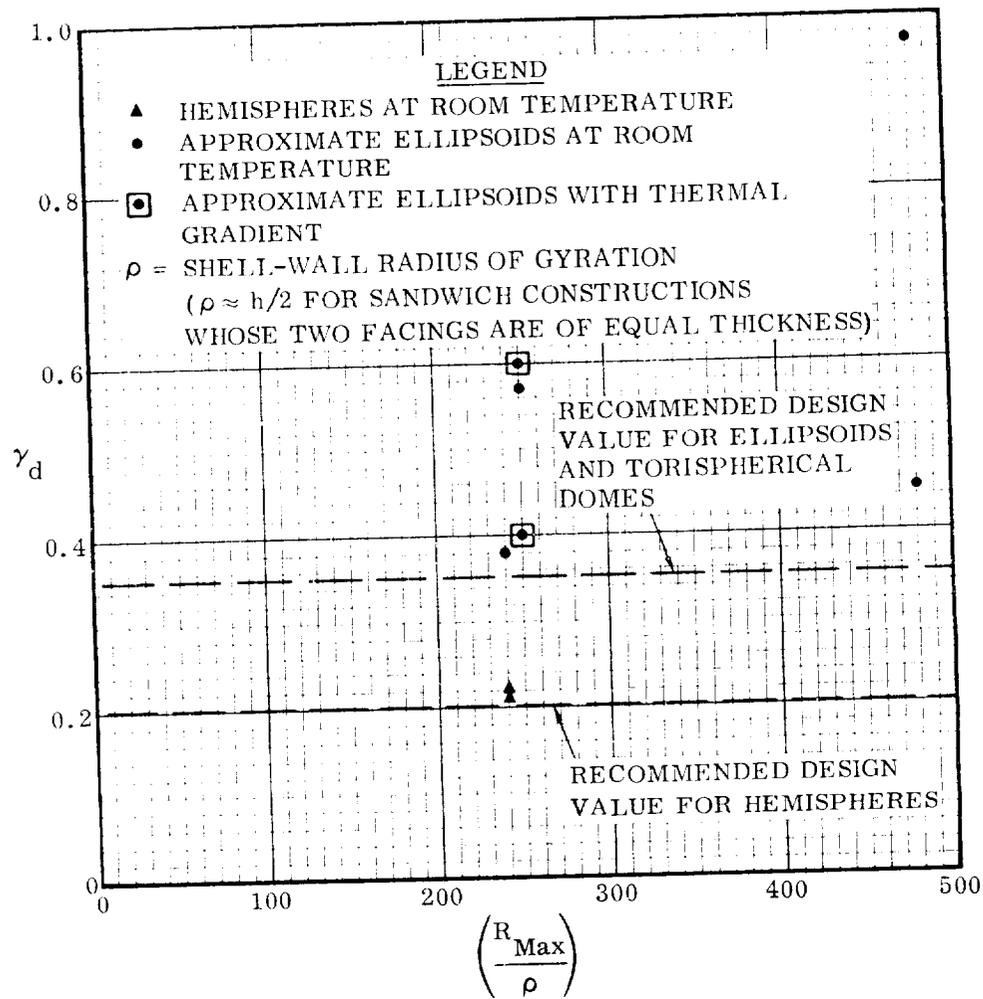
Figure 6.2-3. Knock-Down Factor γ_d for Sandwich Domes Subjected to Uniform External Pressure

To fully understand the information given in Figure 6.2-3, it is important for the reader to be aware of the data reduction techniques employed here. For an explanation of these procedures, reference may be made to the discussion in Section 4.2.1.2.1. Although that section is concerned with sandwich cylinders, the same basic approach was used in analyzing the domes.

Based on Figure 6.2-3, it is recommended that, except where shear crimping occurs, the following values may be used for γ_d:

$$\gamma_d = 0.20 \text{ for hemispheres} \tag{6.2-13}$$

$$\gamma_d = 0.35 \text{ for ellipsoids and torispherical domes} \tag{6.2-14}$$

Insufficient data are available to discern any dependence of the knock-down factor on the ratio R_{Max}/ρ. However it is quite possible that even a large array of data would lead to the same conclusion. This would be consistent with the practice usually accepted for isotropic (non-sandwich) domes.

It is thought that there is physical justification for the use of a γ_d value for hemispheres which is lower than that for ellipsoids and torispherical domes. This justification lies in the fact that, for the latter two configurations, the maximum membrane stresses occur at the apex which is well-removed from the boundary disturbances. On the other hand, the membrane stresses in a hemisphere are uniform over the entire surface. Discontinuity distortions at the boundaries are ignored in classical small-deflection stability theory but, in reality, these deformations can act somewhat like initial imperfections and precipitate buckling. This fact, coupled with the uniform membrane

6-10

stress in the hemisphere, can lead to earlier failure than would be encountered for shapes where the peak membrane stresses do not extend into the boundary regions.

Since the recommended values for γ_d are based on meager test results, the method proposed here is not very reliable and can only be regarded as a "best-available" technique. It should only be used as a rough guideline and final designs must be substantiated by test.

6.2.2 Design Equations and Curves

For sandwich domes of the types shown in Figure 6.1-1 and subjected to uniform external pressure, the critical apex stresses may be computed from the relationships given in the equations on page 6-14 where the subscripts 1 and 2 refer to the separate facings. There is no preference as to which facing is denoted by the subscript 1 or 2. The equations on page 6-14 were obtained by a simple extension of the formulas presented in Section 6.2.1.1. The extension was accomplished in order to cover some situations where the two facings are not made of the same material. This was achieved through the use of equivalent-thickness concepts based on the ratios of the moduli for the respective facings. For cases where the two facings are not made of the same material, the resulting equations are valid only when the behavior is elastic $(\eta = 1)$. Application to inelastic cases $(\eta \neq 1)$ can only be made when both facings are made of the same material. For such configurations, E_1 and E_2 will, of course, be equal.

The buckling coefficients K_c can be obtained from Figure 6.2-4.

The knock-down factor γ_d may be chosen as follows:

When $V_c < 2.0$

    Use $\gamma_d = 0.20$ for hemispheres.

    Use $\gamma_d = 0.35$ for ellipsoids and torispherical domes.

When $V_c \geq 2.0$

    Use $\gamma_d = 1.0$ for hemispheres, ellipsoids, and torispherical domes.

The quantity R_{Max} is the maximum principal radius of curvature for the dome and is measured in units of inches. For all of the shapes shown in Figure 6.1-1, this value occurs at the apex.
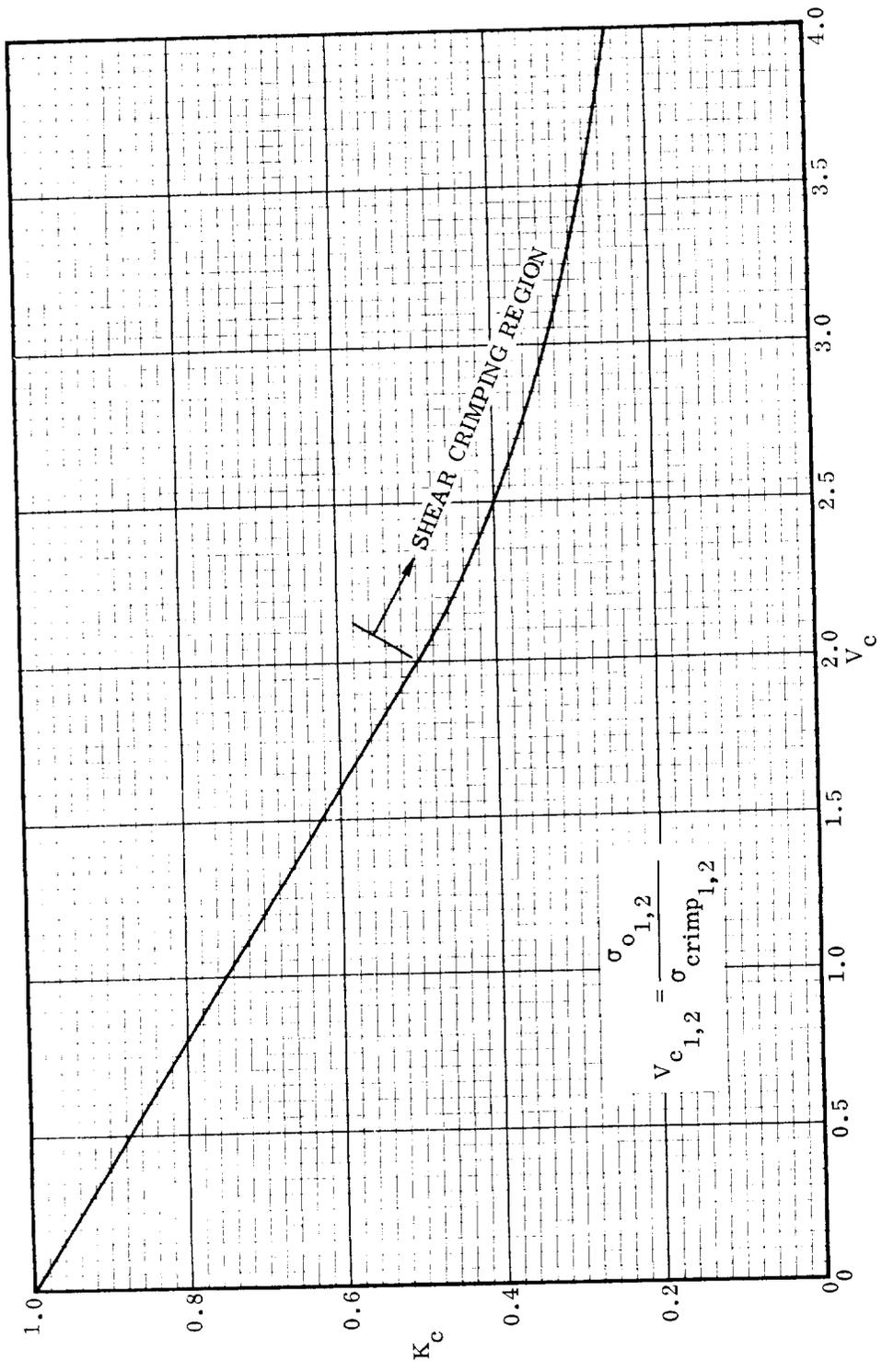
Figure 6.2-4. Buckling Coefficient for Sandwich Domes Subjected to External Pressure

The formulations given here are based on the assumption that the transverse shear stiffness of the core is isotropic. However, in most practical sandwich constructions, this stiffness will vary with direction. In order to apply the given criteria to such structures, one must select a single effective G_c value. Whenever the shear crimping mode is critical ($V_c \leq 2.0$), G_c must be taken equal to the minimum value for the core. In all other cases one must rely on engineering judgment in making an appropriate selection.

The plasticity reduction factor should always be based on the stress at the apex of the dome. For elastic cases, use $\eta = 1$. Whenever the behavior is inelastic, the methods of Section 9 must be employed.

<u>Facing 1</u>

$$\text{Apex } \sigma_{cr_1} = \gamma_d K_{c_1} \sigma_{o_1} \quad (6.2\text{-}15)$$

$$\sigma_{o_1} = \eta E_1 C_o \quad (6.2\text{-}17)$$

<u>Facing 2</u>

$$\text{Apex } \sigma_{cr_2} = \gamma_d K_{c_2} \sigma_{o_2} \quad (6.2\text{-}16)$$

$$\sigma_{o_2} = \eta E_2 C_o \quad (6.2\text{-}18)$$

$$C_o = \frac{h}{R_{Max}} \frac{2\sqrt{(E_1 t_1)(E_2 t_2)}}{\sqrt{1 - \nu_e^2}\,[(E_1 t_1) + (E_2 t_2)]} \quad (6.2\text{-}19)$$

$$\sigma_{crimp_1} = \frac{h^2}{\left[t_1 + \left(\dfrac{E_2}{E_1}\right) t_2\right] t_c} G_c \quad (6.2\text{-}20)$$

$$\sigma_{crimp_2} = \frac{h^2}{\left[\left(\dfrac{E_1}{E_2}\right) t_1 + t_2\right] t_c} G_c \quad (6.2\text{-}21)$$

$$V_{c_1} = V_{c_2} = \frac{\sigma_{o_1}}{\sigma_{crimp_1}} \quad (6.2\text{-}22)$$

$$V_{c_1} = V_{c_2} = \frac{\sigma_{o_2}}{\sigma_{crimp_2}} \quad (6.2\text{-}23)$$

6-14

The critical pressure p_{cr} (in units of psi) may be computed as follows:

$$p_{cr} = \frac{2}{R_{Max}} [\sigma_{cr_1} t_1 + \sigma_{cr_2} t_2]$$

(6.2-24)

In the special case where $t_1 = t_2 = t_f$ and both facings are made of the same material,

Equations (6.2-15) through (6.2-24) can be simplified to the following:

$$\text{Apex } \sigma_{cr} = \gamma_d K_c \sigma_o$$

(6.2-25)

$$\sigma_o = \frac{(\eta E_f)}{\sqrt{1-\nu_e^2}} \frac{h}{R_{Max}}$$

(6.2-26)

$$\sigma_{crimp} = \frac{h^2}{2 t_f t_c} G_c$$

(6.2-27)

$$V_c = \frac{\sigma_o}{\sigma_{crimp}}$$

(6.2-28)

$$p_{cr} = \frac{4}{R_{Max}} (\sigma_{cr} t_f)$$

(6.2-29)

6.3 OTHER LOADING CONDITIONS

No information is available concerning the general instability of dome-shaped sandwich shells under loading conditions other than that of uniform external pressure which is covered in Section 6.2.

Table 6-1. Summary of Design Equations for Instability of Dome-Shaped Shells

NOTATION: σ_{cr} = Critical compressive stress (occurs at apex of dome, psi), η = Plasticity reduction factor (dimensionless), E = Young's modulus (psi), h = Distance between middle surfaces of facings (inches), R_{Max} = Maximum principal radius of curvature for the dome (occurs at apex for all domes considered here, inches), t = Thickness (inches), ν_e = Elastic Poisson's ratio of facings (dimensionless), G_c = Transverse shear modulus of core (psi), p = Uniform external pressure (psi), γ_d = Knock-down factor (dimensionless), M.S. = Margin of safety (dimensionless).

SUBSCRIPTS: 1, 2 denote facing 1 or 2 (there is no preference as to which facing is denoted by the subscript 1 or 2), c denotes core, cr denotes critical value for buckling, f denotes facing, D denotes design value.

Loading Condition	Design Formulas for General Instability
1. UNIFORM EXTERNAL PRESSURE	(a) Apex $\sigma_{cr_{1,2}} = \gamma_d K_{c_{1,2}} \sigma_{o_{1,2}}$ where $K_{c_{1,2}}$ may be obtained from Figure 6.2-4. The knock-down factor γ_d may be chosen as follows: When $V_{c_1} < 2.0$ When $V_{c_1} \geq 2.0$ Use $\gamma_d = 0.20$ for hemispheres. Use $\gamma_d = 1.0$ for hemispheres, ellipsoids, and torispherical domes. Use $\gamma_d = 0.35$ for ellipsoids and torispherical domes. $\sigma_{o_{1,2}} = \eta E_{1,2} C_o$ $C_o = \dfrac{h}{R_{Max}} \dfrac{2\sqrt{(E_1 t_1)(E_2 t_2)}}{\sqrt{1 - \nu_e^2}\,(E_1 t_1) - (E_2 t_2)}$ $\sigma_{crimp_1} = \dfrac{h^2}{\left[t_1 + \left(\dfrac{E_2}{E_1}\right) t_2 \right] t_c} G_c$ $\sigma_{crimp_2} = \dfrac{h^2}{\left[\left(\dfrac{E_1}{E_2}\right) t_1 + t_2 \right] t_c} G_c$

$$V_{c_1} = V_{c_2} = \frac{\sigma_{o,i}}{\sigma_{crimp,i}}$$
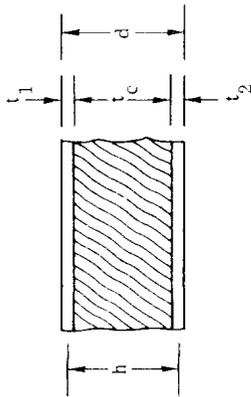
$(V_{c_i}$ are used in obtaining K_{c_i} from Figure 6.2-4)

$$p_{cr} = \frac{2}{R_{Max}} \left(\sigma_{cr,1} t_1 + \sigma_{cr,2} t_2 \right)$$

$$M.S. = \left(\frac{p_{cr}}{p_D} \right) - 1$$

For cases where $V_c \geq 2.0$, take G_c equal to the minimum value for the core. Use judgement in other cases.

For cases where the two facings are not made of the same material, the foregoing equations are valid only when the behavior is elastic. Application to inelastic cases can only be made when both facings are made of the same material.

The plasticity reduction factor η should always be based on the stress at the apex of the dome. Use $\eta = 1.0$ for elastic cases. Refer to Section 9 for η for inelastic cases.

(b) In the special case where $t_1 = t_2 = t_f$ and both facings are made of the same material, Apex $\sigma_{cr} = \gamma_d K_c \sigma_o$ where K_c may be obtained from Figure 6.2-4.

The knock-down factor γ_d may be chosen as specified for case (a) above.

$$\sigma_o = \frac{(\eta E_f)}{\sqrt{1 - \nu_e^2}} \frac{h}{R_{Max}}$$

$$\sigma_{crimp} = \frac{h^2}{2 t_f t_c} G_c$$

$$V_c = \frac{\sigma_o}{\sigma_{crimp}}$$

$(V_c$ is used in obtaining K_c from Figure 6.2-4)

$$p_{cr} = \frac{4}{R_{Max}} \left(\sigma_{cr} t_f \right)$$

$$M.S. = \left(\frac{p_{cr}}{p_D} \right) - 1$$

For cases where $V_c \geq 2.0$, take G_c equal to the minimum value for the core. Use judgement in other cases.

The plasticity reduction factor η should always be based on the stress at the apex of the dome. Use $\eta = 1.0$ for elastic cases. Refer to Section 9 for η for inelastic cases.

REFERENCES

6-1   Yao, J. C., "Buckling of Sandwich Sphere Under Normal Pressure", Journal
        of the Aerospace Sciences, March 1962.

6-2   Plantema, F. J., Sandwich Construction, John Wiley & Sons, Inc., New York,
        Copyright 1966.

6-3   Donnell, L. H., "Stability of Thin-Walled Tubes Under Torsion", NACA
        Technical Report No. 479, 1934.

6-4   Gonzalez, H. M. and Patton, R. J., "Development and Fabrication of 55-Inch
        Diameter Scale Model S-II Common Bulkheads", North American Rockwell,
        Corp. Report No. SDL 468, May 1964.

7

INSTABILITY OF SANDWICH SHELL SEGMENTS

7.1 CYLINDRICAL CURVED PANELS

7.1.1 Axial Compression

7.1.1.1 Basic Principles

It will be helpful here to first consider the case of axially compressed, isotropic (non-sandwich) skin panels for which all four boundaries are simply supported. In such cases, the Schapitz criterion [7-1] furnishes a practical means for the computation of critical stresses. This criterion accounts for the effects of skin-panel geometry as the transition is made from wide panels, which behave essentially as full cylinders, to narrow panels which approach the behavior of flat plates. In particular, Schapitz proposed that one use the following relationships which have been verified by the rederivation of Reference 7-2:

When

$$\sigma_R \leq 2\sigma_p \qquad (7.1\text{-}1)$$

then

$$\sigma_{cr} = \sigma_p + \frac{\sigma_R^2}{4\sigma_p} \qquad (7.1\text{-}2)$$

when

$$\sigma_R > 2\sigma_p \qquad (7.1\text{-}3)$$

then

$$\sigma_{cr} = \sigma_R \qquad (7.1\text{-}4)$$

where,

σ_p = Critical stress for buckling of a simply supported flat plate of the configuration shown in Figure 7.1-1, psi.

σ_R = Critical stress (in units of psi) for buckling of a simply supported complete cylinder of radius R, length a_R, and thickness t_R (see Figure 7.1-1). The quantities R, a_R, and t_R are all measured in units of inches. An empirical knock-down factor should be incorporated here to account for the detrimental effects from initial imperfections.

$$a_R = a_p = a$$

$$b_R = b_p = b$$

$$t_R = t_p = t$$
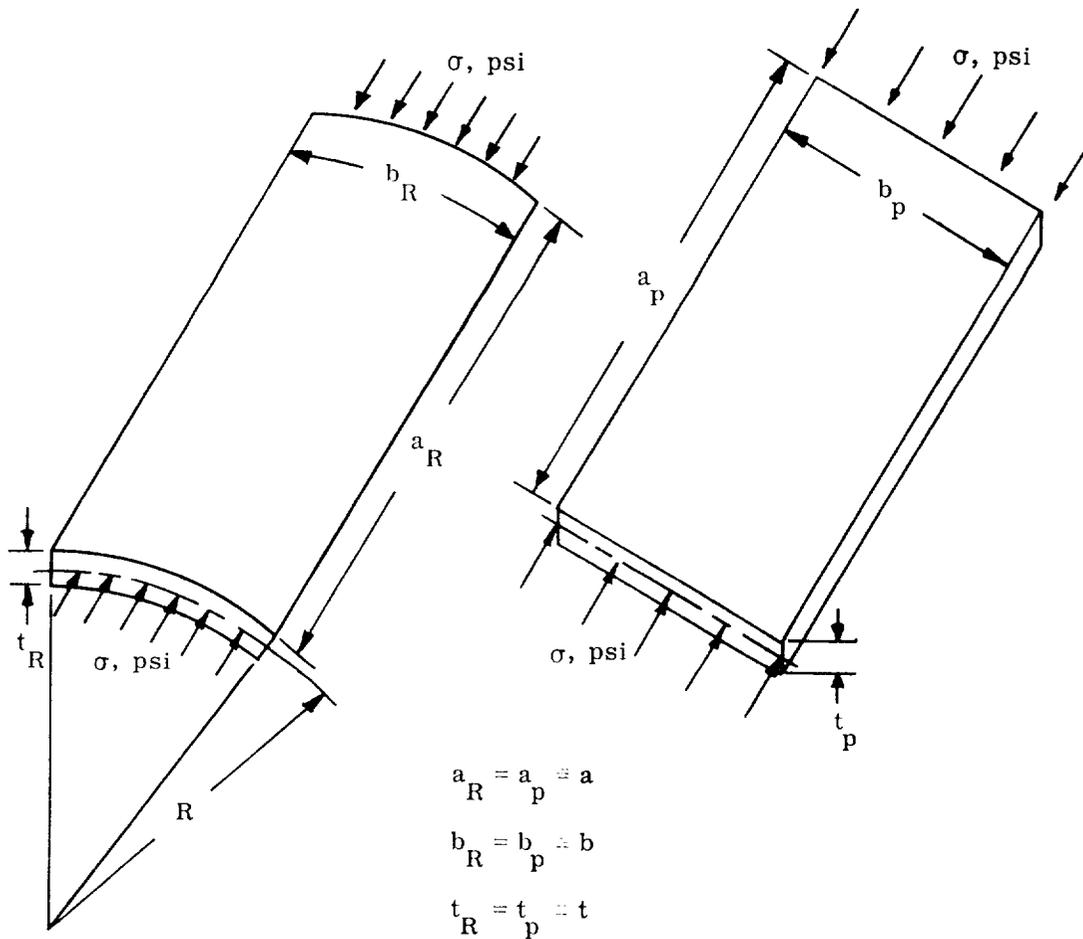
Figure 7.1-1. Cylindrical Panel and Associated Flat-Plate Configuration

b. For sandwich panels which fall in the moderately-stiff or weak-core categories, σ_{cr} should be taken equal to the higher of the two values σ_p and σ_R.

In the course of preparing this handbook, no analysis was made of test data from sandwich panels. Therefore, the reliability of this approach has not been established, and, until experimental substantiation is obtained, one can only regard the method as a "best-available" technique.

In view of the lack of sandwich data comparisons, it is informative to note that a large collection of test results from isotropic (non-sandwich) specimens is evaluated in Reference 7-3 and it is shown there that the Schapitz criterion is a reliable approach for such panels. The test configurations embraced a wide range of $\left(\dfrac{a}{b}\right)$, $\left(\dfrac{b}{R}\right)$, and $\left(\dfrac{R}{t}\right)$ ratios. Narrow, wide, and intermediate panels were included. The K values fell between those for the case where all four boundaries are simply supported and the case where all four boundaries are fully clamped. The results are summarized in the qualitative presentation of Figure 7.1-3. This figure shows the general characteristics and relative positioning for each of the following when displayed in a nondimensional logarithmic format:

a. The theoretical buckling relationship for flat plates.

b. The classical, small-deflection, theoretical buckling relationship for complete cylinders.

c. A lower-bound buckling relationship for complete cylinders. This is obtained by multiplying the values from b; above, by the empirical knock-down factor of Reference 7-4.

d. The design curve based on the Schapitz criterion.
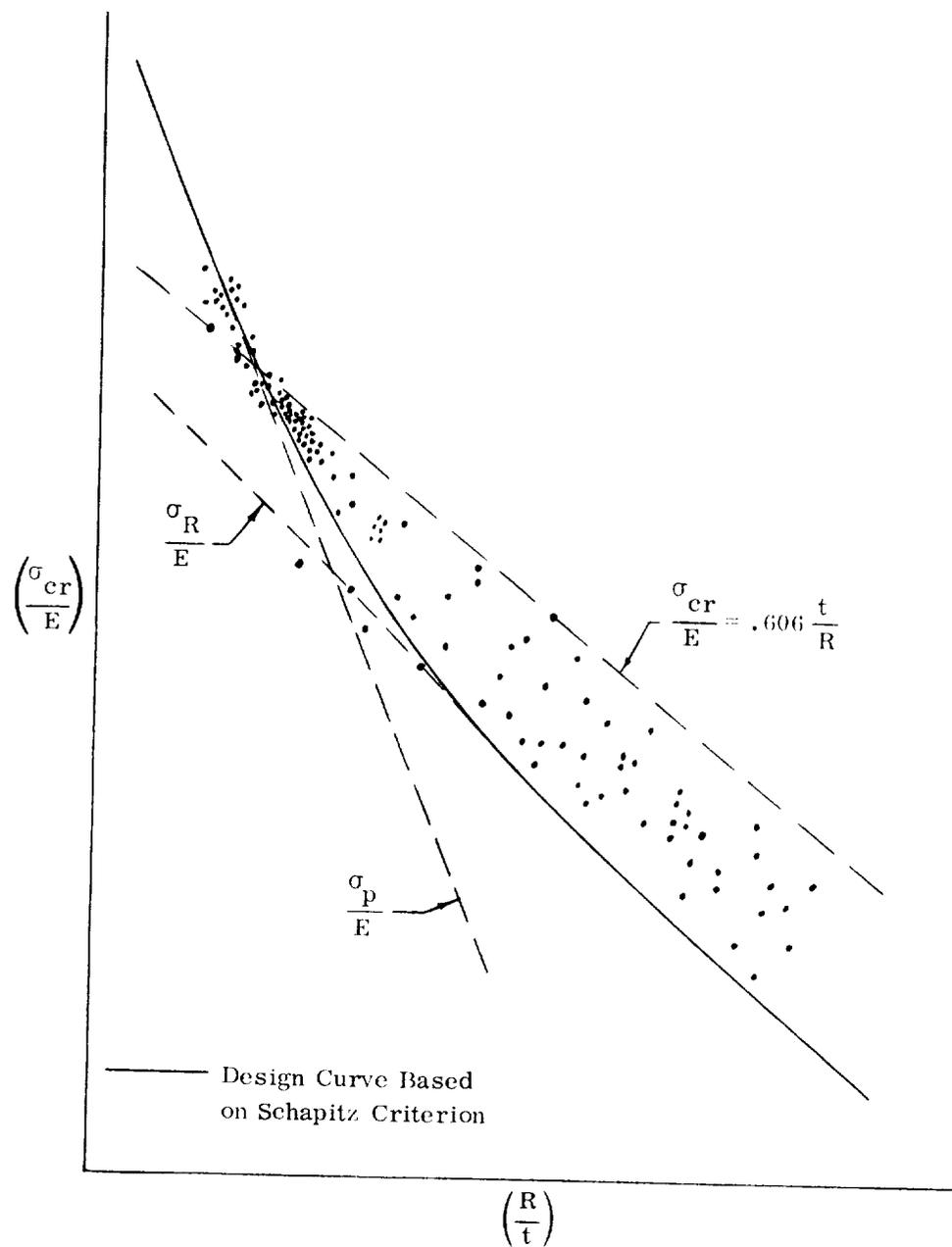
Figure 7.1-3. Schematic Logarithmic Plot of Test Data for Cylindrical Isotropic (Non-Sandwich) Skin Panels Under Axial Compression

Although derived specifically for the case of simple support, this criterion has been

successfully employed [7-3] where the boundaries provide various degrees of rotational

restraint along with the condition of no radial displacement. This was accomplished by

simply adjusting the value for σ_p to correspond with the appropriate edge restraints.

For the case under immediate discussion (non-sandwich skin panels), the Schapitz

criterion can be graphically represented as shown in Figure 7.1-2. A series of design

curves of this type are given in Reference 7-3. The transition curve defined by Equation

(7.1-2) becomes tangent to the full-cylinder curve when $\sigma_R = 2\sigma_p$. For (R/t) values

greater than that of the tangency point, the skin panel behaves as a complete cylinder.

For all other (R/t) values, the transitional relationship applies. Note that the transition

curve asymptotically approaches the line for σ_p. The quantity K denoted in Figure 7.1-2
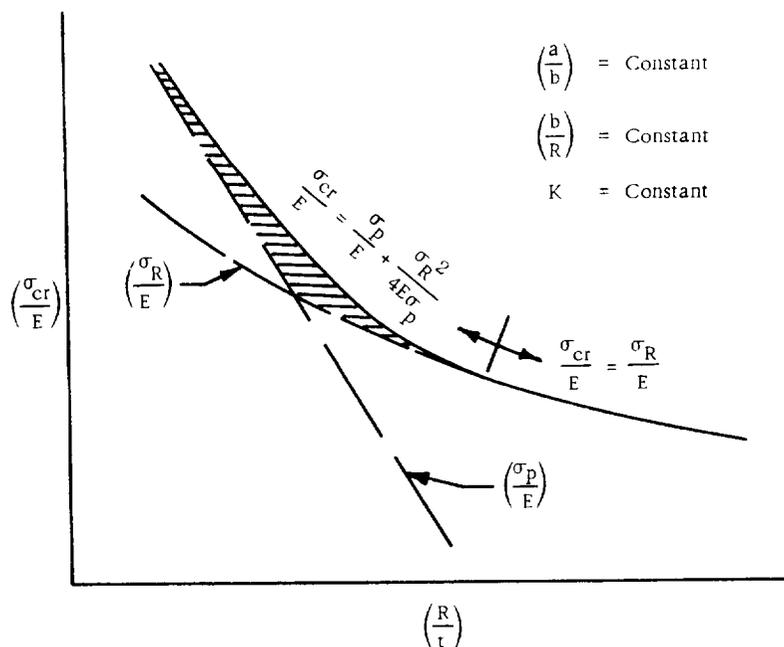
Figure 7.1-2. Schematic Logarithmic Plot of Schapitz Criterion
for Non-Sandwich Cylindrical Skin Panels

is the conventional flat-plate buckling coefficient which is dependent upon the aspect ratio (a/b), boundary conditions, and type of loading. From this figure, it can be seen that, if the critical stress were taken equal to the higher of the two values σ_p and σ_R, one would only be neglecting the transitional strength associated with the cross-hatched region. When $\left(\dfrac{\sigma_R}{\sigma_p}\right) = 1$, neglect of this contribution would result in a design value which is 80 percent of the Schapitz prediction. For all other values of the ratio $\left(\dfrac{\sigma_R}{\sigma_p}\right)$, the differences would be less significant. Indeed, for most ranges of $\left(\dfrac{\sigma_R}{\sigma_p}\right)$, the conservatism introduced by neglecting the cross-hatched area would be quite small.

Since the Schapitz criterion is dependent solely on the values σ_p and σ_R, the speculation is made here that one might extend its application to cylindrical sandwich panels merely by computing σ_p and σ_R from the sandwich design equations and curves which are provided in Sections 3 and 4. However, in making such an extension, one must recognize that the behavior of a sandwich panel is dependent upon the core stiffness. For stiff-core constructions (see Section 4.2), it should be possible to make direct application of Equations (7.1-1) through (7.1-4). On the other hand, in the weak-core region, the sandwich panel will fail by shear crimping, and curvature will not contribute to the buckling strength. In such cases, Equations (7.1-1) through (7.1-4) would yield unconservative predictions. The situation for sandwich constructions having moderately-stiff cores would, of course, fall somewhere between the foregoing limiting cases. Consequently it is recommended here that,

      a.   For stiff-core sandwich panels, Equations (7.1-1) through (7.1-4) can be applied.

Also shown in Figure 7.1-3 are the approximate locations of the test data from the non-sandwich cylindrical panels of References 7-5 through 7-8. During the course of the study reported in Reference 7-3, quantitative plots were made for each of these specimens and the corresponding test points were accurately located on the appropriate graph. Based on these many different plots, the test points were inserted in Figure 7.1-3 in approximation to their actual positions relative to the several basic curves and regions of behavior. This figure shows that all but four of the test points which fall below the design curve lie within the region where the panel behaves essentially as a flat plate. Except for those four points, all of the test data for the regions of transitional and full-cylinder behavior fall between the following two bounds:

a.   The recommended design curve.

b.   The values which would have been predicted if σ_R did not incorporate an empirical knock-down factor.

It is concluded that Figure 7.1-3 verifies the reliability of the Schapitz criterion for the case of isotropic (non-sandwich) skin panels, even where the boundary conditions include some rotational restraint in addition to the requirement of no radial displacement. This conclusion is based partly on the fact that the character of flat-plate buckling is quite different from that exhibited by wide cylindrical panels and complete cylinders. The flat plate can continue to support steadily increasing in-plane loading well into the postbuckling region. This is in contrast to the sudden drop-off in load usually observed for wide panels and full cylinders. Consequently the Schapitz criterion utilizes full theoretical predictions as the limiting case of a

flat plate is approached. One might, therefore, expect that within this region test data will display some small degree of scatter on both sides of the design curve. However, because of the physical behavior cited above, this generally will not lead to any serious structural deficiencies.

7.1.1.2 Design Equations and Curves

For cylindrical sandwich panels subjected to axial compression, the critical stress may be computed from the following:

Stiff-Core Constructions

When

$$\sigma_R \le 2\sigma_p \qquad (7.1\text{-}5)$$

then

$$\sigma_{cr} = \sigma_p + \frac{\sigma_R^2}{4\sigma_p}, \text{ and} \qquad (7.1\text{-}6)$$

when

$$\sigma_R > 2\sigma_p \qquad (7.1\text{-}7)$$

then

$$\sigma_{cr} = \sigma_R \qquad (7.1\text{-}8)$$

Weak-Core and Moderately-Stiff-Core Constructions

$$\sigma_{cr} = \begin{bmatrix} \text{The higher of the two} \\ \text{values } \sigma_p \text{ and } \sigma_R \end{bmatrix} \qquad (7.1\text{-}9)$$

where,

σ_p = Critical axial compressive stress (in units of psi) for the buckling of a flat sandwich plate which has the same boundary conditions as the cylindrical panel and, except for curvature, is of the same geometry as the cylindrical panel (see Figure 7.1-1). No knock-down factor is required in computing this value.

σ_R = Critical axial compressive stress (in units of psi) for the buckling of a complete sandwich cylinder which, except for the circumferential dimension, is identical to the curved panel. An appropriate empirical knock-down factor should be incorporated here to account for the detrimental effects from initial imperfections.

As a rule-of-thumb, one may assume that stiff-core constructions are those which satisfy the inequality

$$V_c \le 0.25 \qquad (7.1\text{-}10)$$

where V_c is computed as specified in Section 4.2.

The quantity σ_p should be computed by using the design equations and curves given in Section 3.

The quantity σ_R should be computed by using the design equations and curves given in Section 4.

A graphical representation of Equations (7.1-5) through (7.1-8) is provided in Figure 7.1-4.

The method given here applies only where all four boundaries are completely restrained against radial displacement. Therefore, no free edges are permitted. Any or all of the four boundaries may include rotational restraint of any degree ranging all the way from a hinged condition to fully clamped.
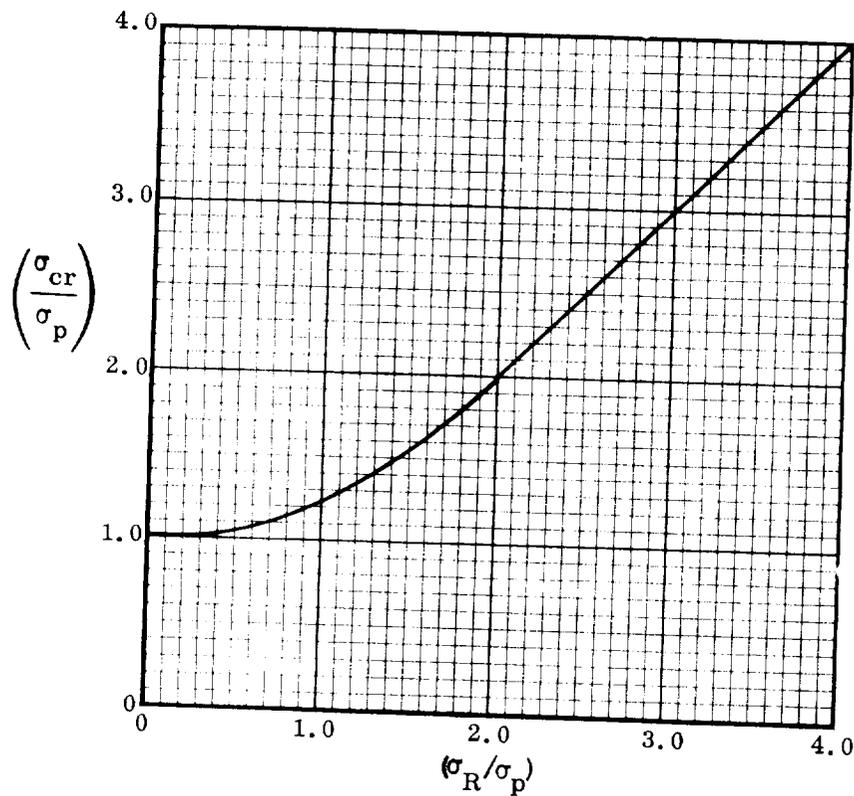
Figure 7.1-4. Graphical Representation of Equations (7.1-5) through (7.1-8)

7-10

7.1.2 Other Loading Conditions

7.1.2.1 Basic Principles

In the preparation of this handbook, almost no consideration was given to the buckling of cylindrical sandwich panels subjected to loadings other than axial compression. Therefore, no firm recommendations can be made here concerning design equations and curves. However, the suggestion is offered that, for such cases, one might consider an extension of the concepts presented in Section 7.1.1. In particular, for all regions of core stiffness, it might be possible to apply the equation

$$\sigma_{cr} = \begin{bmatrix} \text{The higher of the two} \\ \text{values } \sigma_p \text{ and } \sigma_R \end{bmatrix} \tag{7.1-11}$$

if one simply computes the values σ_p and σ_R for the loading condition of interest.

In conformance with the restrictions of Section 7.1.1, the foregoing suggestion applies only when all four boundaries of the panel are completely restrained against radial displacement. Therefore, no free edges are permitted. Any or all of the four boundaries may include rotational restraint of any degree ranging all the way from a hinged condition to fully clamped.

7.1.2.2 Design Equations and Curves

No recommendations are made here.

7.2 OTHER PANEL CONFIGURATIONS

No information is available concerning the instability of sandwich shell segments of shapes other than the cylindrical configurations considered in Section 7.1.

Table 7-1. Summary of Design Equations for Instability of Cylindrical, Curved Panels

NOTATION: σ_{cr} = Critical buckling stress for a cylindrical, curved sandwich panel. (psi)

σ_p = Critical buckling stress for a flat sandwich plate which has the same boundary conditions as the cylindrical panel and, except for curvature, is of the same geometry as the cylindrical panel (see Figure 7.1-1). No knock-down factor is required in computing this value. (psi)

σ_R = Critical buckling stress for a complete sandwich cylinder which, except for the circumferential dimension, is identical to the curved panel. The appropriate empirical knock-down factor should be incorporated here. (psi)

Loading Condition	Design Formulas for General Instability	
	Stiff-Core Constructions	Weak-Core and Moderately-Stiff-Core Constructions
1. AXIAL COMPRESSION	As a rule-of-thumb, one may assume that the panel falls into this category when $$V_c \leq 0.25$$ where V_c is computed as specified in Loading Condition 1 of Table 4-1. When $$\sigma_R \leq 2\sigma_p$$ then $$\sigma_{cr} = \sigma_p + \frac{\sigma_R^2}{4\sigma_p}, \text{ and}$$ when $$\sigma_R > 2\sigma_p$$ then $$\sigma_{cr} = \sigma_R$$ (The above relationships are plotted in Figure 7.1-4)	As a rule-of-thumb, one may assume that the panel falls into this category when $$V_c > 0.25$$ where V_c is computed as specified in Loading Condition 1 of Table 4-1. $$\sigma_{cr} = \left[\begin{array}{c} \text{The higher of the two} \\ \text{values } \sigma_p \text{ and } \sigma_R \end{array} \right]$$

7-12

The quantity, σ_p, should be computed by using the design formulas specified in Loading Condition 1 of Table 3-1. Note that the value of the buckling coefficient, K_M, must be that which applies where all boundary conditions are the same as those for the curved panel. All the restrictions noted in Table 3-1 apply to the calculations for σ_p.

The quantity, σ_R, should be computed by using the design formulas specified in Loading Condition 1 of Table 4-1. All the restrictions noted in Table 4-1 apply to the calculations for σ_R.

The method given here applies only where all four boundaries of the panel are completely restrained against radial displacement. Therefore, no free edges are permitted. Any or all of the four boundaries may include rotational restraint of any degree ranging all the way from a hinged condition to fully clamped.

σ_{cr}, σ_R, and σ_p are based on the actual panel faceplate and core thicknesses.
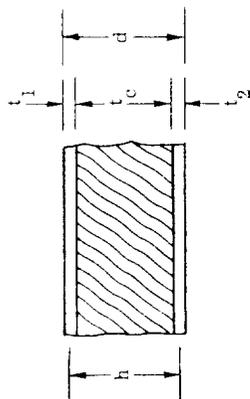
REFERENCES

7-1   Schapitz, E., Festigkeitslehre für den Leichtbau, 2 Aufl., VDI-Verlag GmbH Düsseldorf, Copyright 1963.

7-2   Spier, E. E. and Smith, G. W., "The Schapitz Criterion for the Elastic Buckling of Isotropic Simply Supported Cylindrical Skin Panels Subjected to Axial Compression", Contract NAS8-11181, General Dynamic Convair division Memo AS-D-1029, 31 January 1967.

7-3   Smith, G. W., Spier, E. E., and Fossum, L. S., "The Stability of Eccentrically Stiffened Circular Cylinders, Volume II - Buckling of Curved Isotropic Skin Panels; Axial Compression", Contract NAS8-11181, General Dynamics Convair division Report No. GDC-DDG-67-006, 20 June 1967.

7-4   Seide, P., Weingarten, V. I., and Morgan, E. J., "Final Report on the Development of Design Criteria for Elastic Stability of Thin Shell Structures", STL-TR-60-0000-19425, 31 December 1960.

7-5   Peterson, J. P., Whitley, R. O., and Deaton, J. W., "Structural Behavior and Compressive Strength of Circular Cylinders with Longitudinal Stiffening", TN-D-1251, May 1962.

7-6   Cox, H. L. and Clenshaw, W. J., "Compression Tests on Curved Plates of Thin Sheet Duralumin", British A.R.C. Technical Report R&M No. 1894, November 1941.

7-7   Crate, H. and Levin, L. R., "Data on Buckling Strength of Curved Sheet in Compression", NACA WR L-557, 1943.

7-8   Jackson, K. B. and Hall, A. H., "Curved Plates in Compression", National Research Council of Canada Aeronautical Report AR-1, 1947.

8

EFFECTS OF CUTOUTS ON THE GENERAL INSTABILITY OF SANDWICH SHELLS

In many practical aerospace shell structures, it is required that cutouts be incorporated for purposes of access, lightening, venting, etc. However, no theoretical solutions or experimental data have been published for the general instability of sandwich shells having such penetrations. Even in the case of isotropic (non-sandwich) shell structures, this problem has received little attention. Some theoretical solutions have been accomplished concerning the stress distributions around cutouts in isotropic shells but the authors of this handbook are aware of only one paper (8-1) dealing with the general instability problem, and this paper is not sufficiently comprehensive to provide a practical design criterion.

An obvious need exists for further theoretical and experimental work to be accomplished in this area, and, in view of this situation, no related design recommendations can be made at the present time.

REFERENCE

8-1   Snyder, R. E., "An Experimental Investigation of the Effect of Circular Cutouts on the Buckling Strength of Circular Cylindrical Shells Loaded in Axial Compression," Thesis submitted to the Graduate Faculty of the Virginia Polytechnic Institute in candidacy for the degree of Master of Science in Engineering Mechanics, May 1965.

9

INELASTIC BEHAVIOR OF SANDWICH PLATES AND SHELLS

9.1 SINGLE LOADING CONDITIONS

9.1.1 Basic Principles

For structural members stressed beyond the proportional limit of the material, it is

customary to compute critical loads or stresses through the use of so-called plasticity

reduction factors. In this handbook, such factors are denoted by the symbol η. In

many cases, appropriate formulas for η are established by theoretical derivations

based on plasticity theory but, when this approach proves impractical, one must some-

times resort to empirical expressions. Section 9.1.2 gives the formulations for η

which are recommended in this handbook for various sandwich configurations, types

of loading, and modes of instability. These equations are based on the information

provided in References 9-1 through 9-5 for isotropic (non-sandwich) plates and shells.

Application of these reduction factors involves the trial-and-error procedure outlined

below:

    a.   First, assume $\eta = 1$ and compute the critical stress for the appropriate
configuration, loading condition, and mode of failure.

    b.   If the critical stress computed in a, above, is less than the proportional
limit of the facing material, no further computations are required. How-
ever, if the computed critical stress exceeds the proportional limit, one
must continue as specified below.

    c.   Assume a new value for the critical stress which is in excess of the pro-
portional limit but less than the value computed in a, above.

d.   Based on the stress level assumed in c, above, and the stress-strain curve for the facing material, compute a value for the appropriate plasticity reduction factor. The formulas of Tables 9.1-1 through 9.1-3 can be used for this purpose.

e.   Using the η value computed in d above, recalculate the critical stress.

f.   If the critical stress calculated in e, above, is in reasonable agreement with the value assumed in c, no further computations are required. However, if such agreement is not achieved, one must then repeat the computation cycle starting with c. This iterative procedure must be continued until acceptable agreement is attained between the assumed and the calculated critical stresses.

A numerical example of the foregoing procedure is provided in Section 9.1.2.

9.1.2   Design Equations

Recommended formulas for plasticity reduction factors are given in Tables 9.1-1

through 9.1-3 where

E_f = Compressive Young's modulus of facings, psi.

E_s = Compressive secant modulus of facings, psi.

E_t = Compressive tangent modulus of facings, psi.

G_f = Elastic shear modulus of facings, psi.

G_s = Secant shear modulus of facings, psi.

ν_e = Elastic Poisson's ratio of facings, dimensionless.

ν = Actual Poisson's ratio of facings, dimensionless.

Values for ν can be obtained by using

$$\nu = 0.50 - \left(\frac{E_s}{E_f}\right)\left(0.50 - \nu_e\right) \qquad (9.1-1)$$

or

$$\nu = 0.50 - \left(\frac{3\,G_s}{E_f}\right)\left(0.50 - \nu_e\right) \qquad (9.1-2)$$

The technique for applying the plasticity reduction factors is demonstrated below by

means of a numerical example for an axially compressed sandwich cylinder which is

assumed to be of sufficient length to fall outside the short-cylinder range. It is further

assumed that

a.   both facings are of the same thickness,

b.   both facings are made of the same material, and

c.   the transverse shear properties of the core are isotropic so that
$\theta = \left(G_{xz}/G_{yz}\right) = 1.$

9-3

For such cylinders, Section 4.2.2 specifies that the critical stress for general instability may be computed from

$$\sigma_{cr} = \gamma_c K_c \sigma_o \qquad (9.1\text{-}3)$$

where

$$\sigma_o = \frac{(\eta E_f)}{\sqrt{1 - \nu_e^2}} \frac{h}{R} \qquad (9.1\text{-}4)$$

γ_c is obtained from Figure 4.2-8. K_c is obtained from **Figure** 4.2-7 where

$$V_c = \frac{\sigma_o}{\sigma_{crimp}} \qquad (9.1\text{-}5)$$

and

$$\sigma_{crimp} = \frac{h^2}{2 t_f t_c} G_{xz} \qquad (9.1\text{-}6)$$

For the purposes of the present sample problem, assume that

$$E_f = 10 \times 10^6 \text{ psi}$$

$$\nu_e = 0.30$$

$$R = 32.0''$$

$$h = .320''$$

$$t_f = .020''$$

$$t_c = .300''$$

$$G_{xz} = 20,000 \text{ psi}$$

$$\rho = \frac{h}{2} = .160''$$

$$\frac{R}{\rho} = \frac{32.0''}{.160''} = 200$$

Facing Proportional Limit = 25,000 psi

9-4

By using these values and assuming that $\eta = 1$, it is found that

$$\gamma_c = 0.49$$

$$\sigma_o = 104,900$$

$$\sigma_{crimp} = 170,800$$

$$V_c = 104,900/170,800 = .614$$

$$K_c = 0.85$$

Therefore,

$$\sigma_{cr} = \gamma_c K_c \sigma_o = .49 \times .85 \times 104,900 = 43,600$$

Note that the computed critical stress (43,600 psi) is higher than the proportional limit (25,000 psi) of the facings. Hence the use of $\eta = 1$ cannot be valid and one must now proceed on a trial-and-error basis. That is, one must select an assumed critical stress value which exceeds the proportional limit. For the purposes of this sample problem, suppose that the value $\sigma_{cr} = 30,000$ is selected. By using the stress-strain curve for the facing material, the corresponding plasticity reduction factor can then be computed from the following formula which is taken from Table 9.1-3:

$$\eta = \left[\frac{1 - \nu_e^2}{1 - \nu^2} \right]^{\frac{1}{2}} \frac{\sqrt{E_t E_s}}{E_f} \tag{9.1-7}$$

Suppose that this gives the result that

$$\eta = 0.900$$

so that one now obtains

$$\gamma_c = 0.49 \text{ (remains unchanged)}$$

$$\sigma_o = .900 \times 104,900 = 94,400$$

$$\sigma_{crimp} = 170,800 \text{ (remains unchanged)}$$

$$V_c = 94,400/170,800 = .553$$

$$K_c = 0.86$$

Therefore,

$$\sigma_{cr} = \gamma_c K_c \sigma_o = .49 \times .86 \times 94,400 = 39,800$$

Note that the computed critical stress (39,800 psi) does not agree very closely with the assumed value (30,000 psi). Therefore, another iteration will be performed by selecting a new assumed critical stress, say 35,000 psi. Suppose that by using Equation (9.1-7) the corresponding plasticity reduction factor is found to be

$$\eta = 0.790$$

so that one now obtains

$$\gamma_c = 0.49 \text{ (remains unchanged)}$$

$$\sigma_o = .790 \times 104,900 = 82,900$$

$$\sigma_{crimp} = 170,800 \text{ (remains unchanged)}$$

$$V_c = 82,900/170,800 = .486$$

$$K_c = 0.87$$

Therefore,

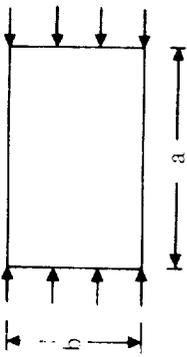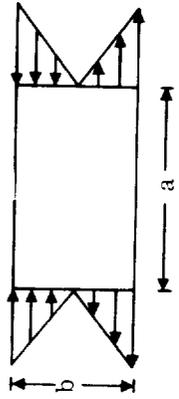$$\sigma_{cr} = \gamma_c K_c \sigma_o = .49 \times .87 \times 82,900 = 35,400$$

Note that the computed critical stress (35,400 psi) is now in reasonable agreement with the assumed value (35,000 psi). Therefore, no further iterations are required and the design value for the critical stress is 35,000 psi.

Table 9-1. Recommended Plasticity Reduction Factors for Local Instability Modes

Mode	Plasticity Reduction Factors		
	Uniaxial Compression With Honeycomb Core	Uniaxial Compression Parallel to Axis of a Corrugated Core	Uniaxial Compression Perpendicular to Axis of a Corrugated Core
Intracellular Buckling (Face Dimpling)	$\eta = \left[\dfrac{1-\nu_e^2}{1-\nu^2}\right]\dfrac{E_s}{E_f}\left[\dfrac{1}{2}+\dfrac{1}{2}\left(\dfrac{1}{4}+\dfrac{3}{4}\dfrac{E_t}{E_s}\right)^{\frac{1}{2}}\right]$	$\eta = \left[\dfrac{1-\nu_e^2}{1-\nu^2}\right]\dfrac{E_s}{E_f}\left[\dfrac{1}{2}+\dfrac{1}{2}\left(\dfrac{1}{4}+\dfrac{3}{4}\dfrac{E_t}{E_s}\right)^{\frac{1}{2}}\right]$	$\eta = \left[\dfrac{1-\nu_e^2}{1-\nu^2}\right]\dfrac{E_t}{E_f}$
Face Wrinkling	For all cases, use $\eta = \dfrac{E_t}{E_f}$		

NOTE: The Shear Crimping failure mode is independent of any plasticity reduction factor.

Table 9-2. Recommended Plasticity Reduction Factors for the General Instability of Flat Sandwich Plates

Loading Condition	Plasticity Reduction Factors
Uniaxial In-Plane Edgewise Compression	* $\eta = \left[\dfrac{1-\nu_e^2}{1-\nu^2}\right] \dfrac{E_s}{E_f} \left[\dfrac{1}{2} + \dfrac{1}{2}\left(\dfrac{1}{4} + \dfrac{3}{4}\dfrac{E_t}{E_s}\right)^{\frac{1}{2}}\right]$
In-Plane Edgewise Bending	* $\eta = \left[\dfrac{1-\nu_e^2}{1-\nu^2}\right] \dfrac{E_s}{E_f} \left[\dfrac{1}{2} + \dfrac{1}{2}\left(\dfrac{1}{4} + \dfrac{3}{4}\dfrac{E_t}{E_s}\right)^{\frac{1}{2}}\right]$
In-Plane Edgewise Shear	$\eta = \dfrac{G_s}{G_f}$

* These formulas for η are not valid when $\dfrac{a}{b}$ is so small that the plate behaves essentially as a wide column. However, it is unlikely that such configurations will be encountered in aerospace applications.

Table 9-3. Recommended Plasticity Reduction Factors for the General Instability of Circular Sandwich Cylinders, Truncated Circular Sandwich Cones, and Axisymmetric Sandwich Domes

Loading Condition	Plasticity Reduction Factors	
	Short Cylinders and Cones	Moderate Length Through Long Cylinders and Cones
Axial Compression	$\eta = \left[\dfrac{1-\nu_e^2}{1-\nu^2}\right]\dfrac{E_t}{E_f}$	$\eta = \left[\dfrac{1-\nu_e^2}{1-\nu^2}\right]^{\frac{1}{2}}\dfrac{\sqrt{E_t E_s}}{E_f}$
Pure Bending	$\eta = \left[\dfrac{1-\nu_e^2}{1-\nu^2}\right]\dfrac{E_t}{E_f}$	$\eta = \left[\dfrac{1-\nu_e^2}{1-\nu^2}\right]^{\frac{1}{2}}\dfrac{\sqrt{E_t E_s}}{E_f}$
External Lateral Pressure	* $\eta = \left[\dfrac{1-\nu_e^2}{1-\nu^2}\right]\dfrac{E_s}{E_f}\left(\dfrac{1}{4} + \dfrac{3}{4}\dfrac{E_t}{E_s}\right)$	
Torsion	** $\eta = \left[\dfrac{1-\nu_e^2}{1-\nu^2}\right]^{\frac{1}{4}}\left(\dfrac{G_s}{G_f}\right)$	
Transverse Shear	** $\eta = \left[\dfrac{1-\nu_e^2}{1-\nu^2}\right]^{\frac{5}{4}}\left(\dfrac{G_s}{G_f}\right)$	
External Pressure	Hemispherical, Ellipsoidal, and Torispherical Domes (All truncated at the equator)	
	$\eta = \left[\dfrac{1-\nu_e^2}{1-\nu^2}\right]^{\frac{1}{2}}\dfrac{\sqrt{E_t E_s}}{E_f}$	

*This formula for η is not valid when the cylinder or cone is so short that it behaves essentially as a long, flat plate. However, it is unlikely that such configurations will be encountered in aerospace applications. Furthermore, it is informative to note that, for such constructions, the given formula for η is conservative.

**This formula for η is not valid when the cylinder or cone is so short that it behaves essentially as a long, flat plate. However, it is unlikely that such configurations will be encountered in aerospace applications. Furthermore, it is informative to note that, for such constructions, the given formula is approximately 13-percent unconservative.

9-9

9.2 COMBINED LOADING CONDITIONS

9.2.1 Basic Principles

As noted in Reference 9-6, only limited information is available on the inelastic stability of shell structures subjected to combined loading conditions. A similar situation exists for flat-plate constructions. Very little theoretical work has been done in these fields due to the complexity of the problem and, in general, related plasticity reduction criteria have not been established. However, in many practical engineering applications, one is confronted with this type of problem and it becomes necessary to determine at least a rough estimate of the critical loading conditions. Toward this end, one should note a fundamental hypothesis of plasticity theory which specifies that, for a given material and when the stress intensity is increasing (loading condition), the stress intensity σ_i is a uniquely defined, single-valued function of the strain intensity e_i. When σ_i is decreasing (unloading condition), the relationship between σ_i and e_i is linear as in a purely elastic case. Based on the octahedral shear law for plane stress conditions, the stress and strain intensities σ_i and e_i can be defined as follows [9-1]:

$$\sigma_i = \sqrt{\sigma_x^2 + \sigma_y^2 - \sigma_x \sigma_y + 3\tau^2} \qquad (9.2-1)$$

$$e_i = \frac{2}{\sqrt{3}} \sqrt{\epsilon_x^2 + \epsilon_y^2 + \epsilon_x \epsilon_y + \epsilon_{xy}^2/4} \qquad (9.2-2)$$

It should be noted that Equation (9.2-1) is sometimes written in the following form to facilitate its use:

$$\sigma_i = (\sigma_x)\sqrt{1 - \gamma + \gamma^2 + 3\lambda^2} \qquad (9.2-1a)$$

where

σ_x = Normal stress in the x direction, psi.

σ_y = Normal stress in the y direction, psi.

τ = Shear stress in the xy plane, psi.

ϵ_x = Normal strain in the x direction, in/in.

ϵ_y = Normal strain in the y direction, in/in.

ϵ_{xy} = Shear strain in the xy plane, in/in.

$\gamma = \sigma_y / \sigma_x$

$\lambda = \tau / \sigma_x$

From the foregoing discussion it can be concluded that, for the case of increasing σ_i (loading condition), the relationship between σ_i and e_i is identical to the conventional stress-strain curve obtained from a uniaxial loading test. It should therefore be evident that although each individual stress component may be less than the proportional limit of the material, the combination of these stresses can give a σ_i value which lies above the proportional limit so that the behavior is actually inelastic. It is important to keep this phenomenon in mind when deciding whether or not plasticity effects must be considered.

Lacking a rigorous approach to the subject stability problem, it is conjectured here that the foregoing generalization of the stress-strain relationship might be used in conjunction with the plasticity reduction factor

$$\eta = \frac{E_t}{E_f}$$ (9.2-3)

9-11

to obtain conservative predictions of inelastic instability under combined loadings. The quantities E_t and E_f are as follows:

E_t Tangent modulus of facing material obtained from the curve of σ_i vs e_i at a prescribed value of σ_i, psi.

E_f Young's modulus of facing material, psi.

The above formula for η was selected in view of its conservative nature. Since the overall procedure suggested here is based purely on an engineering estimation, it is thought that this conservatism is well justified.

The details of the suggested approach are outlined in Section 9.2.2. It is important to keep in mind that this method does not give a rigorous solution, and its reliability has not been evaluated by comparisons against test data. Therefore, this can only be regarded as a "best-available" technique and one should be cautious in its application.

9.2.2 Suggested Method

The method suggested here for analysis of the inelastic stability of sandwich plates and shells first requires that the conventional stress-strain curve for the facing material have the stress coordinates relabeled as σ_i and the strain coordinates relabeled as e_i. By completely ignoring all plasticity considerations ($\eta = 1$), one should then proceed to establish a first-estimate for the critical combined stress condition. This can be achieved by using the appropriate interaction relationships provided in earlier sections of this handbook. In performing this computation, the assumption should be made that for the critical combined stress condition the individual stress components are in the same ratios to each other as exist for the actual applied loading condition. That is, during loading, proportionality between the several individual stress components is maintained. The stresses from the elastic first-estimate computation must then be inserted into the equation

$$\sigma_i = \sqrt{\sigma_x^2 + \sigma_y^2 - \sigma_x \sigma_y + 3\tau^2} \qquad (9.2-4)$$

to determine the associated stress intensity value. If this value does not exceed the proportional limit of the σ_i versus e_i curve, the first-estimate stress values are in fact the critical combination. However, if the related σ_i value exceeds the proportional limit of the σ_i versus e_i curve, the first-estimate results are not valid and one must then resort to the following trial-and-error procedure which is similar to that outlined in Section 9.1:

  a. Assume a new value for σ_i which is in excess of the proportional limit for the σ_i versus e_i curve.

b. For the σ_i value assumed in a, above, compute the plasticity reduction factor

$$\eta = \frac{E_t}{E_f}$$ (9.2-5)

where

   E_t Tangent modulus of the σ_i versus e_i curve, psi.

   E_f Elastic modulus of the σ_i versus e_i curve, psi.

c. Using the η value from b, above, recalculate the critical stress intensity σ_i. This is accomplished by simply multiplying the first-estimate σ_i value by η.

d. If the new value for σ_i computed in c, above, is in reasonable agreement with the σ_i value assumed in a, above, the related plasticity reduction factor η is valid. Then the critical combination of stresses is obtained by multiplying each of the first-estimate stress components by this η value.

If the value of σ_i computed in c, above, is not in reasonable agreement with the σ_i value assumed in a, the related plasticity reduction factor is not valid. One must then repeat the computation cycle starting with a. This iterative procedure must be continued until acceptable agreement is attained between the assumed and the computed σ_i values.

REFERENCES

9-1   Gerard, G., "Plastic Stability Theory of Thin Shells," Journal of the Aeronautical Sciences, April 1957.

9-2   Gerard, G. and Becker, H., "Handbook of Structural Stability, Part I - Buckling of Flat Plates," NACA Technical Note 3781, July 1957.

9-3   Gerard, G. and Becker, H., "Handbook of Structural Stability, Part III - Buckling of Curved Plates and Shells," NACA Technical Note 3783, August 1957.

9-4   Gerard, G., "Compressive and Torsional Buckling of Thin-Wall Cylinders in Yield Region," NACA Technical Note 3726, August 1956.

9-5   Gerard, G., Introduction to Structural Stability Theory, McGraw-Hill Book Company, Inc., 1962.

9-6   Baker, E. H., Cappelli, A. P., Kovalevsky, L., Rish, F. L., and Verette, R. M., "Shell Analysis Manual," Prepared by North American Rockwell, Corp. for the National Aeronautics and Space Administration, Manned Spacecraft Center, Houston, Texas, June 1966.

"The aeronautical and space activities of the United States shall be conducted so as to contribute . . . to the expansion of human knowledge of phenomena in the atmosphere and space. The Administration shall provide for the widest practicable and appropriate dissemination of information concerning its activities and the results thereof."

— NATIONAL AERONAUTICS AND SPACE ACT OF 1958

NASA SCIENTIFIC AND TECHNICAL PUBLICATIONS

TECHNICAL REPORTS: Scientific and technical information considered important, complete, and a lasting contribution to existing knowledge.

TECHNICAL NOTES: Information less broad in scope but nevertheless of importance as a contribution to existing knowledge.

TECHNICAL MEMORANDUMS: Information receiving limited distribution because of preliminary data, security classification, or other reasons.

CONTRACTOR REPORTS: Scientific and technical information generated under a NASA contract or grant and considered an important contribution to existing knowledge.

TECHNICAL TRANSLATIONS: Information published in a foreign language considered to merit NASA distribution in English.

SPECIAL PUBLICATIONS: Information derived from or of value to NASA activities. Publications include conference proceedings, monographs, data compilations, handbooks, sourcebooks, and special bibliographies.

TECHNOLOGY UTILIZATION PUBLICATIONS: Information on technology used by NASA that may be of particular interest in commercial and other non-aerospace applications. Publications include Tech Briefs, Technology Utilization Reports and Notes, and Technology Surveys.

Details on the availability of these publications may be obtained from:

SCIENTIFIC AND TECHNICAL INFORMATION DIVISION

NATIONAL AERONAUTICS AND SPACE ADMINISTRATION
Washington, D.C. 20546